Fakultät für Mathematik, Informatik und Naturwissenschaften | RWTH AACHEN UNIVERSITY

Effect-directed identification and fate analysis of potent antiandrogenic coumarin derivatives in a central European river

Von der Fakultät für Mathematik, Informatik und Naturwissenschaften der RWTH Aachen University
zur Erlangung des akademischen Grades eines
Doktors der Naturwissenschaften genehmigte Dissertation

vorgelegt von

Diplom-Chemiker
Matthias Muschket
aus
Bad Salzungen

Berichter*:* Prof. Dr. rer. nat. Henner Hollert
PD Dr. rer. nat. Werner Brack

Tag der mündlichen Prüfung*:* 07.09.2018

Erklärung

Die vorliegende Dissertation wurde im Department wirkungsorientierte Analytik des UFZ - Helmholtz Zentrum für Umweltforschung in Zusammenarbeit mit dem Lehr- und Forschungsgebiet für Ökosystemanalyse des Institutes für Umweltforschung (Biologie V) der RWTH Aachen unter Betreuung von Herrn Prof. Dr. Henner Hollert und Herrn PD Dr. Werner Brack angefertigt.

Hiermit versichere ich, dass ich die vorliegende Doktorarbeit selbstständig verfasst und keine anderen als die angegebenen Hilfsmittel verwendet habe. Alle Textauszüge und Grafiken, die sinngemäß oder wörtlich aus veröffentlichten Schriften entnommen wurden, sind durch Referenzen gekennzeichnet.

Matthias Muschket Aachen, den 02. Juli 2018

Abstract

Surface waters are adversely affected by the discharge of wastewater that is containing numerous anthropogenic micropollutants. In consequence, endocrine disrupting effects like androgenicity and antiandrogenicity are frequently observed in the aquatic environment. Even if a large list of androgen axis disruptors is available, linking of adverse effects to responsible chemicals is hampered by a great share of this compound group, which is remaining unknown. Structure elucidation of these “unknowns” in environmental mixtures of typically thousands of compounds is extremely challenging even despite powerful tools like effect-directed analysis (EDA) are available. In this thesis, a novel, multidimensional fractionation approach was developed to support EDA of surface waters with endocrine disrupting activity.

In **chapter 2**, four reversed phases were selected with a focus on the separation of androgens and antiandrogens. To this end, a representative mixture of 39 endocrine disrupting compounds (EDCs) was separated on a set of 17 columns with widely differing bond chemistries. After exclusion of columns with poor peak shapes and chromatographic resolution those stationary phases displaying the highest degree of orthogonal separation selectivity for EDCs were depicted using principal component analysis and Spearman rank correlation: aminopropyl-, octadecyl-, and pyrenyl ethyl silica phase. Additionally, a pentafluorophenyl silica phase was chosen due to promising results reported in the literature. A surface water sample with antiandrogenic activity was fractionated in parallel on the four selected columns. The resulting coverage of the virtual two-dimensional separation space with non-target peaks confirmed the high degree of orthogonality of the selected stationary phases. Besides, the separation of co-eluting isobaric compounds led to a 4.8fold increase of the number of detected peaks. Consequently, the fractionation system is facilitating the chemical identification of organic micropollutants by chemical target, suspect and non-target screening using high resolution mass spectrometry.

In **chapter 3**, the established fractionation approach was applied to minimize the complexity of a surface water sample collected close to the effluent of a waste water treatment plant in the river Holtemme in Germany. In concert with a miniaturized luciferase reporter gene cell-based anti-AR-CALUX assay and LC-HRMS/MS non-target screening the highly potent antiandrogen 4-methyl-7-diethylaminocoumarin (C47), as well as the two less active

derivatives 4-methyl-7-ethylaminocoumarin (C47T1) and 4-methyl-7-aminocoumarin (C47T2) were identified. The measured *in vitro* effect was quantitatively confirming C47 as the major cause of antiandrogenicity. Furthermore the antiandrogenic activity of C47 was also observed *in vivo* in spiggin-gfp *Medaka* already at the concentration equal to the concentration in the non-concentrated water extract.

The longitudinal and temporal distribution of C47 and its derivatives along the whole river stretch was investigated in **chapter 4**. A constant exposure of the aquatic ecosystem by the three antiandrogens was observed at all sites downstream of the wastewater treatment plant of Silstedt, which was identified as the continuous source that is releasing C47, C47T1 and C47T2 in the gram per day range. Moreover, all compounds were detected in sediment and biota represented by the ubiquitous species *Gammarus pulex*. In this context, an experimental evaluation did not confirm typically proposed hydrophobic interaction to organic carbon as the driving force of partitioning into sediment but suggested cation binding of these aromatic amines to sediment. Finally, the coumarin derivatives were assessed as persistent as C47 is solely partially degraded to the less antiandrogenic potent C47T1 and C47T2 in the WWTP while a further attenuation of the compounds within the river was solely attributed to dilution by groundwater inflow.

Zusammenfassung

Oberflächengewässer werden durch die Einleitung von Abwasser, das zahlreiche anthropogene Mikroverunreinigungen enthält, negativ beeinträchtigt. Infolgedessen werden in der aquatischen Umwelt häufig endokrine Effekte wie die Androgenität und Antiandrogenität beobachtet. Obwohl eine große Liste von Androgenen und Antiandrogenen bekannt ist, kann auftretenden hormonellen Aktivitäten häufig keine ursächliche Chemikalie zugeordnet werden. Die Strukturaufklärung bisher unbekannter endokriner Disruptoren in Umweltmischungen von typischerweise tausenden von Verbindungen ist trotz leistungsfähiger Werkzeuge wie der wirkungsorientierten Analyse (EDA) äußerst schwierig. In dieser Arbeit wurde ein neuartiger, mehrdimensionaler Fraktionierungsansatz zur Unterstützung der EDA von Oberflächengewässern mit endokriner Aktivität entwickelt.

In **Kapitel 2** wurden vier Umkehrphasen mit Schwerpunkt auf der Trennung von Androgenen und Antiandrogenen ausgewählt. Zu diesem Zweck wurde eine repräsentative Mischung von 39 endokrin wirksamen Verbindungen (EDCs) auf 17 Säulen chromatographisch getrennt. Nach Ausschluss von Säulen mit schlechter Peakform und chromatographischer Auflösung wurden die stationären Phasen mit der höchsten orthogonalen Trennleistung für EDCs mittels Hauptkomponentenanalyse und Spearman-Rankkorrelation ausgewählt: Aminopropyl-, Octadecyl- und Pyrenylethyl-Silica-Phase. Zusätzlich wurde eine Pentafluorphenyl-Silica-Phase entsprechend vielversprechender Ergebnisse aus der Literatur gewählt. Eine Oberflächenwasserprobe mit antiandrogener Aktivität wurde parallel auf den vier ausgewählten Säulen fraktioniert. Die daraus resultierende Deckung des virtuellen zweidimensionalen Trennraumes mit Non-target Peaks bestätigte die hohe Orthogonalität der ausgewählten stationären Phasen. Außerdem führte die Trennung von co-eluierenden isobaren Verbindungen zu einem 4,8-fachen Anstieg der Anzahl der detektierten Peaks. Das Fraktionierungssystem erleichtert somit die chemische Identifizierung von organischen Mikroverunreinigungen durch chemisches Target-, Suspect- und Non-target Screening mittels hochauflösender Massenspektrometrie.

In **Kapitel 3** wurde der etablierte Fraktionierungsansatz angewendet, um die Komplexität einer Oberflächenwasserprobe, welche in der Nähe des Abflusses einer Kläranlage in der Holtemme in Deutschland gesammelt wurde, zu minimieren. In Verbindung mit einem miniaturisierten anti-AR-CALUX-Assay und der Flüssigchromatographie-hochauflösenden

Massenspektrometrie-Kopplung (LC-HRMS) wurden das hochwirksame Antiandrogen 4-Methyl-7-diethylaminocoumarin (C47) sowie die beiden weniger aktiven Derivate 4-Methyl-7-ethylaminocoumarin (C47T1) und 4-Methyl-7-aminocoumarin (C47T2) identifiziert. Der gemessene in vitro-Effekt bestätigte C47 als Hauptursache der Antiandrogenität. Darüber hinaus wurde die antiandrogene Aktivität von C47 auch *in vivo* in spiggin-gfp Medaka bereits in der Konzentration beobachtet, die der Konzentration im nicht konzentrierten Wasserextrakt entspricht.

Die Längs- und Zeitverteilung von C47 und seinen Derivaten entlang der gesamten Flussstrecke wurde in **Kapitel 4** untersucht. Eine konstante Belastung des aquatischen Ökosystems durch die drei Antiandrogene wurde an allen Standorten flussabwärts der Kläranlage von Silstedt beobachtet, die als kontinuierliche Quelle identifiziert wurde und C47, C47T1 und C47T2 im Gramm pro Tag Bereich freisetzt. Darüber hinaus wurden alle Verbindungen in Sedimenten und Biota der ubiquitären Spezies *Gammarus pulex* nachgewiesen. In diesem Zusammenhang bestätigte ein Verteilungsexperiment nicht die typischerweise angenommene hydrophobe Wechselwirkung mit organischem Kohlenstoff als Hauptursache für die Sorption dieser aromatischen Amine an Sediment, sondern wies auf Kationenbindung als treibende Kraft der Sorption hin. Schließlich wurden die Cumarinderivate als persistent beurteilt, da C47 in der Kläranlage nur teilweise zu den weniger aber dennoch antiandrogen wirksamen C47T1 und C47T2 abgebaut wird, während eine Konzentrationsabnahme der Verbindungen innerhalb des Flusses ausschließlich auf eine Verdünnung durch Grundwasserzufluss zurückzuführen ist.

Contents

List of Figures

List of Tables

List of Abbreviations

^{1}D	first separation dimension
2D	two-dimensional
^{2}D	second separation dimension
AOP	adverse outcome pathway
APCI	Atmospheric pressure chemical ionization
AR	androgen receptor
B	Benzylamin
BB	Butylbenzene;
C	Caffein
C18	octadecyl silica
C47	4-methyl-7-diethylaminocoumarin
C47T1	4-methyl-7-ethylaminocoumarin
C47T2	4-methyl-7-aminocoumarin
CALUX	chemically activated luciferase expression
DDE	Dichlorodiphenyldichloroethylene
DDT	Dichlorodiphenyltrichloroethane
DIA	Data-independent
EC50	Median Effect Concentration
EDA	effect-directed analysis
EDCs	endocrine disrupting compounds
EqP	equilibrium partitioning theorie
ERs	estrogen receptors
ESA	Ethane sulfonic acid
ESI	Electrospray ionization
GFP	green fluorescent protein
HDX	Hydrogen−deuterium exchange
HILIC	hydrophilic interaction chromatography
HRMS	high resolution mass spectrometry
IEC	ion-exchange chromatography
Kow	Octanol and water partitioning constant
LC	liquid chromatography
MDLC	multidimensional liquid chromatography
MS	mass spectrometry
MS/MS	Product ion spectra
NH2	Aminopropyl silica
NPC	Normal phase chromatography
O	o-Terphenyl
P	Peak capacity
PBs	Planetary boundaries
PBz	Pentylbenzene
PFP	pentafluorophenyl silica
PFP	Pentafluorophenyl silica

Pl	Phenol
PSA	Primary-secondary amine
PYE	Pyrenyl ethyl silica
RADAR	Rapid androgen disruption adverse outcome reporter
REF	Relative enrichment factor
RLU	Relative light units
RPC	Reversed phase chromatography
RT	Retention time
SEC	Size exclusion chromatography
SPM	Suspended particulate matter
T	Triphenylene
t_0	Dead time
TOC	Total organic carbon content
t_R	Retentionszeit
WFD	European Union Water Framework Directive
WWTP	Waste-water treatment plant

Chapter 1

Introduction

1.1 Human Impact on the Environment and Surface Waters

Our planets environment has been unusually stable during the last 11700 years in terms of temperatures, biogeochemical flows and freshwater availability [1, 2]. This epoch, known as the Holocene, is in serious danger since the humanity is causing devastating changes to the Earth system leading to the transgression of environmental boundaries in which we and other species can live safely [3, 4]. For example, fossil fuel combustion has increased atmospheric CO_2 concentrations by about 35% compared to pre-industrial levels resulting not only in a higher rate of global warming [5] but also in ocean acidification [6]. Other disastrous human activities include big scale forest destruction, the degradation of soil or the changes in the nitrogen and phosphorus cycle [7]. The recent loss of species diversity and thus extinction rates are already 100 to 1000 times above pre-human levels [8]. Within only 240 years Earth may face the sixth mass extinction if human society continues on this path of environmental degradation [9]. A drastic change in human behavior and partly even the acceptance of the overwhelming scientific evidence for the human impact on the environment by decision makers in policy is still missing [10]. However, we have to be aware that a transgression of the planetary boundaries (PBs) most likely does not lead to linear but rather abrupt changes of the relatively stable climate [11, 12] with unprecedented consequences for life on earth. In other words, the huge difference between where we are now and where we might be within only three centuries underlines the great urgency of a change in human behavior [9]. Rockström et al. introduced nine PBs that must not be exceeded in order to stay in the desired holocene state [2].

These PBs include the change in land use, biodiversity loss and chemical pollution which is a major force driving the environment beyond the PBs [2]. The often disastrous effects of man-made chemicals on the ecosystem and human health was displayed in numerous studies [13, 14].

More than 100.000 compounds are produced in the European Union [15] and are daily used in large quantities [16]. An uncertain number of these compounds find their way into the

aquatic environment even leading to the ubiquitous occurrence of some chemicals, as shown for instance for the insect repellent DEET [17]. Typically micropollutants are released from diffuse and point sources having industrial, agricultural and domestic origins [18, 19]. The effluent of wastewater treatment plants is a major point source and can contribute even more than 50% to the flow of small rivers [20]. These chemicals of anthropogenic origin are partially ending up not only in drinking water even despite advanced water treatment [21-23], but also in the food chain [24-26] and can heavily accumulate over several trophic levels via biomagnification [27]. It is important to note that not only big-scale accidents including the discharge of tons of chemicals into the aquatic environment may exert toxic effects but also the occurrence of these trace substances with concentration down to ng L^{-1}, especially when present as mixtures [28].

The increasing, overwhelming evidence of the adverse human impact on the aquatic environment also resulted in a growing awareness of the public and decision makers for the need to defend this good. Water is an essential resource for our planets ecosystem and therefore also for human life. Thus the protection of water from chemical contamination is a major societal goal. Water has been defined as a “heritage which must be protected, defended and treated as such” in the European Union Water Framework Directive (WFD), which is the core legislation to protect European surface waters [29]. Surprisingly, however, only 45 chemicals are regulated by the WFD (Directive 2000/60/EC) in order to achieve a “good chemical status” of all European water bodies by 2027. Thus, even if the WFD is a good starting point for a broad and efficient legislation to protect European water, the findings of Malaj et al. [30] should not be a surprise: the evaluation of monitoring data from 4,000 European sites revealed an adverse impact of organic chemicals on the biodiversity on nearly half of the continental water bodies. The findings were even likely to underestimate the actual risks due to the limitations of the existing monitoring data. Quite a few of the compounds frequently used in the European Union are endocrine disrupting chemicals that may cause adverse effects to aquatic organisms [20, 31-33] or human health [34].

1.2 Endocrine Disrupting Compounds

1.2.1 Definition and Effect of Endocrine Disrupting Compounds

Endocrine disrupting compounds (EDCs) are defined as exogenous substances causing adverse health effects in an intact organism, or its progeny, secondary to changes in endocrine function [35]. EDCs are characterized by the absence of any structural similarity with exception of their small molecular mass that is usually not exceeding 1000 Daltons [36]. They can disturb the development of the endocrine system and its responding organs in humans and wildlife, often exerting permanent and irreversible effects, especially in case of an exposure during prenatal or early postnatal life stages [37]. Thus EDCs are being stated as a significant concern to public health [36]. Effects of hormonally active chemicals present in a mixture act in an additive or sometimes even synergistic manner [38] leading to reproductive abnormalities already at very low levels of exposure [39, 40]. Even worse, endocrine disruptors may not only affect the exposed organism itself but also its progeny over several generations via epigenetic mechanisms [41]. Moreover, some EDCs exhibit multiple hormonal activities [42]. Dichlorodiphenyltrichloroethane (DDT), for example, is an estrogen, while one of its metabolites possess antiandrogenic activity [43]. Contrary to what was originally assumed, on the molecular level EDCs do not only act through the nuclear hormone receptors (e.g., estrogen receptors (ERs), androgen receptors (ARs) or thyroid receptors), but also via nonnuclear steroid receptors, nonsteroid receptors, enzymatic pathways involved in the steroidogenesis and various other mechanisms [42]. Quite a number of adverse effects and diseases in humans can be caused by an exposure of endocrine disruptors, including lower full-scale IQ, motor deficits, obesity and in consequence diabetis mellitus and cardiovascular disease [36].

1.2.2 Androgenic Disrupting Compounds and their Occurrence in Surface Waters

Until now research on EDCs was mainly focused on pathways including the ER [44] and thus on estrogens, which have been shown to be of environmental importance in both sediment [45] and water [46]. In a Canadian lake the collapse of a whole fish population was observed after exposure to low concentrations (5 to 6 ng/L) of the synthetic estrogen 17α-ethynylestradiol, which is used in birth-control pills [46]. However, increasing evidence in environmental research also underlines the importance of androgens and antiandrogens.

The occurrence of this compound class was not only shown in water [47-49] and sediment [50-53] but bioaccumulation also leads to their presence in aquatic biota [34, 47, 54, 55].

Already in 1980 a paper mill was identified as the origin for a masculinization of mosquitofish that was exposed to the androgen-containing effluent [56]. In the meanwhile the androgenic activity of pulp and paper mill effluents was confirmed in mosquitofish by several studies [57, 58]. However, androgens and androgen mimics do not only adversely impact the reproductive health but also the immune system of fish [59]. A variety of xenoandrogens were detected in the aquatic ecosystem, including steroids such as androst-16-en-3-one or nandrolone [60], chlorinated pesticides such as lindane and dichlorodiphenyldichloro-ethylene (DDE) [20] or the fungicide vinclozolin [61].

The presence of antiandrogens at environmental concentrations was correlated to a feminization of non-mammalian vertebrate males [32, 34]. Other studies identified the exposure of antiandrogens to fish populations as the cause for the skewed sex ratio towards females [62, 63]. In the meanwhile several hundreds of man-made chemicals are known to be antiandrogenic active, such as the insecticide isofenphos [64], the disinfectant chloroxylenol [54] or the fungicide dichlorophene [54]. Jobling et al. [32] identified WWTP effluents as an important source of antiandrogen release into English rivers.

The impact of androgenic endocrine disrupting compounds on the wildlife raises concern since strong evidence supports the assumption that wildlife is an important sentinel of human public health [34].

1.2.3 Bioassay supported detection of endocrine disrupting compounds

The increasing awareness on the occurrence of EDCs, including androgens and anti-androgens, in the aquatic environment was particularly supported by the development of bioassays capable to detect endocrine disrupting effects [65]. Today in ecotoxicology a big battery of cellular (*in vitro*) and whole organism (*in vivo*) biotests with numerous different endpoints is accessible [66-68]. The concept of the Adverse Outcome Pathway (AOP) links effects observable in the organ, organism or even whole population level with their underlying causes in the cellular level where gene activation, protein production/depletion or altered signaling can be triggered by molecular initiating events, e.g. receptor/ligand interactions [69]. Biotests for all these levels of the AOP are available.

In vitro bioassays are very popular for the detection and risk assessment of compounds exhibiting a biological activity due to their unique properties: They are sensitive, cheaper and ethically favored compared to whole organism tests and they can be included into high-throughput screening approaches [70-72]. Chemically activated luciferase expression (CALUX) reporter-gene assays have been found to be very sensitive and specific in vitro biosensors of environmental pollutants [73]. They are based on genetically modified cells. Upstream of a receptor fragment, the genomic DNA of receptor-mediated reporter cells is transfected with a reporter gene, e.g. with the firefly luciferase protein, which has luminescence properties [74]. Ligands enter the cell and bind specifically to receptors, which subsequently are translocated to the cell nucleus. There, the ligand-receptor complex binds to specific responsive elements on the DNA to induce the expression of the introduced firefly luciferase gene [65]. The addition of D-luciferin results in an oxygen-dependent bioluminescent reaction and thus light emission at 560 nm [75]. The magnitude of bioluminescence can directly be translated into the extent of the examined effect. Besides agonistic aciticity like estrogenicity or androgenicity, also antagonistic activity, e.g. antiestrogenicity or antiandrogenicity, can be measured if competing endogenous ligands are added [67]. CALUX assays are not only capable to detect endocrine disruptors by their affinity to the ER, AR, progesterone or glucocorticoid receptor [73], but they can also identify genotoxicants [76] or oxidative stressors [76] by non-receptor mediated pathways. These assays are based on the U2OS cell line which is derived from the human osteoblastic osteosarcoma. Thus the predictive value of these *in vitro* assays may be even higher compared to animal models [77].

However, the translation of *in vitro* toxicity into meaningful *in vivo* effects remains challenging [78]. Thus animal tests may provide important data to support or reject first results obtained by the ethically favored *in vitro* and *in silico* methods. Today, in line with this, animal tests are rather used to verify but not to identify toxicity. Sometimes extreme differences between *in vitro* and *in vivo* effects of chemicals are caused by toxicodynamic effects influencing the bioavailabilty of a compound or by toxicokinetic effects such as metabolism and cellular defense mechanisms based on different enzymes [78, 79].

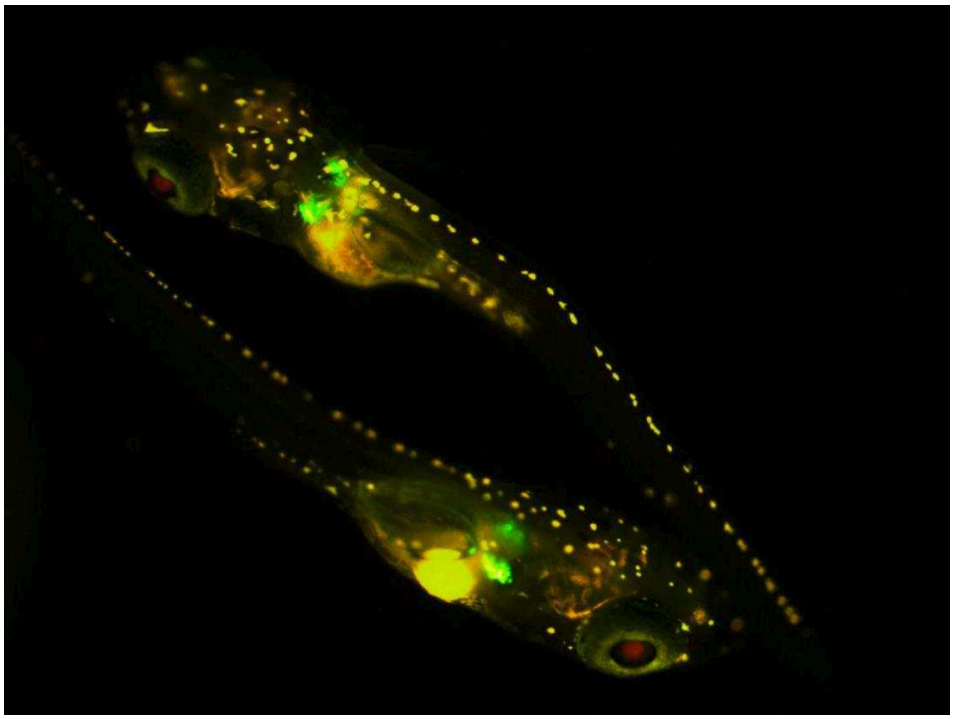

Figure 1-1 Rapid Androgen Disruption Adverse outcome Reporter (RADAR) assay using spiggin-gfp medaka. GFP is formed in consequence of androgen exposure. Image was provided by Andrew J. Tindall, WatchFrog, France.

Various promising *in vivo* assays using fish embryos or larvae are established to tackle ecotoxicological questions within the aquatic environment [80-83]. The spiggin promoter, which is activated by elevated concentrations of androgens, is a well-known response element in the genome of the three-spined stickleback (*Gasterosteus aculeatus*). Sebillot et al. transfected wild-type medaka (*Oryzias latipes*) with the green fluorescent protein (GFP) gene and introduced the spiggin promoter upstream to obtain a rapid, receptor mediated *in vivo* test capable to detect androgens and antiandrogens (Figure 1-1) [83]. The amount of GFP production and thus the magnitude of fluorescence directly correlates with the magnitude of the androgenic effect. Comparable with the luminescent oxyluciferin, that is formed in the reaction of luciferin and luciferase in the CALUX assay, GFP possess an extreme high quantum yield of 88% supporting the assays sensitivity [75].

The development of an immense variety of different *in vitro* and *in vivo* biosensors led to the frequent detection of androgenicity [52, 84, 85] and antiandrogeniciy [86, 87] in the aquatic ecosystem. However, the detection of biological activity alone does not suffice to identify effect causing compounds. Thus, chemical analysis of biological active samples is inevitable for structure elucidation. An approach that offers the necessary linkage between biological activity and chemical analysis is effect-directed analysis (EDA).

1.3 Effect-directed Analysis

Environmental samples are usually containing thousands of compounds with diverse modes of action [88]. The key to identify the most harmful compounds that are driving the toxicity in such a complex mixture is the linkage between the observed effect and the chemical data. A powerful tool to achieve this goal is effect-directed analysis (EDA) [67, 89] if the effect of a sample is caused either by a dominant effect driver or by a mixture of a small number of toxicants, which can be isolated within a limited number of fractions [90]. An overview about the classical scheme of EDA is shown in Figure 1-2. In a first step, the complexity of an environmental sample exhibiting a biological activity is reduced by fractionation. This is typically achieved by liquid chromatography (LC), either in normal or reversed separation mode. The resulting fractions are tested for the relevant endpoint, e.g. androgenicity or estrogenicity, and only the biological active fractions are further fractionated. This separation might be performed in repeated cycles unless the complexity of the sample is essentially reduced. Finally, the active fraction is subjected to chemical analysis in order to identify the toxicant(s).

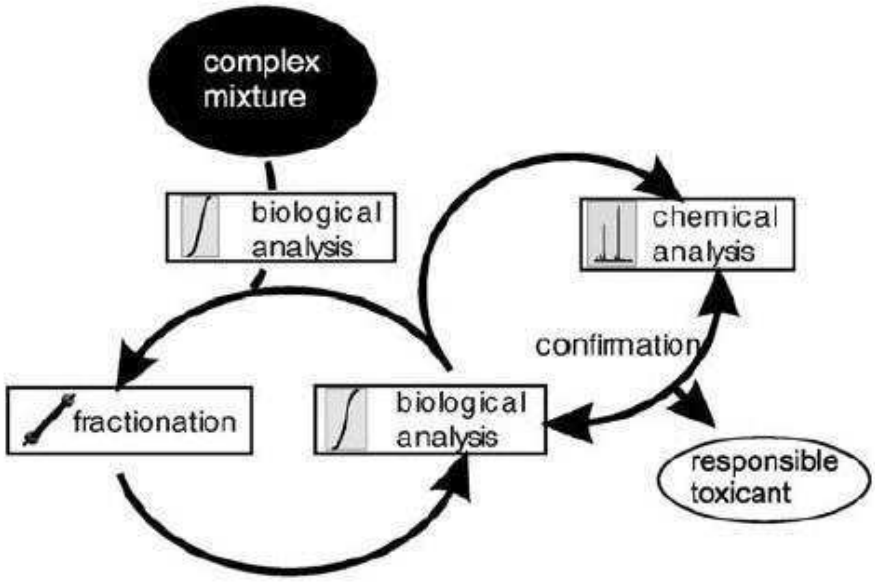

Figure 1-2 Classical Work Flow in EDA [89].

EDA was applied in a variety of environmental compartments, including water [91], sediment [92], biota [93] and air particulate matter [94]. Successful identification of EDCs in the frame of EDA was achieved in the effluent WWTPs [95, 96], in harbor areas [97], in marine sediment [98], in biota [54, 99] and in European river sediment [60]. Antiandrogens have

been identified in North Sea offshore produced water discharges [100], river water [101], sediment [51, 60], fish bile [54] or in tissue of high trophic level animals like the Baikal Seal [102]. Also androgens have been identified in sediment by EDA [60].

Since effect drivers are often unknown, tedious suspect or even non-target screening cannot be circumvented by the more straight forward target analysis. Nowadays, chemical screening is essentially supported by the recent development of high resolution-high mass accuracy mass spectrometers (HRMS) that are routinely coupled to LC in EDA [103-106]. HRMS enables to derive the molecular formula of unknown compounds from their accurate mass and isotope patterns [107]. However, the identification of analytes remains extremely challenging due to a lack of information in LC-MS-databanks [108]. Thus, structure elucidation requires tandem mass spectra (MS/MS) to generate candidate lists that are often containing several thousand of compounds. Candidate selection can be supported by *in silico* fragmentation prediction softwares such as MetFrag [109], which compares measured and predicted fragment patterns. Moreover the prediction of retention time [110] and ionization behavior [111] or the consideration of hydrogen-deuterium exchange [112] and pH-dependent retention time shifts [91] were successfully applied tools to reduce the number of candidates in order to increase the chance of compound identification. A tailor made fractionation approach can help to essentially reduce the number of non-target peaks that need to be evaluated within the chemical analysis.

1.3.1 Fractionation: Generall Considerations

The success of each EDA is essentially influenced by the fractionation and thus by the separation power of the LC, which is mostly the method of choice to achieve a substantial reduction of complexity in the sample of concern. The separation power of a stationary phase can be expressed by the peak capacity (P). It represents the maximum number of theoretically separable analytes [113]. The separation power of a chromatographic system can be enhanced by shallow gradients for the elution [114], by the application of longer columns [115] or by the use of stationary phases with extreme small particle diameter. All these approaches have their inherent drawbacks concerning increasing separation time or backpressure.

The application of two [116, 117] or even more columns [118] for the fractionation of complex samples using the multidimensional liquid chromatography (MDLC) is an alternative

approach to gain separation performance. The peak capacity of a two-dimensional (2D) separation system P_{2D} is defined as the product of the peak capacities of the two coupled separation dimensions [119]:

$$P_{2D} = P_1 P_2 \quad (1)$$

According to equation 1 a 2D systems consisting of two separation dimensions, each characterized by a peak capacity of 100, results in a theoretical P_{2D} of 10.000 [120], thus underlining the potential of such an approach. Nevertheless, this peak capacity is usually not obtained in the praxis, i.e. as a result of back-mixing after compound eluting from the first separation dimension (^{1}D) [118, 121], solvent incompatibility of ^{1}D and second separation dimension (^{2}D) [118, 122], due to sample loss during the transfer of the analytes between the separation dimensions and due to the unavailability of fully orthogonal columns. Orthogonal columns are possessing different separation selectivity and thus statistically unrelated retention of the mixture components [123]. The separation dimensions are frequently coupled online rather than offline to support the reproducibility, to decrease the analysis time and to minimize the risk of compound loss during sample transfer [124]. However, the harmonization of timescales of ^{1}D sampling and ^{2}D separation is a major challenge of MDLC [116, 121, 125] and may be achieved by i.e. the use of multiple parallel columns in the ^{2}D [125], stop and go approaches [124], high ^{2}D flow rates [126] and separation temperatures [127]. Nevertheless, all these approaches are hardly compatible with typically time-consuming biotests, resulting in the application of offline MDLC within the frame of EDA despite the risk of sample loss [105].

Different separation principles were already applied in EDA for fractionation, including not only normal phase (NPC) [128-130], ion-exchange (IEC) [105], size exclusion (SEC) [131] and reverse phase chromatography (RPC) [54, 91] but also affinity-based separation techniques [132]. RPC is frequently applied due to its better reproducibility compared to NPC or IEC [127] and its suitability to separate rather polar, water soluble chemicals since methanol/acetonitril - water mixtures are used as the mobile phase. Furthermore a huge amount of more than 400 reversed phases is available [133], most of them being silica based octadecyl phases [134]. Examples of different stationary phases are given in Figure 1-3.

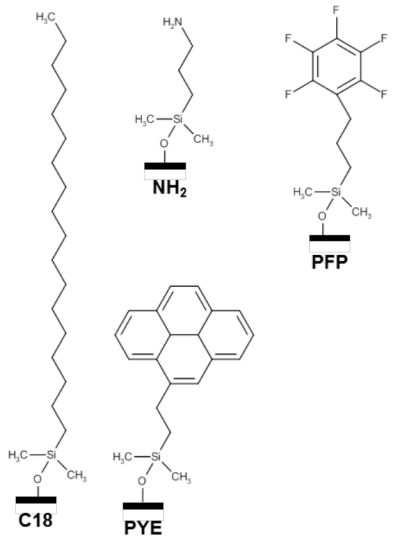

Figure 1-3 Structures of conventional octadecyl (C18), pyrenyl ethyl (PYE), aminopropyl (NH_2) and pentafluorophenyl (PFP) silica phases.

It is important to note that the driving force of retention in RP mode is always non-specific, hydrophobic interactions [65, 126]. Hence the selection of orthogonal RP phases is extremely challenging. Differences in selectivity are the result of specific interactions of the stationary phases with the solutes including polar and ionic interactions and hydrogen bonds.

1.3.2 Fractionation: Selection of RP Phases

There is no agreement on a standard procedure for column selection in the literature. Two frequently used generic methods to determine the selectivity of a chromatographic separation are the hydrophobic subtraction model [135] and the Tanaka protocol [136-139]. In the HSM the selectivity α of stationary phases is characterized by five selectivity parameters including hydrophobic interaction, shape selectivity, hydrogen-bond acidity and basicity and cation-exchange activity [135]. According to the Tanaka protocol retention factors for specific indicator compounds serve as a measure of for instance shape selectivity or ion-exchange capacity (Table 1). In other words, the selection of columns via the TANAKA approach and the HSM-Model is based on the evaluation of retention of an analyte on different columns as a result of certain structural properties, e.g. molecular shape or presence of hydrogen-bond donators.

Table 1 Variables[1] used in Tanaka-Protocol [136].

Tanaka-Variables	Reflected property of the RP phase	Calculation
Retentionsfactor of pentylbenzene (PBz), k_{PB}	The surface area and the surface coverage / ligand density	$k_{PBz} = \frac{t_R - t_0}{t_0}$
Hydrophobicity or hydrophobic selectivity, α_{CH2}	Measure of surface coverage / ligand density	$\alpha_{CH2} = k_{PB} / k_{BB}$
Shape selectivity, $\alpha_{T/O}$	Shape selectivity	$\alpha_{T/O} = k_T / k_O$
Hydrogen bonding capacity, $\alpha_{C/P}$	Number of free silanol groups of the silica	$\alpha_{C/P} = k_C / k_{Pl}$
Ion-exchange capacity at pH 7,6, $\alpha_{B/P}$	Basic ion-exchange capacity	$\alpha_{B/P} = k_B / k_{Pl}$
Ion-exchange capacity at pH 2,7, $\alpha_{B/P}$	Acidic ion-exchange capacity	$\alpha_{B/P} = k_B / k_{Pl}$

Alternatively a promising approach of column selection for the efficient separation of certain compound classes like EDCs might follow a rigorous experimental evaluation of the retention data of a representative mixture of these analytes. Various statistical methods useful for this approach are available in the literature [113, 140-142]. The common principle is the evaluating of the peak distribution within a 2D separation space to measure the degree of orthogonality between two columns. The degree of orthogonality is rising with increasing peak distribution.

According to Gilar et al. [113] the degree of random distribution of analytes within the 2D separation space and thus the degree of orthogonality of any 2D-LC separation system can be described by a simple geometric approach. The 2D separation space is divided into a number of rectangular bins that is equal to the number of data points (i.e, analytes). The degree of orthogonality increased with rising number of occupied bins. Camenzuli and Schoenmakers [140] introduced four lines (Z_-, Z_+, Z_1 and Z_2) crossing the separation space, as

[1] PB: Pentylbenzene; BB: Butylbenzene; T: Triphenylene; O: o-Terphenyl; C: Caffein; Pl: Phenol; B: Benzylamin
t_R: Retentionszeit; t_0: dead time

shown in Figure 1-4. The spread of analytes around these lines increases with a better distribution of analytes within the 2D separation space. The spread around the Z1 is affected by the separation of analytes within the first separation dimension and that one of Z2 by the second dimension while the lines Z_- and Z_+ are influenced by both dimensions. The standard deviation of the distances of the analytes to these lines is calculated to retrieve an A_0 value that is considered as a measure of orthogonality.

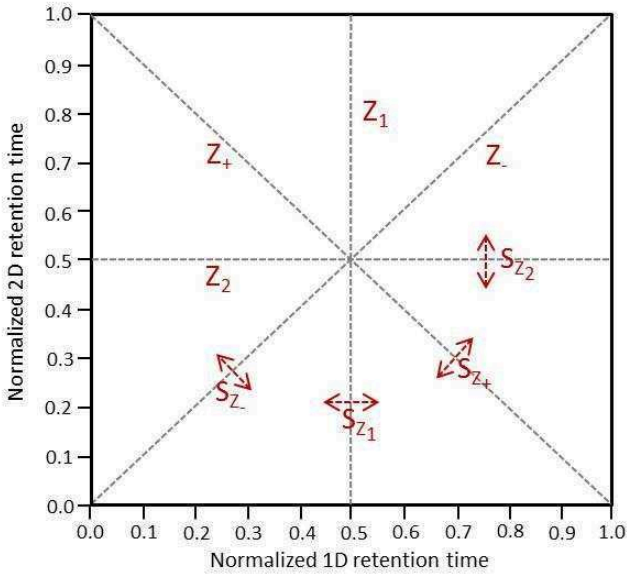

Figure 1-4 Calculation of orthogonality and the spread of peaks by the Asterisk approach.

1.4 Objectives

WWTP effluents are highly complex mixtures of at least hundreds of chemicals [143, 144] with different modes of action. Consequently, antiandrogenic activity is frequently detected in the aquatic environment [86, 87]. Despite a large list of known antiandrogens [145], in many cases only a minor fraction of the activity of an environmental sample can be explained with known androgen axis disruptors. EDA is a valuable tool to identify "unknowns" that are causing adverse effects [95, 96]. However, classical EDA with one-dimensional fractionation may not always be sufficient to reduce the complexity to a degree that allows for the identification of effect drivers. Thus, in the present PhD thesis a multidimensional fractionation approach for EDA of mixtures exhibiting endocrine disrupting activity should be developed and its efficiency demonstrated at a sample taken at a hotspot of antiandrogenicity in the central European river Holtemme. Finally, it was aimed to study the fate of the identified endocrine disruptors within the aquatic ecosystem.

In order to tackle this objective, in **Chapter 2,** a novel fractionation approach was developed for water samples containing EDC by employing a set of reversed phase columns with a focus on androgens and antiandrogens. From a set of 17 columns with widely differing bond chemistries those four stationary phases exhibiting the highest degree of orthogonality for the separation of a representative set of 39 EDCs were selected. The suitability of the method to achieve a significant reduction in the complexity of HRMS data in order to facilitate the compound identification has been examined. For this purpose, the whole non-target peak inventory of an antiandrogenic active river water extract fractionated with the four selected columns was evaluated.

In **Chapter 3**, the successfully established fractionation approach was applied in the frame of an EDA study in combination with a parallel developed, due to sample scarcity miniaturized luciferase reporter gene cell-based anti-AR-CALUX assay. Additionally, state-of-the-art LC-HRMS/MS non-target techniques including *in silico* fragmentation prediction, pH-dependent LC retention time shift and hydrogen-deuterium exchange to unravel the identity of unknown effect drivers were used. Finally the high endocrine disrupting potential of the identified "unknowns" was confirmed *in vivo* in spiggin-gfp Medaka.

In **Chapter 4**, the temporal and spatial distribution of the identified antiandrogens along the whole river stretch was investigated by a retrospective analysis of LC-HRMS/MS data to identify their source and the extent of pollution of the Holtemme. Moreover, their

transformation and distribution in the aquatic ecosystem between water, sediment and biota was analyzed applying equilibrium partitioning theory. Finally, partition coefficients between water and sediment were determined experimentally and compared with estimates based on hydrophobicity to gain insights into the unexpected driving force of sorption to sediment.

Finally, **Chapter 5** provides an overview of all results, a detailed discussion of the findings and addresses potential future research questions.

Chapter 3 is published in the international peer-reviewed journal Environmental Science & Technology. Chapter 1 will be submitted to the international peer-reviewed Journal of Separation Science and Chapter 4 to the international peer-reviewed journal Environmental Pollution.

The appendix provides detailed information on sample extraction, fractionation, biotest results, chemical analysis, data evaluation, spectra of identified compounds and a list containing 385 known or suspected antiandrogens.

1.5 Literature

1. Steffen, W., et al., *Planetary boundaries: Guiding human development on a changing planet.* Science, 2015. **347**(6223).
2. Rockstrom, J., et al., *A safe operating space for humanity.* Nature, 2009. **461**(7263): p. 472-475.
3. McGowan, P.J., *Conservation: Mapping the terrestrial human footprint.* Nature, 2016. **537**: p. 172-173.
4. Vitousek, P.M., et al., *Human Domination of Earth's Ecosystems.* Science, 1997. **277**(5325): p. 494-499.
5. Barnosky, A.D., et al., *Approaching a state shift in Earth/'s biosphere.* Nature, 2012. **486**(7401): p. 52-58.
6. Doney, S.C., et al., *Ocean Acidification: The Other CO2 Problem.* Annual Review of Marine Science, 2009. **1**(1): p. 169-192.
7. Cardinale, M., *Fishery reform: many stocks secure.* Nature, 2011. **476**(7360): p. 282-282.
8. Pimm, S.L., et al., *The Future of Biodiversity.* Science, 1995. **269**(5222): p. 347-350.
9. Barnosky, A.D., et al., *Has the Earth/'s sixth mass extinction already arrived?* Nature, 2011. **471**(7336): p. 51-57.
10. Merino, J.G., et al., *Standing up for science in the era of Trump.* BMJ, 2017. **356**.
11. Dakos, V., et al., *Slowing down as an early warning signal for abrupt climate change.* Proceedings of the National Academy of Sciences, 2008. **105**(38): p. 14308-14312.
12. Scheffer, M., et al., *Anticipating Critical Transitions.* Science, 2012. **338**(6105): p. 344-348.
13. Giger, W., *The Rhine red, the fish dead—the 1986 Schweizerhalle disaster, a retrospect and long-term impact assessment.* Environmental Science and Pollution Research, 2009. **16**(1): p. 98-111.
14. Schirmer, K. and M. Schirmer, *Who is chasing whom? A call for a more integrated approach to reduce the load of micro-pollutants in the environment.* Water Science and Technology, 2008. **57**(1): p. 145-150.
15. Hartung, T. and C. Rovida, *Chemical regulators have overreached.* Nature, 2009. **460**(7259): p. 1080-1081.
16. Kuzmanović, M., et al., *Risk assessment based prioritization of 200 organic micropollutants in 4 Iberian rivers.* Science of The Total Environment, 2015. **503**: p. 289-299.
17. Merel, S. and S.A. Snyder, *Critical assessment of the ubiquitous occurrence and fate of the insect repellent N,N-diethyl-m-toluamide in water.* Environment International, 2016. **96**: p. 98-117.
18. Ritter, K.S.P.S.K.H.P.K.G.M.B.L.L., *SOURCES, PATHWAYS, AND RELATIVE RISKS OF CONTAMINANTS IN SURFACE WATER AND GROUNDWATER: A PERSPECTIVE PREPARED FOR THE WALKERTON INQUIRY.* Journal of Toxicology and Environmental Health, Part A, 2002. **65**(1): p. 1-142.
19. Li, W.C., *Occurrence, sources, and fate of pharmaceuticals in aquatic environment and soil.* Environmental Pollution, 2014. **187**: p. 193-201.
20. Sumpter, J.P., *Endocrine Disrupters in the Aquatic Environment: An Overview.* Acta hydrochimica et hydrobiologica, 2005. **33**(1): p. 9-16.

21. Jones, O.A., J.N. Lester, and N. Voulvoulis, *Pharmaceuticals: a threat to drinking water?* Trends in Biotechnology, 2005. **23**(4): p. 163-167.
22. Zühlke, S., U. Dünnbier, and T. Heberer, *Detection and identification of phenazone-type drugs and their microbial metabolites in ground and drinking water applying solid-phase extraction and gas chromatography with mass spectrometric detection.* Journal of Chromatography A, 2004. **1050**(2): p. 201-209.
23. Reddersen, K., T. Heberer, and U. Dünnbier, *Identification and significance of phenazone drugs and their metabolites in ground- and drinking water.* Chemosphere, 2002. **49**(6): p. 539-544.
24. Riemenschneider, C., et al., *Pharmaceuticals, Their Metabolites, and Other Polar Pollutants in Field-Grown Vegetables Irrigated with Treated Municipal Wastewater.* Journal of Agricultural and Food Chemistry, 2016. **64**(29): p. 5784-5792.
25. Macherius, A., et al., *Uptake of Galaxolide, Tonalide, and Triclosan by Carrot, Barley, and Meadow Fescue Plants.* Journal of Agricultural and Food Chemistry, 2012. **60**(32): p. 7785-7791.
26. Wu, C., et al., *Transfer of wastewater associated pharmaceuticals and personal care products to crop plants from biosolids treated soil.* Ecotoxicology and Environmental Safety, 2012. **85**: p. 104-109.
27. Kelly, B.C., *Food web-specific biomagnification of persistent organic pollutants (vol 317, pg 236, 2007).* Science, 2007. **318**: p. 44-44.
28. Schwarzenbach, R.P., et al., *Global Water Pollution and Human Health*, in *Annual Review of Environment and Resources, Vol 35*. 2010. p. 109-136.
29. Brack, W., et al., *Towards the review of the European Union Water Framework Directive: Recommendations for more efficient assessment and management of chemical contamination in European surface water resources.* Science of The Total Environment, 2017. **576**: p. 720-737.
30. Malaj, E., et al., *Organic chemicals jeopardize the health of freshwater ecosystems on the continental scale.* Proceedings of the National Academy of Sciences, 2014. **111**(26): p. 9549-9554.
31. Söffker, M. and C.R. Tyler, *Endocrine disrupting chemicals and sexual behaviors in fish – a critical review on effects and possible consequences.* Critical Reviews in Toxicology, 2012. **42**(8): p. 653-668.
32. Jobling, S., Burn, R.W., Thorpe, K., Williams, R., Tyler, C., *Statistical modeling suggests that antiandrogens in effluents from wastewater treatment works contribute to widespread sexual disruption in fish living in English rivers.* Environmental Health Perspectives, 2009. **117**(5): p. 797-802.
33. Blaber, S.J.M., *THE OCCURRENCE OF A PENIS-LIKE OUTGROWTH BEHIND THE RIGHT TENTACLE IN SPENT FEMALES OF NUCELLA LAPILLUS (L.).* Journal of Molluscan Studies, 1970. **39**(2-3): p. 231-233.
34. Milnes, M.R., et al., *Contaminant-induced feminization and demasculinization of nonmammalian vertebrate males in aquatic environments.* Environmental Research, 2006. **100**(1): p. 3-17.
35. EuropeanEnvironmentAgency, *European workshop on the impact of endocrine disruptors on human health and wildlife*. 2–4 December 1996, Weybridge, UK. Report of the Proceedings. Report EU 17549., European Commission DG XII, Copenhagen.
36. Diamanti-Kandarakis, E., et al., *Endocrine-Disrupting Chemicals: An Endocrine Society Scientific Statement.* Endocrine Reviews, 2009. **30**(4): p. 293-342.

37. Colborn, T., F.S. vom Saal, and A.M. Soto, *Developmental effects of endocrine-disrupting chemicals in wildlife and humans.* Environmental Health Perspectives, 1993. **101**(5): p. 378-384.
38. Kortenkamp, A., *Ten Years of Mixing Cocktails: A Review of Combination Effects of Endocrine-Disrupting Chemicals.* Environmental Health Perspectives, 2007. **115**(Suppl 1): p. 98-105.
39. Sheehan, D.M., et al., *No threshold dose for estradiol-induced sex reversal of turtle embryos: how little is too much?* Environmental Health Perspectives, 1999. **107**(2): p. 155-159.
40. Rajapakse, N., E. Silva, and A. Kortenkamp, *Combining xenoestrogens at levels below individual no-observed-effect concentrations dramatically enhances steroid hormone action.* Environmental Health Perspectives, 2002. **110**(9): p. 917-921.
41. Anway, M.D. and M.K. Skinner, *Epigenetic Transgenerational Actions of Endocrine Disruptors.* Endocrinology, 2006. **147**(6): p. s43-s49.
42. Sweeney, M.F., et al., *Environmental Endocrine Disruptors: Effects on the human male reproductive system.* Reviews in endocrine & metabolic disorders, 2015. **16**(4): p. 341-357.
43. Kelce, W.R., et al., *Persistent DDT metabolite p,p'–DDE is a potent androgen receptor antagonist.* Nature, 1995. **375**(6532): p. 581-585.
44. Gore, A.C., et al., *Executive Summary to EDC-2: The Endocrine Society's Second Scientific Statement on Endocrine-Disrupting Chemicals.* Endocrine Reviews, 2015. **36**(6): p. 593-602.
45. Grund, S., et al., *The endocrine disrupting potential of sediments from the Upper Danube River (Germany) as revealed by in vitro bioassays and chemical analysis.* Environmental Science and Pollution Research, 2011. **18**(3): p. 446-460.
46. Kidd, K.A., et al., *Collapse of a fish population after exposure to a synthetic estrogen.* Proceedings of the National Academy of Sciences, 2007. **104**(21): p. 8897-8901.
47. Hill, E.M., et al., *Profiles and Some Initial Identifications of (Anti)Androgenic Compounds in Fish Exposed to Wastewater Treatment Works Effluents.* Environmental Science & Technology, 2010. **44**(3): p. 1137-1143.
48. Soto, A.M., et al., *Androgenic and estrogenic activity in water bodies receiving cattle feedlot effluent in Eastern Nebraska, USA.* Environmental Health Perspectives, 2004. **112**(3): p. 346-352.
49. Grover, D.P., et al., *Endocrine disrupting activities in sewage effluent and river water determined by chemical analysis and in vitro assay in the context of granular activated carbon upgrade.* Chemosphere, 2011. **84**(10): p. 1512-1520.
50. Urbatzka, R., et al., *Androgenic and antiandrogenic activities in water and sediment samples from the river Lambro, Italy, detected by yeast androgen screen and chemical analyses.* Chemosphere, 2007. **67**(6): p. 1080-1087.
51. Weiss, J.M., et al., *Masking effect of anti-androgens on androgenic activity in European river sediment unveiled by effect-directed analysis.* Analytical and Bioanalytical Chemistry, 2009. **394**: p. 1385-1397.
52. Kinani, S., et al., *Bioanalytical characterisation of multiple endocrine- and dioxin-like activities in sediments from reference and impacted small rivers.* Environmental Pollution, 2010. **158**(1): p. 74-83.

53. Schmitt, C., et al., *In vivo effect confirmation of anti-androgenic compounds in sediment contact tests with Potamopyrgus antipodarum.* Journal of Environmental Science and Health, Part A, 2013. **48**(5): p. 475-480.
54. Rostkowski, P., et al., *Bioassay-Directed Identification of Novel Antiandrogenic Compounds in Bile of Fish Exposed to Wastewater Effluents.* Environmental Science & Technology, 2011. **45**(24): p. 10660-10667.
55. Katsiadaki, I., et al., *Field surveys reveal the presence of anti-androgens in an effluent-receiving river using stickleback-specific biomarkers.* Aquatic Toxicology, 2012. **122–123**: p. 75-85.
56. Howell, W.M., D.A. Black, and S.A. Bortone, *Abnormal Expression of Secondary Sex Characters in a Population of Mosquitofish, Gambusia affinis holbrooki: Evidence for Environmentally-Induced Masculinization.* Copeia, 1980. **1980**(4): p. 676-681.
57. Ellis, R.J., et al., *In vivo and in vitro assessment of the androgenic potential of a pulp and paper mill effluent.* Environmental Toxicology and Chemistry, 2003. **22**(7): p. 1448-1456.
58. Drysdale, D.T. and S.A. Bortone, *Laboratory induction of intersexuality in the mosquitofish,Gambusia affinis, using paper mill effluent.* Bulletin of Environmental Contamination and Toxicology, 1989. **43**(4): p. 611-617.
59. Milla, S., S. Depiereux, and P. Kestemont, *The effects of estrogenic and androgenic endocrine disruptors on the immune system of fish: a review.* Ecotoxicology, 2011. **20**(2): p. 305-319.
60. Weiss, J., et al., *Identification strategy for unknown pollutants using high-resolution mass spectrometry: Androgen-disrupting compounds identified through effect-directed analysis.* Analytical and Bioanalytical Chemistry, 2011. **400**(9): p. 3141-3149.
61. Kiparissis, Y., et al., *Effects of the antiandrogens, vinclozolin and cyproterone acetate on gonadal development in the Japanese medaka (Oryzias latipes).* Aquatic Toxicology, 2003. **63**(4): p. 391-403.
62. Bayley, M., M. Junge, and E. Baatrup, *Exposure of juvenile guppies to three antiandrogens causes demasculinization and a reduced sperm count in adult males.* Aquatic Toxicology, 2002. **56**(4): p. 227-239.
63. Lor, Y., et al., *Juvenile exposure to vinclozolin shifts sex ratios and impairs reproductive capacity of zebrafish.* Reproductive Toxicology, 2015. **58**: p. 111-118.
64. Kojima, H., et al., *Screening for estrogen and androgen receptor activities in 200 pesticides by in vitro reporter gene assays using Chinese hamster ovary cells.* Environmental Health Perspectives, 2004. **112**(5): p. 524-531.
65. Brack, W., *Effect-Directed Analysis of Complex Environmental Contamination*. The Handbook of Environmental Chemistry, ed. D. Barcelo and A.G. Kostianoy. Vol. 15. 2011, Berlin Heidelberg: Springer.
66. Wernersson, A.-S., et al., *The European technical report on aquatic effect-based monitoring tools under the water framework directive.* Environmental Sciences Europe, 2015. **27**(1): p. 7.
67. Brack, W., et al., *Effect-directed analysis supporting monitoring of aquatic environments — An in-depth overview.* Science of The Total Environment, 2016. **544**: p. 1073-1118.
68. Connon, R.E., J. Geist, and I. Werner, *Effect-Based Tools for Monitoring and Predicting the Ecotoxicological Effects of Chemicals in the Aquatic Environment.* Sensors, 2012. **12**(9): p. 12741.

69. Ankley, G.T., et al., *Adverse outcome pathways: A conceptual framework to support ecotoxicology research and risk assessment.* Environmental Toxicology and Chemistry, 2010. **29**(3): p. 730-741.
70. Froment, J., K.V. Thomas, and K.E. Tollefsen, *Automated high-throughput in vitro screening of the acetylcholine esterase inhibiting potential of environmental samples, mixtures and single compounds.* Ecotoxicology and Environmental Safety, 2016. **130**(Supplement C): p. 74-80.
71. Nagy, S.R., et al., *Identification of Novel Ah Receptor Agonists Using a High-Throughput Green Fluorescent Protein-Based Recombinant Cell Bioassay.* Biochemistry, 2002. **41**(3): p. 861-868.
72. Yueh, M.-F., M. Kawahara, and J. Raucy, *Cell-based high-throughput bioassays to assess induction and inhibition of CYP1A enzymes.* Toxicology in Vitro, 2005. **19**(2): p. 275-287.
73. van der Linden, S.C., et al., *Detection of Multiple Hormonal Activities in Wastewater Effluents and Surface Water, Using a Panel of Steroid Receptor CALUX Bioassays.* Environmental Science & Technology, 2008. **42**(15): p. 5814-5820.
74. Sonneveld, E., et al., *Development of Androgen- and Estrogen-Responsive Bioassays, Members of a Panel of Human Cell Line-Based Highly Selective Steroid-Responsive Bioassays.* Toxicological Sciences, 2005. **83**(1): p. 136-148.
75. Köhler, S., S. Belkin, and R.D. Schmid, *Reporter gene bioassays in environmental analysis.* Fresenius' Journal of Analytical Chemistry, 2000. **366**(6): p. 769-779.
76. van der Linden, S.C., et al., *Development of a panel of high-throughput reporter-gene assays to detect genotoxicity and oxidative stress.* Mutation Research/Genetic Toxicology and Environmental Mutagenesis, 2014. **760**: p. 23-32.
77. van der Burg, B., et al., *Optimization and prevalidation of the in vitro AR CALUX method to test androgenic and antiandrogenic activity of compounds.* Reproductive Toxicology, 2010. **30**(1): p. 18-24.
78. McKim Jr, J.M., *Building a Tiered Approach to In Vitro Predictive Toxicity Screening: A Focus on Assays with In Vivo Relevance.* Combinatorial Chemistry & High Throughput Screening, 2010. **13**(2): p. 188-206.
79. Escher, B. and F. Leusch, *Bioanalytical tools in water quality assessment*. 2012: IWA Publishing, London, UK. 253.
80. Fini, J.-B., et al., *An In Vivo Multiwell-Based Fluorescent Screen for Monitoring Vertebrate Thyroid Hormone Disruption.* Environmental Science & Technology, 2007. **41**(16): p. 5908-5914.
81. Lee, O., J.M. Green, and C.R. Tyler, *Transgenic fish systems and their application in ecotoxicology.* Critical Reviews in Toxicology, 2015. **45**(2): p. 124-141.
82. Brion, F., et al., *Screening Estrogenic Activities of Chemicals or Mixtures In Vivo Using Transgenic (cyp19a1b-GFP) Zebrafish Embryos.* PLOS ONE, 2012. **7**(5): p. e36069.
83. Sébillot, A., et al., *Rapid Fluorescent Detection of (Anti)androgens with spiggin-gfp Medaka.* Environmental Science & Technology, 2014. **48**(18): p. 10919-10928.
84. Parks, L.G., et al., *Masculinization of Female Mosquitofish in Kraft Mill Effluent-Contaminated Fenholloway River Water Is Associated with Androgen Receptor Agonist Activity.* Toxicological Sciences, 2001. **62**(2): p. 257-267.
85. Bandelj, E., et al., *Determination of the androgenic potency of whole effluents using mosquitofish and trout bioassays.* Aquatic Toxicology, 2006. **80**(3): p. 237-248.

86. Stalter, D., et al., *Ozonation and activated carbon treatment of sewage effluents: Removal of endocrine activity and cytotoxicity.* Water Research, 2011. **45**(3): p. 1015-1024.
87. Sousa, A., et al., *Chemical and Biological Characterization of Estrogenicity in Effluents from WWTPs in Ria de Aveiro (NW Portugal).* Archives of Environmental Contamination and Toxicology, 2010. **58**(1): p. 1-8.
88. Busch, W., et al., *Micropollutants in European rivers: A mode of action survey to support the development of effect-based tools for water monitoring.* Environmental Toxicology and Chemistry, 2016. **35**(8): p. 1887-1899.
89. Brack, W., *Effect-directed analysis: a promising tool for the identification of organic toxicants in complex mixtures.* Analytical and Bioanalytical Chemistry, 2003. **377**: p. 397-407.
90. Brack, W., *Effect-directed analysis: a promising tool for the identification of organic toxicants in complex mixtures?* Analytical and Bioanalytical Chemistry, 2003. **377**(3): p. 397-407.
91. Muz, M., et al., *Mutagenicity in Surface Waters: Synergistic Effects of Carboline Alkaloids and Aromatic Amines.* Environmental Science and Technology, 2017. **51**(3): p. 1830-1839.
92. Biselli, S., et al., *Bioassay-directed fractionation of organic extracts of marine surface sediments from the North and Baltic Sea. Part I: Determination and identification of organic pollutants.* Journal of Soils and Sediments, 2005. **5**: p. 171-181.
93. Simon, E., et al., *Challenges in effect-directed analysis with a focus on biological samples.* TrAC Trends in Analytical Chemistry, 2015. **67**(0): p. 179-191.
94. Durant, J. and A. Lafleur, *Effect-Directed Analysis of Mutagens in Ambient Airborne Particles*, in *Effect-Directed Analysis of Complex Environmental Contamination*, W. Brack, Editor. 2011, Springer Berlin Heidelberg. p. 199-235.
95. Grung, M., et al., *Effect-directed analysis of organic toxicants in wastewater effluent from Zagreb, Croatia.* Chemosphere, 2007. **67**(1): p. 108-120.
96. Thomas, K.V., et al., *An assessment of in vitro androgenic activity and the identification of environmental androgens in United Kingdom estuaries.* Environmental Toxicology and Chemistry, 2002. **21**: p. 1456-1461.
97. Houtman, C.J., et al., *Estrogenic and dioxin-like compounds in sediment from Zierikzee harbour identified with CALUX assay-directed fractionation combined with one and two dimensional gas chromatography analyses.* Chemosphere, 2006. **65**: p. 2244-2252.
98. Grote, M., W. Brack, and R. Altenburger, *Identification of toxicants from marine sediment using effect-directed analysis.* Environmental Toxicology, 2005. **20**: p. 475-486.
99. Houtman, C.J., et al., *Identification of estrogenic compounds in fish bile using bioassay-directed fractionation.* Environmental Science and Technology, 2004. **38**: p. 6415-6423.
100. Thomas, K.V., et al., *Effect-Directed Identification of Naphthenic Acids As Important in Vitro Xeno-Estrogens and Anti-Androgens in North Sea Offshore Produced Water Discharges.* Environmental Science & Technology, 2009. **43**(21): p. 8066-8071.
101. Liscio, C., et al., *Methodology for profiling anti-androgen mixtures in river water using multiple passive samplers and bioassay-directed analyses.* Water Research, 2014. **57**: p. 258-269.

102. Suzuki, G., et al., *Identification of Major Dioxin-Like Compounds and Androgen Receptor Antagonist in Acid-Treated Tissue Extracts of High Trophic-Level Animals.* Environmental Science & Technology, 2011. **45**(23): p. 10203-10211.
103. Zaja, R., et al., *Identification of P-Glycoprotein Inhibitors in Contaminated Freshwater Sediments.* Environmental Science & Technology, 2013. **47**(9): p. 4813-4821.
104. Wagner, M., et al., *Identification of Putative Steroid Receptor Antagonists in Bottled Water: Combining Bioassays and High-Resolution Mass Spectrometry.* PLoS ONE, 2013. **8**(8): p. e72472.
105. Gallampois, C.M.J., et al., *Integrated biological–chemical approach for the isolation and selection of polyaromatic mutagens in surface waters.* Analytical and Bioanalytical Chemistry, 2013. **405**(28): p. 9101-9112.
106. Hug, C., et al., *Metabolic transformation as a diagnostic tool for the selection of candidate promutagens in effect-directed analysis.* Environmental Pollution, 2015. **196**(Supplement C): p. 114-124.
107. Krauss, M., *Chapter 15 - High-Resolution Mass Spectrometry in the Effect-Directed Analysis of Water Resources*. 2016: Comprehensive Analytical Chemistry. Elsevier.
108. Brack, W., et al., *How to confirm identified toxicants in effect-directed analysis.* Anal.Bioanal.Chem., 2008. **390**: p. 1959-1973.
109. Ruttkies, C., et al., *MetFrag relaunched: incorporating strategies beyond in silico fragmentation.* Journal of Cheminformatics, 2016. **8**(1): p. 3.
110. Ulrich, N., G. Schüürmann, and W. Brack, *Linear Solvation Energy Relationships as classifiers in non-target analysis—A capillary liquid chromatography approach.* Journal of Chromatography A, 2011. **1218**(45): p. 8192-8196.
111. Gallampois, C.M.J., et al., *Multicriteria Approach To Select Polyaromatic River Mutagen Candidates.* Environmental Science & Technology, 2015. **49**(5): p. 2959-2968.
112. Liu, D.Q., et al., *On-line H/D exchange LC–MS strategy for structural elucidation of pharmaceutical impurities.* Journal of Pharmaceutical and Biomedical Analysis, 2007. **44**(2): p. 320-329.
113. Gilar, M., et al., *Orthogonality of Separation in Two-Dimensional Liquid Chromatography.* Analytical Chemistry, 2005. **77**(19): p. 6426-6434.
114. Gilar, M., et al., *Implications of column peak capacity on the separation of complex peptide mixtures in single- and two-dimensional high-performance liquid chromatography.* Journal of Chromatography A, 2004. **1061**(2): p. 183-192.
115. Sandra, K., et al., *Highly efficient peptide separations in proteomics: Part 1. Unidimensional high performance liquid chromatography.* Journal of Chromatography B, 2008. **866**(1–2): p. 48-63.
116. F. Cacciola, P.J., Z. Hajdu´, P C˘esla, L. Mondello, *Comprehensive two-dimensional liquid chromatography with parallel gradients for separation of phenolic and flavone antioxidants.* Journal of Chromatography A, 2007. **1149**: p. 73-87.
117. Serban Moldoveanu, V.D., *Essentials in Modern HPLC Separations*. 2012, Waltham, USA: Elsevier Verlag.
118. Simpkins, S.W., et al., *Targeted three-dimensional liquid chromatography: A versatile tool for quantitative trace analysis in complex matrices.* Journal of Chromatography A, 2010. **1217**(49): p. 7648-7660.
119. Giddings, J.C., *Two-dimensional separations: concept and promise.* Analytical Chemistry, 1984. **56**(12): p. 1258A-1270A.

120. Sandra, K., et al., *Highly efficient peptide separations in proteomics: Part 2: Bi- and multidimensional liquid-based separation techniques.* Journal of Chromatography B, 2009. **877**(11–12): p. 1019-1039.
121. Groskreutz, S.R., et al., *Selective comprehensive multi-dimensional separation for resolution enhancement in high performance liquid chromatography. Part I: Principles and instrumentation.* Journal of Chromatography A, 2012. **1228**(0): p. 31-40.
122. Dugo, P., et al., *Comprehensive Two-Dimensional Normal-Phase (Adsorption)−Reversed-Phase Liquid Chromatography.* Analytical Chemistry, 2004. **76**(9): p. 2525-2530.
123. Allen, R.C., et al., *Impact of reversed phase column pairs in comprehensive two-dimensional liquid chromatography.* Journal of Chromatography A, 2014. **1361**(0): p. 169-177.
124. Fairchild, J.N., K. Horváth, and G. Guiochon, *Approaches to comprehensive multidimensional liquid chromatography systems.* Journal of Chromatography A, 2009. **1216**(9): p. 1363-1371.
125. Fairchild, J.N., K. Horváth, and G. Guiochon, *Theoretical advantages and drawbacks of on-line, multidimensional liquid chromatography using multiple columns operated in parallel.* Journal of Chromatography A, 2009. **1216**(34): p. 6210-6217.
126. Jandera, P., *Programmed elution in comprehensive two-dimensional liquid chromatography.* Journal of Chromatography A, 2012. **1255**(0): p. 112-129.
127. Stoll, D.R., et al., *Fast, comprehensive two-dimensional liquid chromatography.* Journal of Chromatography A, 2007. **1168**(1): p. 3-43.
128. Zebühr, Y., et al., *An Automated HPLC Separation Method with two Coupled Columns for the Analysis of PCDD/Fs, PCBs and PACs.* Chemosphere, 1993. **27**: p. 1211-1219.
129. Lübcke-von Varel, U., G. Streck, and W. Brack, *Automated fractionation procedure for polycyclic aromatic compounds in sediment extracts on three coupled normal-phase high-performance liquid chromatography columns.* Journal of Chromatography A, 2008. **1185**(1): p. 31-42.
130. Thomas, K.V., et al., *Identification of in vitro estrogen and androgen receptor agonists in North Sea offshore produced water discharges.* Environmental Toxicology and Chemistry, 2004. **23**: p. 1156-1163.
131. Brack, W., et al., *A sequential fractionation procedure for the identification of potentially cytochrome P4501A-inducing compounds.* Journal of Chromatography A, 2003. **986**: p. 55-66.
132. Jonker, N., et al., *Online Magnetic Bead Dynamic Protein-Affinity Selection Coupled to LC−MS for the Screening of Pharmacologically Active Compounds.* Analytical Chemistry, 2009. **81**(11): p. 4263-4270.
133. Vitha, M. and P.W. Carr, *The chemical interpretation and practice of linear solvation energy relationships in chromatography.* Journal of Chromatography A, 2006. **1126**(1–2): p. 143-194.
134. Layne, J., *Characterization and comparison of the chromatographic performance of conventional, polar-embedded, and polar-endcapped reversed-phase liquid chromatography stationary phases.* Journal of Chromatography A, 2002. **957**(2): p. 149-164.
135. Snyder, L.R., J.W. Dolan, and P.W. Carr, *The hydrophobic-subtraction model of reversed-phase column selectivity.* Journal of Chromatography A, 2004. **1060**(1-2): p. 77-116.

136. Euerby, M.R. and P. Petersson, *Chromatographic classification and comparison of commercially available reversed-phase liquid chromatographic columns using principal component analysis.* Journal of Chromatography A, 2003. **994**(1-2): p. 13-36.
137. Euerby, M.R., et al., *Chromatographic classification and comparison of commercially available reversed-phase liquid chromatographic columns containing phenyl moieties using principal component analysis.* Journal of Chromatography A, 2007. **1154**(1-2): p. 138-151.
138. Euerby, M.R., A.P. McKeown, and P. Petersson, *Chromatographic classification and comparison of commercially available perfluorinated stationary phases for reversed-phase liquid chromatography using Principal Component Analysis.* Journal of Separation Science, 2003. **26**(3-4): p. 295-306.
139. Euerby, M.R. and P. Petersson, *Chromatographic classification and comparison of commercially available reversed-phase liquid chromatographic columns containing polar embedded groups/amino endcappings using principal component analysis.* Journal of Chromatography A, 2005. **1088**(1-2): p. 1-15.
140. Camenzuli, M. and P.J. Schoenmakers, *A new measure of orthogonality for multi-dimensional chromatography.* Analytica Chimica Acta, 2014. **838**(Supplement C): p. 93-101.
141. Pellett, J., et al., *"Orthogonal" separations for reversed-phase liquid chromatography.* Journal of Chromatography A, 2006. **1101**(1): p. 122-135.
142. Leonhardt, J., et al., *A new method for the determination of peak distribution across a two-dimensional separation space for the identification of optimal column combinations.* Analytical and Bioanalytical Chemistry, 2016. **408**(28): p. 8079-8088.
143. Munz, N.A., et al., *Pesticides drive risk of micropollutants in wastewater-impacted streams during low flow conditions.* Water Research, 2017. **110**: p. 366-377.
144. Beckers, L.-M., et al., *Characterization and risk assessment of seasonal and weather dynamics in organic pollutant mixtures from discharge of a separate sewer system.* Water Research, 2018. **135**: p. 122-133.
145. Muschket, M., et al., *Identification of Unknown Antiandrogenic Compounds in Surface Waters by Effect-Directed Analysis (EDA) Using a Parallel Fractionation Approach.* Environmental Science & Technology, 2018. **52**(1): p. 288-297.

Chapter 2

LC fractionation on a set of reversed phase columns improves the detection of endocrine disruptors in LC-HRMS screening of surface water extracts

Abstract

Liquid chromatography (LC) coupled to high-resolution mass spectrometry (HRMS) is a powerful tool for the chemical screening of complex environmental mixtures containing potentially harmful micropollutants including endocrine disrupting compounds (EDCs). However, the automated detection of peaks by automated algorithms is challenged by many co-eluting isobaric compounds resulting in “humps” rather than individual peaks, particularly for steroidal EDCs. Thus, we evaluated possible improvements in compound separation and thus peak detection of EDCs by fractionation of complex samples on combinations of different reversed-phase columns. To identify orthogonal stationary phases, retention times of 39 endocrine disruptors separated on 17 different columns were determined and statistically evaluated using principal component analysis and Spearman rank correlation. Based on this evaluation, an octadecyl-, pyrenyl ethyl, aminopropyl and perfluorohexyl modified silica phase were selected for an orthogonal separation. The high degree of orthogonality of these columns was confirmed for the whole non-target peak inventory of a river water extract stemming from automated peak detection. An essential improvement of the separation of co-eluting isobaric compounds resulted in a 4.8-fold increase of the number of detected peaks after fractionation. Hence the application of the proposed column set for fractionation helps to facilitate compound detection and identification in LC-HRMS target and non-target screening.

2.1 Introduction

The contamination of freshwater systems with potentially toxic chemical compounds poses a risk to water resources for human consumption and for aquatic ecosystems on a global scale [1]. Currently about 100,000 organic chemicals are in daily use and are partially released into freshwater ecosystems [2] resulting in environmental mixtures of thousands of chemicals [3] such as personal care products, pharmaceuticals [4], pesticides and biocides. Quite a few of these are endocrine disrupting chemicals (EDCs) that may cause adverse effects to aquatic organisms [5-8] or human health [9].

To characterize these complex mixtures, LC-HRMS has emerged as a powerful technique over the last decade, and different strategies have been developed based on this technique [10]. In target screening, compounds are identified based on available reference standards and thus known retention times, full scan mass spectra and diagnostic MS/MS fragments if possible. A (semi-)quantification is commonly also done [11-13].

Suspect screening starts from known compounds, suspected to occur in the samples considered, but without the availability of a reference standard. Based on molecular formulas, exact masses and isotope patterns can be calculated considering the type of ionization or adduct formation and the ion peaks can be searched in the HRMS data. Whether a found peak originates from the particular suspect has to be further substantiated using additional information (e.g., plausible or predicted retention time and MS/MS spectra).

In contrast to these approaches, non-target screening does not require any pre-selection of compounds, but solely relies on the analytical data. The first step is typically the detection of individual peaks from the raw HRMS data, for which a range of software algorithms are available (e.g., MZmine [14] or xcms [15]). Finally, peak lists (containing m/z, retention time, peak intensity and/or area) are obtained. It should also be noted that the detection of target and suspect compounds can be done by two approaches, (i) by extracting ion chromatograms for each individual suspect ion mass or (ii) from a search of matching ions in the peak list. A benefit of the latter approach is that it is faster to perform (integrating target and suspect screening into non-target screening). Due to the high selectivity of modern HRMS instruments with resolving powers in the range of 30,000 to >200,000, extracted ion chromatograms often show a very low background, and peak detection algorithms allow for a detection of low-intensity peaks as well.

However, for quite a few compounds, still noisy baselines and many overlapping peaks are observed, mainly due to the presence of co-eluting isobaric compounds. Although in target screening these problems can be partly mitigated by using high resolution tandem mass spectrometry, this is no option for suspect or non-target screening. These unresolved humps occur particularly for compounds composed of C, H, and O only. These are prevalent in water samples with high matrix load, suggesting that humic or fulvic acids and maybe other biomolecules of natural origins such as fatty acids are the source of this "matrix background". Unfortunately, many potent EDCs are affected by this problem, such as steroid estrogens (beta-estradiol, estrone), androgens (testosterone, dihydrotestosterone) and gestagens (progesterone). Figure A1 in the Electronic Supplementary Materials shows some contrasting examples ("zero baseline vs. unresolved humps") for a set of known EDCs.

To facilitate the detection in target, suspect and non-target screening and subsequent identification of such compounds, a reduction of complexity is required. A fractionation of the extract is a promising option for this task. Fractionation of water extracts is regularly used in the context of effect-directed analysis, where biologically active compounds are isolated in one or several fractionation – biotesting sequences until a chemical identification of the simplified mixture in a fraction becomes feasible [3]. For this purpose extracts are fractionated with normal or reversed phase liquid chromatography (NPLC/RPLC), mostly with single stationary phases [16-20]. In a few cases a sequence of fractionation steps with different stationary phases was used for a sufficient reduction of complexity [21]. A reduction of sample complexity can also be achieved by comprehensive two-dimensional LC (2D-LC), which is an online coupling based on the same underlying idea. Despite a lot of progress in recent years, 2D-LC has only hardly been used for screening analysis of water samples [22-24].

To achieve a good separation in two dimensions (either offline or online) the selection of reversed phases with an orthogonal selectivity and thus statistically independent retention of mixture components [25] is important. Full orthogonality might be not achievable in RPLC, as it is primarily driven by the solutes' hydrophobicity [26]. Differences in selectivity are the result of specific interactions of the solutes with the stationary phases including hydrogen bonds, polar and ionic interactions. Two frequently used generic methods to determine the selectivity of chromatographic separations are the hydrophobic subtraction model (HSM) [27] and the Tanaka protocol [28-31]. However, such generic approaches to describe

differences in separation selectivity of various stationary phases do not always guarantee for optimal orthogonality for a specific set of compounds. For example, no separation power will be gained if the measured difference in selectivity of two columns is based to a large extent on hydrogen bond acidity, but the compounds of interests have no hydrogen bond acceptor functions [32]. Thus, we consider it more promising to select orthogonal chromatographic systems according to the compound groups of interest in an experimental evaluation.

Thus, the objective of this study was to identify orthogonal RPLC columns for the separation of endocrine disrupting compounds to facilitate their detection and identification in LC-HRMS screening methods and EDA studies. To this end, we separated a mixture of 39 known EDCs with a wide range of physicochemical properties on 17 different RP columns with widely differing chemistry. Two different statistical methods for identifying orthogonal combinations of columns were compared.

To demonstrate the improvement of non-target peak detection after fractionation, a wastewater-impacted surface water extract was separated using the four most promising columns and the obtained fractions were analysed by LC-HRMS along with the raw extract. Here we did not aim to identify unknown compounds, but to verify the column orthogonality using the whole non-target peak inventory.

2.2 Material and Methods

2.2.1 Chemicals

A set of 39 EDCs covering a broad variety of chemicals structures and a wide hydrophobicity rage (log K_{OW} 1.6-6.5) were selected. These compounds were dexamethasone, 17β-trenbolone, norethindrone, androsterone, epi-androsterone, dihydrotestosterone, testosterone, levonorgestrel, medroxyprogesterone, 17α-estradiol, 17β-estradiol, isopimaric acid, abietic acid, estriol, progesterone, hydrocortisone, bisphenol S, isoeugenol, 2-naphthol, 2,2´-dihydroxybiphenyl, genistein, propylparaben, 3-hydroxybiphenyl, benzophenone-3, 1-hydroxypyrene, zearalenone, procymidone, N-benzylphthalimide, carbaryl, propanil, tris-(1-chloro-2-propyl)phosphate, linuron, metolachlor, flutamide, flavone, methylparathion, fenthion, triphenylphosphate and benzylbutylphthalate. A mixture of all compounds at 1 µg/mL was prepared in methanol. The structures, CAS number, log K_{OW} values (calculated with EPI Suite Version 1.68), biological activity and the literature reference are shown in Table A1. Compounds were obtained from Sigma-Aldrich, Dr. Ehrenstorfer, Sigma-Aldrich, Acros, Biomol, Campro, Chiron, SAFC, Alfa Aesar, Roth, Cambridge Isotope Laboratories and Merck at a purity of >98% in almost all cases. LC-MS grade methanol, formic acid and water were obtained from Sigma-Aldrich.

2.2.2 LC columns and MS/MS analysis

Retention times of all compounds were determined on 17 different RP stationary phases with widely differing functional groups (Table 2-1). These phases include three octadecyl-, one diol, two nitrophenyl, one pyrenyl ethyl, one cyanopropyl, one phenylhexyl, one perfluorohexyl, two pentafluorophenyl, one pentabromobenzyl and two aminopropyl silica phases, one polymeric aminopropyl phase and one octadecyl silica column containing a polar embedded group.

For the determination of retention times a HPLC system (Agilent 1260 Infinity) coupled to a tandem mass spectrometer (QTrap 6500, AB Sciex) with an electrospray ionization (ESI) source, all controlled by the Analyst software (version 1.6.2) were used. For details see section A1.1. The injection volume of the standard mixture containing 1 µg/mL of all compounds was 10 µL. The mobile phase consisted of 0.1% formic acid in water (Eluent A) and 0.1% of formic acid in methanol (Eluent B). The gradient elution programs and flow rates were optimized for each column to achieve sufficient retention for all compounds and are shown in Table A2. Separate runs were conducted with single compound standards to distinguish isobaric compounds.

Table 2-1 Columns applied for development of an orthogonal, parallel fractionation approach.

#	Column name	Abbreviation	Supplier	Functionalisation	Specification	Dimension and particle size	Dimension and particle size pre-column
1	Nucleosil 100-5 OH	OH (#1)	Macherey-Nagel	Diol	porous silica	150 x 4.0 mm, 5 µm	3 x 4.0 mm, 5 µm
2	Nucleodur C18 Gravity	C18 (#2)	Macherey-Nagel	Octadecyl	porous silica	250 x 4.0 mm; 5 µm	-
3	Kinetex C18	C18 (#3)	Phenomenex	Octadecyl	core shell silica	100 x 3.0 mm, 2.6 µm	10 x 3.0 mm, 2.6 µm
4	Zorbax Eclipse PAH	PAH (#4)	Agilent	Octadecyl	porous silica	250 x 4.6 mm; 5 µm	12.5 x 4.6 mm, 5 µm
5	Nucleosil 100-5 NO2	NO2 (#5)	Macherey-Nagel	Nitrophenyl	porous silica	250 x 4.0 mm, 5 µm	-
6	Cosmosil NPE	NPE (#6)	Phenomenex	Nitrophenyl	porous silica	250 x 4.6 mm, 5 µm	-
7	Asahipak NH2	NH2 (#7)	Shodex	Aminopropyl	polymer based	150 x 4.6 mm, 5 µm	10 x 4.6 mm, 5 µm
8	Luna NH2	NH2 (#8)	Phenomenex	Aminopropyl	porous silica	150 x 4.6 mm, 5 µm	10 x 4.6 mm, 5 µm
9	Unison NH2	NH2 (#9)	Imtakt	Aminopropyl	porous silica	150 x 4.6 mm, 3 µm	10 x 4.6 mm, 3 µm
10	Cosmosil PYE	PYE (#10)	Nacalai Tesque	Pyrenyl ethyl	porous silica	150 x 4.6 mm, 5 µm	20 x 4.6 mm; 5 µm
11	LiChroCART CN	CN (#11)	Merck	Cyanopropyl	porous silica	125 x 4.0 mm, 5 µm	-
12	Accucore PH	PH (#12)	Thermo Fisher	Phenylhexyl	porous silica	100 x 3.0 mm, 2.6 µm	10 x 3.0 mm, 2.6 µm
13	Fluophase RP	PFH (#13)	Thermo Fisher	Perfluorohexyl	porous silica	150 x 4.6 mm, 5 µm	-
14	Accucore PFP	PFP (#14)	Thermo Fisher	Pentafluorophenyl	core shell silica	150 x 2.1 mm, 2.6 µm	10 x 2.1 mm, 2.6 µm
15	Hypersil Gold PFP	PFP (#15)	Thermo Fisher	Pentafluorophenyl	porous silica	150 x 3.0 mm, 5 µm	-
16	Cosmosil 5PBB-R	PBB (#16)	Nacalai Tesque	Pentabromobenzyl	porous silica	150 x 4.6 mm, 5 µm	-
17	Polaris Amide	N-PEG (#17)	Varian	Embedded amide, octadecyl	porous silica	150 x 4.6 mm, 5 µm	10 x 4.6 mm, 5 µm

2.2.3 Retention data evaluation for column selection

A range of methods have been published to assess the orthogonality of liquid chromatographic separations without an agreement on a standardized procedure [33-37]. In this study the column selection was based on the measure of orthogonality between all pairs of columns by principal component analysis (PCA) and Spearman rank correlation (SRC).
The retention times of the standard mixture (Table A6) separated on the set of 17 columns were normalized according to equation 1:

$$RT_{i(norm)} = \frac{RT_i - RT_{min}}{RT_{max} - RT_{min}} \qquad \text{(eq. 2-1)}$$

where $RT_{i(norm)}$ denotes the normalized retention time of compound i and RT_i its retention time. RT_{min} denotes the retention time of the first and RT_{max} of the last eluting compound [33]. Histograms of the retention data distribution of the standard compounds on each column are shown in Figure A2.

2.2.4 Spearman rank correlation (SRC)

The degree of orthogonality using the Pearson correlation coefficient of a two-dimensional retention time plot has been already applied earlier [25, 34, 38]. We used, however, SRC since the retention data of the 39 standard compounds did not always follow a normal distribution (Figure A3).

2.2.5 Principal component analysis (PCA)

A PCA of the retention data was conducted in R (Version 3.3.2) using the package `psych` Version 1.7.5 [39] to obtain the correlation matrix. SRC was applied. The principal components could not be assumed as independent and thus an oblique-angled rotation with the package `GPArotation` Version 2014.11.1 [40] was conducted and the corresponding loading plot generated.

2.2.6 Sampling and extraction of surface water

The sampling site was located in the small river Holtemme, 1.3 km downstream of the wastewater treatment plant of Silstedt (60,000 person equivalents), Saxony-Anhalt, Germany. The water sample was taken in a 5 L aluminium container, the extraction procedure is described in detail in Hug et al. [41]. In brief, the pH was adjusted to 6.5, the sample was filtered by a glass fibre filter and extracted using a multi-layer cartridge similar to the one described in Huntscha et al. [42] containing in the upper layer Chromabond HR-X (Macherey Nagel) and in the lower layer a mixture of Isolute ENV+ (Biotage), Chromabond HR-XAW and Chromabond HR-XCW. After elution, sample extract was evaporated and finally adjusted to a concentration factor of 1000 in methanol.

2.2.7 Orthogonal fractionation of surface water

Fractionation was performed on four orthogonal stationary phases selected based on the previously described procedure. For the octadecyl- (#2), aminopropyl- (#9) and pentafluorophenyl-modified silica phase (#15) semi-preparative columns (Table A3) were used after upscaling. To this end, on each column 500 µL of the water sample extract (CF 700, 20% MeOH in H_2O) were used. For the pyrenyl ethyl-modified silica phase PYE (#10) the same analytical scale column was used and four times 50 µL extract aliquots (EF = 875, 15% MeOH in H_2O) were separated and the same fractions of each run combined.

The sample extract was injected by a Rheodyne manual valve. A Varian Prostar 210 pump was operating at a flow rate of 2.8 mL min^{-1} for semi-preparative and at 0.8 mL min^{-1} for analytical scale columns. We used 0.1% formic acid (eluent A) and 0.1% formic acid in methanol (eluent B) as mobile phases. Chromatograms were recorded with a Dionex UVD 340U UV/VIS detector at a wavelength of 210 nm. One minute fractions were collected with a Foxy 2000 fraction collector (Teledyne Isco Inc., Lincoln, USA). The software Chromeleon 6.7 (Dionex) was used for instrument control. The fractions were combined according to peak clusters in the UV-Vis chromatogram. Details on the collected fractions and the gradient programs are shown in section A1.2.

For solvent exchange in fractions, water was added to reach a maximum content of 10 vol.-% of methanol. The diluted fractions were frozen at -80°C and freeze dried in an Alpha 2-4 LSG device (Martin Christ, Osterode, Germany). The dried fractions were redissolved in 0.35 mL

of methanol (i.e., CF 1000). A blank sample for each column was prepared by the same fractionation and solvent exchange procedure, but without sample injection.

2.2.8 LC-HRMS analysis of the fractionated river water extract

For LC separation of the fractionated river water extract, an Ultimate 3000 LC system with a Kinetex EVO C18 column (50 x 2.1 mm, 2.6 µm with pre-column 10 x 2.1 mm, Phenomenex) was used at 40°C. Compounds were eluted in a gradient of 0.1% formic acid (Eluent A) and methanol with 0.1% formic acid (Eluent B). The injection volume was 5 µL. The high performance liquid chromatography system was coupled to a Q-Exactive Plus HRMS instrument (Thermo). Full scan spectra in the mass range of m/z 100-1500 were obtained by ESI in positive ionization mode. The nominal resolving power was 140.000 (referenced to m/z 200). Details of the gradient elution program, eluents and mass spectrometric parameters are given in **section A1.3**.

2.2.9 Evaluation of LC-HRMS data

The HRMS raw files were converted to mzML format by ProteoWizard [43]. Subsequently, non-target peaks were detected using MZmine 2.26 [44]. Resulting peak lists include the accurate mass, retention time, height and area of the detected peaks. The peak lists of all fractions were aligned and exported as csv files. For more detailed information of the MZmine workflow and settings see section A1.4.

Evaluation of HRMS peak lists was conducted in RStudio Version 0.98.501. Non-target peaks with a sample-to-blank intensity ratio <10 and an area-to-height ratio >100 (i.e., those stemming from background noise and not resembling Lorentzian peak shapes, see [45]) were removed.

2.3 Results and Discussion

2.3.1 Selection of orthogonal columns

2.3.1.1 Spearman Rank Correlation

Figure 2-1 shows the SRC coefficients for all 136 possible column pairs. For most combinations the correlation coefficients were >0.8, indicating a low orthogonality. This is also illustrated in Figure A3 showing retention time plots for pairs of the C18 column (#2) and all other 16 columns. In contrast, the three aminopropyl phases #7, #8 or #9 showed close correlations with each other, but weak correlations (<0.6 in any case) with any other column (Figure 2-1). Also relatively low correlation coefficients of on average 0.52 were obtained for all combinations with the PYE column (#10).

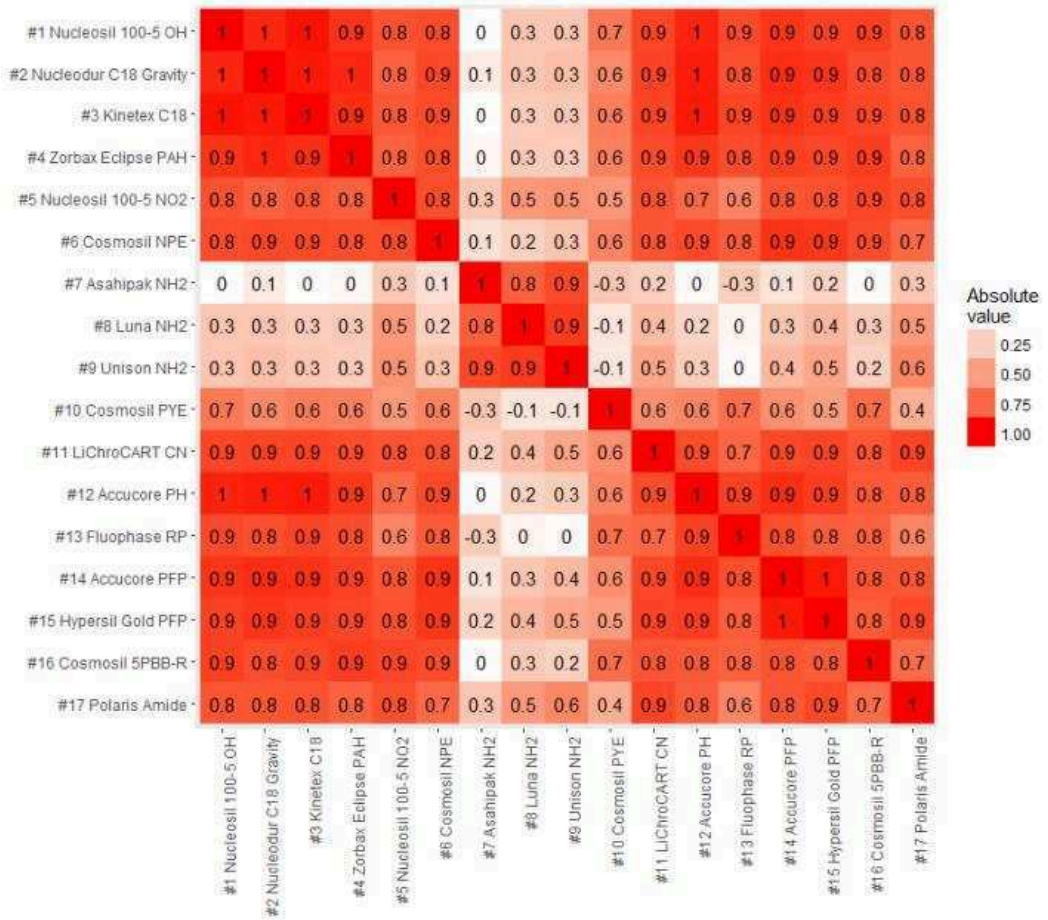

Figure 2-1 Spearman correlation matrix of retention times of the standard mixture compounds on the tested columns. Colors are displayed according to the absolute values of the corresponding correlation.

2.3.1.2 Principal component analysis

The evaluation of retention data by PCA was based on two principal components (PCs) explaining the majority (88%) of the variance within the retention data.

Each vector in the resulting loading plot (Figure 2-2) represents one column and three distinct groups are visible. An angle of 90° between two vectors indicates orthogonal selectivity of the corresponding stationary phases. The first group is formed by the aminopropyl silica phases #7, #8, #9 that are loading to a high percentage on PC 2. Under acidic separation conditions (nominal aqueous pH of 2.6) aminopropyl phases are positively charged [46]. Thus electrostatic repulsion or attraction of ionic analytes by Coulomb interactions is obtained and might be represented by PC 2. Moreover, interactions occur between the electron-deficient, protonated ligand acting as an electron acceptor and the electron-rich π-electron ring systems of analytes.

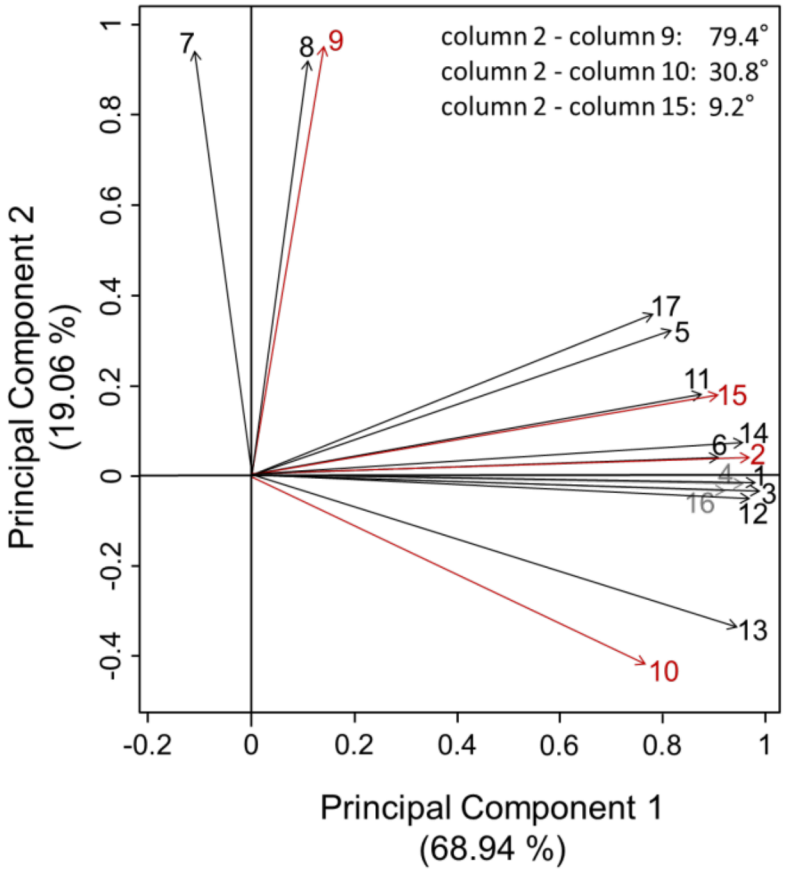

Figure 2-2 Loading plot of the Principal Component Analysis of retention time data from the 17 studied columns. An angle of 90° between two vectors indicates orthogonal selectivity. The angles between the four selected, red marked columns for the final fractionation procedure are displayed.

The group formed by the PYE (#10) and the PFH (#13) columns loads negatively onto PC 2. Hence these phases have specific separation selectivity and display a high degree of orthogonality especially to the three aminopropyl phases. This might be due to their strong ability to act as hydrogen bond acceptors - PYE (#10) with its large aromatic ring system [47] and PFH (#13) with its ligands containing three free electron pairs on each fluorine atom [48]. Valko et al. [49] pointed out that the major difference between different RPC systems is related to their H-bond acceptor properties. Nevertheless, not only the PYE (#10) and the PFH (#13) columns within the set of 17 different stationary phases exhibit H-bond acceptor moieties but also the PH (#12) or PBB (#16) exhibit H-bond acidity but load only slightly negative on PC 2.

The third group, formed by the majority of the tested columns including the octadecyl phases #2 and #3 but also the OH (#1) or PH (#12) highly charge on PC 1 which explains with 69% the majority of variance within the retention data. Thus PC 1 most likely represents hydrophobic interactions which are generally the dominant driver of retention in RPC [26]. All loadings of the columns are given in Table A7.

2.3.1.3 Comparison of the two approaches to determine orthogonality of columns

The evaluation of retention data by SRC and PCA identified the amino propyl phases #7, #8 and #9 and the PYE phase (#10) as those with the highest degree of orthogonality compared to the C18 (#2). Moreover a high degree of different separation selectivity was measured between the aminopropyl phases and the PYE phase (#10) with a SRC between -0.1 and -0.3 (Figure 2-1) and an angle between the corresponding vectors in the PCA plot between 110° and 126°. Only the PCA shows for the PFH (#13) a high degree of orthogonality to C18 (#2). Particularly in the SRC the column group including OH (#1), C18 (#3), PAH (#4) and PH (#12) has the lowest degree of orthogonality if compared to the C18 (#2) phase. Thus the two statistical approaches do not lead to fully consistent results regarding the orthogonality of the examined columns and even regarding the ranking of the columns from low to high degree of orthogonality compared to the C18 (#2). Nevertheless, the degree of orthogonality was high in both approaches for pairs of the NH2 and PYE columns (#7, #8, #9, #10) and C18 (#2).

The chromatogram of the multi-component test compound mixture obtained using the NH2 phase (#9) displayed good peak shapes while the separation on the other two NH2 columns (#7, #8) mostly led to strong peak broadening. Thus, the C18 (#2), the PYE (#10) and the NH2 (#9) were finally selected as orthogonal columns or the fractionation. Additionally the PFP (#15) was selected according to promising results in the literature. It was found to be an effective complement to an octadecyl silica phase for the characterization of sewage treatment plant effluents [22]. Moreover the SRC of 0.5 displayed a rather high degree of orthogonality to NH2 (#9) and PYE (#10). The resulting retention time plots show a high coverage of the 2D separation space confirming the high degree of orthogonality of this set of columns (Figure A4).

2.3.2 Improvement of peak detection for non-target screening after fractionation

Target or non-target screening using HRMS peak detection is massively facilitated if isobaric compounds are separated to prevent unresolved humps in the chromatogram. Additionally the resulting compound specific fragments and distinct retention times of "clean" peaks is supporting the compound identification, especially in non-target screening. Thus, a water sample extract showing antiandrogenic activity was fractionated on a set of columns possessing different selectivity for endocrine disruptors (#2, #9, #10 and #15) to obtain a separation of possibly co-eluting isobaric compounds by at least one column. Chemical analysis of fractions was carried out by LC-HRMS using an analytical scale C18 column followed by automated peak detection in MZmine 2.26.

The absolute number of peaks and the number of common peaks of the water extract and its 114 fractions obtained by chromatographic separation on the four selected columns were determined. In general, a complete recovery of compounds after fractionation cannot be expected due to losses during the fractionation procedure and the following sample treatment including freeze drying. Additionally, a distribution of compounds across more than one fraction will result in lower-intensity peaks, which are not always retrieved by the peak detection algorithm. This is illustrated by an increase of the percentage of common peaks from 66 to 83% if the area cut off value of the peaks in the raw extract is increased from 1×10^5 a.u. to 5×10^7 a.u. (Figure A5), since only high-intensity peaks are detectable after fractionation even in case of a distribution across several fractions. Especially noticeable is the peak broadening, occurring in the separation on the NH2 column (#9). The average number of fractions containing the same analyte is 2.4 for C18 (#2), 2.1 for PFP (#15), 3.7 for PYE (#10) and even 4.4 for NH2 (#9) at an area cut off value of 5×10^6 a.u., indicating the lowest separation power of the latter phase. The following discussion is based on peaks with a minimal peak area of 5×10^6 a.u. in the water extract since no evaluable but for compound identification essential fragment spectra can be expected from smaller peaks after fractionation.

4906 peaks were detected in the water extract before and in average 23,628 in the fractions of the four selected stationary phases after fractionation (Figure 2-3). This 4.8-fold increase of the peak inventory was essentially caused by the desired separation of in the non-

fractionated water extract co-eluting isobars. On average 74% of the 4906 peaks detected in the water extract were also found in the fractions of each stationary phase.

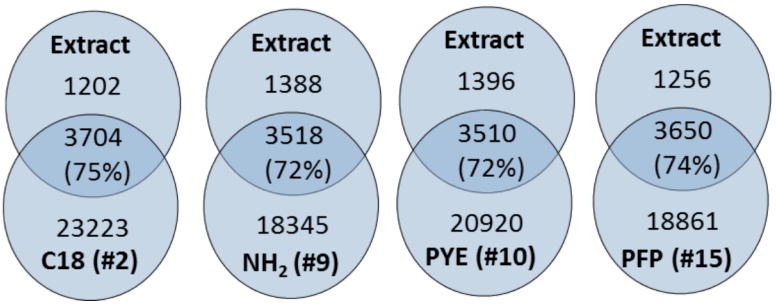

Figure 2-3 Absolute number and number of peaks in common between the raw water extract and all fractions obtained by chromatographic separation of the extract on a C18 (#2), NH2 (#9), PYE (#10) and PFP (#15) phase. Percentage of common peaks refers to the number of peaks of the raw water extract. Cutoff value for the peak area in the non-fractionated water extract was 5×10^6 a.u. and the minimal blank to sample area ratio 10.

The increase of peak numbers after fractionation was not only caused by the better separation of isobaric compounds, but also by a higher number of artefact peaks resulting from improperly picked peaks from the background noise by MZmine, which was indicated for some peaks by their distribution among the fractions. If a compound separates among different fraction during preparative fractionation, it should be detected in the HRMS runs also in consecutive fractions, but not in an early and a late eluting one.

To get an impression of the number of false positives, we examined the distribution of the 23,628 peaks across the fractions (Figure A6, Table A8). A rather random distribution pattern among the different fractions was observed for quite a few peaks. 60% of the peaks were detected in one, 14% in two or three consecutive fractions and 21% in unrelated ones. Automated peak picking is always a compromise between strict settings limiting peak detection to high intensity peaks, losing many of the lower intensity ones, or more “loose” settings to include also smaller and noisier peaks, but with a substantial risk to include also artefacts from background noise [50].

It should be noted, however, that the absence of peaks in one out of a row of consecutive fractions might also be caused by the failure of peak detection if in that fraction an isobaric compound co-elutes, or the peak intensity is suppressed by matrix effects. Thus, employing the presence in consecutive fractions as a prerequisite for the presence of a true compound peak might also result in the erroneous exclusion of compound peaks.

Despite these difficulties, the fractionation resulted in many cases in an improved detection of peaks hidden in a "hump" in the raw extract, as demonstrated for the case of testosterone in Figure 2-4. Its identification within environmental samples is typically hampered by co-eluting compounds. By fractionation on the C18 (#2) column, the broad high-intensity hump for m/z 289.2162 in the raw extract could be partially separated, resulting in several detected individual peaks in the different fractions. Still in all fractions, a smaller background hump is visible besides these clearly distinguishable peaks. Also testosterone could be isolated, picked by MZmine and tentatively identified.

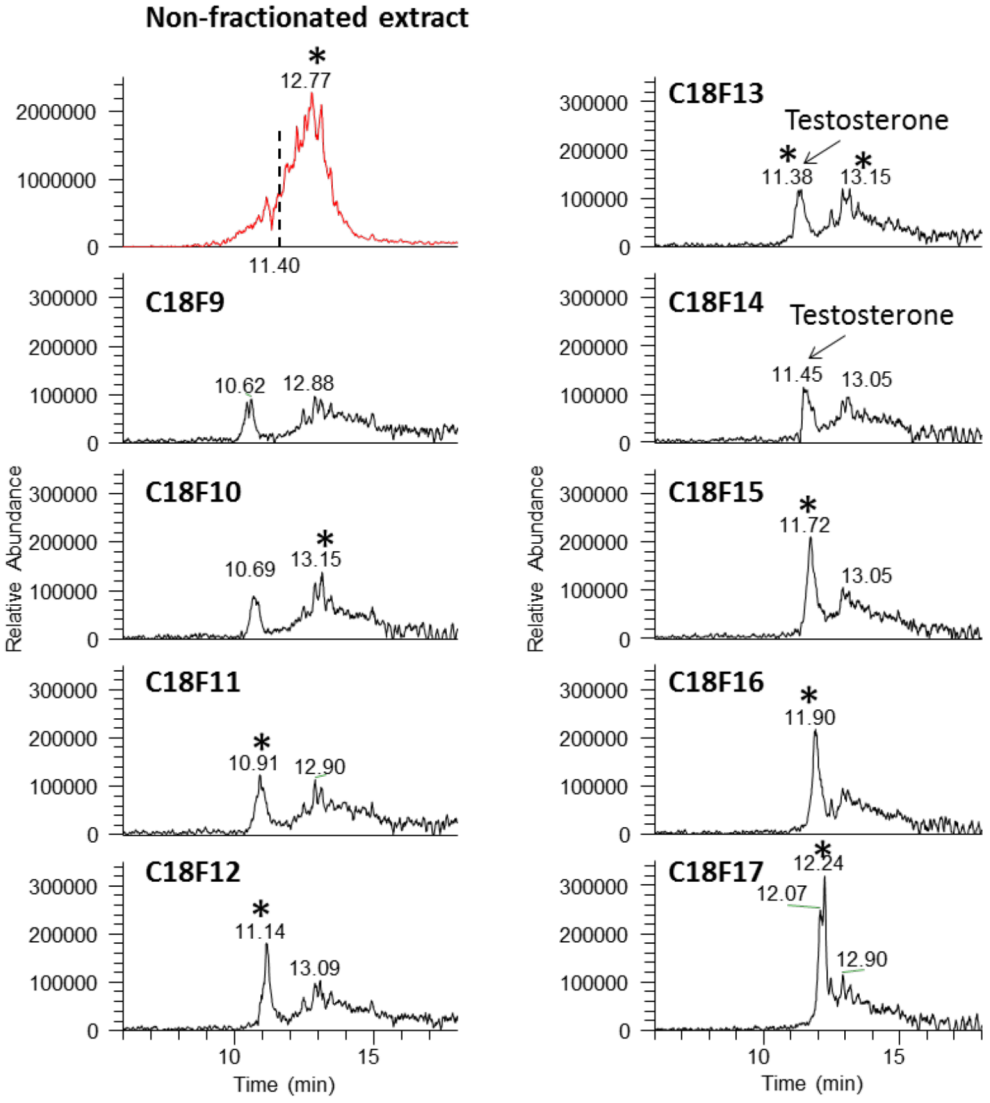

Figure 2-4 Extracted ion chromatograms (XICs) for m/z 289.2162 (at 5ppm mass accuracy) of the raw water extract and some fractions from a fractionation on the C18 (#2) column. Testosterone (Retention time 11.4 minutes) was picked and tentatively identified only after fractionation in fractions C18F13 and C18F14. Peaks picked by MZmine are labelled with an asterisk. Note the different scales for the raw extract and the individual fractions.

Using additionally orthogonal columns increases the probability to obtain a well-separated peak in a fraction of at least one column. This is exemplified for isobars with m/z 207.1379 (Figure A7). A broad, unresolved hump eluting between 6.5 and 12 minutes was separated into less complex mixtures by fractionation. However, various peaks are still co-eluting in the fractions from the C18 column (#2), as seen in C18F3 for the two peaks eluting after 8.82 minutes (Peak #1) and 8.99 minutes (Peak #2). Peak #1 was also co-eluting with isobaric compounds in the fractions from the PFP (#15) and NH2 column (#9), while it was sufficiently separated by fractionation using the PYE column (#10) in the fraction PYEF4. The clean peak #2 was received by fractionation using the PFP column (#15) in fraction PFPF3, by fractionation using the NH2 column (#9) in fraction NH2F7 and by the PYE column (#10) in fraction PYEF5.

2.3.3 Distribution of non-target peaks in a virtual two dimensional separation space

The distribution of all detected non-target peaks within a virtual two dimensional separation space was evaluated in order to verify the degree of orthogonality between the selected columns (#2, #9, #10 and #15), which was previously derived from the small set of endocrine disrupting target compounds. In order to minimize a bias of this evaluation by potentially false positive peaks only those detected in up to five consecutive fractions on all four columns were considered. Furthermore, we only considered fractions for the subsequent data analysis which were collected after 6 min for NH2 (#9), 9 min when using PYE (#10), after 10 minutes for C18 (#2) and PFP (#15) (Table A4). The early eluting fractions were not considered, as many compounds eluted at the column dead time with the LC gradient starting at a high percentage of methanol (50 or 60%) for columns #2, #10 and #15, as most EDCs are rather hydrophobic and thus elute at higher methanol fractions. This results in a reduction of the peak inventory from 23628 to 3452 peaks. The reduced fraction of common peaks is also a result of the challenges of automated peak detection in non-target screening as discussed above.

For visualization of the peak distribution the number of common peaks (Tables A9 to Tables A15) in each fraction combination among all four selected phases was determined (Figure 2-5). Each bin represents a virtual two dimensional fraction containing the common

peaks. An ideal pair of two fully orthogonal columns would result in a homogeneous distribution and an equal number of peaks within each bin of the virtual 2D separation space [33]. The C18 (#2) vs. PFP column (#15) plot (Figure 2-5a) shows only a limited spread of common peaks among the fraction combinations close to the diagonal of the plot. Solely 49% of the bins contain at least one peak. All remaining column pairs pose a higher grade of orthogonality, reflected by a bin-coverage of in between 73 and 88% (Table A16). These findings reflect the statistical evaluation of the reference compounds retention data.

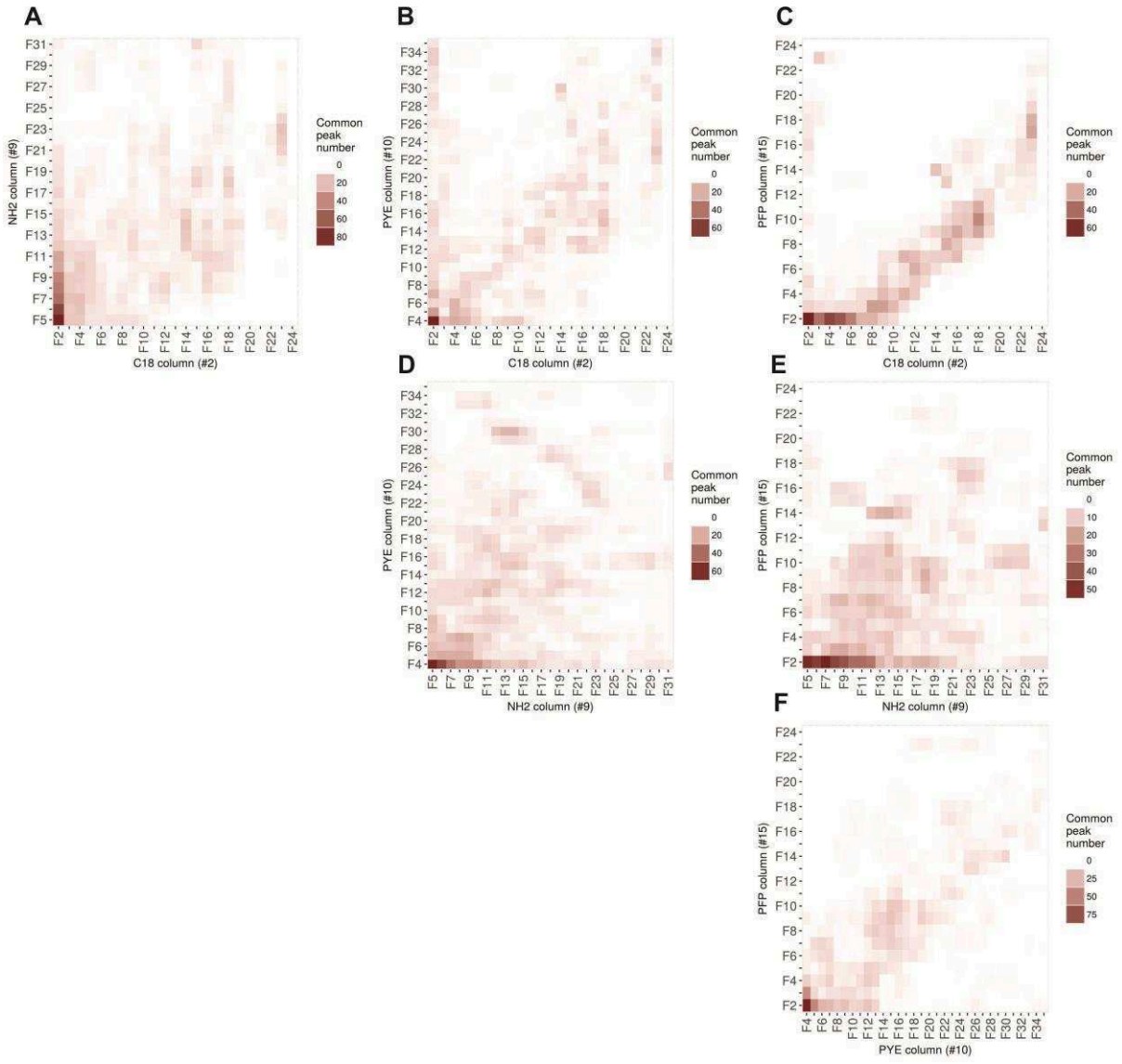

Figure 2-5 Heat map matrix showing the distribution of the number of peaks in common in the virtual 2D separation space of the column pairs C18 (#2) vs. (a) NH2 (#9), (b) PYE (#10) and PFP (#15), of the pairs NH2 (#9) vs. (d) PYE (#10) and PFP (#15) and the pair (f) PYE (#10) vs. PFP (#15).

2.4 Conclusion

Based on a test set of 39 compounds we could identify three reversed-phase columns (octadecyl- (#2), aminopropyl- (#9) and pyrenyl ethyl-modified (#10) silica phases) out of 17 tested with a high degree of orthogonality for the separation of EDCs using PCA and SRC. These methods proved to be effective for this selection due to their capability to provide information on orthogonality among all pairs of columns. The capability of this approach to reduce complex “humps” of co-eluting compounds in LC-HRMS data was proven for a river water extract, which was fractionated on the three columns and additionally on a pentafluorophenyl column based on promising results in the literature [51]. However, the detection of common peaks relies strongly on a well-balanced peak picking in all fractions minimizing false positives and false negatives, which might be compromised by matrix effects and peak broadening.

The proposed approach is a powerful method to facilitate target or suspect screening, and the isolation of unknowns within complex environmental mixtures. This was verified within a recently conducted EDA study [52]. Its success was essentially supported by a tremendous reduction of the data complexity of over 99.9% as a result of the fractionation of the raw water extract on the four proposed reversed phases and resulted in the identification of the highly potent antiandrogen 4-methyl-7-diethylaminocoumarin and two derivatives.

2.5 Acknowledgments

This work was supported by the European FP7 Collaborative Project SOLUTIONS (grant agreement no. 603437). The authors would like to thank Robert Bloch for collecting the sample and Arnold Bahlmann for fruitful discussions concerning the method development. Chemaxon (Budapest, Hungary) is acknowledged for providing an academic license of JChem for Excel.

2.6 Literature

1. Schwarzenbach, R.P., et al., *The Challenge of Micropollutants in Aquatic Systems.* Science, 2006. **313**(5790): p. 1072-1077.
2. Malaj, E., et al., *Organic chemicals jeopardize the health of freshwater ecosystems on the continental scale.* Proceedings of the National Academy of Sciences, 2014. **111**(26): p. 9549-9554.
3. Brack, W., et al., *Effect-directed analysis supporting monitoring of aquatic environments — An in-depth overview.* Science of The Total Environment, 2016. **544**: p. 1073-1118.
4. Runnalls, T.J., et al., *Pharmaceuticals in the Aquatic Environment: Steroids and Anti-Steroids as High Priorities for Research.* Human and Ecological Risk Assessment: An International Journal, 2010. **16**(6): p. 1318-1338.
5. Sumpter, J.P., *Endocrine Disrupters in the Aquatic Environment: An Overview.* Acta hydrochimica et hydrobiologica, 2005. **33**(1): p. 9-16.
6. Söffker, M. and C.R. Tyler, *Endocrine disrupting chemicals and sexual behaviors in fish – a critical review on effects and possible consequences.* Critical Reviews in Toxicology, 2012. **42**(8): p. 653-668.
7. Jobling, S., Burn, R.W., Thorpe, K., Williams, R., Tyler, C., *Statistical modeling suggests that antiandrogens in effluents from wastewater treatment works contribute to widespread sexual disruption in fish living in English rivers.* Environmental Health Perspectives, 2009. **117**(5): p. 797-802.
8. Blaber, S.J.M., *THE OCCURRENCE OF A PENIS-LIKE OUTGROWTH BEHIND THE RIGHT TENTACLE IN SPENT FEMALES OF NUCELLA LAPILLUS (L.).* Journal of Molluscan Studies, 1970. **39**(2-3): p. 231-233.
9. Milnes, M.R., et al., *Contaminant-induced feminization and demasculinization of nonmammalian vertebrate males in aquatic environments.* Environmental Research, 2006. **100**(1): p. 3-17.
10. Krauss, M., H. Singer, and J. Hollender, *LC–high resolution MS in environmental analysis: from target screening to the identification of unknowns*. Analytical and Bioanalytical Chemistry, 2010. **397**(3): p. 943-951.
11. Bletsou, A.A., et al., *Targeted and non-targeted liquid chromatography-mass spectrometric workflows for identification of transformation products of emerging pollutants in the aquatic environment.* TrAC Trends in Analytical Chemistry, 2015. **66**(0): p. 32-44.
12. Ruff, M., et al., *Quantitative target and systematic non-target analysis of polar organic micro-pollutants along the river Rhine using high-resolution mass-spectrometry – Identification of unknown sources and compounds.* Water Research, 2015. **87**: p. 145-154.
13. Vergeynst, L., H. Van Langenhove, and K. Demeestere, *Trends in liquid chromatography coupled to high-resolution mass spectrometry for multi-residue analysis of organic micropollutants in aquatic environments.* TrAC Trends in Analytical Chemistry, 2015. **67**: p. 192-208.
14. Pluskal, T., et al., *MZmine 2: Modular framework for processing, visualizing, and analyzing mass spectrometry-based molecular profile data.* BMC Bioinformatics, 2010. **11**(1): p. 395.

15. Smith, C.A., et al., *XCMS: Processing Mass Spectrometry Data for Metabolite Profiling Using Nonlinear Peak Alignment, Matching, and Identification.* Analytical Chemistry, 2006. **78**(3): p. 779-787.
16. Liscio, C., et al., *Methodology for profiling anti-androgen mixtures in river water using multiple passive samplers and bioassay-directed analyses.* Water Research, 2014. **57**: p. 258-269.
17. Thomas, K.V., et al., *An assessment of in vitro androgenic activity and the identification of environmental androgens in United Kingdom estuaries.* Environmental Toxicology and Chemistry, 2002. **21**: p. 1456-1461.
18. Ellis, R.J., et al., *In vivo and in vitro assessment of the androgenic potential of a pulp and paper mill effluent.* Environmental Toxicology and Chemistry, 2003. **22**(7): p. 1448-1456.
19. Chang, H., et al., *Trace analysis of androgens and progestogens in environmental waters by ultra-performance liquid chromatography–electrospray tandem mass spectrometry.* Journal of Chromatography A, 2008. **1195**(1–2): p. 44-51.
20. Thomas, K.V., et al., *Effect-Directed Identification of Naphthenic Acids As Important in Vitro Xeno-Estrogens and Anti-Androgens in North Sea Offshore Produced Water Discharges.* Environmental Science & Technology, 2009. **43**(21): p. 8066-8071.
21. Gallampois, C.M.J., et al., *Integrated biological–chemical approach for the isolation and selection of polyaromatic mutagens in surface waters.* Analytical and Bioanalytical Chemistry, 2013. **405**(28): p. 9101-9112.
22. Ouyang, X., et al., *Comprehensive two-dimensional liquid chromatography coupled to high resolution time of flight mass spectrometry for chemical characterization of sewage treatment plant effluents.* Journal of Chromatography A, 2015. **1380**(0): p. 139-145.
23. Stephan, S., et al., *Contaminant screening of wastewater with HPLC-IM-qTOF-MS and LC+LC-IM-qTOF-MS using a CCS database.* Analytical and Bioanalytical Chemistry, 2016. **408**(24): p. 6545-6555.
24. Ouyang, X., et al., *Rapid Screening of Acetylcholinesterase Inhibitors by Effect-Directed Analysis Using LC × LC Fractionation, a High Throughput in Vitro Assay, and Parallel Identification by Time of Flight Mass Spectrometry.* Analytical Chemistry, 2016. **88**(4): p. 2353-2360.
25. Allen, R.C., et al., *Impact of reversed phase column pairs in comprehensive two-dimensional liquid chromatography.* Journal of Chromatography A, 2014. **1361**(0): p. 169-177.
26. Brack, W., *Effect-Directed Analysis of Complex Environmental Contamination*. The Handbook of Environmental Chemistry, ed. D. Barcelo and A.G. Kostianoy. Vol. 15. 2011, Berlin Heidelberg: Springer.
27. Snyder, L.R., J.W. Dolan, and P.W. Carr, *The hydrophobic-subtraction model of reversed-phase column selectivity.* Journal of Chromatography A, 2004. **1060**(1-2): p. 77-116.
28. Euerby, M.R. and P. Petersson, *Chromatographic classification and comparison of commercially available reversed-phase liquid chromatographic columns using principal component analysis.* Journal of Chromatography A, 2003. **994**(1-2): p. 13-36.
29. Euerby, M.R., et al., *Chromatographic classification and comparison of commercially available reversed-phase liquid chromatographic columns containing phenyl moieties*

using principal component analysis. Journal of Chromatography A, 2007. **1154**(1-2): p. 138-151.
30. Euerby, M.R., A.P. McKeown, and P. Petersson, *Chromatographic classification and comparison of commercially available perfluorinated stationary phases for reversed-phase liquid chromatography using Principal Component Analysis.* Journal of Separation Science, 2003. **26**(3-4): p. 295-306.
31. Euerby, M.R. and P. Petersson, *Chromatographic classification and comparison of commercially available reversed-phase liquid chromatographic columns containing polar embedded groups/amino endcappings using principal component analysis.* Journal of Chromatography A, 2005. **1088**(1-2): p. 1-15.
32. Johnson, A.R., et al., *Identifying orthogonal and similar reversed phase liquid chromatography stationary phases using the system selectivity cube and the hydrophobic subtraction model.* Journal of Chromatography A, 2012. **1249**(0): p. 62-82.
33. Gilar, M., et al., *Orthogonality of Separation in Two-Dimensional Liquid Chromatography.* Analytical Chemistry, 2005. **77**(19): p. 6426-6434.
34. Gilar, M., et al., *Comparison of Orthogonality Estimation Methods for the Two-Dimensional Separations of Peptides.* Analytical Chemistry, 2012. **84**(20): p. 8722-8732.
35. Camenzuli, M. and P.J. Schoenmakers, *A new measure of orthogonality for multi-dimensional chromatography.* Analytica Chimica Acta, 2014. **838**(Supplement C): p. 93-101.
36. Leonhardt, J., et al., *A new method for the determination of peak distribution across a two-dimensional separation space for the identification of optimal column combinations.* Analytical and Bioanalytical Chemistry, 2016. **408**(28): p. 8079-8088.
37. Liu, Z., D.G. Patterson, and M.L. Lee, *Geometric Approach to Factor Analysis for the Estimation of Orthogonality and Practical Peak Capacity in Comprehensive Two-Dimensional Separations.* Analytical Chemistry, 1995. **67**(21): p. 3840-3845.
38. D'Attoma, A., C. Grivel, and S. Heinisch, *On-line comprehensive two-dimensional separations of charged compounds using reversed-phase high performance liquid chromatography and hydrophilic interaction chromatography. Part I: Orthogonality and practical peak capacity considerations.* Journal of Chromatography A, 2012. **1262**(Supplement C): p. 148-159.
39. Revelle, W. *psych: Procedures for Personality and Psychological Research*. 2017; Available from: https://CRAN.R-project.org/package=psych Version = 1.7.5.
40. Bernaards, C.A. and R.I. Jennrich, *Gradient Projection Algorithms and Software for Arbitrary Rotation Criteria in Factor Analysis.* Educational and Psychological Measurement, 2005. **65**(5): p. 676-696.
41. Hug, C., et al., *Microbial reporter gene assay as a diagnostic and early warning tool for the detection and characterization of toxic pollution in surface waters.* Environmental Toxicology and Chemistry, 2015. **34**(11): p. 2523-2532.
42. Huntscha, S., et al., *Multiresidue analysis of 88 polar organic micropollutants in ground, surface and wastewater using online mixed-bed multilayer solid-phase extraction coupled to high performance liquid chromatography-tandem mass spectrometry.* Journal of Chromatography A, 2012. **1268**: p. 74-83.
43. Chambers, M.C., et al., *A cross-platform toolkit for mass spectrometry and proteomics.* Nat Biotech, 2012. **30**(10): p. 918-920.

44. Pluskal, T., et al., *MZmine 2: Modular framework for processing, visualizing, and analyzing mass spectrometry-based molecular profile data.* Bmc Bioinformatics, 2010. **11**(1): p. 1-11.
45. Hug, C., et al., *Identification of novel micropollutants in wastewater by a combination of suspect and nontarget screening.* Environmental Pollution, 2014. **184**(0): p. 25-32.
46. Fariss, M.W. and D.J. Reed, *High-performance liquid chromatography of thiols and disulfides: Dinitrophenol derivatives*, in *Methods in Enzymology*. 1987, Academic Press. p. 101-109.
47. Tanaka, N., et al., *Effect of stationary phase structure on retention and selectivity in reversed-phase liquid chromatography.* Journal of Chromatography A, 1982. **239**: p. 761-772.
48. Marchand, D.H., et al., *Column selectivity in reversed-phase liquid chromatography: VIII. Phenylalkyl and fluoro-substituted columns.* Journal of Chromatography A, 2005. **1062**(1): p. 65-78.
49. Valko, K., et al., *Rapid Method for the Estimation of Octanol / Water Partition Coefficient (Log Poct) from Gradient RP-HPLC Retention and a Hydrogen Bond Acidity Term (Sigma alpha2H).* Current Medicinal Chemistry, 2001. **8**(9): p. 1137-1146.
50. Hu, M., et al., *Optimization of LC-Orbitrap-HRMS acquisition and MZmine 2 data processing for nontarget screening of environmental samples using design of experiments.* Analytical and Bioanalytical Chemistry, 2016. **408**(28): p. 7905-7915.
51. Ouyang, X., et al., *Comprehensive two-dimensional liquid chromatography coupled to high resolution time of flight mass spectrometry for chemical characterization of sewage treatment plant effluents.* Journal of Chromatography A, 2015. **1380**: p. 139-145.
52. Muschket, M., et al., *Identification of Unknown Antiandrogenic Compounds in Surface Waters by Effect-Directed Analysis (EDA) Using a Parallel Fractionation Approach.* Environmental Science & Technology, 2018. **52**(1): p. 288-297.

Chapter 3

Identification of Unknown Antiandrogenic Compounds in Surface Waters by Effect-Directed Analysis (EDA) Using a Parallel Fractionation Approach

Abstract

Among all the nuclear-receptor mediated endocrine disruptive effects, antiandrogenicity is frequently observed in aquatic environments and may pose a risk to aquatic organisms. Linking these effects to responsible chemicals is challenging and a great share of antiandrogenic activity detected in the environment has not been explained yet. To identify drivers of this effect at a hot spot of antiandrogenicity in the German river Holtemme, we applied effect-directed analysis (EDA) including a parallel fractionation approach, a downscaled luciferase reporter gene cell-based anti-AR-CALUX assay and LC-HRMS/MS non-target screening. We identified and confirmed the highly potent antiandrogen 4-methyl-7-diethylaminocoumarin (C47) and two derivatives in the active fractions. The relative potency of C47 to the reference compound flutamide was over 5.2, while the derivatives were less potent. C47 was detected at a concentration of 13.7 µg/L, equal to 71.4 µg flutamide equivalents per liter (FEq/L) in the non-concentrated water extract that was posing an antiandrogenic activity equal to 45.5 (±13.7 SD) FEq/L. Thus, C47 was quantitatively confirmed as the major cause of the measured effect in vitro. Finally, the antiandrogenic activity of C47 and one derivate was confirmed in vivo in spiggin-gfp Medaka. An endocrine disrupting effect of C47 was observed already at the concentration equal to the concentration in the non-concentrated water extract, underlining the high risk posed by this compound to the aquatic ecosystem. This is of some concern since C47 is used in a number of consumer products indicating environmental as well as human exposure.

This chapter is based on the article:

Identification of Unknown Antiandrogenic Compounds in Surface Waters by Effect-Directed Analysis (EDA) Using a Parallel Fractionation Approach

Matthias Muschket, Carolina di Paolo, Andrew J. Tindall, Gerald Touak, Audrey Phan, Martin Krauss, Kristina Kirchner, Thomas-Benjamin Seiler, Henner Hollert, Werner Brack:

Environmental Science&Technology, Volume 52, 2018, pages 288-297

3.1 Introduction

Aquatic organisms are exposed to numerous man-made androgens and antiandrogens [1]. Bioaccumulation leads to the presence of androgenic and antiandrogenic activity not only in water [2-4] and sediment [5-8] but also in aquatic biota [2, 9-11] resulting in adverse effects on reproductive health. The first report on masculinization of mosquitofish caused by androgen-containing paper mill effluent dates back to 1980 [12]. Moreover the observations of Mila et al. [13] indicate the impact of androgens on the immune system of fish. Other studies have demonstrated that feminization of non-mammalian vertebrate males was correlated to environmental concentrations of antiandrogens [11, 14]. Laboratory studies have also confirmed that the skewed sex ratio towards females in fish can be induced by exposure to antiandrogens [15, 16]. These facts raise concerns, since not only is the impact of this class of pollutants on wildlife well documented, but there is also evidence that wildlife might act as a sentinel for human health [11].

Sources that have been demonstrated to release (anti)androgens into freshwater systems are effluents from livestock feedlot [3], pulp mills [17, 18], the leather industry [19] and wastewater treatment plants [2, 20-23]. Identified androgens present in the aquatic environment include chlorinated pesticides such as dichlorodiphenyldichloroethylene (DDE) and lindane [1], steroids such as androst-16-en-3-one or nandrolone [24] which are used as anabolic drugs to improve sport performance, and fungicides such as vinclozolin [25]. Antiandrogenic activity has been reported for example for the disinfectant chloroxylenol [9], the fungicide dichlorophene [9] and the insecticide isofenphos [26]. Bioassays frequently detect androgenic [7, 27, 28] and antiandrogenic [29-32] activity in environmental samples. However, in many cases, only a minor part of the effect can be explained by known androgen axis disruptors. Effect-directed analysis (EDA) is a powerful tool for identifying unknown toxicants in environmental samples exhibiting a specific mode of action [33, 34]. It has been used successfully to identify estrogenic [35] and antiandrogenic [36] compounds. For instance, Weiss et al. [6] tentatively identified the antiandrogenic PAHs benzo[a]anthracene and fluoranthene in sediments while Thomas et al. [36] identified petrogenic naphthenic acids in north sea offshore produced water discharges as antiandrogens. In EDA effect drivers are classically identified by effect testing, sequential fractionation and chemical analysis of active fractions. The application of EDA at hotspots of

contamination identified by effect-based monitoring is a promising strategy for identifying environmentally relevant chemicals exhibiting a specific effect. Using this strategy, the River Holtemme (Saxony Anhalt, Germany) has been identified as a hotspot of antiandrogenic effects detectable in river water extracts with the anti-AR-CALUX assay (unpublished data).

The objective of this study was to unravel the causes of antiandrogenicity in the River Holtemme using an EDA approach, combining a new fractionation method using four columns with optimized orthogonal separation selectivity in parallel to separate mixtures of endocrine disruptors. Active fractions were identified with a downscaled luciferase reporter gene cell-based anti-AR-CALUX assay that has been recently developed [37]. For structure elucidation of non-target peaks shared by the active fractions of the four orthogonal stationary phases, *in-silico* fragmentation prediction by Metfrag, pH-Dependent LC Retention and hydrogen−deuterium exchange (HDX) [38, 39] were conducted. Finally the antiandrogenicity of the compounds identified *in vitro* was confirmed at a higher biological level [40] *in-vivo* in the spiggin-gfp medaka model [41].

3.2 Material and Methods

3.2.1 Chemicals and Reagents

Information on all chemicals, reagents and solvents used is given in Table A1.

3.2.2 Sampling, Extraction and Fractionation of Surface Water.

The water was sampled in the river Holtemme, 1.3 km downstream of the WWTP of Silstedt (60,000 person equivalents), Saxony-Anhalt, Germany. It was concentrated using a combination of four sorbents in a multi-layer cartridge, eluted simultaneously from all four sorbents and fractionated by RP-HPLC in a parallel approach on four columns optimized for orthogonality (Table 3-1): octadecyl-, pentafluorophenyl-, aminopropyl and pyrenyl ethyl-modified silica phase. One-minute fractions of the water extract were collected and combined according to peak clusters in the UV-Vis chromatogram. For method blanks, LC-MS grade water was injected. More details on the extraction and fractionation procedure, as well as an overview on the gradients used for fractionation (Table B2) and collected fractions (Table B3) is given in the appendix, section B1.1.

Table 3-1 Suppliers, functionalization and dimension of stationary silica phases and the corresponding guard columns applied in this study.

Column name	Supplier	Functionalisation	Dimension	Dimension pre-column
Nucleodur C18 Gravity	Macherey-Nagel	Octadecyl	250 x 10.0 mm, 5 µm	10 x 10 mm, 5 µm
Hypersil Gold PFP	Thermo Fisher	Pentafluorophenyl	250 x 10.0 mm, 5 µm	10 x 10 mm, 5 µm
Unison NH2	Imtakt	Aminopropyl	150 x 10.0 mm, 3 µm	10 x 10 mm, 3 µm
Cosmosil PYE	Nacalai Tesque	Pyrenyl ethyl	150 x 4.6 mm, 5 µm	20 x 4.6 mm, 5 µm

3.2.3 anti-AR-CALUX Assay

Cell culture and assay performance

The human osteoblastic osteosarcoma U2OS cell line stably co-transfected with an expression construct for the human AR and a respective reporter construct was provided by

BioDetection Systems BV (BDS, Amsterdam, the Netherlands) and cultured as previously described [42, 43].

Cells were exposed to a dilution series of the non-fractionated river water sample with a relative enrichment factor (REF) of 1.25 - 12.5 in 96-well plates in co-exposure with a non-saturating dihydrotestosterone (DHT) concentration equivalent to the EC50 in the agonistic assay (4.2×10^{-10} M) in a final volume of 200 µL exposure medium per well. Each plate contained a serial dilution of the reference antiandrogen flutamide (10^{-9} – 10^{-5} M), solvent controls (1% DMSO) and DHT controls (4.2×10^{-10} M DHT). All conditions were performed in triplicate wells in each test. All exposure conditions and wells contained 1% DMSO. Exposure and measurement were performed according to regular protocols [37]. Tests to evaluate the water sample extract were repeated in three replicates. Non-specific expression or inhibition of the luciferase gene, as well as luminescence of the candidate chemicals itself were excluded with the Cytotox CALUX assay [44]. For single and recombined fractions as well as method blanks, low-volume procedures for dosing and exposure were applied in dilution series to obtain a 75% reduction of the required sample volume compared to the regular protocol [37].

Cell viability of at least 80 % after exposure was verified by the MTT-assay [45] measuring the amount of formazan with a microplate spectrophotometer (Tecan Infinite® M200, Tecan, Switzerland) at an absorbance wavelength of 492 nm. Details of the procedure are found in Di Paolo et al. [37, 46].

Data analysis

Results are presented as magnitude of AR response, obtained by normalizing the average of measured relative light units (RLU) from co-exposed cells versus the average of RLU values of cells exposed in the DHT-control condition [47]. Sigmoidal dose-response fit of results was obtained by constraining top to 100 and bottom to zero using a two parameter logistic equation using GraphPad Prism version 7.01

Toxicity equivalent concentrations [48] were calculated to assess the biological recovery of activity after fractionation and for the evaluation of the portion of antiandrogenic effect caused by the identified compounds within the water extract. The chemically determined flutamide equivalent $FEq_{chem,i}$ (µg FEQ/L) of compound i was calculated from the simultaneously determined EC50 of flutamide ($EC50_{flutamide}$) and compound i ($EC50_i$) and the concentration c_i of compound i (eq. 3-1).

The biologically determined flutamide equivalents of the sample FEq_{bio} was calculated from the simultaneously determined EC50 value of flutamide and the sample ($EC50_{sample}$) and the relative enrichment factor of the sample at its EC50 value ($REF_{sample\ EC50}$) (eq. 2).

$$FEq_{chem,i} = EC50_{flutamide} \cdot \frac{c_i}{EC50_i} \quad \text{(eq. 3-1)}$$

$$FEq_{bio} = EC50_{flutamide} \cdot \frac{1}{REF_{sample\ EC50}} \quad \text{(eq. 3-2)}$$

3.2.4 Structure elucidation of the antiandrogenic compounds

Analysis was performed with an Ultimate 3000 LC system connected to a Q-Exactive Plus HRMS instrument (all from Thermo). For separation, a Kinetex EVO C18 column (50 x 2.1 mm, 2.6 µm with pre-column 10 x 2.1 mm, Phenomenex) was used at 40°C. Details of the gradient elution program and the eluents are given in Table B4. Full scan MS data was obtained by electrospray (ESI) and atmospheric pressure chemical ionization (APCI) in positive and negative mode (ESI+, ESI-, APCI+ and APCI-) in the mass range of m/z 100-1000 at a nominal resolving power of 140.000 (referenced to m/z 200).

Suspect screening for 302 known or suspected antiandrogens was carried out using Tracefinder Version 3.2 (Thermo). The suspect list is shown the accompanying Excel file, Table B7.

For non-target screening, peak lists were obtained from the full scan chromatograms using the software MZmine 2.17 [49]. Product ion spectra (MS/MS) were acquired with a data-dependent MS/MS acquisition with an inclusion list containing common masses of all active fractions from the preparative fractionation at a nominal resolving power of 35.000 using 50% or 55% normalized collision energy. Molecular formulas based on accurate mass and isotope patterns were assigned using XCalibur (Thermo). Experimental MS/MS spectra were compared against those predicted for candidate structures retrieved from ChemSpider (Royal Society of Chemistry) using the software MetFrag 2.2 (command line version 54) [50]. Besides the match of predicted and experimental MS/MS spectra, hydrogen-deuterium exchange (HDX) [38] and pH-dependent LC retention time (RT) shift at pH 2.6, 6.4 and 10.0 [38] were used for candidate selection. A literature survey for available data concerning antiandrogenic activity was carried out for candidates of potentially highest environmental

relevance reflected by a high number of references in ChemSpider. For detailed information on the Settings of MzMine, HDX and pH-Dependent LC Retention see appendix, section B1.3.

3.2.5 Chemical and effect confirmation of antiandrogens

The chemical identity of tentatively identified compounds was confirmed by comparison with RTs and MS/MS spectra of reference standards. To assess the contribution of the confirmed compounds to the observed antiandrogenicity, they were quantified and tested at the corresponding concentration level in the anti-AR-CALUX assay.

For internal matrix matched quantification in the water extract, an internal calibration standard containing verapamil-d6, atrazine-$^{13}C_3$ and bezafibrate-d4 was added to the water extract and the mixed analyte standards at concentration levels of 0.1, 0.5, 1, 2, 5, 10, 20, 50, 100, 200, and 500 ng/mL. The concentrations of the internal calibration standards were 95 ng/mL. Peak integration, compound calibration and quantification were carried out in TraceFinder 3.2 (Thermo).

3.2.6 Rapid Androgen Disruption Adverse outcome Reporter (RADAR) assay

The RADAR assay was performed using a stable line of medaka eleuthero-embryos harboring the spiggin1-gfp transgene as previously described [41]. Briefly, day post hatch zero medaka fry were exposed to the test chemicals or control solutions in six-well plates. Five fry were exposed per well in four replicates for 96 h at 26 °C with a 14:10 light:dark cycle to stock solutions and controls in DMSO at a final concentration of 0.2 % DMSO in all exposure solutions. All solutions were renewed every 24 h. For each experiment, fry were exposed to the test compounds or the solvent control in the presence or absence of 17α-methyltestosterone (17MT, 3 µg/L). Exposure in the presence of 17MT allowed inhibition of 17MT induced fluorescence to be quantified. The reference androgen receptor antagonist flutamide was also tested in the presence of 17MT for comparison.

Following 96 h of exposure fry were anaesthetized by immersion in a 200 mg/L solution of MS222 and positioned in order to reveal their dorsal surface. A Leica MZ10F fluorescent (Leica Microsystems) fitted with a TXD 14C camera (Baumer), ET-GFP long-pass filters (excitation 480/40, emission 510LP, Leica) and a 200 W Lumen fluorescence source (Prior

Scientific) was used to capture a color image of the mesonephros of each fry. The GFP signal was quantified using ImageJ [51] as previously described [41]. Two independent replicate experiments were carried out for each set of conditions. In all cases the two replicate experiments gave similar results, therefore data from all groups were normalized to the mean of the solvent control group containing 17MT and pooled.

Data analysis and statistics were carried out in Prism version 5.04 (GraphPad Software). When the groups being compared followed a Gaussian distribution, a Students T-Test (pairwise comparison) or one-way ANOVA and Dunnett's post-test (comparing multiple groups) were carried out. When the data of one or more groups did not follow a Gaussian distribution, a Mann-Whitney test (pairwise comparison) or Kruskal-Wallis and Dunn's post-test (comparing multiple groups) were carried out. All unspiked groups were compared with the solvent control group, all spiked groups were compared to the solvent control containing 17MT.

3.3 Results and Discussion

3.3.1 Identification of Antiandrogenic Active Fractions

The water extract reduced the magnitude of AR response of DHT to 79 % ± 9 % at REF 1.25 in the anti-AR-CALUX assay with a concentration-dependent decrease to 17 % ± 2% at REF 12.5 (Figure B1). Extrapolation of the concentration-response relationship according to eq. (3-2) indicates the presence of 46 ± 14 µg FEq/L antiandrogens in the non-concentrated water extract.

Fractionation of the water extract on octadecyl- (C18), pentafluorophenyl- (PFP), aminopropyl- (NH2) and pyrenyl ethyl (PYE) silica and subsequent testing for antiandrogenic activity in a miniaturized anti-AR-CALUX assay [37] showed one active fraction with an AR response between 37 and 65 % for each column (Figure 3-1). Only one additional fraction (F13 of the NH2 phase separation) showed a slight antiandrogenic response (75 ± 1.2%) (Figure 3-1c), but was not further considered due to its relatively low bioactivity.

At the same REF values, no cytotoxicity was observed in the MTT-assay in any fraction or the water extract. The fractionation method blanks did not show any antiandrogenic activity in the relevant concentration range between a REF of 1.25 and 12.5.

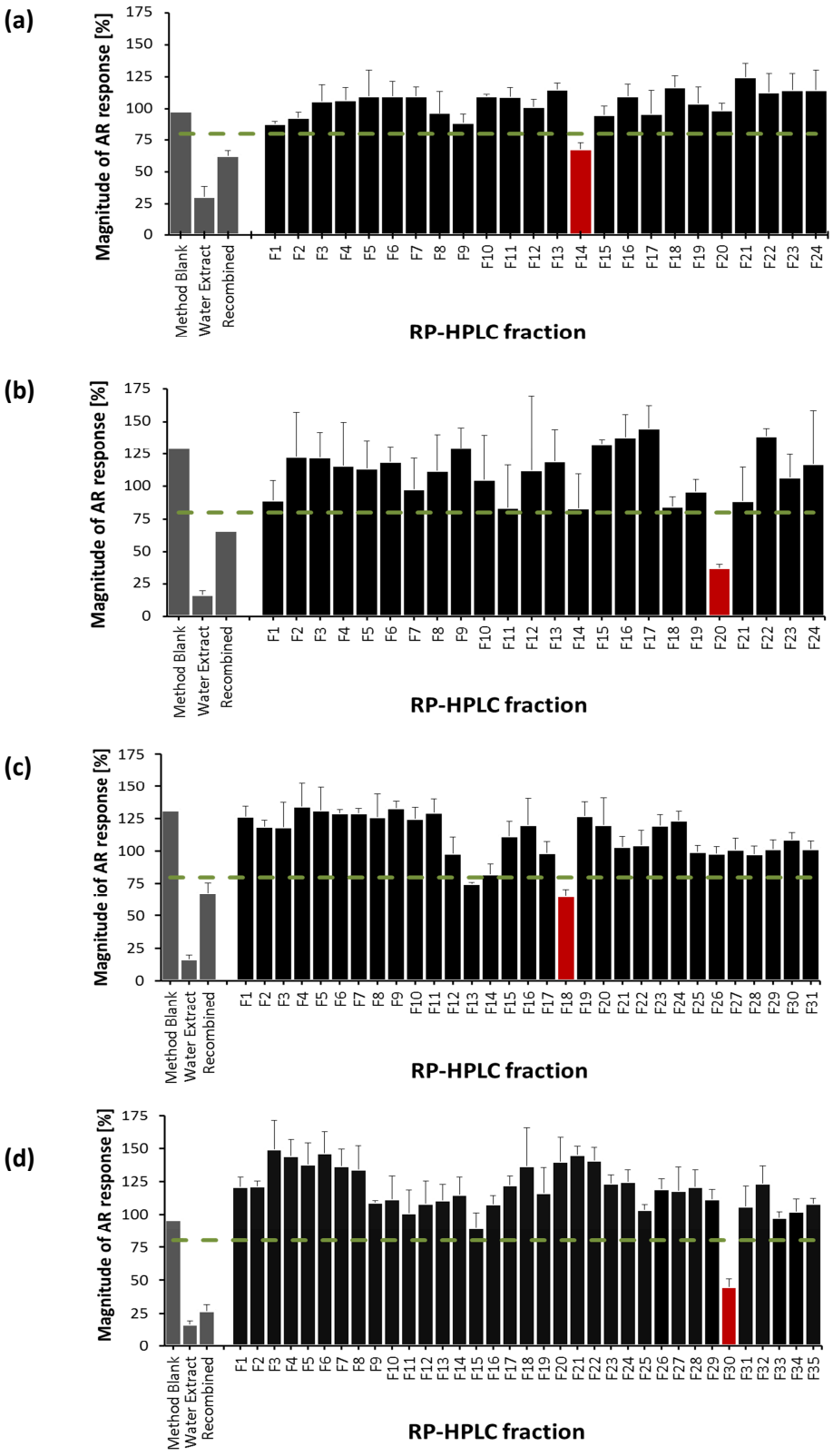

Figure 3-1 Magnitude of AR response in the downscaled anti-AR-CALUX assay of the water extract, recombined fractions and single fractions obtained with four different columns: (a) C18, (b) PFP (c) NH2 and (d) PYE. Red bars represent the identified active fractions. Fractions with values under the dashed line at 80% AR response are defined as antiandrogenic. REF was 6.25 for (a) and 12.5 for (b) – (d).

3.3.2 Suspect Screening for known Antiandrogens

Active fractions were screened with LC-HRMS for common antiandrogenic suspects addressing 302 of 385 known or suspected antiandrogens retrieved in the literature (Table B7) that are potentially ionizable in ESI or APCI.

Amongst others the river water extract was fractionated on a semi-preparative octadecyl silica column. For chemical analysis an analytical scale octadecyl silica column was coupled online to a mass detector. A standard mixture containing 36 androgenic endocrine disrupting compounds (Table A5) was separated on both columns to derive a high correlation of retention times (R^2=0.94), as displayed in Figure 3-2. Peaks of the active fraction collected between 25 and 26 min were eluting between 11.37 and 11.54 min if separated on an analytical scale octadecyl silica column. Thus the chemical analysis of the active fractions was constrained to peaks eluting between 10 and 13 min.

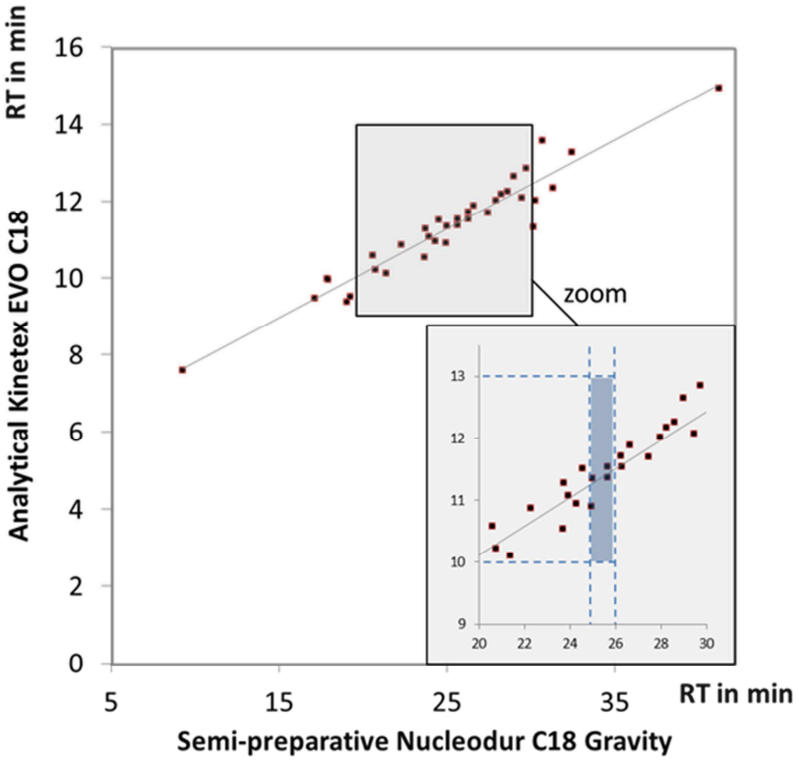

Figure 3-2 Correlation of retention times of 36 androgenic endocrine disrupting compounds on analytical Kinetex C18 and semi-preaparative Nucleodur C18 column with R^2=0.9356.

In total 34 masses assigned to 45 tentatively identified suspects were detected, as shown in section S2.3 of SI. Ten masses were present within two and the remaining 24 masses solely within one active fraction. Thus, none of the suspects fulfilled the candidate selection criteria.

3.3.3 Non-Target Screening, Compound Identification and Confirmation

3.3.3.1 Reduction of the number of peaks

Non-target screening (ESI+/- and APCI +/-) identified common peaks with the same monoisotopic mass, retention time and isotope pattern within all active fractions eluting between 10 and 13 minutes from the analytical scale octadecyl silica column for structure elucidation. For ESI+, on average 7477 peaks were picked by the automated peak detection in MZmine in each active fraction before (Figure 3-3a) and 3108 after (Figure 3-3b) blank substraction. Any combination of two and three active fractions shared on average 730 (Figure 3-3c) and 286 peaks (Figure 3-3d), respectively. All four active fraction had 147 peaks in common (Figure 3-3e) but solely 24 of them eluted within the RTs window between 10 and 13 min (Figure 3-3f). The manual evaluation of non-target peaks in XCalibur led to an elimination of another 21 candidate peaks either due to similar or higher peak intensity in non-active fractions and corresponding blanks despite the conducted blank removal or due to a false-positive automated peak picking by MZmine within in background noise. Thus solely three peaks were present in all active fractions corresponding to a tremendous MS-data reduction of 99.96% underlining the power of the fractionation approach (Figure 3-3g).

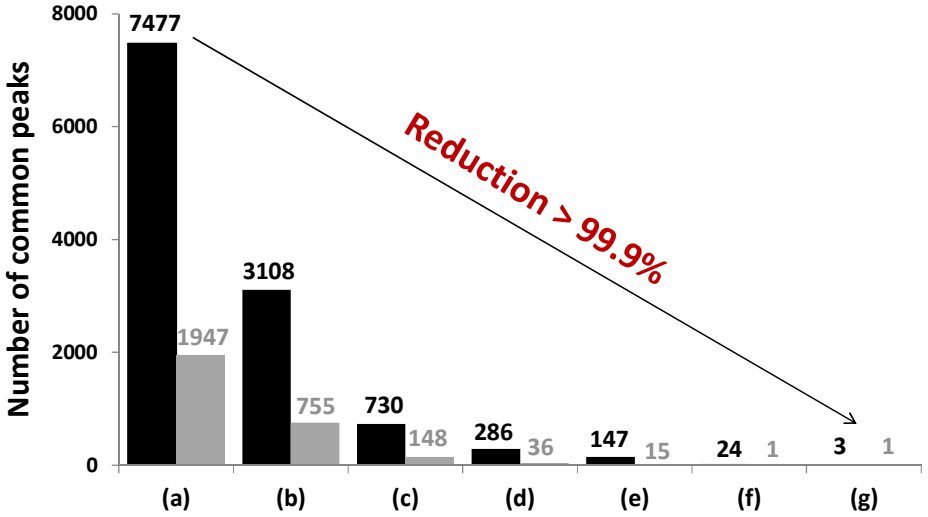

Figure 3-3 Overview of MS-data reduction by the parallel fractionation approach. Peaks were obtained by ESI (black bars) and APCI (grey bars) in positive mode. The average number of peaks in single active fractions (a) before and (b) after blank subtraction and the average number of peaks in common in any combination of (c) two, (d) three or (e) four active fractions is shown. Consideration of (f) the RT window (10min ≤ RT ≤ 13min) and (g) manual evaluation led to a further reduction of the number of common peaks.

The remaining three peaks (#1 - #3) are displayed in the Table 3-1. Molecular formulas based on accurate mass and isotope patterns were assigned. With APCI+ only peak #1 was detected in all active fractions but with a lower intensity than in ESI+. In ESI/APCI- no common peaks were detected in all active fractions. Thus the following non-target analysis was conducted for the HRMS/MS data received by ESI+ for the active fraction collected from the fractionation on the C18 column.

Table 3-2 Overview on five non-target peaks detected commonly in all active fractions C18F14, PFPF20, PYEF30 and NH2F18. Three peaks were eluting within and two peaks outside of the retention time window between 10 and 13 min.

#	m/z $[M+H]^+$	Retention time	Candidates in ChemSpider	Compound name	Molecular formula	CAS
1	232.1332	11.40 min	6931	4-methyl-7-diethylaminocoumarin (C47)	$C_{14}H_{18}NO_2$	91-44-1
2	233.1361	11.40 min	-	4-methyl-7-diethylaminocoumarin (C47)	$C_{13}{}^{13}C_1H_{18}NO_2$	91-44-1
3	208.1332	11.13 min	8569	Unknown	$C_{12}H_{18}O_2N$	
4	204.1019	9.75 min	3792	4-methyl-7-ethylaminocoumarin (C47T1)	$^{12}C_{12}H_{14}NO_2$	28821-18-3
5	176.0706	7.00 min	1190	4-methyl-7-aminocoumarin (C47T2)	$^{12}C_{10}H_{10}NO_2$	26093-31-2

3.3.3.2 Structure elucidation of three common peaks within the active fractions

Peaks #1 and #2 are the monoisotopic and the $^{13}C_1$ isotopologue peak of the same compound. For peak #1 6931 candidates were found in total in the Chemspider database with 195 structures exhibiting both a Metfrag score of at least 0.7 and a minimum of 10 reference compounds. Within this group 18 compounds displayed a score of higher than 0.9. By far the highest number of references (155) and a high score of 0.94 were assigned to the candidate 4-methyl-7-diethylaminocoumarin (C47). The *in silico* fragmentation prediction by Metfrag explained 17 of the obtained 19 most abundant fragment peaks. Moreover, the predicted logK_{OW} value of 3.22 fitted to the observed RT, as shown in Table B5. In addition, peak #1 was detected in positive but not in negative ionization mode. This is plausible since C47 can only be ionized by protonation.

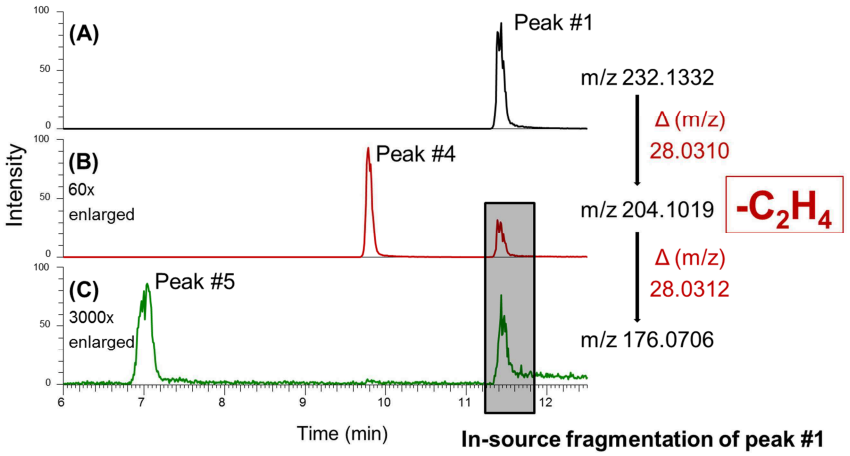

Figure 3-4 Extracted ion chromatograms of peak #1 and its two dealkylated transformation products from LC-HRMS analysis of the active fraction collected from the fractionation on the C18 column.

Two non-target peaks (#4 and #5), exhibiting a mass difference to peak #1 corresponding to one, respectively two ethyl groups, were considered since they were not only detected at 9.75 (peak #4) and 7.00 min (peak #5) respectively (Table 3-1), but also with the same RT as peak #1 due to in-source fragmentation of C47. This is shown in the extracted ion chromatogram of the active fraction (Figure 3-4).

The fractionated sample was collected in the effluent of a WWTP. N-Deethylation is a well-known transformation reaction of micropollutants in activated sludge [52] supporting the evidence for C47 as a candidate for peak #1 which contains two ethyl groups at the terminal

aryl core. The chemical identity of the non-target peak #1 and its dealkylated transformation products 4-methyl-7-ethylaminocoumarin (C47T1) and 4-methyl-7-aminocoumarin (C47T2) was confirmed using authentic reference standards, as shown in Figure 3-5 for C47 and for its derivatives in the section A2.4. The presence of peak #4 and #5 in the active fractions despite their lower hydrophobicity compared to C47 suggests some transformation during sample processing after fractionation. However, by far the highest signal intensity within the fractions of the octadecyl silica phase was observed in fraction C18F6 for peak #4 and in fraction C18F1 for peak #5, as shown in Figure B6.

Among the 8569 candidates for peak #3 (Table 3-1) a total number of 338 exhibit a Metfrag score higher than 0.7 and at least 10 references in ChemSpider which are believed to reflect reasonable cutoff values [38]. Ciclopirox, the candidate having the most references in ChemSpider (277) was the only candidate with a suggested environmental relevance and literature indications for antiandrogenic potency [53]. Moreover its predicted $\log K_{OW}$ value of 2.73 is in the same range of other antiandrogens eluting in a RT window between 10 and 13 minutes, as shown in the appendix, Table B5. However, the identity of the non-target peak #3 could not be confirmed using the authentic reference standard of ciclopirox due to different fragment ion patterns of peak #3 and ciclopirox in LC-HRMS/MS, even if identical RTs were observed (Figure B5). A possible coelution of ciclopirox with an isobaric compound was disproved by different common fragment intensities derived from the standard and the environmental sample.

A combination of HDX and pH-dependent retention, which was successfully applied for the identification of unknown mutagens in surface waters [38, 39], was utilized for a further reduction of the candidate list. Out of the 338 candidates, a total number of 252 structures were selected after HDX. The consideration of pH-dependent retention led to a final list of 126 compounds without any outstanding candidate. Thus, the compound related to peak #3 remained unidentified.

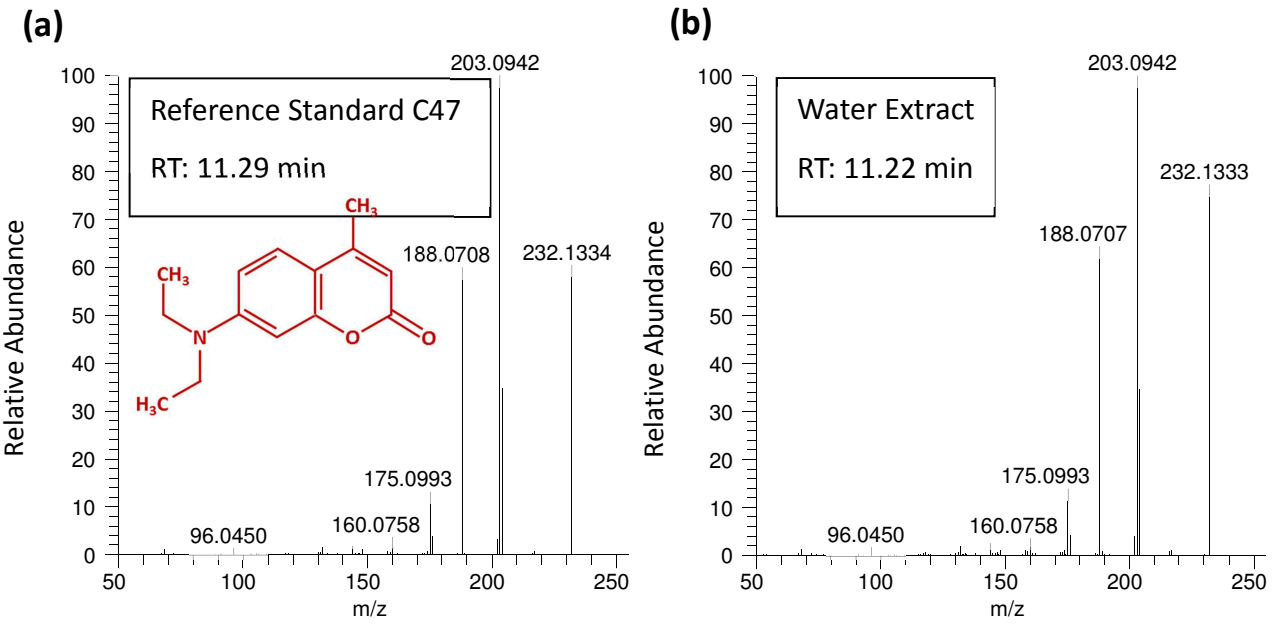

Figure 3-5 Fragment ion spectra (HCD 50) of (a) C47 and (b) peak #1 with m/z 232.1332 at RT 11.22 min from the water extract (REF 76). The mass spectrum is available in MassBank (https://massbank.eu/MassBank) with accession UA006401 (splash10-0gz0000000-db9037e4cce830af7e43).

3.3.4 Contribution of Identified Compounds to the Samples Antiandrogenicity

The assumed antiandrogenic activity of C47 was supported by the literature. Several derivatives, all joining a coumarin scaffold, have been already reported as antiandrogens [54-56] with up to 50 fold higher antiandrogenic potency than bicalutamide which is a major antiandrogen in clinical use worldwide [56]. Additionally C47 was already assessed as antiandrogenic in the Tox21 AR-LUC MDAkb2 antagonist assay using a human breast cell line [53].

The antiandrogenic activity of the identified compounds was verified in the anti-AR-CALUX assay. The corresponding concentration-response curves are shown in the Figure B7. The contribution of the compounds to the antiandrogenic activity of the water extract was estimated from their concentrations determined by internal matrix-matched quantification by LC-HRMS and their relative potency values to flutamide in the anti-AR-CALUX assay. All values are displayed in the Table B6.

C47 was detected at a concentration of 13.7 µg/L, equal to 71.4 µg FEq/L, in the water extract (REF=1). The corresponding concentration-response curves of the water extract and

C47 are well in agreement (Figure 3-6). At the EC50 the compound was calculated to explain 157% of the water extracts total antiandrogenic activity, which is within the uncertainty of the method. The bioassay method uncertainty is estimated to be within one order of magnitude, in accordance with the variation expected for the main acceptance criteria of the bioassay i.e. the flutamide IC50 (1.1 - 10.7 × 10− 7 M) [43].

This is the first study reporting the high antiandrogenic activity of this compound with an EC50 of 23.2 µg/L and thus 5.2-fold higher potency than the reference compound flutamide.

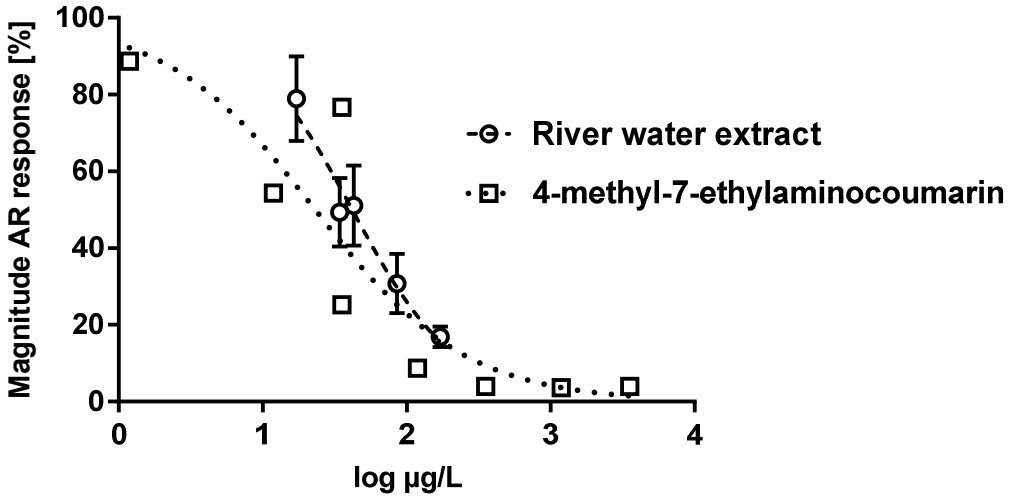

Figure 3-6 Magnitudes of AR response (%) versus concentrations of C47 in the antagonistic AR-CALUX assay. The C47 reference standard was tested in one and the water extract in three tests (error bars indicate the 95% confidence interval).

For the transformation product C47T1 an EC50 of 30.8 µg/L displayed a slightly lower antiandrogenic potency than its parent compound C47 but still exhibited a 3.7-fold higher potency than flutamide. The observed concentration in the water extract (REF=1) was 3.9 µg/L, equal to 14.5 µg FEq/L. It contributed to 31.8% of the extract total antiandrogenic activity. The potency of the transformation product C47T2 (EC50 371.1 µg/L) is 5.8-fold lower than the one of flutamide. It contributed only to 0.4% of the extract total antiandrogenic activity due to its comparatively low concentration of 1.1 µg/L, equal to 0.2 µg FEq/L, in the non-concentrated water extract.

3.3.5 spiggin-gfp medaka (RADAR assay)

The antiandrogenic activity of C47, C47T1 and C47T2 was confirmed at the organism level using the spiggin-gfp medaka model [41]. An initial range-finder experiment indicated that C47 at 10 mg/L was lethal to 90 % of the tested medaka fry after 24 h. C47T1 (10 mg/L) was lethal to 10 % of fry after 96 h and 10 % of fry were immobile following 96 h exposure to C47T2 at 10 mg/L. No toxicity was observable after 96 h exposure to any of the three molecules at 1 mg/L or 0.1 mg/L.

With the observed toxicity in mind, spiggin-gfp medaka fry were exposed to C47, C47T1 or C47T2 at 1 mg/L alone or at a range of concentrations from 1 mg/L to 0.1 mg/L in the presence of 17MT (Figure 3-7a). The two transformation products, but not C47, showed very weak pro-androgenic activity at 1 mg/L in the absence of 17MT. In the presence of 17MT, the transformation product C47T2 showed no antiandrogenic activity at any of the concentrations tested. However, both C47 and C47T1 demonstrated almost total inhibition of 17MT induced androgen axis activity at 0.1 mg/L and 0.5 mg/L respectively.

In light of the potent antiandrogenicity observed for C47 and C47T1, full concentration response curves were performed for these two molecules in addition to the reference androgen receptor antagonist flutamide (Figure 3-7b). The concentrations tested covered the full effect range from inactivity to complete inhibition of the 17MT induced fluorescence. Using the modelled curves, EC50 values were determined as: 62 µg/L, 32 µg/L and 69 µg/L for flutamide, C47 and C47T1 respectively, indicating that C47 is a more powerful inhibitor of androgen axis activity than flutamide. These results confirm the evaluation via the antiAR-CALUX assay. C47T1 showed a concentration-dependent antiandrogenic effect and a weaker antiandrogenic activity than C47. C47 displays an antiandrogenic effect already at concentrations equal to the concentration in the water extract at REF=1, thus suggesting an adverse impact of this compound on the aquatic ecosystem.

Figure B8 shows that C47 also exhibits a weak estrogenic activity in medaka, confirming results previously obtained *in vitro* with the Tox21 Era-BLA antagonist assay [53]. This indicates that in addition to the androgen receptor antagonism observed *in vitro* with the antiAR-CALUX assay, a second mechanism of antiandrogenicity may be present *in vivo*. Estrogens have previously been shown to inhibit androgen axis activity *in vivo* [41, 57, 58], presumably through their well-documented ability to upregulate aromatase expression [59]

resulting in increased conversion of androgens to estrogens and reducing the concentration of circulating androgens. Further studies will help to shed light on the relative importance of the two mechanisms of antiandrogenicity.

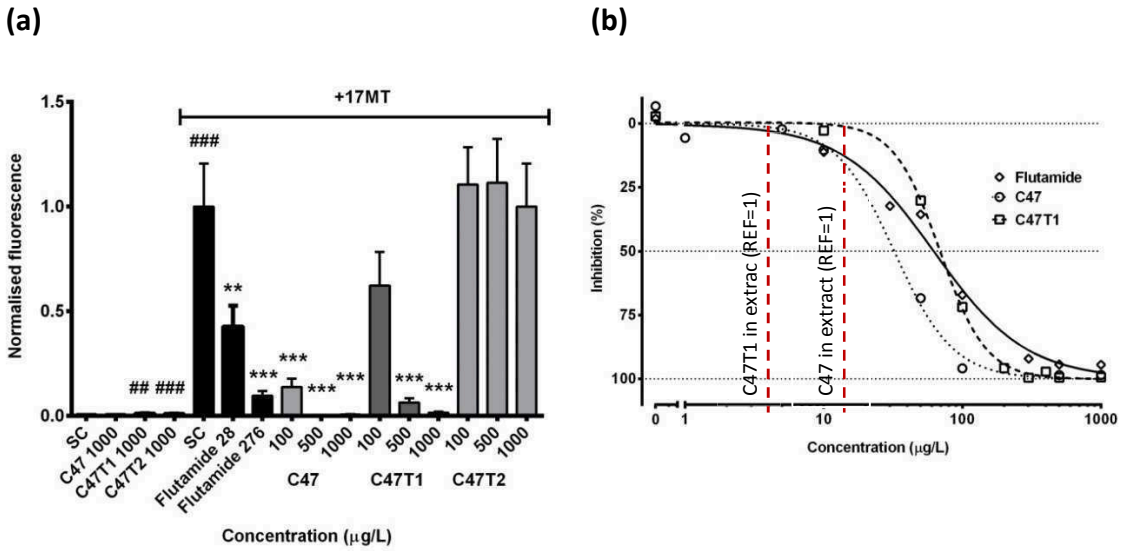

Figure 3-7 Fluorescent detection of antiandrogenic activity with the RADAR assay.
A: Confirmation of the in vivo antiandrogenic activity of C47 in spiggin-gfp medaka by inhibition of fluorescence production. Statistical significance in the absence of co-treatment, compared to the solvent control group (SC), is indicated by: ## (P < 0.01) and ### (P < 0.001). Statistical significance in the presence of 17-methyltestosterone (17MT), compared to the 17MT alone group (SC+17MT), is indicated by: ** (P < 0.01) and * (P < 0.001). Mean and standard error of the mean are shown.**
B: Full concentration-response curves for the two antiandrogenic contaminants (C47 and C47T1) compared to the reference antiandrogenic pharmaceutical flutamide. The graph indicates similar EC50s for flutamide and C47T1, but a lower EC50 for C47. All three molecules achieved complete inhibition of androgen dependent fluorescence production. The concentration of the two compounds in the non-concentrated water extract is marked by vertical lines.

3.4 Conclusion

The present study demonstrated the power of the novel EDA approach using parallel orthogonal fractionation procedures, miniaturized *in vitro* tests, state-of-the-art LC-HRMS/MS non-target techniques and organism level confirmation procedures to identify and confirm environmentally relevant endocrine disruptors in complexly contaminated water samples. This study is clearly underlining that not only effect-based monitoring of pro-

and antiandrogenic activity should be integrated into the water framework directive but also EDA as an important tool to identify endocrine disruptors in pollutes sites [60]. The identified compound C47 was demonstrated to be a highly potent environmental contaminant that acts as an androgen receptor antagonist. The antiandrogenic potency of C47 *in vivo* was demonstrated to be higher than that of the reference antiandrogenic pharmaceutical flutamide. This is of some concern since C47 is used in a number of consumer products, including bathroom air fresheners at concentrations up to 1 %. Screening of other molecules belonging to the coumarin class for endocrine activity is therefore recommended.

3.5 Acknowledgements

Thanks to Melis Muz for fruitful discussions concerning the non-target analysis. Thanks to Monika Lam, Jochen Kuckelkorn and Simone Hotz at RWTH for the support with the bioassays. Thanks to Tobias Schulz (UFZ, Leipzig, Germany) for his help concerning the fractionation apparatus and for processing the MassBank records. Thanks to BioDetection Systems BV (BDS, Amsterdam, The Netherlands) for supplying the cell line and respective culture and method protocols. Thanks to Promega GmbH, Germany, and to Tecan Group Ltd., Switzerland, for their contribution to this study as a partner of the Students Lab Fascinating Environment at Aachen Biology and Biotechnology (ABBt). Chemaxon (Budapest, Hungary) is acknowledged for providing an academic license of JChem for Excel. This study was mainly supported by the European FP7 Collaborative Project SOLUTIONS (grant agreement no. 603437) and partially supported by the EDA EMERGE ITN project within the EU Seventh Framework Program (FP7-PEOPLE-2011-ITN) under the grant agreement number 290100.

3.6 Literature

1. Sumpter, J.P., *Endocrine Disrupters in the Aquatic Environment: An Overview.* Acta hydrochimica et hydrobiologica, 2005. **33**(1): p. 9-16.
2. Hill, E.M., et al., *Profiles and Some Initial Identifications of (Anti)Androgenic Compounds in Fish Exposed to Wastewater Treatment Works Effluents.* Environmental Science & Technology, 2010. **44**(3): p. 1137-1143.
3. Soto, A.M., et al., *Androgenic and estrogenic activity in water bodies receiving cattle feedlot effluent in Eastern Nebraska, USA.* Environmental Health Perspectives, 2004. **112**(3): p. 346-352.
4. Grover, D.P., et al., *Endocrine disrupting activities in sewage effluent and river water determined by chemical analysis and in vitro assay in the context of granular activated carbon upgrade.* Chemosphere, 2011. **84**(10): p. 1512-1520.
5. Urbatzka, R., et al., *Androgenic and antiandrogenic activities in water and sediment samples from the river Lambro, Italy, detected by yeast androgen screen and chemical analyses.* Chemosphere, 2007. **67**(6): p. 1080-1087.
6. Weiss, J.M., et al., *Masking effect of anti-androgens on androgenic activity in European river sediment unveiled by effect-directed analysis.* Analytical and Bioanalytical Chemistry, 2009. **394**: p. 1385-1397.
7. Kinani, S., et al., *Bioanalytical characterisation of multiple endocrine- and dioxin-like activities in sediments from reference and impacted small rivers.* Environmental Pollution, 2010. **158**(1): p. 74-83.
8. Schmitt, C., et al., *In vivo effect confirmation of anti-androgenic compounds in sediment contact tests with Potamopyrgus antipodarum.* Journal of Environmental Science and Health, Part A, 2013. **48**(5): p. 475-480.
9. Rostkowski, P., et al., *Bioassay-Directed Identification of Novel Antiandrogenic Compounds in Bile of Fish Exposed to Wastewater Effluents.* Environmental Science & Technology, 2011. **45**(24): p. 10660-10667.
10. Katsiadaki, I., et al., *Field surveys reveal the presence of anti-androgens in an effluent-receiving river using stickleback-specific biomarkers.* Aquatic Toxicology, 2012. **122–123**: p. 75-85.
11. Milnes, M.R., et al., *Contaminant-induced feminization and demasculinization of nonmammalian vertebrate males in aquatic environments.* Environmental Research, 2006. **100**(1): p. 3-17.
12. Howell, W.M., D.A. Black, and S.A. Bortone, *Abnormal Expression of Secondary Sex Characters in a Population of Mosquitofish, Gambusia affinis holbrooki: Evidence for Environmentally-Induced Masculinization.* Copeia, 1980. **1980**(4): p. 676-681.
13. Milla, S., S. Depiereux, and P. Kestemont, *The effects of estrogenic and androgenic endocrine disruptors on the immune system of fish: a review.* Ecotoxicology, 2011. **20**(2): p. 305-319.
14. Jobling, S., Burn, R.W., Thorpe, K., Williams, R., Tyler, C., *Statistical modeling suggests that antiandrogens in effluents from wastewater treatment works contribute to widespread sexual disruption in fish living in English rivers.* Environmental Health Perspectives, 2009. **117**(5): p. 797-802.

15. Bayley, M., M. Junge, and E. Baatrup, *Exposure of juvenile guppies to three antiandrogens causes demasculinization and a reduced sperm count in adult males.* Aquatic Toxicology, 2002. **56**(4): p. 227-239.
16. Lor, Y., et al., *Juvenile exposure to vinclozolin shifts sex ratios and impairs reproductive capacity of zebrafish.* Reproductive Toxicology, 2015. **58**(Supplement C): p. 111-118.
17. Jenkins, R.L., et al., *Production of Androgens by Microbial Transformation of Progesterone in Vitro: A Model for Androgen Production in Rivers Receiving Paper Mill Effluent.* Environmental Health Perspectives, 2004. **112**(15): p. 1508-1511.
18. Ellis, R.J., et al., *In vivo and in vitro assessment of the androgenic potential of a pulp and paper mill effluent.* Environmental Toxicology and Chemistry, 2003. **22**(7): p. 1448-1456.
19. Kumar, V., C. Majumdar, and P. Roy, *Effects of endocrine disrupting chemicals from leather industry effluents on male reproductive system.* The Journal of Steroid Biochemistry and Molecular Biology, 2008. **111**(3): p. 208-216.
20. Runnalls, T.J., et al., *Pharmaceuticals in the Aquatic Environment: Steroids and Anti-Steroids as High Priorities for Research.* Human and Ecological Risk Assessment: An International Journal, 2010. **16**(6): p. 1318-1338.
21. Kirk, L.A., et al., *Changes in estrogenic and androgenic activities at different stages of treatment in wastewater treatment works.* Environmental Toxicology and Chemistry, 2002. **21**(5): p. 972-979.
22. Tan, B.L.L., et al., *Comprehensive study of endocrine disrupting compounds using grab and passive sampling at selected wastewater treatment plants in South East Queensland, Australia.* Environment International, 2007. **33**(5): p. 654-669.
23. Thomas, K.V., et al., *An assessment of in vitro androgenic activity and the identification of environmental androgens in United Kingdom estuaries.* Environmental Toxicology and Chemistry, 2002. **21**: p. 1456-1461.
24. Weiss, J.M., et al., *Identification strategy for unknown pollutants using high-resolution mass spectrometry: Androgen-disrupting compounds identified through effect-directed analysis.* Anal. Bioanal. Chem., 2011. **400**(9): p. 3141-3149.
25. Kiparissis, Y., et al., *Effects of the antiandrogens, vinclozolin and cyproterone acetate on gonadal development in the Japanese medaka (Oryzias latipes).* Aquatic Toxicology, 2003. **63**(4): p. 391-403.
26. Kojima, H., et al., *Screening for estrogen and androgen receptor activities in 200 pesticides by in vitro reporter gene assays using Chinese hamster ovary cells.* Environmental Health Perspectives, 2004. **112**(5): p. 524-531.
27. Parks, L.G., et al., *Masculinization of Female Mosquitofish in Kraft Mill Effluent-Contaminated Fenholloway River Water Is Associated with Androgen Receptor Agonist Activity.* Toxicological Sciences, 2001. **62**(2): p. 257-267.
28. Bandelj, E., et al., *Determination of the androgenic potency of whole effluents using mosquitofish and trout bioassays.* Aquatic Toxicology, 2006. **80**(3): p. 237-248.
29. Stalter, D., et al., *Ozonation and activated carbon treatment of sewage effluents: Removal of endocrine activity and cytotoxicity.* Water Research, 2011. **45**(3): p. 1015-1024.
30. Sousa, A., et al., *Chemical and Biological Characterization of Estrogenicity in Effluents from WWTPs in Ria de Aveiro (NW Portugal).* Archives of Environmental Contamination and Toxicology, 2010. **58**(1): p. 1-8.

31. Liscio, C., et al., *Methodology for profiling anti-androgen mixtures in river water using multiple passive samplers and bioassay-directed analyses.* Water Research, 2014. **57**(Supplement C): p. 258-269.
32. Ma, D., L. Chen, and R. Liu, *Removal of novel antiandrogens identified in biological effluents of domestic wastewater by activated carbon.* Science of The Total Environment, 2017. **595**(Supplement C): p. 702-710.
33. Brack, W., et al., *Effect-directed analysis supporting monitoring of aquatic environments — An in-depth overview.* Science of The Total Environment, 2016. **544**: p. 1073-1118.
34. Brack, W., *Effect-directed analysis: a promising tool for the identification of organic toxicants in complex mixtures.* Analytical and Bioanalytical Chemistry, 2003. **377**: p. 397-407.
35. Lübcke-von Varel, U., et al., *Polar compounds dominate in vitro effects of sediment extracts.* Environmental Science & Technology, 2011. **45**: p. 2384.
36. Thomas, K.V., et al., *Effect-Directed Identification of Naphthenic Acids As Important in Vitro Xeno-Estrogens and Anti-Androgens in North Sea Offshore Produced Water Discharges.* Environmental Science & Technology, 2009. **43**(21): p. 8066-8071.
37. Di Paolo, C., et al., *Downscaling procedures reduce chemical use in androgen receptor reporter gene assay.* Science of The Total Environment, 2016. **571**: p. 826-833.
38. Muz, M., et al., *Mutagenicity in Surface Waters: Synergistic Effects of Carboline Alkaloids and Aromatic Amines.* Environmental Science and Technology, 2017. **51**(3): p. 1830-1839.
39. Muz, M., et al., *Identification of Mutagenic Aromatic Amines in River Samples with Industrial Wastewater Impact.* Environmental Science & Technology, 2017. **51**(8): p. 4681-4688.
40. Brack, W., et al., *How to confirm identified toxicants in effect-directed analysis.* Anal.Bioanal.Chem., 2008. **390**: p. 1959-1973.
41. Sébillot, A., et al., *Rapid Fluorescent Detection of (Anti)androgens with spiggin-gfp Medaka.* Environmental Science & Technology, 2014. **48**(18): p. 10919-10928.
42. van der Burg, B., et al., *Optimization and prevalidation of the in vitro AR CALUX method to test androgenic and antiandrogenic activity of compounds.* Reproductive Toxicology, 2010. **30**(1): p. 18-24.
43. Di Paolo, C., et al., *Downscaling procedures reduce chemical use in androgen receptor reporter gene assay.* Science of The Total Environment, 2016. **571**(Supplement C): p. 826-833.
44. van der Linden, S.C., et al., *Development of a panel of high-throughput reporter-gene assays to detect genotoxicity and oxidative stress.* Mutation Research/Genetic Toxicology and Environmental Mutagenesis, 2014. **760**: p. 23-32.
45. Blaha, L.H., M.; Murphy, M.; Jones PD.; Giesy JP., *Procedure for determination of cell viability/cytotoxicity using the MTT bioassay.* 2004.
46. Di Paolo, C., et al., *p53 induction and cell viability modulation by genotoxic individual chemicals and mixtures.* Environmental Science and Pollution Research, 2017.
47. He, Y., et al., *Effect of Ozonation on the Estrogenicity and Androgenicity of Oil Sands Process-Affected Water.* Environmental Science & Technology, 2011. **45**(15): p. 6268-6274.

48. Escher, B.I., et al., *Toxic equivalent concentrations (TEQs) for baseline toxicity and specific modes of action as a tool to improve interpretation of ecotoxicity testing of environmental samples.* Journal of Environmental Monitoring, 2008. **10**(5): p. 612-621.
49. Pluskal, T., et al., *MZmine 2: Modular framework for processing, visualizing, and analyzing mass spectrometry-based molecular profile data.* Bmc Bioinformatics, 2010. **11**(1): p. 1-11.
50. Ruttkies, C., et al., *MetFrag relaunched: incorporating strategies beyond in silico fragmentation.* Journal of Cheminformatics, 2016. **8**(1): p. 3.
51. Schneider, C.A., W.S. Rasband, and K.W. Eliceiri, *NIH Image to ImageJ: 25 years of image analysis.* Nat Meth, 2012. **9**(7): p. 671-675.
52. Gulde, R., et al., *Systematic Exploration of Biotransformation Reactions of Amine-Containing Micropollutants in Activated Sludge.* Environmental Science & Technology, 2016. **50**(6): p. 2908-2920.
53. U.S.EPA. *(Environmental Protection Agency) 2017. Endocrine Disruptor Screening Program (EDSP). Available: http://www.epa.gov/endo/ [accessed 27 March 2017]*. 2017.
54. Shen, H.C., et al., *In Silico Discovery of Androgen Receptor Antagonists with Activity in Castration Resistant Prostate Cancer.* Molecular Endocrinology, 2012. **26**(11): p. 1836-1846.
55. Voet, A., et al., *The Discovery of Novel Human Androgen Receptor Antagonist Chemotypes Using a Combined Pharmacophore Screening Procedure.* ChemMedChem, 2013. **8**(4): p. 644-651.
56. Kandil, S., A.D. Westwell, and C. McGuigan, *7-Substituted umbelliferone derivatives as androgen receptor antagonists for the potential treatment of prostate and breast cancer.* Bioorganic & Medicinal Chemistry Letters, 2016. **26**(8): p. 2000-2004.
57. Jolly, C., et al., *Detection of the anti-androgenic effect of endocrine disrupting environmental contaminants using in vivo and in vitro assays in the three-spined stickleback.* Aquatic Toxicology, 2009. **92**(4): p. 228-239.
58. Katsiadaki, I., et al., *Use of the Three-Spined Stickleback (Gasterosteus aculeatus) As a Sensitive in Vivo Test for Detection of Environmental Antiandrogens.* Environmental Health Perspectives, 2006. **114**(Suppl 1): p. 115-121.
59. Hinfray, N., et al., *Brain and gonadal aromatase as potential targets of endocrine disrupting chemicals in a model species, the zebrafish (Danio rerio).* Environmental Toxicology, 2006. **21**(4): p. 332-337.
60. Brack, W., et al., *Towards the review of the European Union Water Framework Directive: Recommendations for more efficient assessment and management of chemical contamination in European surface water resources.* Science of The Total Environment, 2017. **576**: p. 720-737.

Chapter 4

Occurrence and distribution of 4-methyl-7-diethyl-aminocoumarin and two derivatives emitted from a point source in a small river

Abstract

Recently, the potent antiandrogen 4-methyl-7-diethylaminocoumarin (C47), as well as the derivatives 4-methyl-7-ethylaminocoumarin (C47T1) and 4-methyl-7-aminocoumarin (C47T2) were identified with effect-directed analysis of surface water from the River Holtemme in Germany. The aim of this study was to investigate the longitudinal and temporal distribution of C47 and its derivatives along the whole river stretch. In order to better understand sources and sinks, we investigated possible deviations from equilibrium partitioning between the compartments water, sediment and biota represented by the ubiquitous species *Gammarus pulex*. To this end, partition coefficients were determined experimentally and compared with estimates based on hydrophobicity suggesting cation binding as the driving force for deviations. The wastewater treatment plant (WWTP) of Silstedt was identified as a continuous source that is releasing these compounds in the gram per day range. Furthermore we verified the hypothesized transformation of C47 into C47T1 and C47T2 within the WWTP. The study was based on non-target LC-HRMS/MS data that were retrospectively analyzed highlighting the value of digital freezing LC-high resolution MS/MS data.

This chapter is a manuscript which will be submitted as:

Matthias Muschket, Liza-Marie Beckers, Pedro A. Inostroza, Tobias Schulze, Werner Brack, Martin Krauss: Occurrence and distribution of 4-methyl-7-diethyl-aminocoumarin and two derivatives emitted from a point source in a small river

4.1 Introduction

In a recent study we identified 4-methyl-7-diethylaminocoumarin (C47) as a potent antiandrogenic compound in surface water from the river Holtemme (Saxony-Anhalt, Germany). Simultaneously, two similar compounds 4-methyl-7-ethylaminocoumarin (C47T1) and 4-methyl-7-aminocoumarin (C47T2) were found and considered as likely transformation products of C47 [1] based on the fact than N-dealkylation is a commonly observed microbial transformation pathway [2]. Antiandrogenic effects of C47 have been observed without pre-concentration in the water extract, and to a lesser extent for C47T1 and C47T2 *in-vitro* in the cell-based antiAR-CALUX assay [3] and were confirmed *in-vivo* in spiggin-gfp *Medaka* [4].

Derivatives of coumarin can be found all over the plant kingdom [5] and are used in various consumer products, such as bathroom air fresheners, due to their olfactory properties. Synthetic coumarin, derivatives, particularly if substituted at position 7 with an electron donating group, such as the 7-aminocoumarins, exhibit strong fluorescence and thus are used as fluorescent probes and optical brighteners [6]. The occurrence and distribution of the three coumarin derivatives C47, C47T1 and C47T2 in the aquatic environment has not been described before in the literature. In the study of Loos et al. [7] C47 was among the target compounds, but could not be detected in surface waters from Northern Italy.

The aim of the present study was 1) to examine the longitudinal and temporal distribution of C47, C47T1 and C47T2 within the River Holtemme to unequivocally confirm the source and temporal variation and to get a first idea on persistence, 2) to determine concentrations of all three compounds in influent and effluent of the wastewater treatment plant (WWTP) through which these compounds are discharged into the river in order to test the hypothesis that C47T1 and C47T2 are formed from C47 in the WWTP and 3) to investigate the distribution among water, sediment and biota represented by *Gammarus pulex* in order to better understand sources and sinks in the river itself. To this end, we investigated possible deviations from equilibrium partitioning using experimentally determined partition coefficients as well as estimates based on hydrophobicity.

This analysis was carried on non-target full-scan LC-HRMS/MS data from the River Holtemme compiled over four years. While for C47 and C47T2 calibration standards had been measured simultaneously with all samples, the quantification of C47T1 was conducted retrospectively

with newly acquired calibration sets. To assess the comparability of simultaneous and retrospective calibration, we used the corresponding data for C47 and C47T2.

4.2 Material and Methods

4.2.1 Chemical and Reagents

The reference compounds 4-methyl-7-diethylaminocoumarin, 4-methyl-7-ethylaminocoumarin, 4-methyl-7-aminocoumarin, carbamazepine, metazachlor ethane sulfonic acid, 1H-benzotriazole, 4-methyl-1H-benzotriazole and the isotope-labelled internal standards bezafibrate-d4, atrazine-$^{13}C_3$, and imidacloprid-d4 were obtained from different sources and had a purity of >98%. LC-MS grade methanol, water, ethyl acetate, acetonitrile and formic acid were obtained from Sigma-Aldrich. Acetone, dichloromethane, hexane were of LC grade and supplied by Merck, magnesium sulfate and sodium chloride (both analysis grade) by Sigma-Aldrich, and primary-secondary amine (PSA) by Agilent.

4.2.2 Study area and sample overview

The River Holtemme has a length of 47 km and is a tributary to the River Bode located in Saxony-Anhalt, Germany (Figure 1). While its upper stretches are located in the forested Harz mountains national park, its lower stretches are characterized by intensive agriculture. The river passes through the towns of Wernigerode and Halberstadt, and receives effluents from two wastewater treatment plants (WWTPs) at Silstedt (60,000 population equivalent, serving Wernigerode and surrounding villages) and Halberstadt (60,000 population equivalents). To assess the contamination of the Holtemme with C47, C47T1 and C47T2 we analyzed water, sediment and *Gammarus pulex* samples from the sites given in Figure 4-1. Geographical names and coordinates of sampling sites are given in Table C1.

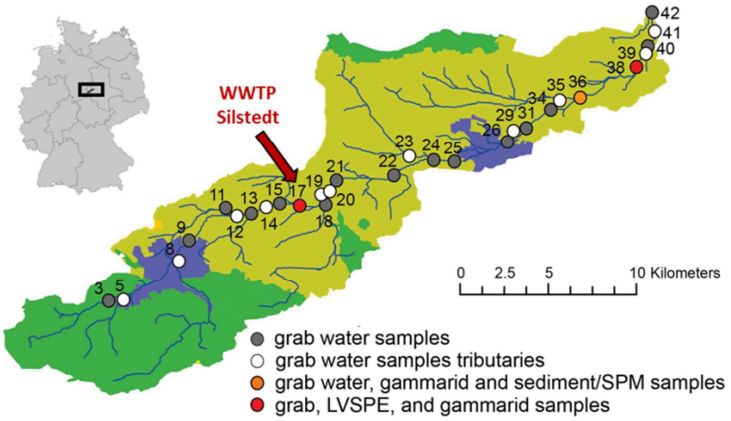

Figure 4-1 Map showing the Holtemme and the sampling sites. Sediment, *Gammarus pulex* and water samples using a LVSPE device were sampled at the sites marked in red. Grab samples of a water package were sampled along the whole river course at the sampling sites in grey. Green areas indicate forests; olive areas indicate agriculture areas and blue represents main settlements.

Table 4-1: Overview of the different sampling campaigns, dates and sites and information on the used calibration (LVSPE: large volume solid phase extraction of water).

Sampling campaign	Sample Type	Sample Date	Sampling Sites	Type of simultaneous calibration for C47 and C47T2	Type of retrospective calibration for all compounds
#1	Grab water Sample	6-Oct-2015	Holtemme River: 3, 9, 11, 13, 15, 17, 18, 21, 22, 24, 25, 26, 31, 34, 36, 38, 40, 42 Tributaries: 5, 8, 12, 14, 19, 20, 23, 29, 35, 39, 41	Matrix-matched, direct injection	Matrix-matched, direct injection
#2	Grab water Sample	9/10-Oct and 12/13-Okt-2017	Influent and Effluent of WWTP Silstedt	Matrix-matched, direct injection	Matrix-matched, direct injection
#3	LVSPE	monthly, Mar until Nov 2014	3, 17, 38	Method- and matrix-matched by small-scale SPE	Method- and matrix-matched by small-scale SPE
#4	LVSPE	monthly, Mar until Nov 2015	3, 17, 38	Method- and matrix-matched by small-scale SPE	Method- and matrix-matched by small-scale SPE
#5	LVSPE	monthly, Mar until Nov 2016	3, 17, 38	Method- and matrix-matched by small-scale SPE	Method- and matrix-matched by small-scale SPE
#6	Sediment /SPM	7-Apr-2016	17, 36, 38	Method- and matrix-matched	Solvent calibration considering recovery, matrix effects are accounted for by IS
#7	Gammarus	7-Apr-2016	17, 36, 38	Method- and matrix-matched	Solvent calibration considering recovery, matrix effects are accounted for by IS

4.2.3 Sampling and sample preparation

4.2.3.1 LVSPE sampling of surface water

Time-proportional composite water samples (28 days) were taken using on-site large volume solid phase extraction (LVSPE) [8] over three years during March to November (Table 1). To this end, 100 L of water were extracted on site using 10 g of Chromabond HR-X (Machery-Nagel) within 14 days, and samples of two consecutive 14 day intervals were combined. The sampling frequency for each sub-sample was 100 min (site 17) or 60 min (sites 3, 38), respectively. Prior to extraction, the water was filtered using glass fiber deep filters (pore size 0.63 µm, Sartopure GF+ MidiCap, Sartorius) to remove suspended particulate matter (SPM). Each cartridge was eluted in the laboratory after drying with a nitrogen stream and freeze-drying according to Välitalo et al. [9]. In brief, cartridges were sequentially eluted with 100 mL of ethyl acetate, 100 mL of methanol, 100 mL of methanol containing 1% formic acid and finally 100 mL of methanol containing 2% 7N ammonia in methanol. Combined extracts were reduced to a final concentration factor of 1000 and neutralized to pH 7 ± 0.5. Afterwards, the eluate was filtered through GF/F (Whatman) filters to remove residual precipitates and stored at -20 °C. The final equivalent concentration was 1 L extracted water per 1 mL extract. Machine blanks were prepared simulating a 200 L sample as detailed in Schulze et al. [8]. For LC-MS/MS and LC-HRMS analysis a 100 µL aliquot was transferred into a 2 mL autosampler vial with glass insert, 60 µL of water, 30 µL of methanol, and 10 µL of an internal standard mixture (1 µg/mL in methanol) were added.

4.2.3.2 Grab Sampling of surface water

To assess the longitudinal concentration profile of the River Holtemme, grab samples were taken on 6 Oct, 2015 at 18 sites along the whole river course by following the same water package downstream, thus synchronizing sampling with the flow velocity. In addition, 11 tributaries and the effluents of the Silstedt and Halberstadt WWTPs were sampled.

Aliquots of 1 mL were transferred into 2 mL auto-sampler vials and stored at -20°C. Prior to analysis, 25 µL of an internal standard mixture in methanol, containing isotope-labelled compounds at 40 ng/mL, 25 µL of methanol, and 10 µL of 2 M ammonium formate buffer (pH 3.5) were added.

4.2.3.3 Sampling of WWTP influent and effluent

From the influent and effluent of the WWTP Silstedt, twelve consecutive two hour composite samples were taken on 9/10 Oct. 2017 and 12/13 Oct. 2017, respectively, accounting for the hydraulic retention time of 72 hours. Each sample was composed from sub-samples taken every 2 min by an automatic sampler used in the routine monitoring by the WWTP operator. Samples were stored at -20°C. For analysis, sample aliquots of 20 µL were diluted 50-fold in LC-MS grade water, and the internal standard mixture, methanol and buffer were added as for the surface water samples.

4.2.3.4 Gammarus pulex

Gammarus pulex was sampled in April 2016 according to a protocol by Hering et al. [10] at the sites 17, 36 and 38 (Table 4-1). In brief, 20 habitat-weighted samples were taken from an area of one m^2 at each site with a Surber sampler (500 µm mesh size). A subset of 24 specimens with different size classes was collected to avoid bias caused by different ages and stored at -20°C. Homogenisation was carried out by pulverized liquid extraction [11] and the extraction procedure followed a modified QuEChERS protocol according to Inostroza et al. [12]. In brief, 900 mg of thawed gammarids were homogenized in 4 mL of acetonitrile:water (1:1 *v/v*), mixed with 200 mg of NaCl and 800 mg of anhydrous $MgSO_4$ and shaken for 1 min. Following centrifugation (4000 × *g*, 5 minutes), 3.5 mL of the acetonitrile phase were transferred to a glass vial containing 50 mg of primary-secondary amine for clean-up and 400 mg of anhydrous $MgSO_4$. The vials were vortexed for 60 s and centrifuged at 4000 × *g* for 5 min. The supernatant was concentrated at room temperature under a nitrogen stream to dryness, reconstituted in 500 mL of methanol and filtered with a PTFE syringe filter (pore size 0.45 µm, Phenomenex).

4.2.3.5 Sediment

Using a stainless-steel scoop, sediment was collected on 7th of April 2016 from the top 5 cm of 10 points within an area of 5 m^2 at sampling site 36, where a sedimentation zone is created by a weir. Beyond site 36 and a nearby located second weir no further sedimentation zones exist and the river bottom is characterized by large stones. Thus, we used stainless steel traps [13] at sites 17 and 38 to collect suspended particulate matter

(SPM) as a proxy between 9th of March and 7th of April 2016. Samples were transported to the laboratory in cooling boxes at 4°C. Sediment was homogenized overnight, freeze dried, sieved to <63mm and stored at -20°C. Total organic carbon content (TOC) was determined according to DIN 19539 (2016) by solid combustion using a LECO C-230 Carbon Analyser. Samples were extracted by pressurized liquid extraction (Dionex ASE 200) followed by clean-up steps according to Massei et al. [14] with minor modifications [15]. In brief, 5 g of the freeze-dried samples were extracted twice at 100°C using a mixture of ethyl acetate and acetone (50:50). Two blanks (diatomaceous earth) were processed in parallel to verify the absence of contaminations. Clean-up by normal-phase chromatography was done using an alumina/silica gel column. Ethyl acetate/acetone extracts were mixed with deactivated silica gel and evaporated to dryness by a rotary evaporator. The silica was loaded onto the alumina/silica gel column and eluted with hexane, dichloromethane and methanol. The mixed dichloromethane/methanol fraction was evaporated close to dryness, re-dissolved in 1 mL of methanol and filtered with cellulose acetate syringe filter (pore size 0.45 µm). For quantification an internal standard mixture at a level of 100 ng mL^{-1} in vial was added.

4.2.4 LC-HRMS analysis

Analysis of environmental samples for C47, C47T1 and C47T2 was performed with an UltiMate 3000 LC system coupled to a quadrupole-Orbitrap instrument (QExactive Plus), equipped with a heated electrospray ionization (ESI) source (all from Thermo). A Kinetex EVO C18 column (50 x 2.1 mm, 2.6 µm particle size, Phenomenex) with a pre-column (C18 EVO, 5 x 2.1 mm) and a 0.2 µm inline filter was used for chromatographic separation in a column oven set to 40°C. For the direct injection of water samples, injection volume was 100 µL, for LVSPE, sediment and gammarid extracts, it was 5 µL. The mobile phase gradient used is shown in Table C2. MS analysis was carried out in positive ion mode in the mass range of m/z 100-1000 at a nominal resolving power of 70.000 (referenced to m/z 200) and data-independent (DIA) MS/MS experiments at a nominal resolving power of 35,000. For DIA isolation windows of 50 mass units (i.e., m/z ranges 97-147, 144-194, 191-241, 238-288, 285-335, 332-382, 379-429, 426- 476) and 280 mass units (i.e., m/z ranges 460-740, 730-1010) were used. Peak integration, calibration and quantification were carried out in TraceFinder 3.2 (Thermo).

Grab water samples in the longitudinal profile of the whole river stretch for carbamazepine, metazachlor ethane sulfonic acid, 1H-Benzotriazole and the sum of 4+5-Methyl-1H-benzotriazole (which could not be distinguished) were analyzed using a HPLC system (Agilent 1260 Infinity) coupled to a tandem mass spectrometer (QTrap 6500, AB Sciex) with an electrospray ionization (ESI) source, all controlled by the Analyst software (version 1.6.2). Details are described in [16].

Method detection limit (MDL) were obtained based on replicate analyses of samples of the same concentration using spiking levels that were 5 to 10 times higher than the lowest detected concentration of the compound [17]. The MDL of the directly injected and extracted water samples was between 2.7 and 6.2 ng/L and between 0.4 and 1.2 ng/L, respectively (Table C3). The MDL ranged from 5.0 to 8.0 ng/g TOC in sediment and from 0.2 to 0.3 ng/g wet weight in *Gammarus pulex*.

4.2.5 Simultaneous and retrospective quantification

While a simultaneous quantification for C47 and C47T2 could be carried out, as calibration standards were already run during the sample analysis (as part of a larger compound mixture), C47T1 had to be quantified by retrospective analysis, i.e., the samples measured up to two years earlier were quantified with newly measured calibration standards. To assess the performance of this approach, we compared the concentrations derived retrospectively (c_{retro}) and simultaneously (c_{sim}) for C47 and C47T2 by calculating the deviation according to equation 1:

$$Deviation\ [\%] = \left|\left(\frac{c_{retro} \cdot 100}{c_{sim}}\right) - 100\right| \qquad \text{eq. 4-1}$$

Additionally, a triplicate analysis of the calibration standards (see below) was done with at least 4 weeks distance of time in between the measurements to calculate the variability of the retrospective quantification of C47, C47T1 and C47T2.

Bezafibrate-d4, atrazine-$^{13}C_3$ and imidacloprid-d4 were used as internal standards for C47, C47T1 and C47T2, respectively to correct for matrix effects. Different sets of calibration standards were prepared for grab water samples, for samples collected by LVSPE and for sediment and *Gammarus pulex* samples, as shown in Table 4-1.

Based on the results of these comparisons (section 4.1), concentrations in the individual samples were calculated for C47 and C47T2 using the simultaneous calibration and for C47T1 using the retrospective calibration, which was corrected by the average deviation of C47 and C47T2 between the simultaneous and retrospective calibration.

4.2.5.1 Calibration for direct LC-HRMS analysis of grab water samples and WWTP influent/effluent

For both simultaneous and retrospective matrix-matched calibration we used 1 mL of water from a pristine stream in the upper Harz Mountains (Wormsgraben). We added 25 µL of diluted standard solutions of C47, C47T1 and C47T2 in methanol to yield calibration standards at 1, 2, 5, 10, 20, 50, 100, 200, 500, 1000, 2000, 5500 and 9000 ng/L of the analytes. To each vial, 25 µL of internal standard mixture (40 ng/mL) and 10 µL of a 2 M ammonium formate buffer (pH 3.5) were added. All solutions were stored at -20^{o}C.

4.2.5.2 Calibration for samples collected by LVSPE

For simultaneous and retrospective method- and matrix-matched calibration of the LVSPE extracts, we used a laboratory-scale SPE procedure. A mixed stock solution in methanol was spiked into Wormsgraben water to yield 250 mL with a concentration of 0.1, 0.5, 1, 2, 5, 10, 20, 50, 100, 200, 500, 1000, 2000 and 5000 ng/L.

Cartridges containing 200 mg of Chromabond® HR-X were conditioned with 5 mL of ethyl acetate, 5 mL of methanol and 10 mL of LC-MS grade water before the extraction by SPE to match the sample preparation procedure. Elution was done with 5 ml of ethyl acetate and 2 mL of methanol containing 1% formic acid, followed by 2 mL of methanol containing 2% 7N ammonia in methanol. All extracts were evaporated to dryness under nitrogen and reconstituted to 250 µL in methanol to obtain a concentration factor of 1000. 100µL aliquots of each extract were spiked with 10 µL of the internal standard mixture (1 µg ml^{-1}) and brought to a final volume of 200 µL methanol/water (70:30) for analysis.

4.2.5.3 Calibration for extracts of sediment and Gammarus pulex

For simultaneous, method-matched calibration of sediments, analyte standards were spiked into ethyl acetate:acetone (simulating the PLE extracts) at levels corresponding to 0.1, 0.2, 0.5, 1, 2, 5, 10, 20, 50, 100, 200 and 500 ng/mL final concentration in vial and processed as sediment extracts as described above. For simultaneous, method-matched calibration of

gammarids, the analytes were spiked into 900 µL of water (simulating the gammarids) at the same levels as for sediments and processed as the *Gammarus* samples (described above).

For retrospective calibration of C47T1 in sediments and *Gammarus*, we decided against the laborious method-matched calibration and prepared calibration standrds by dilution in methanol. To this end, the stock solution was diluted in methanol to yield concentrations of 0.1, 0.2, 0.5, 1, 2, 5, 10, 20, 50, 100, 200 and 500 ng/mL and 100 ng/mL of the internal standard mixture were added. While the matrix effects were accounted for by the internal standard calibration, we had to correct the obtained values by the recoveries over the sample processing procedure. We thus assumed recoveries for C47T1 between those for C47 and C47T2 due to the structural similarity. For quantification in *Gammarus pulex* the recoveries were 90% for C47 and 88% for C47T2, thus we used 89% forC47T1. For the quantification in sediment the recovery was 67% for C47 and 72% for C47T2, thus we used a recovery of 70% for the extraction of C47T1.

4.2.6 Elimination rates

The elimination rates Eli_{CD} of the coumarin derivatives (CD) along the 13-km river stretch between the effluent of the WWTP of Silstedt and Halberstadt were calculated in relation to the persistent carbamazepine (CBZ) according to Kunkel and Radke [18] by equation 4-2.

$$Eli_{CD} = \left(1 - \frac{\frac{\sum c_{CD,Site\ B}}{\sum c_{CD,Site\ A}}}{\frac{\sum c_{CBZ,Site\ B}}{\sum c_{CBZ,Site\ A}}}\right) \cdot 100\% \qquad \text{eq. 4-2}$$

The concentration of the coumarin derivative at site A and B is represented by $c_{CD,Site\ A}$ and $c_{CD,SiteB}$ respectively whereas $c_{CBZ,\ SiteA/B}$ is indicates the concentration of CBZ at these locations.

4.2.7 Freely dissolved concentrations

Freely dissolved water concentrations $c_{fd,W}$ were assumed to be equivalent to the measured water concentration $c_{m,W}$ due to the DOC-poor Holtemme river water.

The freely dissolved concentration in sediment $c_{fd,S}$ was derived by applying equation (4-3) where $c_{m,S}$ is the measured sediment concentration, f_{OC} is representing the organic carbon fraction in sediment and K_{OC} the partitioning constant between the sediment organic carbon and pore-water.

$$c_{fd,S} = \frac{c_{m,S}}{f_{OC} \cdot K_{OC}} \quad \text{eq. 4-3}$$

Freely dissolved concentrations in *Gammarus pulex* $c_{fd,G}$ were calculated from measured concentrations $c_{m,G}$ using eq. 4-4 assuming only the lipid f_{Lipid} and protein fraction $f_{Protein}$ as relevant phases for an absorption of micropullutants. K_{LW} is representing the lipid water and K_{PW} the protein water partitioning constant.

$$c_{fd,G} = \frac{c_{m,G}}{1 + f_{Lipid} \cdot K_{LW} + f_{Protein} \cdot K_{PW}} \quad \text{eq. 4-4}$$

K_{OC}, as well as the partitioning constant between octanol and water (K_{OW}) were predicted by EPI Suite v4.11 (US EPA, 2012) [19]. K_{LW} and K_{PW} were derived according to equation (4-5) [20] and (4-6) [21], respectively.

$$K_{LW} = K_{OW} \quad \text{eq. 4-5}$$

$$K_{PW} = 0.05 \cdot log K_{OW} \quad \text{eq. 4-6}$$

4.2.8 Experimental determination of sediment K_{OC} values

Sediment-water K_{OC} values of C47, C47T1 and C47T2 were determined in a batch sorption experiment. To this end, sediment from the Saale river near Calbe with a similar OC content (65 g/kg) not containing any residues of these compounds was used.

The experiments were set up for each compound individually at five concentration levels by adding 0.1, 0.5, 2, 10, and 50 µg into a glass centrifuge tube with PTFE-lined screw cap containing 0.5 g of sediment (< 63 µm) and 10 mL of 0.005 M $CaCl_2$ solution. The sediment had been previously equilibrated with the $CaCl_2$ solution for 24 hours. Samples were shaken during the whole exposure time of 168 hours on a horizontal shaker at 60 rpm. Control samples without sediment were set up for all compounds. At 4, 8, 24, 72 and 168 hours of exposure at 20°C, the tubes were centrifuged at $5000 \times g$ for 5 minutes and aliquots of 15 or 30 µL were taken from each vial using a pipette. We considered this small removal of volume as negligible for the calculations. For analysis, aliquots were diluted appropriately in LC-MS grade water and 5 volume-% of methanol were added.

Samples were analysed by ESI-LC-MS/MS using an Agilent 1260 LC coupled to an ABSciex QTrap 6500 MS, which was operated in positive ion mode. Two MS/MS transitions for each compound recorded in selected reaction monitoring mode. For details on LC and MS conditions see appendix C1.3. For calibration, mixed standards of all compounds were prepared in LC-MS grade water at 15 levels between 1 and 50,000 ng/L. Five volume-% of methanol were added for analysis.

Sediment-water partitioning constants K for C47, C47T1 and C47T2 at the sorption times (t_S) of 4, 8, 24, 72 and 168 hours were derived by equation 4-7 and are displayed in Figure C4.

$$K = \frac{c_{m,S}}{c_{m,W}} \cdot f_{OC} \qquad \text{eq. 4-7}$$

The K_{OC} values for the sediment-water partitioning in equilibrium were derived by fitting the results to the exponential equation 4-8.

$$K = K_{OC} \cdot (1 - e^{-b \cdot t_s}) \qquad \text{eq. 4-8}$$

4.3 Results and Discussion

4.3.1 Performance of the retrospective calibration

The deviation of the retrospective and simultaneous quantification was compared for C47 and C47T2 for the different sets of samples investigated, the results are shown as an overview in Figure C1 (Appendix). The retrospective quantification led to an overestimation of the concentrations of in average 11% (C47) and 17% (C47T2) in non-concentrated water samples, 29% (C47) and 45% (C47T2) in LVSPE processed water samples, 12% (C47) and 16% (C47T2) in samples of *Gammarus pulex* whereas the concentrations within sediment were retrospectively underestimated by about 31% (C47) and 80% (C47T2).

The differences between retrospective and simultaneous calibration show that the performance of the instrumental analysis changes over time, which is not surprising, as LC columns deteriorate with increasing use resulting in a stronger peak tailing, and a contamination of the MS with sample residues resulting in decreasing sensitivity. While a regular cleaning of the ion source and rinsing of the column was performed, a more intense cleaning of the ion lens system and a change of the LC column was done only at specific intervals. Thus, for a retrospective calibration, the instrument performance state is randomly different from the one during the simultaneous calibration, which results in a variability of about 18% (Table C4) as indicated by the triplicate injection of the same calibration standards with a four week time span in between.

Isotope-labelled internal standards with different structure but similar retention time to coumarin derivates were used throughout the study to minimize the impact of different instrument performance. Observed differences between simultaneous and retrospective calibration might stem therefore from the fact that analytes and internal standards are likely differently affected by the instrument performance. This is likely the case for the directly injected water samples and the LVSPE samples, for which a matrix- and method-matched calibration was carried out. Obviously, systematic, unintentional differences between the sample preparation methods (e.g., stock solution preparation errors, dosing errors, etc.) might also contribute to a deviation. In case of the sediment and gammarid samples, we used a calibration prepared in solvent rather than a method-matched one. Here, the observed deviations are somewhat larger, suggesting that an additional variation is added through different matrix effects and the use of a single average recovery values for correcting for compound losses during sample preparation.

Overall, the results suggest that within a typical error margin of about 20-30% a retrospective quantification of compounds from LC-HRMS screening data is possible. To obtain a more comparable dataset, we calculated concentrations of C47 and C47T2 using the simultaneous calibration and of C47T1 using the retrospective calibration, which was corrected by the average deviation of C47 and C47T2 between the simultaneous and retrospective calibration for the individual datasets.

4.3.2 Longitudinal concentration profile

Water from the River Holtemme was sampled synchronized with the water flow at 18 sites. These samples together with the samples from 11 tributaries were analyzed to determine the longitudinal concentration profile of the three coumarin derivatives along the whole river stretch from the town of Wernigerode to the confluence with the river Bode 42 km further downstream. As shown in Figure 4-2, C47 and its two derivatives were detected along the whole river course downstream of the WWTP Silstedt (17) along with high concentrations of the wastewater marker compounds carbamazepine, benzotriazole, and 4+5-Methyl-1H-benzotriazole. Thus the WWTP Silstedt was clearly the source of discharge into the river. Correspondingly, all three compounds were detected in the effluent from the WWTP Silstedt at concentrations of 1.0 (C47), 1.2 (C47T1) and 1.6 µg/L (C47T2). In contrast to the effluent form the WWTP Silstedt, none of the compounds could be detected in the effluent of the WWTP Halberstadt, consequently no concentration increase was observed as for the three wastewater marker compounds.

In nine of the eleven tributaries, also none of the coumarin derivatives could be detected, while in some of them the wastewater markers benzotriazole, methylbenzotriazole and carbamazepine indicate an input of municipal wastewater (Figure C2). The two tributaries furthest downstream (39 and 41) contained levels similar to those of the Holtemme along with the three wastewater markers. These tributaries are connected upstream to the Holtemme, thus the water samples there is stemming probably to a large extent form the Holtemme itself.

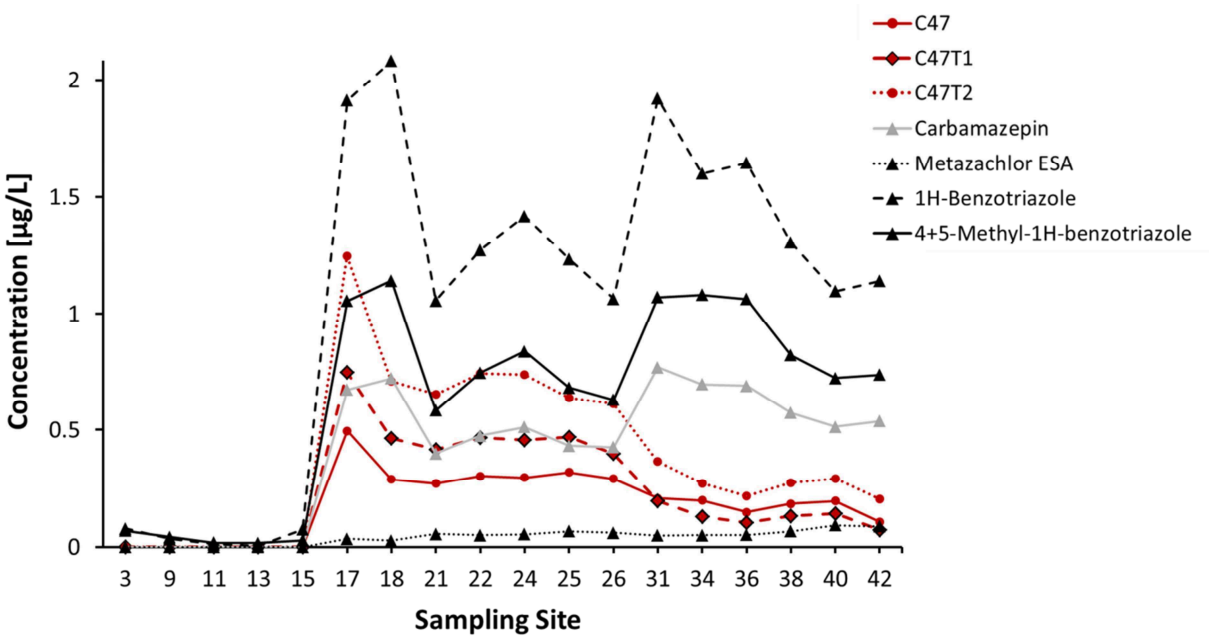

Figure 4-2 Concentration profiles of C47, C47T1, C47T2, the persistent wastewater tracers carbamazepine, 4+5-Methylbenzotriazole and Benzotriazole, as well as the groundwater marker Metazachlor ESA in the longitudinal profile of the Holtemme on 06 Oct 2015.

The concentrations of C47, C47T1 and C47T2 decrease by about 47% between sites 17 and 26. In order to understand the underlying process we calculated the elimination rates relative to the persistent marker carbamazepine for this river. The concentration profile of CBZ as a measure for the percentage of WWTP effluent in the Holtemme water discharged by the WWTP Silstedt was in good agreement with concentration profiles of other wastewater effluent markers such as 4+5-methylbenzotriazole and benzotriazole, as shown in Figure 4-2. Thus, C47, C47T1 and C47T2 concentrations were normalized to CBZ according to equation 4-2 in order to compensate for dilution. Normalized values lower than one indicate attenuation by transformation [18], sorption to sediment, SPM, biofilms and other biota [22, 23] or evaporation. Low relative elimination rates between the site 17 and the reverence site 26 of C47 (8%), C47T1 (16%) and C47T2 (22%) indicate dilution to be the main cause of the strong concentration decrease. Along this stretch, the concentration of metazachlor ethane sulfonic acid (ESA) increased from 33.9 ng/L at site 17 to 59 ng/L at site 26, suggesting that the diluting water contained substantial concentrations of this compound. As it was not detected in any of the tributaries contributing in this river stretch, and the ESA transformation products of chloroacetanilide herbicides are well-known groundwater contaminants in agricultural areas [24], this suggest that an inflow of groundwater is the main cause of this dilution. Additionally the concentration gradient

between the pollutants in the WWTP effluent and the uncontaminated surface water is supporting the fast dilution of the WWTP plume within about 5 km of the river stretch between site 17 and 21. Downstream between sites 21 and 26 no further reduction of C47 and CBZ concentrations was observed, while the concentrations of C47T1 and C47T2 slightly decreased by 5 and 6%, respectively, which is well within the analytical uncertainty. In contrast, higher elimation rates between sites 31 and 42 of C47 (26%), C47T1 (46%) and C47T2 (19%) indicate that the attenuation especially of C47T1 in this river stretch is not solely based on dilution.

In general, C47 and its derivatives show only a limited elimination due to photodegradation, biotransformation or sorption in the Holtemme which was also supported by the low solar irradiation during the sampling on a cloudy day in October and the absence of a significant hyporheic zone in the Holtemme which is known to be of crucial relevance for microbial transformation in rivers [18].

4.3.3 Seasonal variation in LVSPE samples

The temporal concentration variations were assessed from 96 28-day composite samples that were collected in spring, summer and autumn from 2014 to 2016 by LVSPE upstream of Wernigerode (site 3), downstream of the WWTP Silstedt (17) and at Nienhagen (38). Within these three years none of the coumarin derivatives could be detected at site 3. At site 17 and 38, all three compounds were present in all samples, with higher concentrations at site 17 than in the corresponding sample at site 38 (Figure 4-3). This suggests a continuous emission of these compounds from the WWTP Silstedt. Concentrations at site 17 varied within a factor of 5 to 10 for each compound within each year and average concentrations were in the same order of magnitude observed in the longitudinal profile on 6 Oct 2016 (1.6 vs. 0.5 µg/L for C47, 0.8 vs. 0.7 µg/L for C47T1 and 0.7 vs. 1.2 µg/L for C47T2). No trend within the concentration profiles between the seasons or the three years could be observed. In contrast, the concentrations ratios of the three compounds, especially that of C47 to C47T2 showed a large variation, e.g. in 2015 it was varying between 0.8 and 36.9 at site 17 (Figure C3). These findings suggest either the release of a mixture into the WWTP containing a varying composition of the three coumarins or a varying transformation efficiency of the WWTP Silstedt (assuming that C47T1 and C47T2 are formed there from C47 during biological treatement).

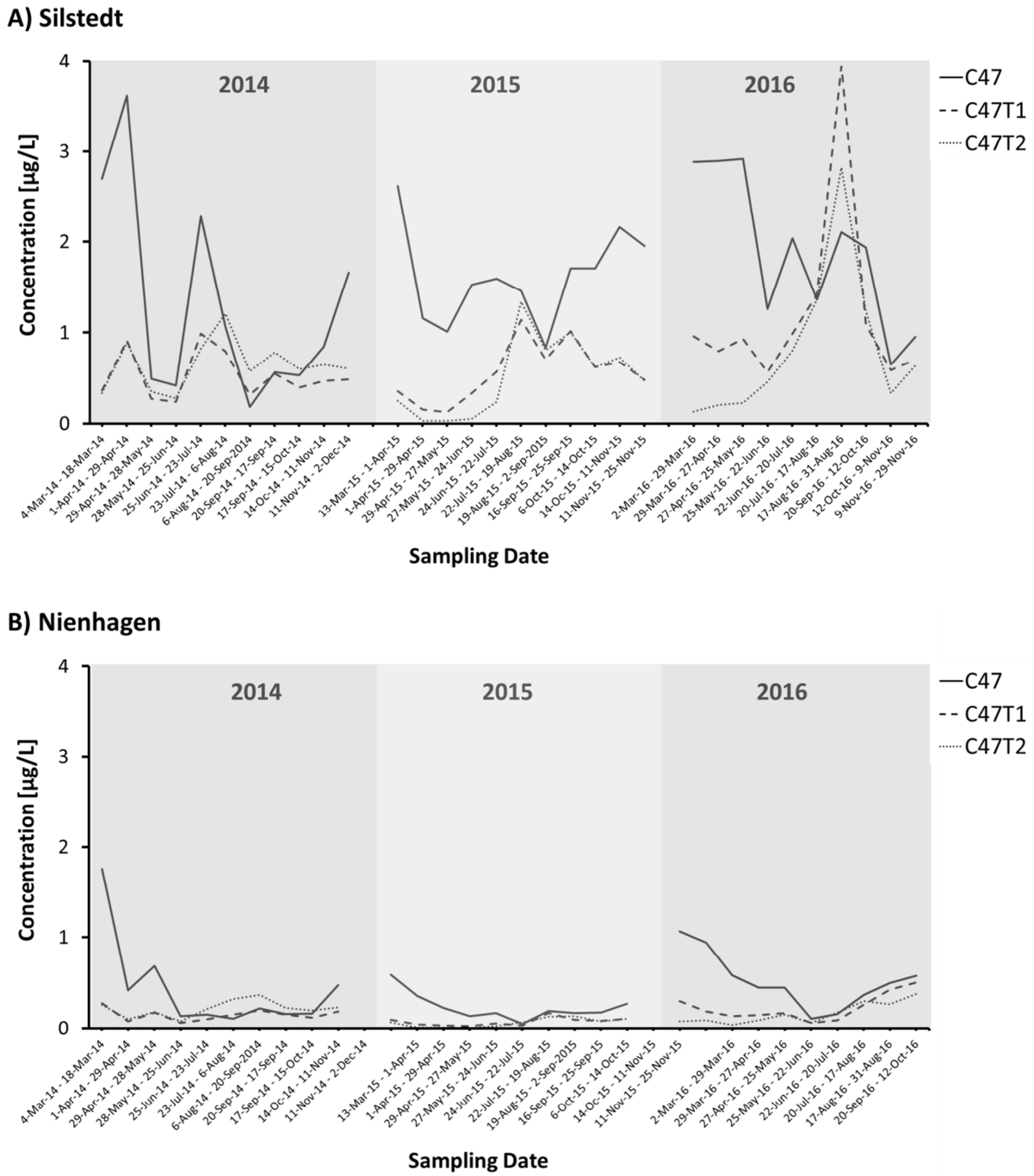

Figure 4-3 Temporal concentration profile in 28 days composite LVSPE samples of C47, C47T1 and C47T2 collected at Silstedt (17) and Nienhagen (38) between 2014 and 2016.

4.3.4 Transformation in the WWTP Silstedt

The well-known transformation of secondary and tertiary amines by N-dealkylation in activated sludge [2] raised the hypothesis that C47T1 and C47T2 are originating from such a transformation of C47 within the WWTP Silstedt. To this end, the influent to the WWTP Silstedt was sampled at the 9 Oct 2017 in 2 hour intervals and the corresponding effluent on 12 Oct 2017 accounting for the hydraulic retention time of 72 hours (Figure 4-4). The

representativeness of the effluent was checked based on the concentrations of the coumarin derivatives in the river water downstream of the WWTP effluent discharge, which were in the same order of magnitude as the monthly average samples from this site taken between 2014 and 2016: the concentrations of C47, C47T1 and C47T2 at site 17 were 1.6, 0.7 and 0.7 µg/L, respectively.

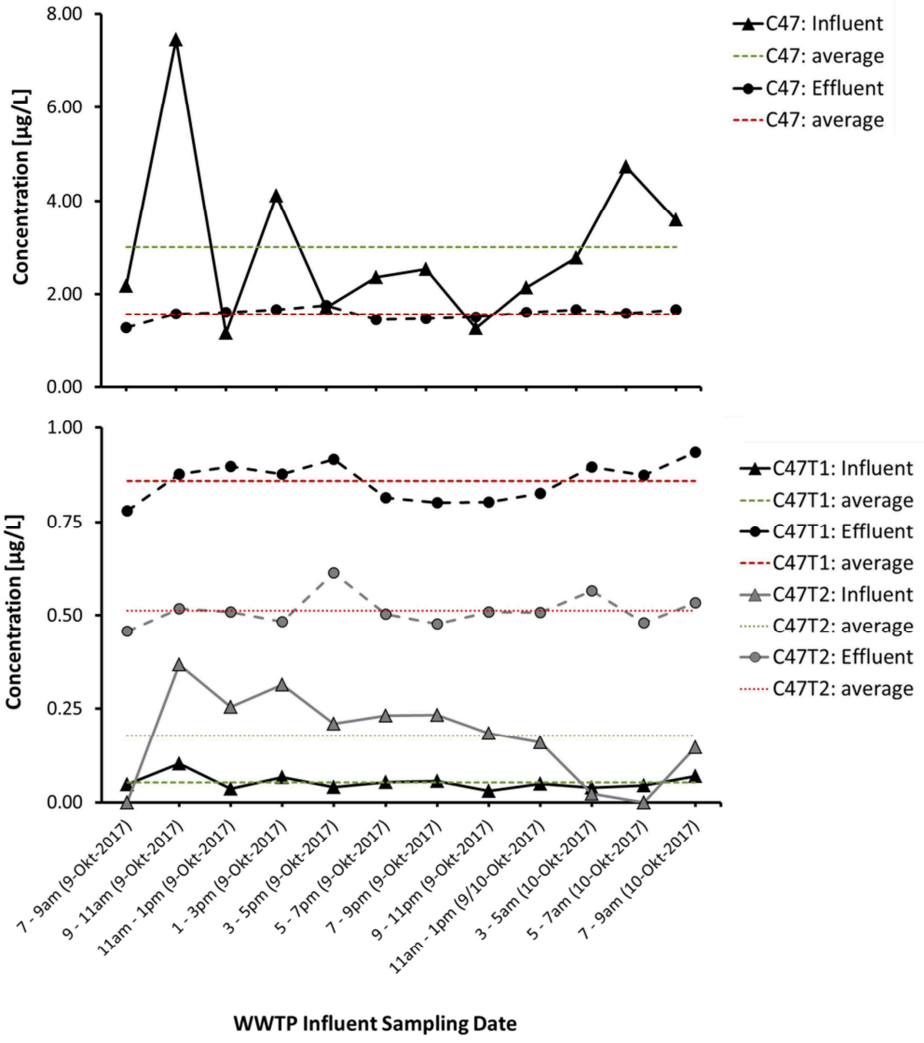

Figure 4-4 Concentration profiles of (A) C47 and (B) C47T1 and C47T2 in the influent (continuous line) and the effluent (dashed line) of the WWTP Silstedt in march 2017. Effluent was sampled 72 hours after the influent to account for the hydraulic retention time of the WWTP.

The fluctuation of coumarin concentrations in the two-hour influent samples was leveled out to a large extent in the effluent, as it could be expected for a well-mixed WWTP system with a large hydraulic retention time. The suspected biotransformation of C47 is confirmed by the decrease of the average concentration from 3.0 to 1.6 µg/L during the WWTP passage

treatment and the simultaneously occurring concentration increase of C47T1 (from 0.1 to 0.9 µg/L) and C47T2 (from 0.2 to 0.5 µg/L). Applying a molar concentration balance approach of the average concentrations on 9 Oct 2017 shows that the transformed amount of C47 (65.9 mmol/L of 137.8 mmol/L in the influent) can be well explained by the formed amounts of C47T1 (formation of 42.1 mmol/L) and C47T2 (formation of 20.4 mmol/L).

4.3.5 Water/sediment distribution and uptake into *Gammarus pulex*

In order to get an understanding of the fate of the coumarins in the Holtemme the distribution between water, sediment (or suspended particulate matter, SPM) and biota (*Gammarus pulex*) was analyzed using equilibrium partitioning theorie (EqP) [25]. Freely dissolved concentrations of the coumarins in the three environmental compartments were calculated according to eq. 4-3 to 4-6 for the sites downstream of the WWTP Silstedt (17), Gross Quenstedt (36) and Nienhagen (38). While *Gammarus pulex* and sediment at site 36 was sampled on 7 Apr 2016 upsteam of a weir creating a sedimentation zone [26], SPM was collected between 9th of March and 7th of April 2016 at site 17 and 38 using stainless steel traps. In order to avoid a bias of the evaluation by potential variations of the water concentrations, the concentrations determined by LVSPE from 29 Mar to 27 Apr 2016 were used for these calculations. As no LVSPE samples were available for site 36, the concentration from the nearby site 38 was used, as in the stretch in between no significant tributaries are located.

Based on the predicted K_{OW} values of C47 (1660), C47T1 (151) and C47T2 (14) the by eq. 4-4 calculated average ratio of the freely dissolved concentrations between gammarid and water is 0.1, 12.1 and 14.4 for C47, C47T1 and C47T2, respectively (Figure 4-5a). Thus, all coumarins are near equilibrium partitioning at all sampling sites since activity ratios in a range of 0.1 – 10 are expected to reflect conditions close to equilibrium [15]. Hence, the body burden of *Gammarus pulex* can be estimated from water concentrations of the coumarins applying EqP. An impact of cation exchange on the sorption to sediment was considered possible as for other aromatic amines [27], which is currently not covered in common K_{OC} prediction models based on structure [28]. Thus, partition coefficients between sediment organic matter and water (K) at initial water concentration of the three coumarin derivatives of 0.01, 0.05 and 5 µg/mL were estimated after exposure in between 4 and 168 hours in a batch sorption experiment by eq. 4-7. K values showed a strong increase within

the first 72 hours of sorption time to sediment, while the increase was much smaller up to 168 hours, suggesting that the system was close to equilibrium after 168 hours (Figure C4). Partitioning coefficients between sediment organic matter and water in equilibrium (K_{OC}) were derived from fitted K values applying eq. 4-8 (Table C5). K_{OC} values were higher for lower initial concentrations of all three compounds, indicating on a strong concentration-dependency of sorption. This strong concentration dependency of partitioning constants may be caused by sorption sites with different affinity for cation exchange, as already reported in the literature [27, 29]. Thus, we did not use a single K_{OC} value for each compound to determine freely dissolved concentrations in the sediment porewater, but calculated these from non-linear sorption isotherms based on the measured sediment concentrations. These nonlinear isotherms were approximated using the Freundlich equation which showed a good fit of the data (Figure C5).

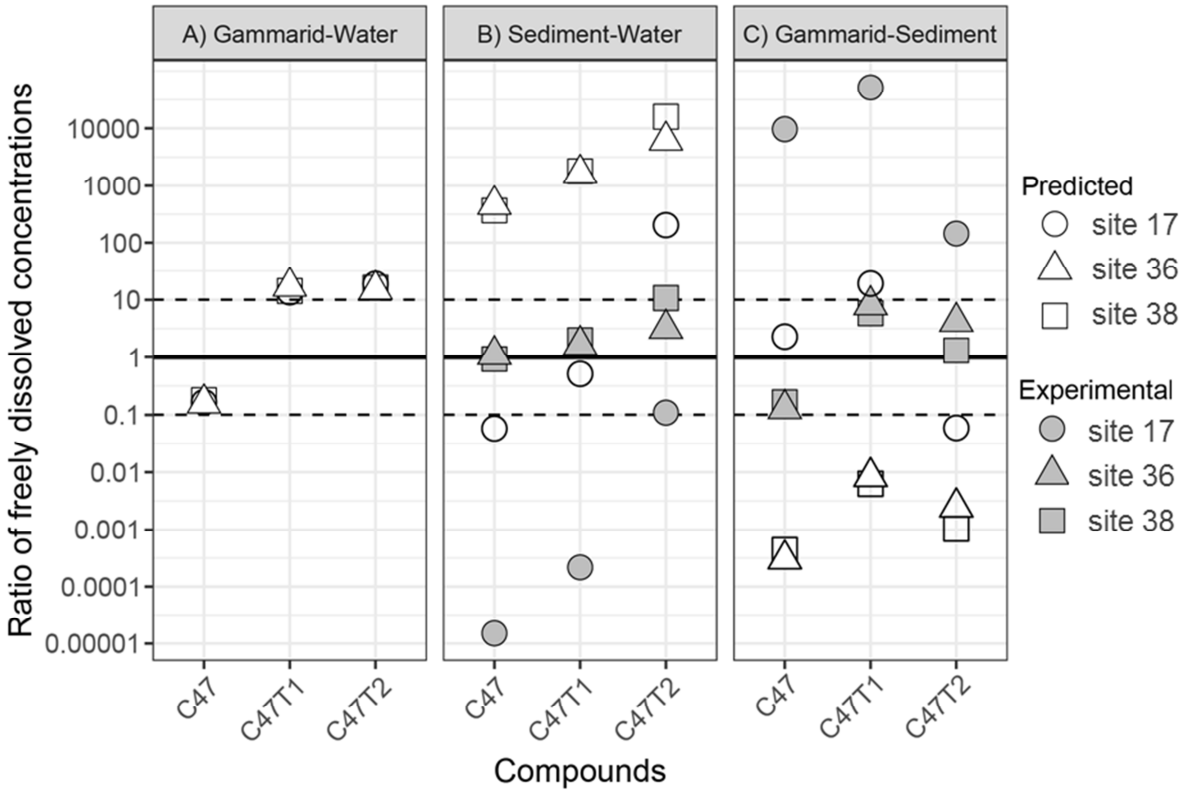

Figure 4-5 Ratio of calculated freely dissolved concentrations in gammarid tissues ($c_{fd,B}$ (lipid, protein)), water ($c_{fd,\ W}$) and sediment ($c_{fd,\ S}$) when assuming partitioning only between gammarid lipid and protein fractions, water and the sedimentary organic matter for C47, C47T1 and C47T2 in the Holtemme river. Ratios were calculated for sites 17, 36 and 38 on the basis of predicted and experimental derived Koc values. Equilibrium partitioning is considered in the range of 0.1 ≤ ratio ≤ 10.

The partitioning of the coumarins between sediment and water is close to equilibrium in the sedimentation zone at site 36 and at site 38 (Figure 4-5b). In contrast, ratios of the freely dissolved concentrations of 2 x 10^{-5} (C47), 2 x 10^{-4} (C47T1) and 0.1 (C47T2) document non-equilibrium conditions for C47 and C47T1 close to the WWTP Silstedt at site 17. This suggests a contact time of the coumarins with the trapped SPM that is not sufficient to reach equilibrium of partitioning at this site with high coumarin concentrations in the water phase. For C47T1 and especially for C47T2 a trend of the partitioning towards high ratios of freely dissolved concentrations between sediment and water up to 11.8 (Table C6) is most likely caused by N-dealkylation of C47 within the sediment pore water resulting in increasing amounts of its transformation products. In general, low water concentrations support the partitioning to sediment. A very similar picture was observed for the partitioning of the compounds between gammarid and sediment (Figure 4-5c). Again, all coumarins are close to equilibrium of partitioning downstream of the River Holtemme at sites 36 and 38. However, high ratios of the freely dissolved concentrations with values of 8 x 10^3 (C47), 6 x 10^4 (C47T1) and 1 x 10^2 (C47T2) proof non-equilibrium conditions at site 17.

Alternatively to the described experimental determination, partitioning constants can be generated more straight forward by prediction models, as recently reported for a wide set of emerging, polar micropollutants in a study of Inostroza et al. [15]. However, the Koc values predicted by EPI Suite (US EPA, 2012) [19] for C47, C47T1 and C47T2 between water and sediment deceed the concentration dependent K_{OC} values, derived by the batch sorption experiment, for an initial water concentration of 5 and 0.01 µg/mL in average 24 and even 92 times, respectively (Table C5). This leads to a completely reversed in-situ picture of the coumarin distribution between sediment and water, as well as between gammarid and sediment: conditions close to equilibrium partitioning are identified for C47 and C47T1 at site 17 if predicted Koc values are considered for the calculations (Figure 4-5). In contrast, 332 (C47), 1510 (C47T1) and even 12988 (C47T2) times higher freely dissolved concentrations in sediment than in water are received at site 38 which was identified as in equilibrium of partitioning by consideration of the reliable, experimentally derived Koc values (Table C6). These observations clearly underline that K_{OW} based prediction models are not appropriate to evaluate the partitioning of aromatic amines between water and sediment. This is an inherent drawback of these approaches since coulomb interactions are by far the most potent intermolecular forces. Their massive influence on the partitioning of

sulfonamides to soil organic matter [27] or on the sorption of other aromatic amines to soil even at pH values greater than pK_a+2 [29] was already demonstrated. Furthermore, biased predictions may be attributed to the presence of strongly adsorbing black carbon in the sediment, as found in Lake Michigan [30].

4.4 Conclusion

The WWTP of Silstedt was identified as the source that is continuously discharging the antiandrogens C47, C47T1 and C47T2 in the gram per day range into the River Holtemme. This is leading constantly to water concentration in the low µg/L range at all sites downstream the river course. It was shown, that the attenuation of coumarins in the river is mainly caused by dilution while transformation was of minor importance. Even within the WWTP Silstedt, the hypothesized N-dealkylation of C47 to the less potent but still antiandrogenic active C47T1 and C47T2 was incomplete thus pointing on their high persistency. In addition to water, sediment and biota was analyzed in order to observe the fate of contamination. Experimentally derived partition constants between water and sediment exceeded the estimates based on hydrophobicity up to 92-fold thus suggesting ionic interactions. Not only sediment but also the model macroinvertebrate *Gammarus pulex* was identified as a sink of the coumarin derivatives. Even if emission of C47 and its derivatives to the Holtemme ceases, the sediment might act as a long-term source of contamination [31].

4.5 Acknowledgments

This work was supported by the European FP7 Collaborative Project SOLUTIONS (grant agreement no. 603437). We thank Jörg Ahlheim, Aleksandra Piotrowska and Margit Petre for their help concerning the sampling and extraction of sediment and *Gammarus pulex* samples.

4.6 Literature

1. Muschket, M., et al., *Identification of Unknown Antiandrogenic Compounds in Surface Waters by Effect-Directed Analysis (EDA) Using a Parallel Fractionation Approach.* Environmental Science & Technology, 2018. **52**(1): p. 288-297.
2. Gulde, R., et al., *Systematic Exploration of Biotransformation Reactions of Amine-Containing Micropollutants in Activated Sludge.* Environmental Science & Technology, 2016. **50**(6): p. 2908-2920.
3. Di Paolo, C., et al., *Downscaling procedures reduce chemical use in androgen receptor reporter gene assay.* Science of The Total Environment, 2016. **571**(Supplement C): p. 826-833.
4. Sébillot, A., et al., *Rapid Fluorescent Detection of (Anti)androgens with spiggin-gfp Medaka.* Environmental Science & Technology, 2014. **48**(18): p. 10919-10928.
5. Lacy, A. and R. O'Kennedy, *Studies on Coumarins and Coumarin-Related Compounds to Determine their Therapeutic Role in the Treatment of Cancer.* Current Pharmaceutical Design, 2004. **10**(30): p. 3797-3811.
6. Kitamura, N., et al., *Synthesis, absorption, and fluorescence properties and crystal structures of 7-aminocoumarin derivatives.* Journal of Photochemistry and Photobiology A: Chemistry, 2007. **188**(2): p. 378-386.
7. Loos, R., G. Hanke, and S.J. Eisenreich, *Multi-component analysis of polar water pollutants using sequential solid-phase extraction followed by LC-ESI-MS.* Journal of Environmental Monitoring, 2003. **5**(3): p. 384-394.
8. Schulze, T., et al., *Assessment of a novel device for onsite integrative large-volume solid phase extraction of water samples to enable a comprehensive chemical and effect-based analysis.* Science of The Total Environment, 2017. **581-582**: p. 350-358.
9. Välitalo, P., et al., *Effect-based assessment of toxicity removal during wastewater treatment.* Water Research, 2017. **126**(Supplement C): p. 153-163.
10. Hering, D., et al., *Overview and application of the AQEM assessment system.* Hydrobiologia, 2004. **516**(1): p. 1-20.
11. Miller, T.H., et al., *Pharmaceuticals in the freshwater invertebrate, Gammarus pulex, determined using pulverised liquid extraction, solid phase extraction and liquid chromatography–tandem mass spectrometry.* Science of The Total Environment, 2015. **511**: p. 153-160.
12. Inostroza, P.A., et al., *Body burden of pesticides and wastewater-derived pollutants on freshwater invertebrates: Method development and application in the Danube River.* Environmental Pollution, 2016. **214**: p. 77-85.
13. Schulze, T., et al., *The German Environmental Specimen Bank - sampling, processing, and archiving sediment and suspended particulate matter.* Journal of Soils and Sediments, 2007. **7**(6): p. 361-367.
14. Massei, R., et al., *A sediment extraction and cleanup method for wide-scope multitarget screening by liquid chromatography–high-resolution mass spectrometry.* Analytical and Bioanalytical Chemistry, 2018. **410**(1): p. 177-188.
15. Inostroza, P.A., et al., *Chemical activity and distribution of emerging pollutants: Insights from a multi-compartment analysis of a freshwater system.* Environmental Pollution, 2017. **231**(Part 1): p. 339-347.

16. Beckers, L.-M., et al., *Characterization and risk assessment of seasonal and weather dynamics in organic pollutant mixtures from discharge of a separate sewer system.* Water Research, 2018. **135**: p. 122-133.
17. US-EPA, *Definition and Procedure for the Determination of the Method Detection Limit.* 40 CFR 17 Part 136, Appendix B to Part 136 Revision 1.11, 2011.
18. Kunkel, U. and M. Radke, *Fate of pharmaceuticals in rivers: Deriving a benchmark dataset at favorable attenuation conditions.* Water Research, 2012. **46**(17): p. 5551-5565.
19. US EPA (2012): Estimation Program Interface Suite, v., *Estimation Program Interface (EPI) Suite (TM) for Microsoft Windows, v 4.11 United States Environmental Protection Agency, Washington, DC, USA*. 2007, United States Environmental Protection Authority.
20. Schwarzenbach, R.P., P.M. Gschwend, and D.M. Imboden, *Environmental Organic Chemistry*. 2003, Hoboken, New Jersey: John Wiley & Sons, Inc.
21. deBruyn, A.M.H. and F.A.P.C. Gobas, *The sorptive capacity of animal protein.* Environmental Toxicology and Chemistry, 2007. **26**(9): p. 1803-1808.
22. Radke, M., et al., *Dynamics and Attenuation of Acidic Pharmaceuticals along a River Stretch.* Environmental Science & Technology, 2010. **44**(8): p. 2968-2974.
23. Kunkel, U. and M. Radke, *Reactive Tracer Test To Evaluate the Fate of Pharmaceuticals in Rivers.* Environmental Science & Technology, 2011. **45**(15): p. 6296-6302.
24. Huntscha, S., et al., *Input Dynamics and Fate in Surface Water of the Herbicide Metolachlor and of its Highly Mobile Transformation Product Metolachlor ESA.* Environmental Science & Technology, 2008. **42**(15): p. 5507-5513.
25. Di Toro, D.M., et al., *Technical basis for establishing sediment quality criteria for nonionic organic chemicals using equilibrium partitioning.* Environmental Toxicology and Chemistry, 1991. **10**(12): p. 1541-1583.
26. Inostroza, P.A., et al., *Anthropogenic Stressors Shape Genetic Structure: Insights from a Model Freshwater Population along a Land Use Gradient.* Environmental Science & Technology, 2016. **50**(20): p. 11346-11356.
27. Richter, M.K., et al., *Cation Binding of Antimicrobial Sulfathiazole to Leonardite Humic Acid.* Environmental Science & Technology, 2009. **43**(17): p. 6632-6638.
28. MacKay, A.A. and D. Vasudevan, *Polyfunctional Ionogenic Compound Sorption: Challenges and New Approaches To Advance Predictive Models.* Environmental Science & Technology, 2012. **46**(17): p. 9209-9223.
29. Li, H., et al., *Role of pH in partitioning and cation exchange of aromatic amines on water-saturated soils.* Chemosphere, 2001. **44**(4): p. 627-635.
30. Burkhard, L.P., P.M. Cook, and M.T. Lukasewycz, *Organic Carbon−Water Concentration Quotients (Πsocs and πpocs): Measuring Apparent Chemical Disequilibria and Exploring the Impact of Black Carbon in Lake Michigan.* Environmental Science & Technology, 2008. **42**(10): p. 3615-3621.
31. Brack, W., et al., *Bioassay-directed identification of organic toxicants in river sediment in the industrial region of Bitterfeld (Germany) - A contribution to hazard assessment.* Archives of Environmental Contamination and Toxicology, 1999. **37**: p. 164-174.

Chapter 5

Summary

A great variety of endocrine disruptors has been identified and is frequently present in environmental mixtures of typically thousands of compounds. The objective of this PhD study was to develop and apply an efficient approach to support effect-directed analysis of effect drivers in a water sample posing antiandrogenic activity. In case of the identification of so far unknown endocrine disrupting chemicals, an assessment of their fate within the aquatic ecosystem of the German river Holtemme and their behavior during the wastewater treatment should be done.

To this end, a novel fractionation approach using four orthogonal reversed stationary phases was established in Chapter 2. In chapter 3, this method was applied in the frame of an EDA study to unravel the effect drivers at a hotspot of antiandrogenicity found close to a WWTP in the German river Holtemme, which is a typical small European stream that is impacted by agriculture, municipal and industrial wastewater, as well as urban runoff [1]. The bioactivity of the fractions was determined using a miniaturized luciferase reporter gene cell-based anti-AR-CALUX assay [2]. For chemical analysis state-of-the-art LC-HRMS/MS non-target techniques including *in silico* fragmentation prediction, pH-dependent LC retention time shift and hydrogen-deuterium exchange were applied to unravel the identity of unknown effect drivers. The potent antiandrogenic activity of the identified "unknowns" was confirmed *in vivo* in spiggin-gfp Medaka. In Chapter 4, the temporal and longitudinal distribution of the three identified antiandrogens along the whole river course was investigated by a retrospective analysis of LC-HRMS/MS data. Moreover their source, transformation and distribution in the aquatic ecosystem between water, sediment and biota were examined. Finally, the estimated partitioning constants between sediment and water were compared with experimentally derived ones to gain insights into the driving force of sorption to sediment.

The results of each chapter are summarized in the following sections, discussed in detail and placed in the context of the current state of research. Gaps in knowledge that require further research are identified.

5.1 Liquid chromatography high resolution mass spectrometry: A powerful technique to characterize complex environmental mixtures

Aquatic organisms are exposed to numerous man-made androgens and antiandrogens [3] potentially resulting in adverse effects on the exposed organisms itself or even its progeny [4, 5]. Amongst others, adverse impacts on the immune system of fish were demonstrated [6], as well as the feminization of fish [7, 8] and non-mammalian vertebrate males [9, 10]. Identified sources that are releasing (anti-)androgens into the aquatic environment are paper mill effluents [11], pulp mills [12, 13], the leather industry [14] or wastewater treatment plants [15-19]. The structure of androgens and antiandrogens is extremely diverse. In freshwater systems identified androgens include chlorinated pesticides such as DDE and lindane [3], fungicides like vinclozolin [20] or the steroid nandrolone [21]. Detected antiandrogens are the disinfectant chloroxylenol [22], the insecticide isofenphos [23], the fungicide dichlorophene [22] or bisphenol A which is one of the chemicals with the highest production volume worldwide [24]. Even though these compounds are often present at subnanogram per liter concentrations they can still cause essential endocrine disrupting effects in the organism due to bioconcentration. Despite a large list of hundreds of known (anti-)androgens, the presence of a large number of unknown ones in the environment is to be assumed and need to be identified. LC-HRMS has emerged as a powerful technique to detect water-soluble contaminants. However, only a limited number of compounds for LC-MS screening has so far been included in existing structural databases like MassBank [25], which are consequently containing only a negligible proportion of the 100,000 substances used daily alone in the EU. Hence target screening approaches are neither sufficient to detect the growing number of (anti-)androgens nor to ensure a high quality of European water bodies in general [26].

Chemical non-target analysis is a promising method to overcome the limitation of target and suspect screening [27]. The challenge of this approach is the identification of individual toxicants and thus relevant peaks within environmental samples that are typically containing thousands of compounds [28]. A general difficulty in non-target screening that is hampering structure elucidation is the enormous amount of structures that can be assigned to the detected masses even in case of using HRMS which is usually allowing for a precise assignment of molecular formulae according to accurate mass and isotopic pattern. To

simplify this proverbial search for the needle in the haystack within highly complex LC-HRMS/MS data different prioritization techniques have been applied to identify "unknowns".

A straight forward approach is the focus on contaminants containing halogen atoms posing distinct isotope patterns since biological activity has been frequently related to halogens in the molecular structure [29]. The presence of these elements is helping to significantly limit the otherwise often hardly manageable number of candidate structures [30-32]. Diagnostic derivatization is an alternative technique for data prioritization [33] and was successfully applied, among others, to detect and identify aromatic amines in river water [34, 35]. Often intensity thresholds are set since no evaluable but for compound identification essential fragment spectra can be expected from peaks under device-specific minimal peak intensities [36, 37]. Moreover a focus on predominant signals can be promising [32] since high peak intensities are often related to high concentrations and thus to relevant pollutions. However, this relation does not always apply due to analyte specific, often strongly differing ionization efficiencies in conjunction with sample matrix effects possibly leading to ion suppression or enhancement [38].

All these prioritization techniques run empty if the often unknown analyte of concern, that is exhibiting a certain activity, is not even detected. Thus, a fundamental challenge for compound identification using LC-MS, especially for non-target screening approaches, are co-eluting isobaric compounds resulting in "humps" rather than individual, "clean" peaks thus hampering the very first step of HRMS data analysis which is typically a software based detection of individual peaks. This is where fractionation comes into play since it can significantly reduce sample complexity and thus decisively support the peak picking algorithms if a separation system tailored to the separation problem is used. This challenge is the objective of chapter 2 and will be discussed in the following section.

5.2 Compound class specific fractionation of EDCs on orthogonal stationary phases with a focus on androgens and antiandrogens

Solely in a few cases of EDA a sequence of fractionation steps with different stationary phases has been applied to reduce complexity [39] despite the significant increase of separation power through the use of MDLC [40]. Within this study, three stationary phases

(octadecyl-, aminopropyl- and pyrenyl ethyl-modified silica phases) were identified from a set of 17 columns as those exhibiting the highest degree of orthogonality for the separation of a set of 39 EDCs. The hydrophilic character of these compounds excludes the use of rather nonpolar solvents like hexane or dichloromethane applied in classical NPC or the use of an high initial percentage of organic modifier as applied in hydrophilic interaction chromatography (HILIC) that can be classified as “mixed-mode” chromatography [41]. Thus, RPC was applied using methanol - water mixtures as the mobile phase to avoid the risk of precipitation of a big portion of water soluble, hydrophilic compounds within hydrophobic NPC solvents. Moreover, RPC displays numerous advantages over NPC. It is best understood which facilitate the method development, it provides an outstanding separation power, is flexible concerning the analytes that shall be separated and is much more reproducible then NPC [42]. Furthermore RPC is compatible to mass spectrometry which enables to perform an online split of the volatile eluate between the fraction collector and a mass detector to generate HRMS data simultaneously with the fractionation.

In order to prove the potential of the novel fractionation approach to generate “clean” peaks a water sample extract showing antiandrogenic activity was separated on the selected three columns and additionally on a pentafluorophenyl column based on promising results in the literature [43]. Particular attention was paid to the compatibility of the separation system with effect-directed analysis. The in this context usually performed sequential fractionation approach [28] is very time consuming since all fractions are subjected to typically long-lasting bioassays and the planning of every new cycle of the multidimensional fractionation is based on the biotest results. Additionally, compound losses in each step may accumulate during the procedure (e.g., three consecutive fractionation-concentration steps with each 70% recovery will result in an overall recovery of a compound of just 34% after the third step), lowering the chances of identification. Thus, a new parallel fractionation approach was developed that is exploiting the different selectivity of orthogonal RP phases but avoiding the shortcomings of sequential fractionation procedures.

One inherent drawback of this approach is the complication of the data analysis since the basic principle of compound identification is not any more the focus on the reduced set of peaks that are classically left after repeated cycles of fractionation within the bioactive fraction(s) but a restriction to those peaks that the toxic fractions isolated on different columns have in common. In this context it is very challenging to identify on the one hand

those peaks that are characteristic for the active fractions and on the other hand non-specific peaks that are also present in various non-active fractions. However, even after the setting of a peak area threshold of minimal 5×10^6 a.u. in the non-fractionated water extract, only 60% of the peaks were detected in one, but 14% in two or three consecutive fractions and 21% even in unrelated ones. This is raising the question how to distinguish between characteristic, “clean” non-target peaks, within the background noise false positively picked peaks and isobars with different chemical structures that were separated during the fractionation but are coeluting on the analytical scale C18 phase prior to the mass spectrometric detection thus belonging to unrelated fractions. To make things even more complicated, the peak detection itself may be hampered by the applied parallel fractionation approach since “clean” but broad peaks are possibly not detected within all consecutive fractions due to strongly varying matrix effects that may substantially decrease the analytes ionization efficiency in some but not all analyte containing fractions. Moreover peak detection might be biased by coeluting isobars in some fractions that are leading to huge peak humps.

The consideration of fragment ion spectra would be extremely helpful to support the differentiation between false positive and relevant common peaks within the toxic fractions. However, this cannot be achieved manually for tens of thousands of peaks and software for this purpose is not available, yet. Furthermore, the results suggest to improve existing peak picking algorithms. Automated peak picking with available algorithms is always a compromise between sensitive settings to avoid false negative detection of small and noisy peaks including the substantial risk of peak picking within the background noise or more rigorous settings to predominantly detect peaks with good shapes and high intensity to prevent false positive picking [44]. MDLC with its sophisticated techniques for online coupling of the separation dimensions is clearly superior to the parallel fractionation approach with regard to peak picking but is hardly compatible with EDA. The online coupling enables the straight forward generation of multiple second dimension separations [45] leading to multiple data points and thus three dimensional peaks [42]. The software based, automatized peak detection of these peaks is substantially more robust.

Despite these challenges concerning the peak picking the desired separation of within one separation dimension coeluting peaks was indicated by a 4.8 fold increase of the peak number: 4906 peaks were detected in the water extract before and in average 23,628 in the

fractions of the four selected stationary phases after fractionation. The improved detection of peaks hidden in a “hump” in the raw extract was demonstrated for testosterone which belongs to the steroidal EDCs whose automated detection is typically challenged by many co-eluting isobaric compounds. The tentative identification of testosterone was only achieved after the fractionation of a broad, unresolved hump into various isobars using a C18 column. The results also proof the need to apply a whole set of columns for the fractionation as shown for the isobars with m/z 207.1379. Here the isobar with a retention time of 8.82 minutes was only separated by fractionation using the PYE column while this column could not ensure for the separation of other peaks like that one of testosterone.

According to the findings of Gilar et al. [46] an ideal pair of two fully orthogonal columns would result in a homogeneous distribution of peaks within a 2D separation space. Against this background, the results of the column selection, which were obtained by statistical evaluation of retention data using Spearman Rank correlation and principal component analysis, were reassessed. To this end, the peak distribution of the non-target peaks of each column pair was visualized in a virtual 2D separation space. To a great extent a coincidence of the distribution of the reference compounds and the whole non-target peak inventory in the 2D separation spaces underlined the validity of our column selection approach. This clearly showes that a rigorous experimental evaluation of the retention data of a representative mixture is a productive approach to measure the degree of orthogonality of a set of different stationary phases and thus is a useful alternative to generic selection methods like the hydrophobic subtraction model [47] or the Tanaka protocol [48-51].

After verifying the potential of the parallel fractionation approach to efficiently separate EDCs in Chapter 2, the approach was integrated into an EDA study in Chapter 3 with the aim to identify unknown effect drivers within a river water sample with antiandrogenic activity.

5.3 Identification of unknown antiandrogens in a surface water sample by EDA using a novel, parallel fractionation approach

EDA is a powerful tool for identifying unknown toxicants in environmental samples with a specific mode of action [28, 52]. It has been used to identify various EDCs like estrogens [53], androgens [54] or antiandrogens [54, 55]. The starting assumption of each EDA is that the major portion of an observed effect of the sample of concern can be explained by specific

effect drivers which are present either as individual compounds or as mixtures consisting of few compounds [52]. Effect drivers are usually identified by effect testing, fractionation and chemical analysis of active fractions. Thus, the success of EDA is essentially influenced by the fractionation procedure aiming on the reduction of the samples complexity. The within this study applied fractionation approach resulted in a tremendous reduction of the raw water extract data complexity of over 99.9% and therefore laid the foundation for the identification of 4-methyl-7-diethylaminocoumarin (C47), 4-methyl-7-ethylaminocoumarin (C47T1) and 4-methyl-7-aminocoumarin (C47T2) [56]. This is clearly underlining the power of this novel tool that was specifically developed for EDA.

In addition to the possibility of reducing sample complexity, which can essentially support the structural elucidation, fractionation has another important property: Weiss et al. [54] demonstrated that toxicity screening of non-fractionated sediment extracts may be insufficient to evaluate the full *in vitro* endocrine disrupting potential of the total mixture if masking effects are formed by androgen receptor agonists and antagonists. Similar effects were observed for other receptor mediated pathways including estrogen receptor assays. Estrogens are frequently detected in the environment [57, 58]. However, environmental samples typically do not only contain estrogens but may additionally comprise non-estrogenic confounders that can form three types of interference: toxic masking, antagonistic modulation or synergistic modulation [59]. Toxic masking is caused by a reduction or even complete erasure of the estrogenic response due to toxic chemicals that are co-occuring in a mixture with estrogens. Antagonistic modulation occurs if non-toxic confounders of estrogens are decreasing estrogenicity by reducing the uptake of estrogens or if anti-estrogens are present. The co-occurrence of estrogens and anti-estrogens were observed in sediment samples taken from the Certak oxbow lake in the czech republic [60], as well as in a WWTP influent [61] and also wastewater effluents [62]. Synergistic modulation is to be understood as a modulation of the toxicokinetic behavior of estrogens by non-estrogenic compounds. Our fractionation approach is specifically developed to separate endocrine disruptors and its confounders and thus may be an important tool to unravel such effects in endocrine active water samples in future studies.

However, even after fractionation the interpretation of biotest results may not always be straightforward, as demonstrated in this EDA study. Mostly the magnitude of AR response of the fractions received by the separation of the river water extract was significantly above

100%, which mistakenly indicate the presence of androgens. Various factors may be investigated in future studies to better understand this effect. On the one hand in the water sample present chemicals are potentially stimulating the growth of the cells leading to a higher number of androgen receptors and thus an increase of the magnitude of AR response. Alternatively a modulation of membrane permeability, which is a common phenomenon in aquatic biotests [63-65], might enhance the uptake of the agonistic dihydrotestosteron which is used for a co-exposure of the test system. Furthermore, a nonspecific expression of the luciferase gene, as well as luminescence of the candidate chemicals itself could possibly cause this shift but was excluded via a constant response of the cytotox CALUX assay [66] in the presence of C47, C47T1 and C47T2. Also toxic masking due to the presence of cytotoxic compounds in the water extract that may result in a reduction of cell viability was ruled out using the MTT-assay [67].

In order to determine the explainable proportion of the samples total antiandrogenic activity, the individual effects of the identified toxicants were considered in a mixture toxicity approach. Additive effects are observed most widely [68]. The assumption of concentration addition is applied for the mixtures of anticipated similar modes of action and the assumption of independent action for those with diverse but non-interactive modes of action [69]. The rare upward and downward deviations from predicted additivity indicate synergism and antagonism, respectively [69]. EDCs are usually following concentration addition and the rarely observed deviations from additivity were always small [70-72]. Thus, also the effect of antiandrogens can be predicted by dose addition [68], as shown for mixtures of procymidone and vinclozolin [73, 74], mixtures of the pesticides deltamethrin, methiocarb and prochloraz [75] or of the five phthalates butyl-benzyl phthalate, di-butyl phthalate, di-(2-ethylhexyl) phthalate, di- (isobutyl) phthalate and di-propyl phthalate [76]. Therefore, the concept of concentration addition was applied using toxicity equivalent concentrations [77] of the *in vitro* responses of the three identified coumarins. In this manner, the entire antiandrogenic effect of the sample could be explained.

The identification of potent antiandrogenic compounds in the Holtemme raised the question about their source and fate and thus is being investigated in chapter 4 of this thesis.

5.4 Exposure of a whole aquatic ecosystem by potent antiandrogen disrupting chemicals

The pollution of rivers by compounds of anthropogenic origin was already reported for numerous substances including paracetamol [78], the in consumer products frequently applied bitterest substance denatonium [79] and quaternary triphenylphosphonium compounds that are used worldwide by the chemical industry [80]. Often compounds are only emerging after they are already being released for years into the environment. In this context the importance of cost and time efficient retrospective screening for the backtracking of anthropogenic compounds in existing HRMS data should not be underestimated [81, 82]. It was successfully applied not only to detect pollutants in environmental samples [83-85] but also to prove drug abuse by analyzing human hair [86] and human urine [87, 88] or to screen food for pesticide metabolites [89].

The present study verified the unique advantage of LC-HRMS/MS which allows not only for a retrospective screening but also a quantitative analysis of environmental samples stemming from water, soil and biota even years after the record of full-scan HRMS spectra. The WWTP Silstedt was identified as the source that is continuously discharging the antiandrogens C47, C47T1 and C47T2 in the gram per day range into the River Holtemme. In other words, the well-known N-dealkylation of micropollutants in activated sludge [90], that has also been observed for C47 and C47T1 in the WWTP Silstedt, does not suffice for a total degradation of these harmful compounds to the less antiandrogenic active C47T2. This is resulting in water concentration of the three toxicants in the low µg/L range at all sites downstream the river course.

Already in the past, numerous studies pointed on the insufficient degradation efficiency of (anti-)androgens in WWTPs with the associated risk for aquatic organisms already at much lower concententration than found in this study, namely at concentrations in the ng or sub-ng/L range [16]. Antiandrogenic activity was also found in the effluents from WWTPs in Ria de Aveiro, Portugal [91] and the UK [92]. In the study of Stalter et al. [61] antiandrogenicity was not detected within the WWTP influent but after the secondary clarifier due to the removal of androgens and associated masking effects. However, solely 63% of this antiandrogenicity was removed during the following ozonation. This means that antiandrogenicity was not removed but even generated by the wastewater treatment. In

contrast to this finding, 99% of the antiandrogenic activity of the influent was removed by the WWTP of Guangzhou, China [93]. Androgenicity was found at the WWTP of Santiago, Portugal [61], in the UK [17] or Australia [18]. Svenson et al. [94] pointed on the importance of secondary treatment whereby the reduction of androgenic activity was enhanced from in between 26-42% to in between 96-99%. All these results in cojunction with our findings illustrate the need for further research aiming on a comprehensive degradation of (anti-) androgenic endocrin disrupting compounds in WWTPs in order to minimize the risks possed by WWTP effluents to the aquatic ecosystem.

In general, attenuation of chemicals from surface waters can be induced by transformation [95], evaporation and sorption to sediment, SPM, biofilms and other biota [96, 97]. In the River Holtemme dilution by groundwater was identified as the major cause of the concentration decrease of the coumarin derivatives along the river stretch. As a consequence of the continuous, years lasting release of the coumarin derivatives into the river a partitioning of these anthropogenic pollutions into other environmental compartments and thus the exposure of the entire aquatic ecosystem was hypothesized. Thus, the distribution of these compounds between water, sediment and the model macroinvertebrate *gammarus pulex* was investigated using equilibrium partitioning theory (EqP) [98]. A significant pollution not only of the sediment but also a considerable body burden of the aquatic biota was demonstrated. Interestingly, inconclusive freely dissolved concentrations in sediment led to the finding that the partitioning of the coumarin derivatives between water and sediment cannot be estimated by predicted partitioning constants K_{OC}. The experimentally derived, concentration dependent partitioning constants exceeded the predicted ones up to 92-times thus pointing on ionic interactions at sorption sites with different affinity for cation exchange as the predominant intermolecular force between the coumarins and the sediment. This interpretation is supported by the literature where the strong impact of cation binding on the sorption of sulfonamides to soil organic matter [99] or on the sorption of other aromatic amines to soil even at pH values greater than pK_a+2 [100] has already been reported. Hence, consideration of the influence of cationic interactions on the sorption of other deprotonable chemicals may be of decisive importance to also understand their fate in the aquatic ecosystem. In contrast, the authors of a recently published study addressing the distribution of polar, emerging pollutants in the Holtemme [101] attributed potentially erroneous predictions of partitioning coefficients to a

possible disequilibrium of partitioning as a result of slow desorption kinetics or the presence of strongly adsorbing black carbon in the sediment, as found in Lake Michigan [102].

The identification of the river sediment as a potent sink of the coumarins is of concern since it will transform to a source of this contamination resulting in a long-term exposure of the ecosystem possibly over many years even after their release is ceased. This forecast is supported by various studies including the study of Brack et al. [103] where relatively polar xenobiotics like the pesticide n-tributyltin or the herbicide prometryn were detected in sediment of the river Spittelwasser even 7 years after the close down of a majority of the chemical production sites in this area.

The results of chapter 3 proof that EDA can play a vital role in the identification of unknown, water soluble EDCs when used in concert with the novel, in Chapter 2 described, parallel fractionation approach, state-of-the-art chemical-analytical non-target techniques, miniaturized *in vitro* tests [2] and organism level confirmation procedures [104]. The retrospective analysis of mass spectrometric data from the River Holtemme for the identified antiandrogens C47, C47T1 and C47T2 in water, sediment and biota revealed the contamination of all compartments of the aquatic ecosystem along the whole river stretch downstream the WWTP Silstedt.

5.5 Literature

1. Beckers, L.-M., et al., *Characterization and risk assessment of seasonal and weather dynamics in organic pollutant mixtures from discharge of a separate sewer system.* Water Research, 2018. **135**: p. 122-133.
2. Di Paolo, C., et al., *Downscaling procedures reduce chemical use in androgen receptor reporter gene assay.* Science of The Total Environment, 2016. **571**(Supplement C): p. 826-833.
3. Sumpter, J.P., *Endocrine Disrupters in the Aquatic Environment: An Overview.* Acta hydrochimica et hydrobiologica, 2005. **33**(1): p. 9-16.
4. Anway, M.D. and M.K. Skinner, *Epigenetic Transgenerational Actions of Endocrine Disruptors.* Endocrinology, 2006. **147**(6): p. s43-s49.
5. EuropeanEnvironmentAgency, *European workshop on the impact of endocrine disruptors on human health and wildlife*. 2–4 December 1996, Weybridge, UK. Report of the Proceedings. Report EU 17549., European Commission DG XII, Copenhagen.
6. Milla, S., S. Depiereux, and P. Kestemont, *The effects of estrogenic and androgenic endocrine disruptors on the immune system of fish: a review.* Ecotoxicology, 2011. **20**(2): p. 305-319.
7. Bayley, M., M. Junge, and E. Baatrup, *Exposure of juvenile guppies to three antiandrogens causes demasculinization and a reduced sperm count in adult males.* Aquatic Toxicology, 2002. **56**(4): p. 227-239.
8. Lor, Y., et al., *Juvenile exposure to vinclozolin shifts sex ratios and impairs reproductive capacity of zebrafish.* Reproductive Toxicology, 2015. **58**: p. 111-118.
9. Milnes, M.R., et al., *Contaminant-induced feminization and demasculinization of nonmammalian vertebrate males in aquatic environments.* Environmental Research, 2006. **100**(1): p. 3-17.
10. Jobling, S., Burn, R.W., Thorpe, K., Williams, R., Tyler, C., *Statistical modeling suggests that antiandrogens in effluents from wastewater treatment works contribute to widespread sexual disruption in fish living in English rivers.* Environmental Health Perspectives, 2009. **117**(5): p. 797-802.
11. Howell, W.M., D.A. Black, and S.A. Bortone, *Abnormal Expression of Secondary Sex Characters in a Population of Mosquitofish, Gambusia affinis holbrooki: Evidence for Environmentally-Induced Masculinization.* Copeia, 1980. **1980**(4): p. 676-681.
12. Jenkins, R.L., et al., *Production of Androgens by Microbial Transformation of Progesterone in Vitro: A Model for Androgen Production in Rivers Receiving Paper Mill Effluent.* Environmental Health Perspectives, 2004. **112**(15): p. 1508-1511.
13. Ellis, R.J., et al., *In vivo and in vitro assessment of the androgenic potential of a pulp and paper mill effluent.* Environmental Toxicology and Chemistry, 2003. **22**(7): p. 1448-1456.
14. Kumar, V., C. Majumdar, and P. Roy, *Effects of endocrine disrupting chemicals from leather industry effluents on male reproductive system.* The Journal of Steroid Biochemistry and Molecular Biology, 2008. **111**(3): p. 208-216.
15. Hill, E.M., et al., *Profiles and Some Initial Identifications of (Anti)Androgenic Compounds in Fish Exposed to Wastewater Treatment Works Effluents.* Environmental Science & Technology, 2010. **44**(3): p. 1137-1143.

16. Runnalls, T.J., et al., *Pharmaceuticals in the Aquatic Environment: Steroids and Anti-Steroids as High Priorities for Research.* Human and Ecological Risk Assessment: An International Journal, 2010. **16**(6): p. 1318-1338.
17. Kirk, L.A., et al., *Changes in estrogenic and androgenic activities at different stages of treatment in wastewater treatment works.* Environmental Toxicology and Chemistry, 2002. **21**(5): p. 972-979.
18. Tan, B.L.L., et al., *Comprehensive study of endocrine disrupting compounds using grab and passive sampling at selected wastewater treatment plants in South East Queensland, Australia.* Environment International, 2007. **33**(5): p. 654-669.
19. Thomas, K.V., et al., *An assessment of in vitro androgenic activity and the identification of environmental androgens in United Kingdom estuaries.* Environmental Toxicology and Chemistry, 2002. **21**: p. 1456-1461.
20. Kiparissis, Y., et al., *Effects of the antiandrogens, vinclozolin and cyproterone acetate on gonadal development in the Japanese medaka (Oryzias latipes).* Aquatic Toxicology, 2003. **63**(4): p. 391-403.
21. Weiss, J., et al., *Identification strategy for unknown pollutants using high-resolution mass spectrometry: Androgen-disrupting compounds identified through effect-directed analysis.* Analytical and Bioanalytical Chemistry, 2011. **400**(9): p. 3141-3149.
22. Rostkowski, P., et al., *Bioassay-Directed Identification of Novel Antiandrogenic Compounds in Bile of Fish Exposed to Wastewater Effluents.* Environmental Science & Technology, 2011. **45**(24): p. 10660-10667.
23. Kojima, H., et al., *Screening for estrogen and androgen receptor activities in 200 pesticides by in vitro reporter gene assays using Chinese hamster ovary cells.* Environmental Health Perspectives, 2004. **112**(5): p. 524-531.
24. Vandenberg, L.N., et al., *Bisphenol-A and the Great Divide: A Review of Controversies in the Field of Endocrine Disruption.* Endocrine Reviews, 2009. **30**(1): p. 75-95.
25. Horai, H., et al., *MassBank: a public repository for sharing mass spectral data for life sciences.* Journal of Mass Spectrometry, 2010. **45**(7): p. 703-714.
26. Brack, W., et al., *Towards the review of the European Union Water Framework Directive: Recommendations for more efficient assessment and management of chemical contamination in European surface water resources.* Science of The Total Environment, 2017. **576**: p. 720-737.
27. Krauss, M., H. Singer, and J. Hollender, *LC–high resolution MS in environmental analysis: from target screening to the identification of unknowns.* Analytical and Bioanalytical Chemistry, 2010. **397**(3): p. 943-951.
28. Brack, W., *Effect-directed analysis: a promising tool for the identification of organic toxicants in complex mixtures.* Analytical and Bioanalytical Chemistry, 2003. **377**: p. 397-407.
29. Butt, C.M., D. Wang, and H.M. Stapleton, *Halogenated Phenolic Contaminants Inhibit the In Vitro Activity of the Thyroid-Regulating Deiodinases in Human Liver.* Toxicological Sciences, 2011. **124**(2): p. 339-347.
30. Nurmi, J., J. Pellinen, and A.L. Rantalainen, *Critical evaluation of screening techniques for emerging environmental contaminants based on accurate mass measurements with time-of-flight mass spectrometry.* Journal of Mass Spectrometry, 2012. **47**(3): p. 303-312.
31. Ruff, M., et al., *Quantitative target and systematic non-target analysis of polar organic micro-pollutants along the river Rhine using high-resolution mass-*

spectrometry – Identification of unknown sources and compounds. Water Research, 2015. **87**: p. 145-154.
32. Liscio, C., et al., *Methodology for profiling anti-androgen mixtures in river water using multiple passive samplers and bioassay-directed analyses.* Water Research, 2014. **57**(Supplement C): p. 258-269.
33. Muz, M., et al., *Nontargeted detection and identification of (aromatic) amines in environmental samples based on diagnostic derivatization and LC-high resolution mass spectrometry.* Chemosphere, 2017. **166**: p. 300-310.
34. Muz, M., et al., *Identification of Mutagenic Aromatic Amines in River Samples with Industrial Wastewater Impact.* Environmental Science & Technology, 2017. **51**(8): p. 4681-4688.
35. Muz, M., et al., *Mutagenicity in Surface Waters: Synergistic Effects of Carboline Alkaloids and Aromatic Amines.* Environmental Science and Technology, 2017. **51**(3): p. 1830-1839.
36. Muschket, M., et al., *LC fractionation on a set of reversed phase columns improves the detection of endocrine disruptors in LC-HRMS screening of surface water extracts.* Manuscript in preparation.
37. Schymanski, E.L., et al., *Strategies to Characterize Polar Organic Contamination in Wastewater: Exploring the Capability of High Resolution Mass Spectrometry.* Environmental Science & Technology, 2014. **48**(3): p. 1811-1818.
38. Matuszewski, B.K., M.L. Constanzer, and C.M. Chavez-Eng, *Strategies for the Assessment of Matrix Effect in Quantitative Bioanalytical Methods Based on HPLC–MS/MS.* Analytical Chemistry, 2003. **75**(13): p. 3019-3030.
39. Gallampois, C.M.J., et al., *Integrated biological–chemical approach for the isolation and selection of polyaromatic mutagens in surface waters.* Analytical and Bioanalytical Chemistry, 2013. **405**(28): p. 9101-9112.
40. Giddings, J.C., *Two-dimensional separations: concept and promise.* Analytical Chemistry, 1984. **56**(12): p. 1258A-1270A.
41. Singer, D., et al., *Separation of Multiphosphorylated Peptide Isomers by Hydrophilic Interaction Chromatography on an Aminopropyl Phase.* Analytical Chemistry, 2010. **82**(15): p. 6409-6414.
42. Stoll, D.R., et al., *Fast, comprehensive two-dimensional liquid chromatography.* Journal of Chromatography A, 2007. **1168**(1): p. 3-43.
43. Ouyang, X., et al., *Comprehensive two-dimensional liquid chromatography coupled to high resolution time of flight mass spectrometry for chemical characterization of sewage treatment plant effluents.* Journal of Chromatography A, 2015. **1380**: p. 139-145.
44. Hu, M., et al., *Optimization of LC-Orbitrap-HRMS acquisition and MZmine 2 data processing for nontarget screening of environmental samples using design of experiments.* Analytical and Bioanalytical Chemistry, 2016. **408**(28): p. 7905-7915.
45. Groskreutz, S.R., et al., *Selective comprehensive multi-dimensional separation for resolution enhancement in high performance liquid chromatography. Part I: Principles and instrumentation.* Journal of Chromatography A, 2012. **1228**(0): p. 31-40.
46. Gilar, M., et al., *Orthogonality of Separation in Two-Dimensional Liquid Chromatography.* Analytical Chemistry, 2005. **77**(19): p. 6426-6434.

47. Snyder, L.R., J.W. Dolan, and P.W. Carr, *The hydrophobic-subtraction model of reversed-phase column selectivity.* Journal of Chromatography A, 2004. **1060**(1-2): p. 77-116.
48. Euerby, M.R. and P. Petersson, *Chromatographic classification and comparison of commercially available reversed-phase liquid chromatographic columns using principal component analysis.* Journal of Chromatography A, 2003. **994**(1-2): p. 13-36.
49. Euerby, M.R., et al., *Chromatographic classification and comparison of commercially available reversed-phase liquid chromatographic columns containing phenyl moieties using principal component analysis.* Journal of Chromatography A, 2007. **1154**(1-2): p. 138-151.
50. Euerby, M.R., A.P. McKeown, and P. Petersson, *Chromatographic classification and comparison of commercially available perfluorinated stationary phases for reversed-phase liquid chromatography using Principal Component Analysis.* Journal of Separation Science, 2003. **26**(3-4): p. 295-306.
51. Euerby, M.R. and P. Petersson, *Chromatographic classification and comparison of commercially available reversed-phase liquid chromatographic columns containing polar embedded groups/amino endcappings using principal component analysis.* Journal of Chromatography A, 2005. **1088**(1-2): p. 1-15.
52. Brack, W., et al., *Effect-directed analysis supporting monitoring of aquatic environments — An in-depth overview.* Science of The Total Environment, 2016. **544**: p. 1073-1118.
53. Lübcke-von Varel, U., et al., *Polar compounds dominate in vitro effects of sediment extracts.* Environmental Science & Technology, 2011. **45**: p. 2384.
54. Weiss, J.M., et al., *Masking effect of anti-androgens on androgenic activity in European river sediment unveiled by effect-directed analysis.* Analytical and Bioanalytical Chemistry, 2009. **394**: p. 1385-1397.
55. Thomas, K.V., et al., *Effect-Directed Identification of Naphthenic Acids As Important in Vitro Xeno-Estrogens and Anti-Androgens in North Sea Offshore Produced Water Discharges.* Environmental Science & Technology, 2009. **43**(21): p. 8066-8071.
56. Muschket, M., et al., *Identification of Unknown Antiandrogenic Compounds in Surface Waters by Effect-Directed Analysis (EDA) Using a Parallel Fractionation Approach.* Environmental Science & Technology, 2018. **52**(1): p. 288-297.
57. Norihide, N., et al., *Identification of estrogenic compounds in wastewater effluent.* Environmental Toxicology and Chemistry, 2004. **23**(12): p. 2807-2815.
58. Mika, P., et al., *Sediments are major sinks of steroidal estrogens in two United Kingdom rivers.* Environmental Toxicology and Chemistry, 2004. **23**(4): p. 945-952.
59. Frische, T., et al., *Toxic masking and synergistic modulation of the estrogenic activity of chemical mixtures in a yeast estrogen screen (YES).* Environmental Science and Pollution Research, 2009. **16**(5): p. 593-603.
60. Macikova, P., et al., *Longer-term and short-term variability in pollution of fluvial sediments by dioxin-like and endocrine disruptive compounds.* Environmental Science and Pollution Research, 2014. **21**(7): p. 5007-5022.
61. Stalter, D., et al., *Ozonation and activated carbon treatment of sewage effluents: Removal of endocrine activity and cytotoxicity.* Water Research, 2011. **45**(3): p. 1015-1024.

62. Snyder, S.A., et al., *Identification and quantification of estrogen receptor agonists in wastewater effluents.* Environmental Science and Technology, 2001. **35**: p. 3620-3625.
63. Beresford, N., et al., *Issues Arising When Interpreting Results from an in Vitro Assay for Estrogenic Activity.* Toxicology and Applied Pharmacology, 2000. **162**(1): p. 22-33.
64. Rajapakse, N., D. Ong, and A. Kortenkamp, *Defining the Impact of Weakly Estrogenic Chemicals on the Action of Steroidal Estrogens.* Toxicological Sciences, 2001. **60**(2): p. 296-304.
65. Hutchinson, T.H., et al., *Acute and chronic effects of carrier solvents in aquatic organisms: A critical review.* Aquatic Toxicology, 2006. **76**(1): p. 69-92.
66. van der Linden, S.C., et al., *Development of a panel of high-throughput reporter-gene assays to detect genotoxicity and oxidative stress.* Mutation Research/Genetic Toxicology and Environmental Mutagenesis, 2014. **760**: p. 23-32.
67. Blaha, L.H., M.; Murphy, M.; Jones PD.; Giesy JP., *Procedure for determination of cell viability/cytotoxicity using the MTT bioassay.* 2004.
68. A. Kortenkamp, T.B., M. Faust 2009, *State of the art report on mixture toxicity. Final Report to the European Commission under Contract Number 070307/2007/485103/ETU/D.1. European Commission, Brussels, Belgium. [cited 04 June 2013]. Available from: http://ec.europa.eu/environment/chemicals/pdf/report_Mixture%20toxicity.pdf*
69. Rolf, A., et al., *Simplifying complexity: Mixture toxicity assessment in the last 20 years.* Environmental Toxicology and Chemistry, 2013. **32**(8): p. 1685-1687.
70. Charles, G.D., et al., *Assessment of Interactions of Diverse Ternary Mixtures in an Estrogen Receptor-α Reporter Assay.* Toxicology and Applied Pharmacology, 2002. **180**(1): p. 11-21.
71. Crofton, K.M., et al., *Thyroid-Hormone–Disrupting Chemicals: Evidence for Dose-Dependent Additivity or Synergism.* Environmental Health Perspectives, 2005. **113**(11): p. 1549-1554.
72. Rajapakse, N., et al., *Deviation from Additivity with Estrogenic Mixtures Containing 4-Nonylphenol and 4-tert-Octylphenol Detected in the E-SCREEN Assay.* Environmental Science & Technology, 2004. **38**(23): p. 6343-6352.
73. Nellemann, C., et al., *The Combined Effects of Vinclozolin and Procymidone Do Not Deviate from Expected Additivity in Vitro and in Vivo.* Toxicological Sciences, 2003. **71**(2): p. 251-262.
74. Gray, J.L.E., et al., *Effects of environmental antiandrogens on reproductive development in experimental animals.* Human Reproduction Update, 2001. **7**(3): p. 248-264.
75. Birkhøj, M., et al., *The combined antiandrogenic effects of five commonly used pesticides.* Toxicology and Applied Pharmacology, 2004. **201**(1): p. 10-20.
76. Howdeshell, K.L., et al., *A Mixture of Five Phthalate Esters Inhibits Fetal Testicular Testosterone Production in the Sprague-Dawley Rat in a Cumulative, Dose-Additive Manner.* Toxicological Sciences, 2008. **105**(1): p. 153-165.
77. Escher, B.I., et al., *Toxic equivalent concentrations (TEQs) for baseline toxicity and specific modes of action as a tool to improve interpretation of ecotoxicity testing of environmental samples.* Journal of Environmental Monitoring, 2008. **10**(5): p. 612-621.

78. Tran, N.H., et al., *Occurrence and suitability of pharmaceuticals and personal care products as molecular markers for raw wastewater contamination in surface water and groundwater.* Environmental Science and Pollution Research, 2014. **21**(6): p. 4727-4740.
79. Lege, S., et al., *Denatonium – A so far unrecognized but ubiquitous water contaminant?* Water Research, 2017. **112**(Supplement C): p. 254-260.
80. Schlüsener, M.P., U. Kunkel, and T.A. Ternes, *Quaternary Triphenylphosphonium Compounds: A New Class of Environmental Pollutants.* Environmental Science & Technology, 2015. **49**(24): p. 14282-14291.
81. Schymanski, E.L., et al., *Non-target screening with high-resolution mass spectrometry: critical review using a collaborative trial on water analysis.* Analytical and Bioanalytical Chemistry, 2015. **407**(21): p. 6237-6255.
82. Aceña, J., et al., *Advances in liquid chromatography–high-resolution mass spectrometry for quantitative and qualitative environmental analysis.* Analytical and Bioanalytical Chemistry, 2015. **407**(21): p. 6289-6299.
83. Gago-Ferrero, P., et al., *Extended Suspect and Non-Target Strategies to Characterize Emerging Polar Organic Contaminants in Raw Wastewater with LC-HRMS/MS.* Environmental Science & Technology, 2015. **49**(20): p. 12333-12341.
84. Hernández, F., et al., *Current use of high-resolution mass spectrometry in the environmental sciences.* Analytical and Bioanalytical Chemistry, 2012. **403**(5): p. 1251-1264.
85. Hernández, F., et al., *Investigation of pharmaceuticals and illicit drugs in waters by liquid chromatography-high-resolution mass spectrometry.* TrAC Trends in Analytical Chemistry, 2014. **63**: p. 140-157.
86. Vogliardi, S., et al., *Simultaneous LC-HRMS determination of 28 benzodiazepines and metabolites in hair.* Analytical and Bioanalytical Chemistry, 2011. **400**(1): p. 51-67.
87. Jiménez Girón, A., et al., *Development and validation of an open screening method for diuretics, stimulants and selected compounds in human urine by UHPLC–HRMS for doping control.* Analytica Chimica Acta, 2012. **721**: p. 137-146.
88. Sundström, M., et al., *A high-sensitivity ultra-high performance liquid chromatography/high-resolution time-of-flight mass spectrometry (UHPLC-HR-TOFMS) method for screening synthetic cannabinoids and other drugs of abuse in urine.* Analytical and Bioanalytical Chemistry, 2013. **405**(26): p. 8463-8474.
89. Polgár, L., et al., *Retrospective screening of relevant pesticide metabolites in food using liquid chromatography high resolution mass spectrometry and accurate-mass databases of parent molecules and diagnostic fragment ions.* Journal of Chromatography A, 2012. **1249**: p. 83-91.
90. Gulde, R., et al., *Systematic Exploration of Biotransformation Reactions of Amine-Containing Micropollutants in Activated Sludge.* Environmental Science & Technology, 2016. **50**(6): p. 2908-2920.
91. Sousa, A., et al., *Chemical and Biological Characterization of Estrogenicity in Effluents from WWTPs in Ria de Aveiro (NW Portugal).* Archives of Environmental Contamination and Toxicology, 2010. **58**(1): p. 1-8.
92. Katsiadaki, I., et al., *Field surveys reveal the presence of anti-androgens in an effluent-receiving river using stickleback-specific biomarkers.* Aquatic Toxicology, 2012. **122–123**: p. 75-85.

93. Li, J., et al., *Analysis of Environmental Endocrine Disrupting Activities Using Recombinant Yeast Assay in Wastewater Treatment Plant Effluents.* Bulletin of Environmental Contamination and Toxicology, 2010. **84**(5): p. 529-535.
94. Svenson, A. and A.-S. Allard, *Occurrence and Some Properties of the Androgenic Activity in Municipal Sewage Effluents.* Journal of Environmental Science and Health, Part A, 2004. **39**(3): p. 693-701.
95. Kunkel, U. and M. Radke, *Fate of pharmaceuticals in rivers: Deriving a benchmark dataset at favorable attenuation conditions.* Water Research, 2012. **46**(17): p. 5551-5565.
96. Radke, M., et al., *Dynamics and Attenuation of Acidic Pharmaceuticals along a River Stretch.* Environmental Science & Technology, 2010. **44**(8): p. 2968-2974.
97. Kunkel, U. and M. Radke, *Reactive Tracer Test To Evaluate the Fate of Pharmaceuticals in Rivers.* Environmental Science & Technology, 2011. **45**(15): p. 6296-6302.
98. Di Toro, D.M., et al., *Technical basis for establishing sediment quality criteria for nonionic organic chemicals using equilibrium partitioning.* Environmental Toxicology and Chemistry, 1991. **10**(12): p. 1541-1583.
99. Richter, M.K., et al., *Cation Binding of Antimicrobial Sulfathiazole to Leonardite Humic Acid.* Environmental Science & Technology, 2009. **43**(17): p. 6632-6638.
100. Li, H., et al., *Role of pH in partitioning and cation exchange of aromatic amines on water-saturated soils.* Chemosphere, 2001. **44**(4): p. 627-635.
101. Inostroza, P.A., et al., *Chemical activity and distribution of emerging pollutants: Insights from a multi-compartment analysis of a freshwater system.* Environmental Pollution, 2017. **231**(Part 1): p. 339-347.
102. Burkhard, L.P., P.M. Cook, and M.T. Lukasewycz, *Organic Carbon−Water Concentration Quotients (Πsocs and πpocs): Measuring Apparent Chemical Disequilibria and Exploring the Impact of Black Carbon in Lake Michigan.* Environmental Science & Technology, 2008. **42**(10): p. 3615-3621.
103. Brack, W., et al., *Bioassay-directed identification of organic toxicants in river sediment in the industrial region of Bitterfeld (Germany) - A contribution to hazard assessment.* Archives of Environmental Contamination and Toxicology, 1999. **37**: p. 164-174.
104. Sébillot, A., et al., *Rapid Fluorescent Detection of (Anti)androgens with spiggin-gfp Medaka.* Environmental Science & Technology, 2014. **48**(18): p. 10919-10928.

Chapter 6

Conclusion

Effect-directed analysis is a powerful tool to unravel the identity of “unknown” chemicals with a biological activity. Parallel fractionation efficiently facilitates the effect-directed analysis of highly complex mixtures of thousands of compounds. It is less time-consuming then the classically applied sequential fractionation approach where the planning of every new cycle of the multidimensional fractionation is based on the biotest results [1]. In contrast, the novel, parallel fractionation approach allows all fractions obtained by chromatographic separation on a set of orthogonal columns to be simultaneously subjected to typically long-lasting bioassays. Furthermore, the accumulation of compound losses occurring in the sequential approach is avoided and thus the chance for compound identification is maximized. Hence, the parallel fractionation scheme combines the advantages of one-dimensional fractionation in terms of time-efficiency and minimization of compound loss with the gain of separation power achieved by multidimensional separation.

The inherent drawback of the novel approach is the complication of data analysis where common peaks of the toxic fraction have to be identified. However, the need to distinguish between characteristic and non-specific peaks, which may be detected within the background noise, is extremely challenging, especially in case of low peak intensities. The consideration of fragment ion spectra would support this differentiation but needs to be implemented into software based tools to allow for an automatized characterization of thousands of peaks.

Although the research in the field of endocrine disrupting activity present in the aquatic environment is rightly focusing on steroidal compounds, this work clearly points to the danger also posed by non-steroidal xenobiotics by identifying 4-methyl-7-diethylaminocoumarin (C47) and two derivatives as the potent drivers of antiandrogenicity in the German river Holtemme [2]. Besides C47, which is used as fluorescent probes and optical brighteners [3], a huge list of hundreds of other endocrine disrupting xenobiotics is known with many of them being frequently used in consumer products. One example is the

antiandrogenic [4] and estrogenic [5] bisphenol A which is one of the chemicals with the highest production volume worldwide [6].

The analysis of the temporal and longitudinal concentration profile of C47 and its derivatives, namely 4-methyl-7-ethylaminocoumarin (C47T1) and 4-methyl-7-aminocoumarin (C47T2), revealed a constant exposure of the aquatic ecosystem by these toxicants along the whole river stretch downstream of Silstedt. Furthermore, the sediment and the model macroinvertebrate *Gammarus pulex* were shown to be sinks of the coumarin derivatives. This is of some concern, because not only adverse effects on the health of aquatic organisms can be expected, as demonstrated *in vivo* in spiggin-gfp *Medaka,* but since the sediment might act as a long-term source of contamination even after the emission of C47 and its derivatives into the Holtemme ceases. The persistency of these compounds further increases the risk to the environment. In the wastewater treatment plant of Silstedt, which has been identified as the point source of these chemicals, C47 is only partially degraded to its less potent but still antiandrogenic transformation products C47T1 and C47T2, while a decrease of the concentrations in the river was only attributed to dilution.

These findings clearly stress the fact that not only effect-based monitoring of pro- and antiandrogenic activity should be integrated into the European water framework directive but also EDA to identify unknown endocrine disruptors in pollutes sites [7]. Furthermore an improvement of WWTPs to ensure an efficient removal of antiandrogenic activity should be in the focus of future studies in order to protect water which is an essential resource for our planets ecosystem and therefore also for human life.

6.1 Literature

1. Brack, W., *Effect-directed analysis: a promising tool for the identification of organic toxicants in complex mixtures.* Analytical and Bioanalytical Chemistry, 2003. **377**: p. 397-407.
2. Muschket, M., et al., *Identification of Unknown Antiandrogenic Compounds in Surface Waters by Effect-Directed Analysis (EDA) Using a Parallel Fractionation Approach.* Environmental Science & Technology, 2018. **52**(1): p. 288-297.
3. Kitamura, N., et al., *Synthesis, absorption, and fluorescence properties and crystal structures of 7-aminocoumarin derivatives.* Journal of Photochemistry and Photobiology A: Chemistry, 2007. **188**(2): p. 378-386.
4. Wang, H., et al., *Anti-androgenic mechanisms of Bisphenol A involve androgen receptor signaling pathway.* Toxicology, 2017. **387**: p. 10-16.
5. Moreman, J., et al., *Acute Toxicity, Teratogenic, and Estrogenic Effects of Bisphenol A and Its Alternative Replacements Bisphenol S, Bisphenol F, and Bisphenol AF in Zebrafish Embryo-Larvae.* Environmental Science & Technology, 2017. **51**(21): p. 12796-12805.
6. Vandenberg, L.N., et al., *Bisphenol-A and the Great Divide: A Review of Controversies in the Field of Endocrine Disruption.* Endocrine Reviews, 2009. **30**(1): p. 75-95.
7. Brack, W., et al., *Towards the review of the European Union Water Framework Directive: Recommendations for more efficient assessment and management of chemical contamination in European surface water resources.* Science of The Total Environment, 2017. **576**: p. 720-737.

Appendix A

Supplementary information for chapter 2

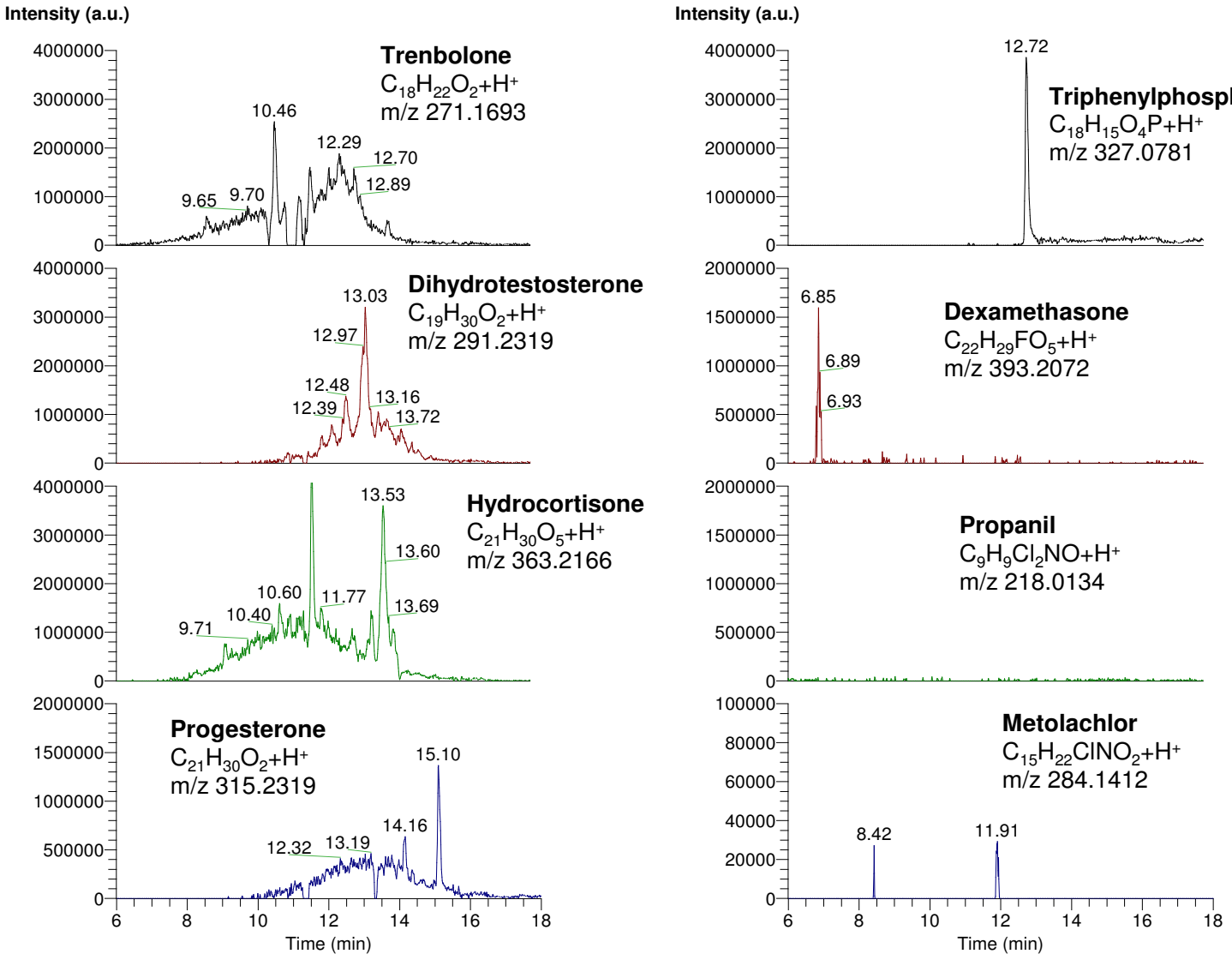

Figure A1 Examples for extracted ion chromatograms (5 ppm window) of endocrine disrupting compound ions which show a strong background "hump" (left side) and which show a low or zero baseline (right side). The sample is the surface water extract described in the main text analysed by LC-HRMS in ESI+ mode at a resolving power of 140,000 (referenced to m/z 200). Except for Triphenylphosphate (retention time 12.72 min) and Metolachlor (retention time 11.91 min), none of the compounds could be confirmed from this data.

A1 Materials and Methods

Table A1 Endocrine disrupting compounds used for the method development. log K_{ow} values were predicted using EPI Suite v4.11 (US EPA, 2012) [1].

Compound	CAS	Structure	log K_{ow}	Activity
Dexamethasone	50-02-2	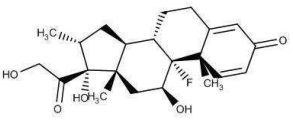	1.72	Glucocorticoid [2]
17β-Trenbolone	10161-33-8		2.65	Androgenic [3]
Norethindrone	68-22-4	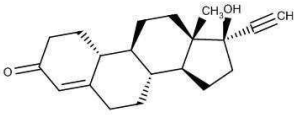	2.99	Progestagenic [4]
Androsterone	53-41-8	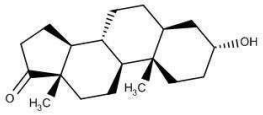	3.07	Androgenic [5]
Epi-Androsterone	481-29-8	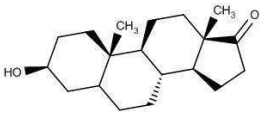	3.07	Androgenic [5]
Dihydrotestosterone	521-18-6	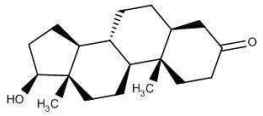	3.07	Androgenic [6,7]
Testosterone	58-22-0	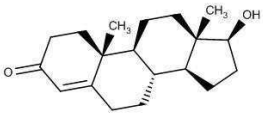	3.27	Androgenic [8]
Levonorgestrel	797-63-7	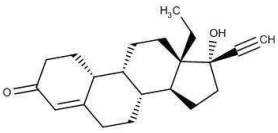	3.48	Progestagenic [9]
Medroxyprogesterone	520-85-4	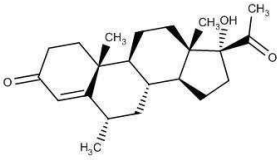	3.5	Androgen receptor affinity [10]
17α-Estradiol	57-91-0	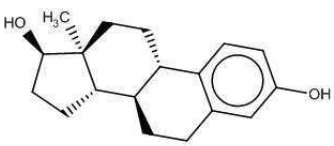	3.94	Estrogenic

17β-Estradiol	50-28-2		3.94	Estrogenic
Isopimaric Acid	5835-26-7	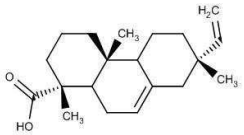	6.45	Antiandrogenic [11]
Abietic Acid	514-10-3	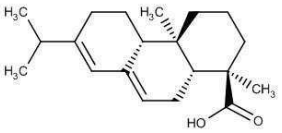	6.46	Antiandrogenic [11]
Estriol	50-27-1	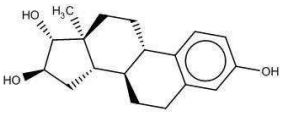	2.81	Estrogenic
Progesterone	57-83-0	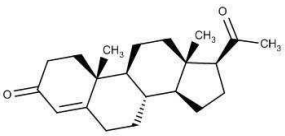	3.67	Progestagenic
Hydrocortisone	50-23-7	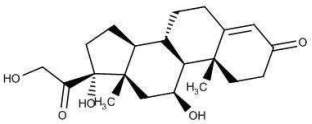	1.62	Androgen receptor affinity [10]
Bisphenol S	80-09-1	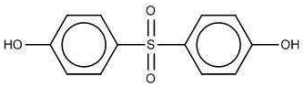	1.65	Estrogenic [12]
Isoeugenol	97-54-1	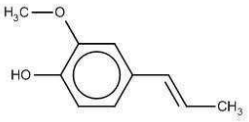	2.65	Androgen receptor affinity [10]
2-Naphthol	135-19-3	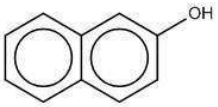	2.69	Antiandrogenic [11]
2,2´-Dihydroxybiphenyl	1806-29-7	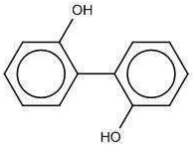	2.8	Antiandrogenic [13]
Genistein	446-72-0	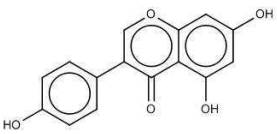	2.84	Androgen receptor affinity [10]
Propylparaben	94-13-3	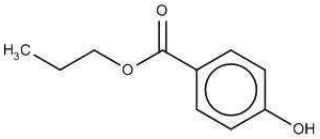	2.98	Androgen receptor affinity [10]

3-Hydroxybiphenyl	580-51-8	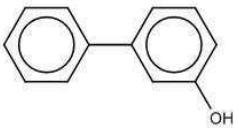	3.28	Androgen receptor affinity [10]
Benzophenone-3	131-57-7	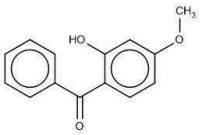	3.52	Antiandrogenic [11,14,13]
1-Hydroxypyrene	5315-79-7	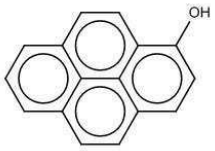	4.45	Antiandrogenic [13]
Zearalenone	17924-92-4	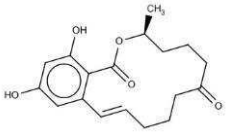	3.58	Antiandrogenic [13]
Procymidone	32809-16-8	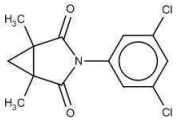	2.59	Antiandrogenic [15]
N-Benzylphthalimide	2142-01-0	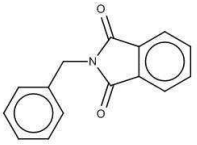	3.22	Androgen receptor affinity [10]
Carbaryl	63-25-2	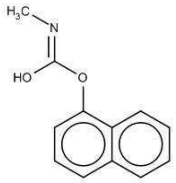	2.35	Androgen receptor affinity [10]
Propanil	709-98-8	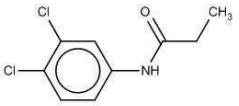	2.88	Antiandrogenic [15,10]
Tris (1-chloro-2-propyl)phosphate	13674-84-5	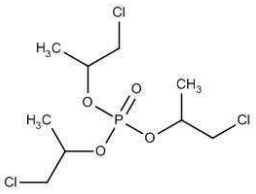	2.89	Antiandrogenic [16]
Linuron	330-55-2	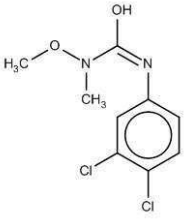	2.91	Antiandrogenic [17,15]

Metolachlor	51218-45-2	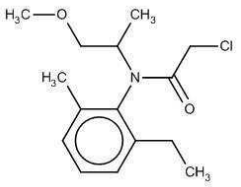	3.24	Androgen receptor affinity [10]
Flutamide	13311-84-7	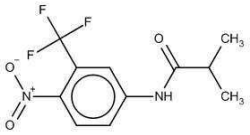	3.51	Antiandrogenic [13]
Flavone	525-82-6	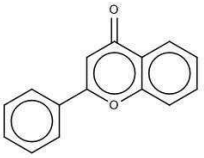	3.51	Androgen receptor affinity [10]
Methylparathion	298-00-0	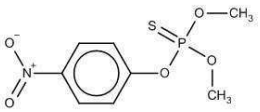	2.75	Antiandrogenic [15]
Fenthion	55-38-9	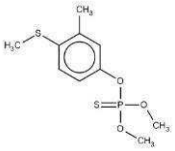	4.08	Antiandrogenic [15]
Triphenylphosphate	115-86-6	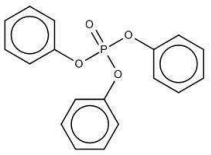	4.7	Androgen receptor affinity [10]
Benzylbutylphthalate	85-68-7	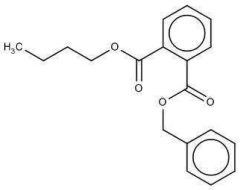	4.84	Antiandrogenic [6,10]

A1.1 LC-MS/MS analysis on different columns

The Agilent 1260 HPLC system involved a degasser, a quaternary pump, a thermostated autosampler and a column oven. The gradients for each column are shown in Table A2. All separations were carried out at a column oven temperature of 20°C. After the gradient separation finished, an isopropanol rinsing step of two minutes was included prior to re-equilibration.

Table A2 Gradients used for chromatographic separation on different columns: Eluent A was 0.1% formic acid in water, eluent B was 0.1% formic acid in methanol.

#	Stationary Phase	Flow rate	% Eluent B			
		[mL/min]	0 min	1 min	31 min	41 min
1	Nucleosil 100-5 OH	0.6	10	10	70	95
2	Nucleodur C18 Gravity	0.6	50	50	95	95
3	Kinetex	0.6	20	20	95	95
4	Zorbax Eclipse PAH	0.6	40	40	95	95
5	Nucleosil 100-5 NO2	0.6	20	20	95	95
6	Cosmosil NPE	0.8	30	30	95	95
7	Asahipak NH2	0.6	20	20	95	95
8	Luna NH2	0.6	5	5	95	95
9	Unison NH2	0.6	5	5	95	95
10	Cosmosil PYE	0.8	60	60	95	95
11	LiChroCART CN	0.6	20	20	95	95
12	Accucore PH	0.4	30	30	95	95
13	Fluophase RP	0.6	30	30	95	95
14	Accucore PFP	0.2	40	40	95	95
15	Hypersil Gold PFP	0.3	60	60	95	95
16	Cosmosil 5PBB-R	0.8	50	50	95	95
17	Polaris Amide	0.6	40	40	95	95

For mass spectrometric analysis multiple reaction monitoring (MRM) was used. The detection of analytes was conducted in positive and negative electrospray ionization mode. The source parameters for both modes were as follows: Ion source temperature was 500°C, ionisation voltage 3.5 kV (positive mode) and -3.5 kV (negative mode), gas 1 pressure was 45

a.u. , gas 2 pressure 50 a.u., curtain gas pressure 40 a.u., entrance lens potential voltage was 10 V (positive mode) and -10 V (negative mode), respectively. The dwell time for the mass transitions was set to 10 ms for all analytes. Peak detection and compound confirmation was done with the MultiQuant 3.0 software (ABSciex).

A1.2 Parallel fractionation of the river water extract

Table A3 Columns used for parallel fractionation.

Column name	Supplier	Functionalisation	Dimension and particle size	Dimension and particle size pre-column
Nucleodur C18 Gravity	Macherey-Nagel	Octadecyl	250 x 10.0 mm, 5 µm	10 x 10 mm, 5 µm
Unison NH2	Imtakt	Aminopropyl	150 x 10.0 mm, 3 µm	10 x 10 mm, 3 µm
Hypersil Gold PFP	Thermo Fisher	Pentafluorophenyl	250 x 10.0 mm, 5 µm	10 x 10 mm, 5 µm
Cosmosil PYE (#10)	Nacalai Tesque	Pyrenyl ethyl	150 x 4.6 mm, 5 µm	20 x 4.6 mm, 5 µm

All fractionations were carried out with 0.1% formic acid in water (A) and 0.1% of formic acid in methanol (B). Due to the different retention characteristics of the selected columns, the LC gradients used were adapted for each column based on the separation of the reference compound mixture. The preparative fractionation on the octadecyl-, aminoproyl- and pentafluorophenyl silica phase were carried out using the same gradients as applied for the separation of the test mixture containing 39 EDCs on the corresponding analytical scale C18 (#2), NH2 (#9) and PFP column (#10) at a flow rate of 2.8 mL/min (Table A2). Also the same, optimized gradient as applied for the separation of the test mixture was acquired for the analytical scale PYE column (#10) at a flow rate of 0.8 mL/min. All collected fractions are shown in Table S4.

Table A4 Overview of fractions collected by the parallel fractionation procedure on four orthogonal columns. Bold marked fractions were considered for data evaluation.

	Retention time window of fraction [min]			
Fraction name	**C18 #2**	**NH2 #9**	**PYE #10**	**PFP #15**
F1	1-10	1-3	2-3	3-10
F2	**10-14**	3-4	3-6	**10-12**
F3	**14-15**	4-5	6-9	**12-13**
F4	**15-16**	5-6	**9-12**	**13-14**
F5	**16-17**	**6-7**	**12-13**	**14-15**
F6	**17-18**	**7-8**	**13-14**	**15-16**
F7	**18-19**	**8-9**	**14-15**	**16-17**
F8	**19-20**	**9-10**	**15-16**	**17-18**
F9	**20-21**	**10-11**	**16-17**	**18-19**
F10	**21-22**	**11-12**	**17-18**	**19-20**
F11	**22-23**	**12-13**	**18-19**	**20-21**
F12	**23-24**	**13-14**	**19-20**	**21-22**
F13	**24-25**	**14-15**	**20-21**	**22-23**
F14	**25-26**	**15-16**	**21-22**	**23-24**
F15	**26-27**	**16-17**	**22-23**	**24-25**
F16	**27-28**	**17-18**	**23-24**	**25-26**
F17	**28-29**	**18-19**	**24-25**	**26-27**
F18	**29-30**	**19-20**	**25-26**	**27-28**
F19	**30-31**	**20-21**	**26-27**	**28-29**
F20	**31-32**	**21-22**	**27-28**	**29-30**
F21	**32-33**	**22-23**	**28-29**	**30-31**
F22	**33-34**	**23-24**	**29-30**	**31-32**
F23	**34-40**	**24-25**	**30-31**	**32-40**
F24	**40-49**	**25-26**	**31-32**	**40-50**
F25		**26-27**	**32-33**	
F26		**27-28**	**33-34**	
F27		**28-29**	**34-35**	
F28		**29-30**	**35-36**	
F29		**30-35**	**36-37**	
F30		**35-40**	**37-38**	
F31		**40-46**	**38-39**	
F32			**39-40**	
F33			**40-42**	
F34			**42-44**	
F35			**44-46**	

A1.3 LC-HRMS analysis

Chromatographic separation of the fractions was carried out using the gradient shown in Table A. Eluent C was used for rinsing the column after compound separation.

Table A5 LC gradient program.

Time [min]	Eluent A: 0.1% formic acid [%]	Eluent B: 0.1% formic acid in MeOH [%]	Eluent C: Isopropanol/Acetone 50/50 (v/v) [%]	Flow rate [mL/min]
0.0	95	5	0	0.30
1.0	95	5	0	0.30
13.0	0	100	0	0.30
24.0	0	100	0	0.30
24.1	5	10	85	0.35
26.2	5	10	85	0.35
26.3	95	5	0	0.35
31.9	95	5	0	0.35
32.0	95	5	0	0.30

For electrospray ionization in positive ion mode a H-ESI II source with the following settings was used: sheath gas flow rate 45 a.u., auxiliary gas flow rate 1 a.u., auxiliary gas heater temperature 300°C, spray voltage 3.80 kV, capillary temperature 300°C, S-lens RF level 70 a.u. The instrument was externally calibrated prior to analysis over the m/z range 74-1321 resulting in a mass accuracy < 2 ppm.

A1.4 HRMS data evaluation

Peak lists of the full scan data of all fractions were generated by MZmine 2.26 [18]. The noise cut-off of the mass detection within individual scans was set to 5000. The minimum time span for chromatogram building was set to 0.15 min, the minimum height to 10,000 a.u., and the m/z tolerance to 0.001 m/z. Smoothing of chromatograms was done using a filter width of 7. Settings for Deconvolution by local minimum search were: Chromatographic threshold 80%, search minimum in RT range 0.15 min, minimum relative height 20%, minimum absolute height 60,000 a.u., min ratio of peak top/edge 3.0 and peak duration range 0.15 to 4 min. The peak lists were aligned with the join aligner, the m/z tolerance was set to 0.001 m/z and 7 ppm and the RT range was 0.15 min.

A2 Results

A2.1 Retention Data of 39 EDCs on 17 different RPs

Table A6 Overview about retention times (in minutes) of 39 EDCs on 17 reversed phases. All runs were performed as a triplett. Displayed are the average retention times. Standard deviation of retention times was in average 0.016 min but never higher than 0.043 min per column. No carry over was observed.

Compound	#1 Nucleosil 100-5 OH	#2 Nucleodur C18 Gravity	#3 Kinetex C18	#4 Zorbax Eclipse PAH	#5 Nucleosil 100-5 NO2	#6 Cosmosil NPE	#7 Asahipak NH2	#8 Luna NH2	#9 Unison NH2	#10 Cosmosil PYE	#11 LiChroCART CN	#12 Accucore PH	#13 Fluophase RP	#14 Accucore PFP	#15 Hypersil Gold PFP	#16 Cosmosil 5PBB-R	#17 Polaris Amide
Dexamethasone	18.96	20.57	17.31	19.32	15.17	24.45	17.10	8.72	12.23	19.22	10.36	13.37	17.51	16.27	7.56	20.35	16.81
17β-Trenbolone	20.56	22.29	18.08	23.88	17.42	26.96	19.71	9.85	14.96	30.58	11.67	14.98	20.88	19.06	9.44	26.79	19.16
Norethindrone	22.86	23.74	19.32	24.10	18.17	27.45	19.50	9.27	15.01	33.18	12.57	16.63	22.39	20.75	10.34	25.70	20.18
Androsterone	28.48	30.70	23.62	29.68	18.89	28.21	20.49	10.07	15.50	30.16	17.75	21.90	24.37	23.48	14.02	28.35	24.98
Epi-Androsterone	26.30	28.26	21.90	29.88	19.33	28.35	20.13	10.07	15.50	36.83	21.41	19.37	24.37	23.48	13.07	29.89	24.55
Dihydro-testosterone	26.30	28.98	22.23	30.10	19.64	28.91	21.03	10.07	15.50	38.90	20.23	19.83	24.37	23.48	13.49	30.61	24.98
Testosterone	23.46	25.64	20.18	26.88	18.77	28.51	18.83	9.37	14.28	43.43	15.52	17.55	23.59	22.39	12.16	28.85	21.60
Levonorgestrel	25.61	26.62	21.16	30.10	19.84	29.01	20.21	10.20	15.93	36.57	13.68	19.29	23.82	22.93	12.42	29.56	22.51
Medroxy-progesterone	27.51	28.60	22.43	27.92	21.09	30.40	20.15	11.53	15.02	41.62	14.49	20.70	24.08	25.13	14.81	29.91	23.70
17α-estradiol	23.41	25.13	20.28	23.98	19.26	25.51	20.40	13.08	18.94	15.28	14.34	16.98	18.50	20.34	11.48	23.89	25.17
17β-estradiol	23.41	24.57	20.01	25.08	19.48	25.90	24.82	12.59	18.94	18.14	15.52	16.12	18.50	20.34	11.48	26.03	26.52
Isopimaric Acid	41.01	41.23	30.43	37.54	25.59	31.62	28.45	19.75	22.67	30.39	20.18	30.11	29.06	30.41	24.17	33.64	36.01
Abietic Acid	41.01	41.23	30.43	37.04	25.93	31.62	28.45	19.75	22.82	30.39	19.83	30.11	28.61	30.41	24.17	33.35	36.01
Estriol	-	14.37	13.46	15.19	15.05	20.87	20.42	8.36	15.36	8.63	11.11	8.21	12.63	13.04	6.35	17.98	18.02
Progesterone	28.58	30.25	23.18	32.32	23.14	33.16	21.60	12.13	16.05	-	15.77	21.92	26.66	27.93	16.94	35.68	24.43

Hydrocortisone	14.89	17.94	15.00	17.19	12.71	22.85	14.61	5.40	9.43	18.81	7.68	10.26	15.14	12.74	6.26	19.14	14.70
Bisphenol S	8.44	9.29	8.49	8.57	14.80	20.19	28.78	13.58	18.14	4.70	9.64	6.07	9.54	9.75	5.32	10.01	12.59
Isoeugenol	13.40	21.39	15.49	21.30	12.87	21.43	27.04	12.93	16.83	9.99	10.74	11.48	15.83	15.87	8.58	16.75	18.82
2-Naphthol	11.10	19.26	13.56	18.99	13.81	20.72	31.13	15.52	19.11	7.55	11.60	11.04	12.93	14.30	7.95	16.60	20.18
2,2´-Dihydroxybiphenyl	10.05	19.05	13.44	17.86	11.30	20.45	29.58	13.09	17.79	8.16	9.62	11.46	12.42	11.78	6.62	13.78	18.77
Genistein	16.73	17.88	15.54	18.31	21.90	26.41	39.53	16.26	22.37	13.42	13.30	10.87	14.04	18.29	10.09	22.70	24.00
Propylparaben	14.97	20.75	15.87	19.69	12.29	21.13	26.07	10.69	16.52	8.34	10.10	12.27	17.15	15.94	8.47	14.59	19.55
3-Hydroxybiphenyl	18.41	23.69	17.79	22.66	16.56	23.49	31.80	16.48	20.70	11.22	14.05	15.05	16.11	17.49	9.47	19.03	23.34
Benzophenone-3	26.06	29.46	21.85	28.92	20.88	29.64	33.89	14.03	20.41	22.96	15.99	19.40	21.04	25.66	16.66	28.27	25.00
1-Hydroxypyrene	30.82	31.32	23.02	32.17	26.71	30.33	41.34	25.68	25.44	20.12	19.49	19.57	17.93	27.24	20.28	35.20	34.32
Zearalenone	25.82	26.26	20.75	24.42	22.70	29.77	27.13	13.99	19.04	29.63	15.38	18.10	19.74	25.65	16.67	27.85	25.17
Procymidone	21.30	27.47	20.23	26.65	19.04	30.26	28.02	9.46	17.14	20.44	15.59	18.10	20.48	22.72	12.92	22.70	22.65
N-Benzylphthalimide	22.06	25.66	19.33	25.27	18.71	27.74	31.78	11.22	18.01	27.84	14.78	17.15	19.19	20.80	11.46	28.56	20.64
Carbaryl	12.95	17.13	13.41	18.38	13.43	20.68	23.87	11.99	15.82	9.01	11.04	10.34	14.11	13.37	6.68	15.98	14.91
Propanil	17.12	24.95	18.19	24.47	15.85	26.11	26.50	11.16	17.93	12.80	12.67	15.21	18.04	20.70	12.49	20.26	23.23
Tris (1-chloro-2-propoyl) phosphate	22.93	24.55	19.48	24.41	12.45	25.68	19.85	7.80	13.23	15.87	12.87	17.84	21.41	20.58	9.96	17.32	19.61
Linuron	18.34	24.30	18.05	24.75	16.75	27.12	27.18	12.10	17.66	13.69	13.51	15.06	17.95	21.07	12.26	21.01	21.72
Metolachlor	24.87	27.95	21.11	26.93	14.92	26.73	17.70	9.01	12.78	22.69	12.07	19.53	23.16	23.00	11.56	23.31	20.89
Flutamide	21.03	24.99	19.28	23.54	16.90	28.69	25.70	9.30	17.90	15.26	14.87	17.17	23.65	25.43	16.84	18.21	23.53
Flavone	25.72	26.26	20.35	29.09	21.55	28.68	28.76	15.42	19.30	29.72	15.11	16.66	20.98	22.76	13.34	31.03	21.59
Methylparathion	19.77	23.94	18.32	23.27	18.02	28.84	32.12	10.30	18.48	20.69	15.02	16.90	20.44	22.50	12.10	22.90	20.71
Fenthion	29.14	30.15	23.04	28.38	21.02	29.94	30.88	14.16	20.81	23.09	18.28	22.25	21.59	25.40	15.89	28.83	25.25
Triphenylphosphat	32.35	29.75	23.83	28.22	21.22	28.29	26.30	15.37	19.74	21.87	18.23	23.32	23.50	25.86	16.19	27.88	24.34
Benzylbutyl-phthalate	33.59	32.47	25.23	30.10	21.98	30.05	28.35	14.71	19.63	25.84	18.47	24.89	24.76	27.67	18.49	29.56	26.60

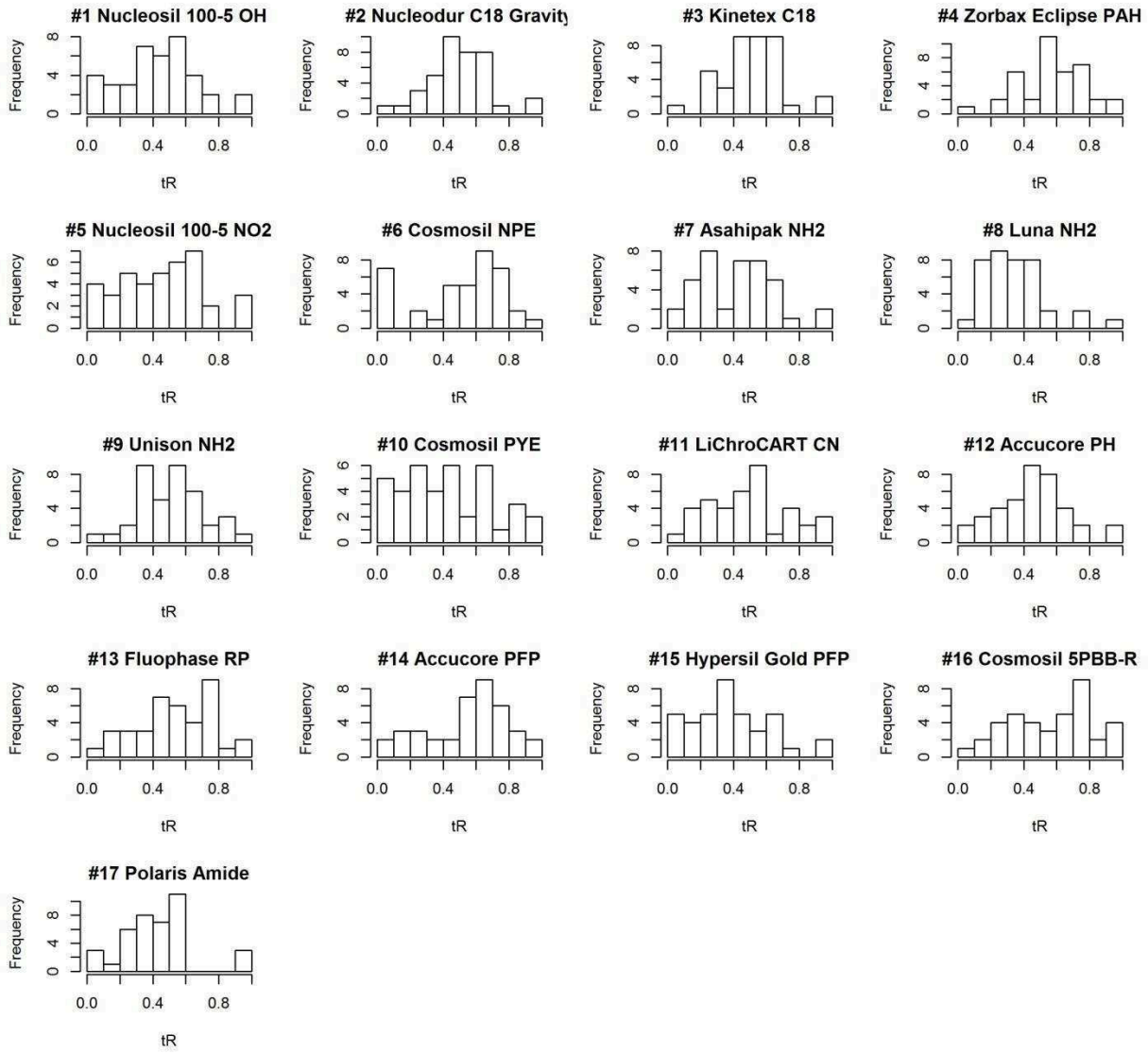

Figure A2 Histograms of the normalized retention times of the 39 EDCs on the 17 test columns.

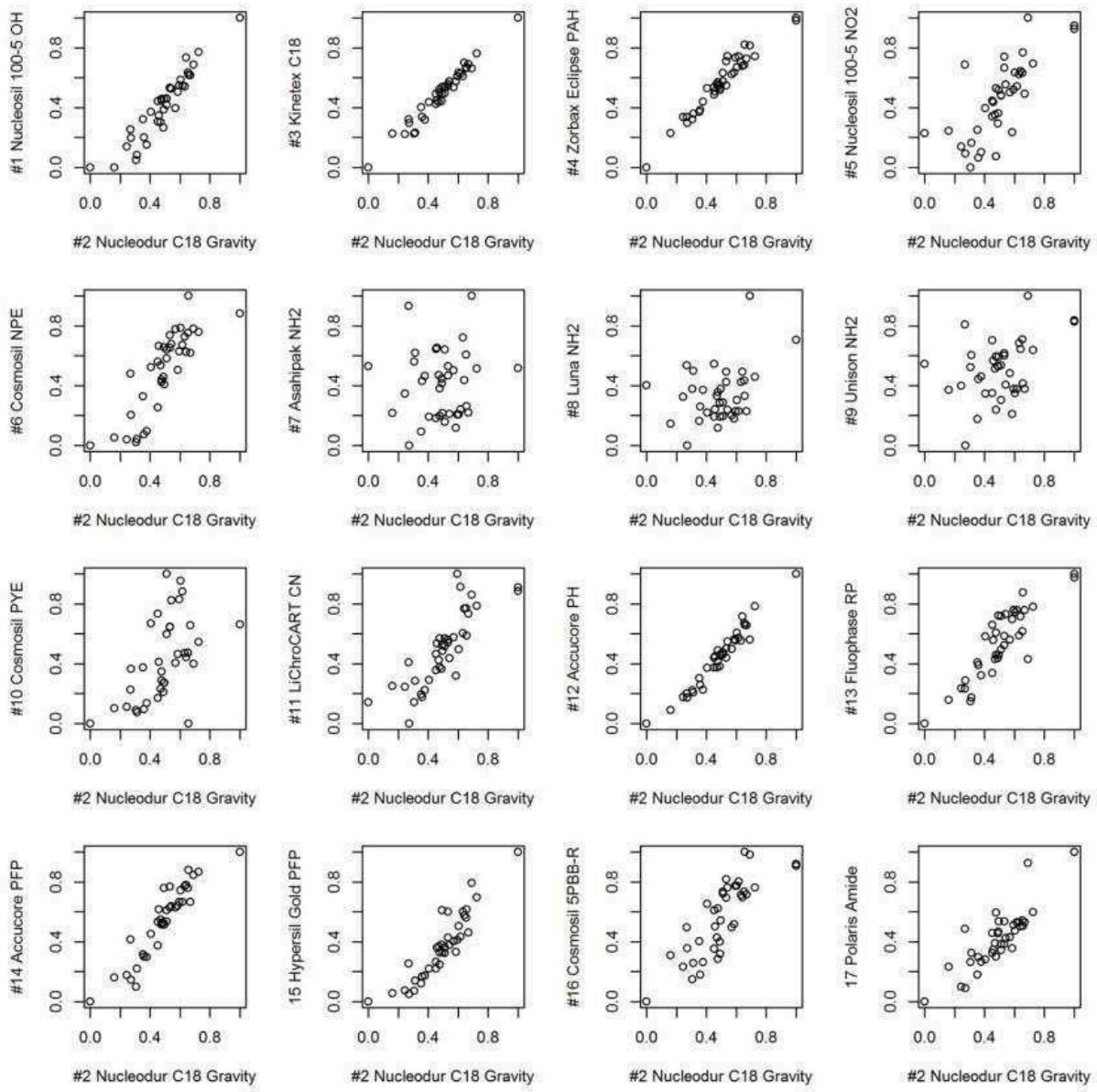

Figure A3 Plots of normalized retention times of the 39 EDCs on 16 columns against those on the reference C18 column (#2).

A2.2 Evaluation of retention data

Table A7 Loading of columns on principal component 1 and 2.

#	Column	Loading on PC1	Loading on PC2	Angle to reference column #2 [degree]
1	Nucleosil 100-5 OH	0.98	-0.02	3.1
2	Nucleodur C18 Gravity	0.96	0.03	0.0
3	Kinetex	0.98	-0.03	3.7
4	Zorbax Eclipse PAH	0.96	-0.03	3.6
5	Nucleosil 100-5 NO2	0.81	0.31	18.9
6	Cosmosil NPE	0.92	0.03	0.2
7	Asahipak NH2	-0.11	0.94	94.9
8	Luna NH2	0.11	0.91	81.0
9	Unison NH2	0.14	0.94	79.4
10	Cosmosil PYE	0.76	-0.42	30.8
11	LiChroCART CN	0.88	0.18	9.5
12	Accucore PH	0.97	-0.05	4.9
13	Fluophase RP	0.95	-0.35	22.0
14	Accucore PFP	0.95	0.07	2.3
15	Hypersil Gold PFP	0.91	0.18	9.2
16	Cosmosil 5PBB-R	0.92	-0.04	4.3
17	Polaris Amide	0.78	0.35	22.3

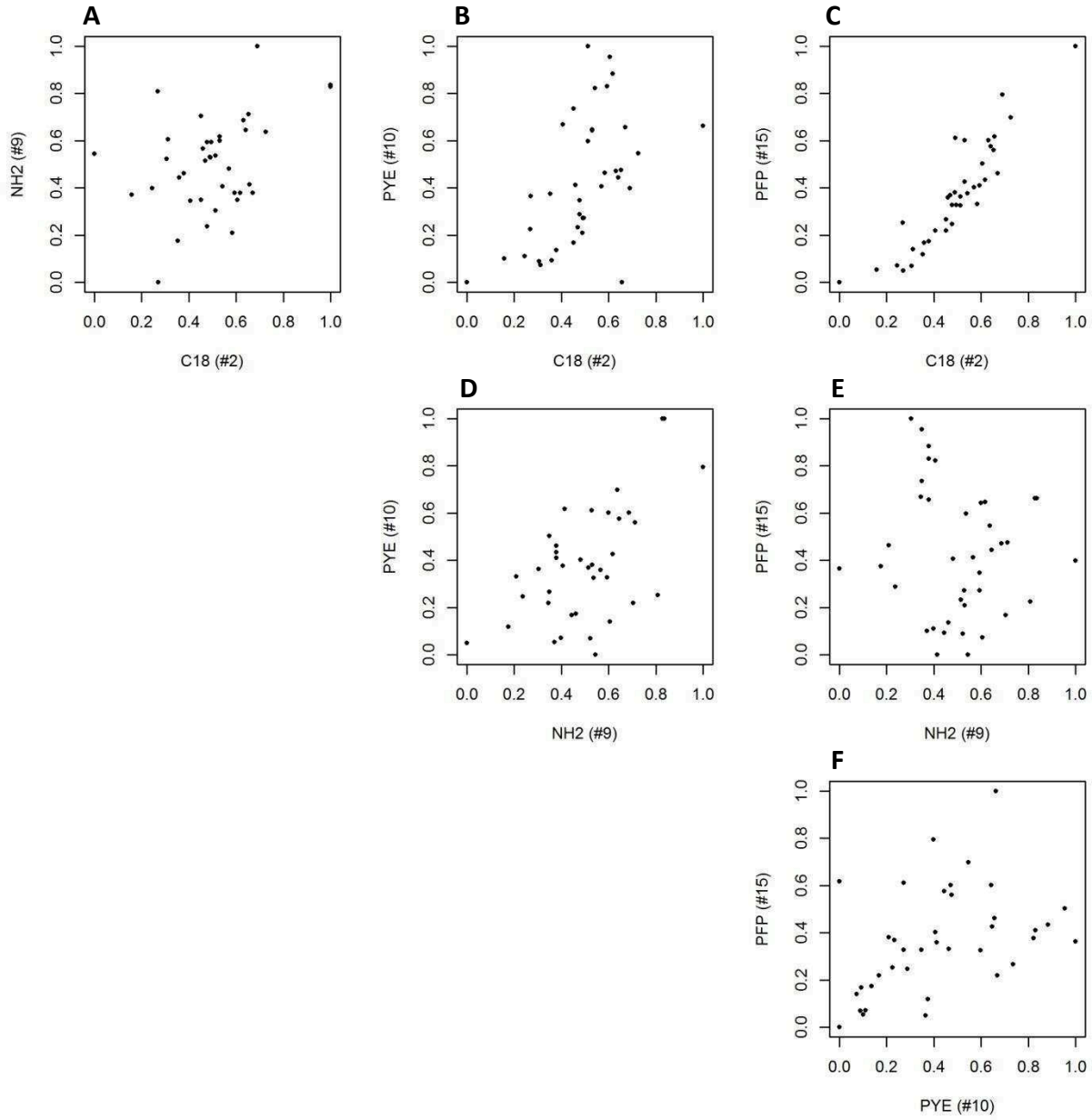

Figure A4 Plots of normalized retention times of the column pairs C18 (#2) vs. (a) NH2 (#9), (b) PYE (#10) and (c) PFP (#15), of the pairs NH2 (#9) vs. (d) PYE (#10) and (e) PFP (#15) and (f) the pair PYE (#10) vs. PFP (#15).

S2.3 Evaluation of the whole non-target peak inventory

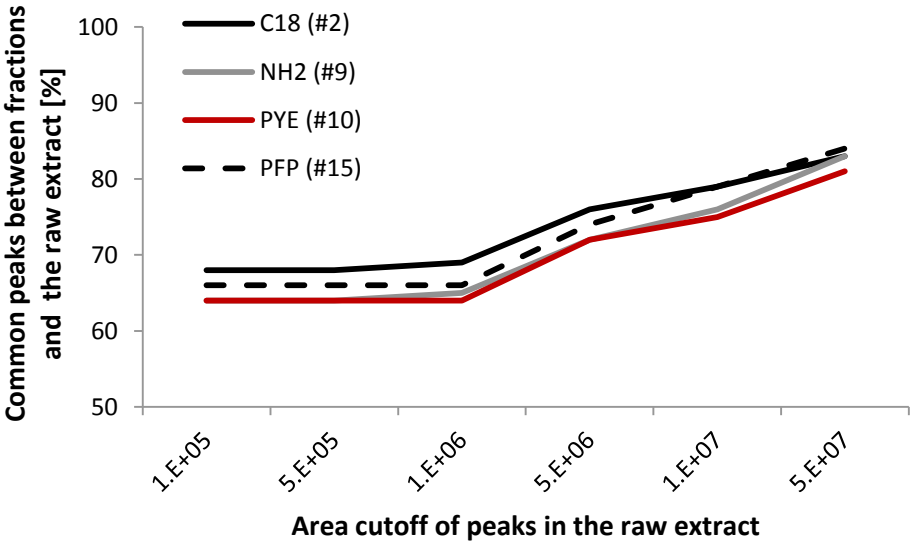

Figure A5 Influence of the area cutoff in the extract on the number of common peaks between the fractions of the C18 (#2), PFP (#15), PYE (#10) and NH2 column (#9) and the raw water extract.

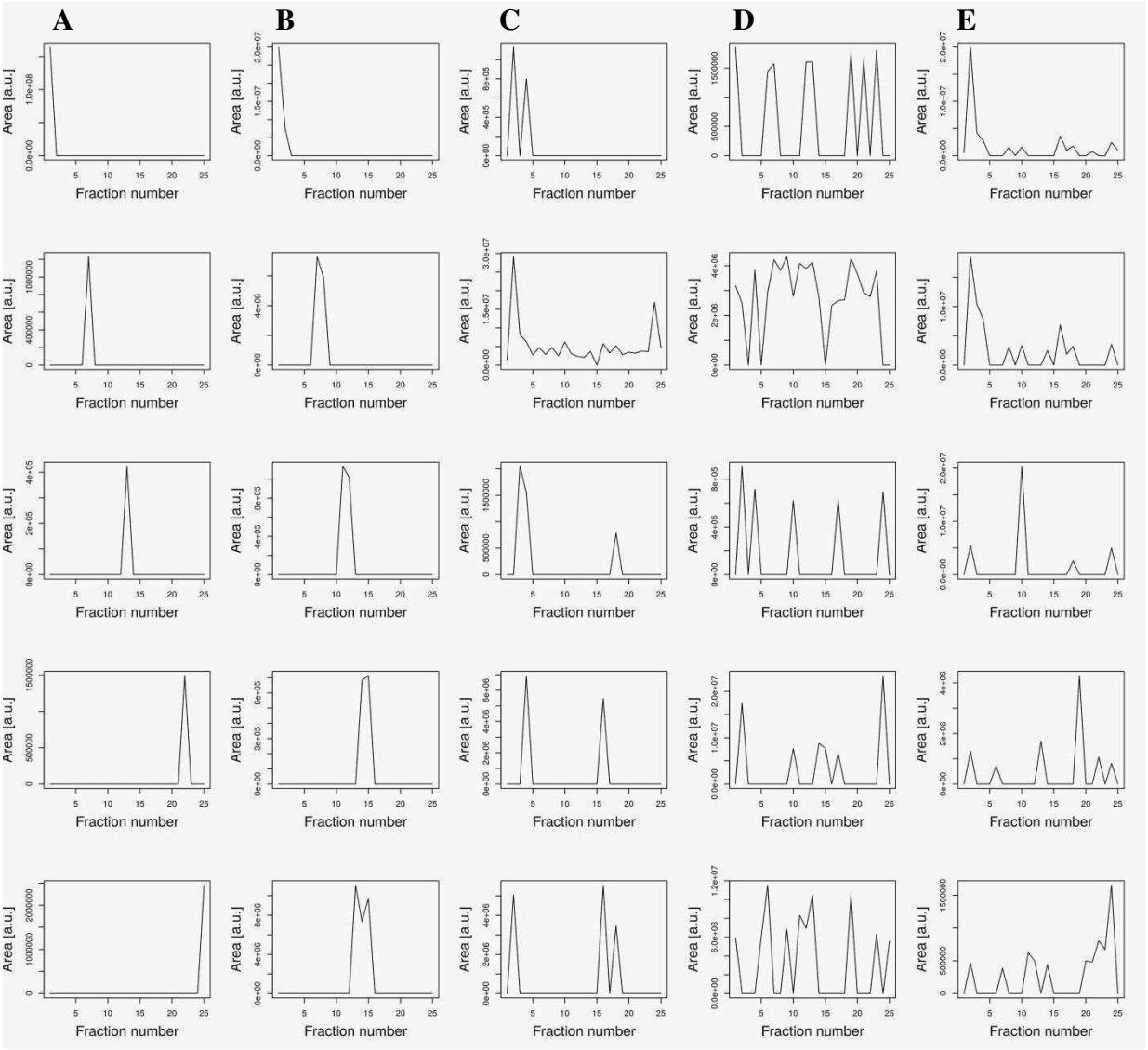

Figure A6 Overview about different distribution patterns of the automatically picked non-target peaks across the preparative fractions of the C18 column (#2). (a) 60% of the peaks were collected and picked in one, (b) 14% in two or three adjacent fractions and (c-e) 21% in non-consecutive fractions.

Table A8 Overview about the average number of peaks received by automated peak detection in one to five fractions of the four stationary phases.

	Number of peaks detected	Number of peaks detected in consecutive fractions
within one fraction	14272	-
within two fraction	3889	2665
within three fraction	1374	514
within four fraction	717	161
within five fraction	464	69

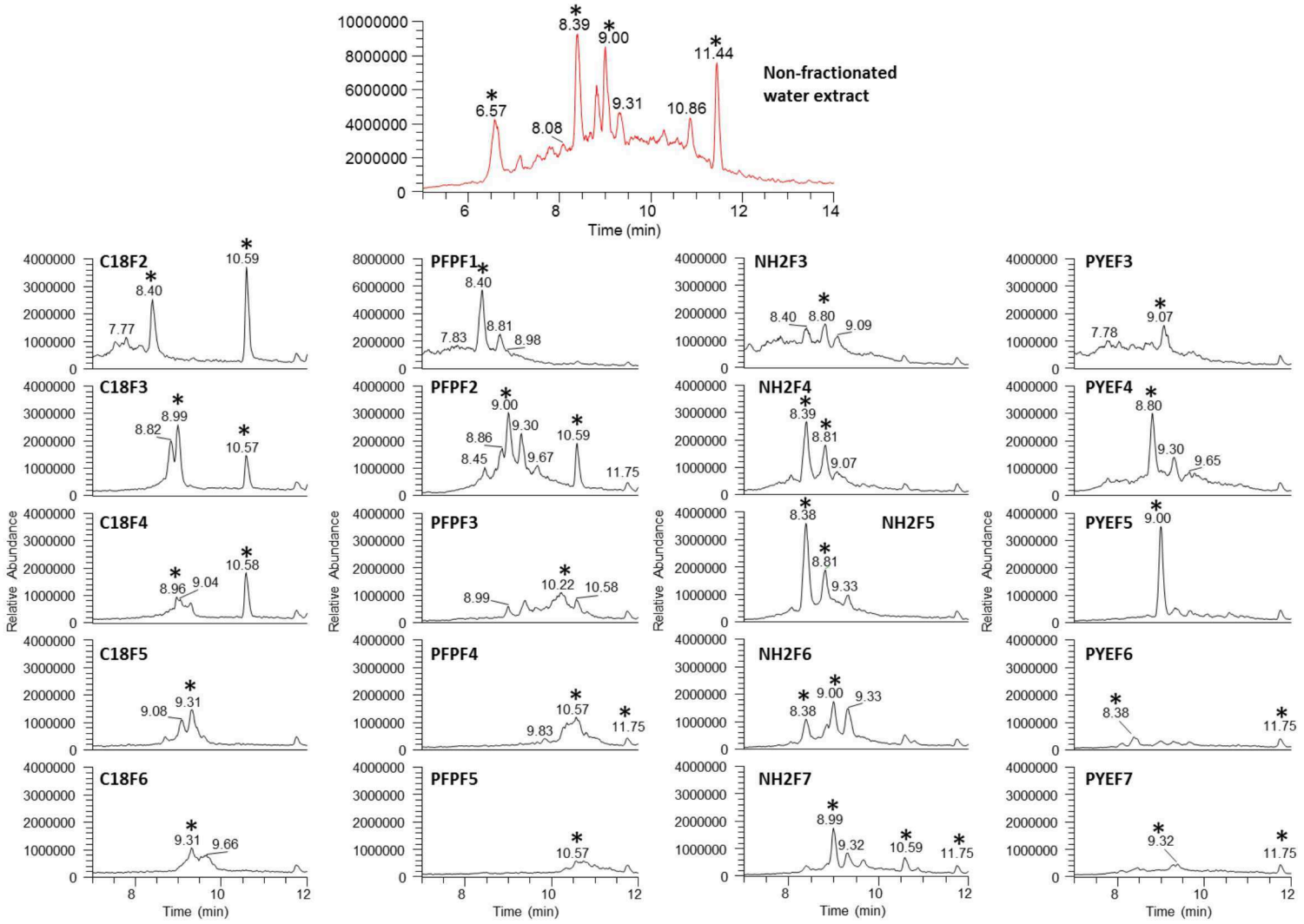

Figure A7 XICs of the mass 207.1379 (at 5ppm mass accuracy) of the raw water extract and some fractions from a fractionation on the C18 (#2), PFP (#15), NH2 (#9) and PYE (#10) columns. Peaks picked by MZMine are labelled with an asterisk. Note the different scales for the raw extract and the individual fractions.

Table A9 Overview about the number of peaks in each fraction of the C18 column (#2).

Fractions	C18F2	C18F3	C18F4	C18F5	C18F6	C18F7	C18F8	C18F9	C18F10	C18F11	C18F12	C18F13	C18F14	C18F15	C18F16	C18F17	C18F18	C18F19	C18F20	C18F21	C18F22	C18F23	C18F24
C18F2	511	33	4	0	0	0	0	0	0	0	0	0	0	0	0	0	0	0	0	0	0	0	0
C18F3	33	183	39	5	0	0	0	0	0	0	0	0	0	0	0	0	0	0	0	0	0	0	0
C18F4	4	39	193	56	2	0	0	0	0	0	0	0	0	0	0	0	0	0	0	0	0	0	0
C18F5	0	5	56	196	35	0	0	0	0	0	0	0	0	0	0	0	0	0	0	0	0	0	0
C18F6	0	0	2	35	181	27	0	0	0	0	0	0	0	0	0	0	0	0	0	0	0	0	0
C18F7	0	0	0	0	27	129	26	0	0	0	0	0	0	0	0	0	0	0	0	0	0	0	0
C18F8	0	0	0	0	0	26	140	37	5	0	0	0	0	0	0	0	0	0	0	0	0	0	0
C18F9	0	0	0	0	0	0	37	197	42	4	0	0	0	0	0	0	0	0	0	0	0	0	0
C18F10	0	0	0	0	0	0	5	42	138	30	1	0	0	0	0	0	0	0	0	0	0	0	0
C18F11	0	0	0	0	0	0	0	4	30	167	65	3	0	0	0	0	0	0	0	0	0	0	0
C18F12	0	0	0	0	0	0	0	0	1	65	190	30	1	0	0	0	0	0	0	0	0	0	0
C18F13	0	0	0	0	0	0	0	0	0	3	30	110	16	3	0	0	0	0	0	0	0	0	0
C18F14	0	0	0	0	0	0	0	0	0	0	1	16	98	16	1	1	0	0	0	0	0	0	0
C18F15	0	0	0	0	0	0	0	0	0	0	0	3	16	159	31	1	0	0	0	0	0	0	0
C18F16	0	0	0	0	0	0	0	0	0	0	0	0	1	31	150	27	0	0	0	0	0	0	0
C18F17	0	0	0	0	0	0	0	0	0	0	0	0	1	1	27	106	29	0	0	0	0	0	0
C18F18	0	0	0	0	0	0	0	0	0	0	0	0	0	0	0	29	149	25	0	0	0	0	0
C18F19	0	0	0	0	0	0	0	0	0	0	0	0	0	0	0	0	25	81	4	0	0	0	0
C18F20	0	0	0	0	0	0	0	0	0	0	0	0	0	0	0	0	0	4	32	8	0	0	0
C18F21	0	0	0	0	0	0	0	0	0	0	0	0	0	0	0	0	0	0	8	41	12	0	0
C18F22	0	0	0	0	0	0	0	0	0	0	0	0	0	0	0	0	0	0	0	12	59	10	0
C18F23	0	0	0	0	0	0	0	0	0	0	0	0	0	0	0	0	0	0	0	0	10	121	1
C18F24	0	0	0	0	0	0	0	0	0	0	0	0	0	0	0	0	0	0	0	0	0	1	6

Table A10 Overview about the number of common peaks of fractions of the C18 (#2) and PFP column (#15).

Fractions	C18F2	C18F3	C18F4	C18F5	C18F6	C18F7	C18F8	C18F9	C18F10	C18F11	C18F12	C18F13	C18F14	C18F15	C18F16	C18F17	C18F18	C18F19	C18F20	C18F21	C18F22	C18F23	C18F24
PFPF2	127	93	127	123	85	51	40	30	14	3	0	0	0	1	0	0	0	0	1	0	0	0	0
PFPF3	14	24	24	36	45	35	61	67	57	20	4	0	0	0	0	0	0	0	0	0	0	0	0
PFPF4	10	10	13	12	29	28	32	55	30	63	44	4	1	1	0	0	0	0	0	0	0	0	0
PFPF5	13	3	7	9	8	13	18	41	20	38	47	33	6	6	0	0	0	0	0	0	0	0	0
PFPF6	4	0	1	4	5	6	8	25	19	32	69	39	23	19	6	2	1	0	0	0	0	0	0
PFPF7	1	0	3	5	16	9	2	16	18	38	48	26	25	37	47	5	4	0	0	0	0	0	0
PFPF8	1	0	2	1	21	10	1	4	8	9	15	8	11	38	30	30	19	2	0	0	0	0	0
PFPF9	2	0	2	0	4	4	7	3	1	6	12	14	13	26	38	33	39	20	1	0	0	0	0
PFPF10	5	0	2	1	1	0	1	0	0	0	3	5	4	13	19	30	71	39	5	1	0	0	1
PFPF11	2	0	0	0	0	2	3	0	1	2	0	0	1	8	18	15	32	23	4	7	6	1	0
PFPF12	2	0	0	0	0	2	2	1	0	3	3	1	1	4	6	1	14	18	4	11	10	6	0
PFPF13	0	0	0	5	4	2	0	0	0	1	0	3	1	37	3	3	6	5	8	5	7	6	0
PFPF14	4	0	0	0	0	0	0	0	0	0	0	1	26	10	3	5	3	3	12	8	13	9	0
PFPF15	11	0	0	0	0	0	0	0	0	0	0	0	0	1	14	10	7	2	1	7	13	21	0
PFPF16	10	1	0	1	0	0	0	0	0	0	1	0	1	0	5	6	6	4	0	7	15	25	0
PFPF17	8	1	0	0	0	0	0	0	0	0	1	0	0	0	0	0	2	1	0	0	7	41	0
PFPF18	9	7	0	0	0	0	0	0	0	0	0	0	0	0	0	1	0	0	1	1	4	29	1
PFPF19	7	6	0	0	0	0	0	0	0	0	0	0	0	0	0	0	0	0	1	0	0	11	0
PFPF20	5	1	0	0	0	0	0	0	0	0	0	0	0	0	0	0	0	1	0	0	0	5	0
PFPF21	1	0	2	0	0	0	0	0	0	0	0	0	1	0	0	0	0	0	1	0	0	5	0
PFPF22	0	0	0	0	0	0	0	0	0	0	0	0	0	0	0	0	0	0	0	0	0	7	3
PFPF23	0	20	5	2	0	0	2	0	0	0	0	1	0	0	0	0	1	0	0	1	1	1	3
PFPF24	2	0	0	0	0	0	1	0	0	0	0	0	0	0	0	0	1	0	1	0	0	0	0

Table A11 Overview about the number of common peaks of fractions of the C18 (#2) and PYE column (#10).

Fractions	C18F2	C18F3	C18F4	C18F5	C18F6	C18F7	C18F8	C18F9	C18F10	C18F11	C18F12	C18F13	C18F14	C18F15	C18F16	C18F17	C18F18	C18F19	C18F20	C18F21	C18F22	C18F23	C18F24
PYEF4	109	41	58	46	41	27	26	41	37	18	9	0	0	1	0	0	0	0	0	0	0	0	0
PYEF5	38	14	34	33	30	18	8	11	16	20	16	5	0	1	1	1	1	0	0	0	0	1	0
PYEF6	19	16	30	23	10	4	6	11	9	11	12	8	0	2	20	1	0	0	0	0	0	0	0
PYEF7	34	8	13	38	16	10	14	11	8	18	22	9	5	3	21	1	1	1	0	0	0	0	0
PYEF8	20	5	8	30	11	13	12	5	10	9	8	15	7	6	2	1	1	1	0	0	0	0	0
PYEF9	15	4	6	14	13	14	14	12	4	4	5	6	2	10	5	4	1	0	0	0	0	0	0
PYEF10	14	6	5	4	10	4	14	16	12	13	14	11	2	6	7	2	4	2	0	0	0	0	0
PYEF11	15	10	12	6	5	4	5	16	12	16	13	7	6	10	2	3	1	0	0	0	0	0	1
PYEF12	18	15	7	11	15	9	13	22	11	16	15	11	1	18	13	14	9	5	0	1	0	0	0
PYEF13	15	16	8	7	13	8	10	13	12	25	25	10	5	19	17	16	10	9	0	1	1	1	0
PYEF14	11	5	2	2	3	4	5	10	4	15	21	11	11	2	6	7	12	11	0	0	1	1	0
PYEF15	14	6	4	5	22	10	6	19	11	9	19	11	10	9	15	11	39	10	3	3	5	1	0
PYEF16	14	11	13	4	8	10	2	6	9	10	20	19	11	12	13	20	36	15	6	6	7	1	0
PYEF17	9	12	5	4	4	7	6	9	3	11	18	17	10	12	18	20	18	15	3	2	6	3	0
PYEF18	5	12	4	3	4	4	4	5	3	16	34	4	4	14	4	4	14	8	1	1	5	4	0
PYEF19	5	12	7	4	4	2	7	10	5	8	12	15	14	18	11	6	18	8	0	3	4	8	0
PYEF20	3	9	3	2	2	3	2	6	1	1	2	8	8	9	13	6	6	5	0	4	0	6	0
PYEF21	4	3	3	1	2	3	3	9	1	1	0	2	5	6	10	6	5	6	2	2	2	8	0
PYEF22	6	6	8	4	0	0	1	5	1	0	1	2	0	2	7	5	9	7	0	2	5	16	0
PYEF23	4	5	4	6	4	1	1	3	1	0	1	0	0	3	8	7	9	9	3	1	8	22	0
PYEF24	6	5	2	5	4	3	2	1	1	3	1	1	1	0	5	6	14	3	2	1	0	14	0
PYEF25	10	7	6	3	3	1	4	0	1	3	1	1	2	24	3	4	11	3	3	3	4	17	1
PYEF26	16	10	7	1	0	2	3	1	2	4	1	0	2	32	3	3	0	3	4	5	5	7	1
PYEF27	17	9	2	1	1	2	3	1	1	2	1	0	1	10	3	4	10	1	6	3	4	8	0
PYEF28	17	3	1	0	0	0	0	0	0	0	1	2	3	5	5	3	7	1	9	7	4	5	0

Fractions	C18F2	C18F3	C18F4	C18F5	C18F6	C18F7	C18F8	C18F9	C18F10	C18F11	C18F12	C18F13	C18F14	C18F15	C18F16	C18F17	C18F18	C18F19	C18F20	C18F21	C18F22	C18F23	C18F24
PYEF29	19	1	0	0	0	0	0	2	1	0	0	1	10	4	3	4	3	2	2	7	2	13	1
PYEF30	14	2	1	1	0	0	3	1	0	0	0	1	26	2	4	3	3	4	0	4	10	10	1
PYEF31	13	1	2	0	0	0	3	1	0	0	0	1	3	2	4	0	2	1	0	4	11	2	1
PYEF32	14	1	0	0	0	1	1	0	0	2	0	1	0	3	4	0	0	0	0	1	6	5	0
PYEF33	26	0	1	1	1	0	1	1	0	2	0	1	0	10	19	4	0	0	0	0	1	11	1
PYEF34	27	0	1	1	1	0	0	1	0	2	2	0	0	1	3	5	0	0	0	0	4	20	2
PYEF35	13	1	0	0	8	4	0	0	0	0	0	0	0	1	1	0	0	0	0	0	0	10	0

Table A12 Overview about the number of common peaks of fractions of the C18 (#2) and NH2 column (#9).

Fractions	C18F2	C18F3	C18F4	C18F5	C18F6	C18F7	C18F8	C18F9	C18F10	C18F11	C18F12	C18F13	C18F14	C18F15	C18F16	C18F17	C18F18	C18F19	C18F20	C18F21	C18F22	C18F23	C18F24
NH2F5	147	39	42	16	23	22	21	22	15	3	4	2	4	0	0	1	0	0	1	0	0	0	0
NH2F6	113	40	42	28	28	16	21	21	11	17	9	1	2	0	3	2	1	1	0	0	0	0	0
NH2F7	82	32	34	33	24	13	21	19	5	16	18	5	6	6	20	2	1	1	0	0	0	0	0
NH2F8	71	30	30	36	29	13	15	25	13	26	47	20	6	12	32	9	9	5	2	0	0	0	0
NH2F9	68	31	30	41	32	8	9	24	16	23	39	20	9	16	29	10	11	4	1	1	0	0	1
NH2F10	45	23	34	34	19	11	5	12	18	14	16	10	7	16	21	16	18	9	2	2	0	2	0
NH2F11	38	28	29	44	20	14	15	21	14	14	11	11	10	29	29	20	19	10	2	2	1	2	0
NH2F12	23	20	17	24	16	13	13	31	14	10	9	9	29	19	19	12	19	14	1	8	5	2	0
NH2F13	19	13	16	7	28	21	12	28	13	11	12	7	27	13	15	6	16	13	0	4	3	6	0
NH2F14	23	12	15	8	29	19	16	27	16	14	16	13	30	14	22	14	18	18	2	2	7	11	1
NH2F15	18	11	9	8	13	13	17	13	11	8	14	16	17	12	13	13	9	13	5	2	13	7	0
NH2F16	10	7	7	7	4	5	13	14	7	10	28	12	8	11	10	9	8	7	4	3	8	9	1
NH2F17	15	7	14	7	6	7	6	8	6	10	21	8	7	18	10	10	16	9	2	1	4	7	2
NH2F18	15	11	13	9	6	3	6	10	5	5	10	9	11	20	12	4	26	9	3	0	2	8	1
NH2F19	16	10	8	7	6	2	1	6	0	6	13	4	5	14	9	3	14	5	1	3	1	4	0
NH2F20	11	5	3	6	5	2	0	6	6	8	9	1	3	4	7	2	4	5	0	3	2	8	1
NH2F21	11	4	2	6	4	2	1	10	10	13	12	3	1	5	6	4	2	2	0	0	4	18	2
NH2F22	4	3	1	2	2	5	4	7	12	13	18	3	1	8	5	7	5	2	0	3	8	28	0
NH2F23	4	4	3	3	4	5	3	9	7	10	19	3	2	6	2	7	7	3	2	1	7	30	0
NH2F24	1	2	2	0	1	3	1	5	0	1	8	7	0	4	2	5	3	1	0	0	1	18	0
NH2F25	2	1	1	0	0	2	5	2	1	2	3	9	0	0	2	5	22	0	1	0	0	7	0
NH2F26	3	0	2	1	0	0	4	0	6	5	5	4	0	2	3	1	21	1	0	0	0	5	0
NH2F27	3	2	4	6	0	0	1	2	5	7	7	2	0	3	2	1	12	1	0	0	0	4	0
NH2F28	3	3	4	6	0	0	0	2	4	5	7	2	0	3	2	3	10	2	0	0	0	3	0
NH2F29	9	6	5	12	3	7	5	5	7	12	11	3	2	8	4	2	12	3	0	0	0	5	0
NH2F30	7	1	3	5	1	7	7	5	3	1	1	1	4	5	3	3	5	0	0	0	0	1	0
NH2F31	6	1	2	1	2	7	6	5	5	1	0	1	5	34	6	4	2	4	0	1	1	1	0

Table A13 Overview about the number of common peaks of fractions of the NH2 (#9) and the PYE column (#10).

Fractions	NH2F5	NH2F6	NH2F7	NH2F8	NH2F9	NH2F10	NH2F11	NH2F12	NH2F13	NH2F14	NH2F15	NH2F16	NH2F17	NH2F18	NH2F19	NH2F20	NH2F21	NH2F22	NH2F23	NH2F24	NH2F25	NH2F26	NH2F27	NH2F28	NH2F29	NH2F30	NH2F31
PYEF4	112	107	65	55	56	44	44	30	29	27	28	20	16	16	12	12	18	22	24	6	7	3	6	6	15	10	7
PYEF5	33	44	41	46	38	22	22	17	16	16	14	10	15	14	8	7	10	15	15	2	2	0	6	7	9	8	4
PYEF6	25	27	35	33	30	20	20	15	11	14	11	12	16	7	3	1	2	4	5	10	7	3	4	3	5	2	0
PYEF7	20	19	39	41	37	21	33	19	7	15	12	6	10	4	4	2	6	10	10	13	9	8	9	6	14	8	4
PYEF8	22	18	18	27	24	16	12	12	13	16	12	12	6	4	6	6	3	3	2	1	4	5	3	1	7	2	1
PYEF9	19	16	9	21	22	17	16	15	13	13	8	9	6	4	5	3	4	2	2	0	1	1	0	0	6	2	2
PYEF10	10	14	7	20	17	11	14	14	10	10	6	7	8	7	7	4	7	6	7	1	0	0	0	0	6	3	5
PYEF11	16	14	12	10	17	12	14	10	9	9	7	13	11	7	5	3	4	5	6	3	2	0	1	0	3	1	1
PYEF12	14	14	13	15	24	24	29	18	12	15	18	15	13	13	12	4	6	8	7	4	3	3	3	2	5	5	1
PYEF13	12	18	14	21	17	28	34	26	18	16	14	12	11	20	20	11	7	8	8	4	0	4	4	5	6	2	3
PYEF14	6	9	7	16	12	9	16	17	15	13	7	5	10	15	12	5	4	1	3	1	1	0	0	1	2	2	4
PYEF15	13	8	4	16	19	18	20	22	45	41	26	8	8	12	9	3	1	7	8	3	20	15	7	6	10	4	7
PYEF16	11	8	6	13	22	21	21	19	23	31	30	14	10	13	4	3	4	5	5	2	21	15	8	9	10	5	6
PYEF17	6	7	9	17	19	25	26	17	10	12	15	15	13	14	5	2	3	1	2	2	1	0	1	4	6	3	4
PYEF18	4	8	15	36	27	17	25	14	8	7	4	5	9	10	8	4	3	2	2	1	1	2	1	1	2	1	0
PYEF19	8	11	17	14	14	17	16	16	11	14	9	4	11	11	8	8	7	5	5	1	3	8	5	4	5	3	1
PYEF20	5	5	2	5	7	3	3	12	10	13	7	5	5	5	4	6	5	4	3	1	1	3	3	3	4	2	0
PYEF21	3	3	4	4	3	6	11	14	13	20	6	3	2	6	3	2	2	0	4	4	2	1	1	1	3	1	1
PYEF22	6	5	5	7	4	7	6	7	7	12	4	6	3	0	0	0	2	11	13	8	2	1	2	3	2	1	1
PYEF23	5	3	3	7	5	4	3	8	8	12	13	12	8	1	0	0	2	14	13	5	2	0	1	1	1	0	0
PYEF24	5	4	3	5	9	8	3	4	5	5	2	3	4	0	0	0	6	13	9	4	3	1	0	0	1	0	0
PYEF25	6	3	3	3	8	9	8	3	1	7	4	3	1	1	0	4	10	11	6	4	0	0	1	1	3	0	23
PYEF26	8	7	2	4	6	7	4	2	1	3	4	1	1	5	5	7	6	4	0	0	0	1	1	1	3	0	31
PYEF27	8	7	5	6	5	5	2	2	4	6	6	4	8	14	10	7	6	4	1	1	0	2	1	0	0	0	4
PYEF28	4	1	1	2	4	2	2	0	1	4	5	4	4	8	7	3	1	1	0	2	2	1	1	1	0	0	1

Fractions	NH2F5	NH2F6	NH2F7	NH2F8	NH2F9	NH2F10	NH2F11	NH2F12	NH2F13	NH2F14	NH2F15	NH2F16	NH2F17	NH2F18	NH2F19	NH2F20	NH2F21	NH2F22	NH2F23	NH2F24	NH2F25	NH2F26	NH2F27	NH2F28	NH2F29	NH2F30	NH2F31
PYEF29	2	0	0	0	2	1	4	10	9	11	8	10	4	2	2	2	3	1	2	3	2	1	1	1	0	0	2
PYEF30	4	1	0	0	0	1	6	26	26	27	12	8	2	2	1	0	1	0	4	5	1	1	1	1	1	0	4
PYEF31	4	1	0	0	0	1	5	8	5	7	2	1	0	0	1	0	1	0	0	0	0	0	0	0	0	0	1
PYEF32	2	1	1	1	1	1	3	1	0	0	0	2	2	0	1	1	0	0	0	0	0	0	0	0	2	0	0
PYEF33	1	1	0	10	14	13	17	3	1	0	0	3	3	1	0	0	0	0	0	0	0	0	0	0	1	0	0
PYEF34	1	1	0	4	6	4	6	2	1	2	3	3	6	7	3	2	2	1	1	0	0	1	1	1	1	0	0
PYEF35	1	1	0	0	3	2	1	2	7	6	5	0	2	5	3	2	2	0	0	0	0	1	1	1	1	0	0

Table A14 Overview about the number of common peaks of fractions of the NH2 (#9) and PFP column (#15).

Fractions	NH2F5	NH2F6	NH2F7	NH2F8	NH2F9	NH2F10	NH2F11	NH2F12	NH2F13	NH2F14	NH2F15	NH2F16	NH2F17	NH2F18	NH2F19	NH2F20	NH2F21	NH2F22	NH2F23	NH2F24	NH2F25	NH2F26	NH2F27	NH2F28	NH2F29	NH2F30	NH2F31
PFPF2	121	123	115	98	106	87	97	68	30	24	29	20	30	29	23	15	14	8	9	4	5	3	6	7	19	13	9
PFPF3	34	35	35	58	55	39	46	31	21	26	14	12	7	9	6	5	8	13	12	4	3	1	1	0	6	4	3
PFPF4	18	33	24	19	27	25	36	24	26	38	21	10	13	12	4	9	13	22	23	9	4	2	2	2	11	5	3
PFPF5	8	15	16	26	23	23	27	17	21	30	16	17	15	11	7	5	8	9	7	10	10	5	4	3	10	4	5
PFPF6	12	13	18	57	43	23	20	22	26	23	22	24	14	12	8	4	5	8	8	2	1	0	2	2	6	3	4
PFPF7	7	8	31	42	41	29	35	26	41	37	18	13	9	12	12	8	8	9	5	3	4	9	8	5	9	5	5
PFPF8	3	4	6	6	12	14	17	15	35	45	26	10	12	23	15	6	2	5	5	4	3	8	6	6	10	7	7
PFPF9	6	8	5	10	12	16	18	25	19	23	26	17	26	28	12	9	3	4	7	4	4	3	4	5	9	4	1
PFPF10	1	1	1	13	9	16	24	22	19	21	20	11	14	20	11	9	4	3	3	0	20	22	14	14	14	3	0
PFPF11	3	2	1	0	4	11	14	22	18	21	10	8	9	6	3	1	1	3	3	0	6	7	9	10	10	2	3
PFPF12	2	2	1	0	0	5	6	10	11	16	8	9	8	5	5	4	5	6	6	1	1	1	1	1	4	1	1
PFPF13	1	0	1	4	4	1	2	2	2	7	5	5	4	3	5	3	9	8	4	1	0	1	0	0	0	1	32
PFPF14	1	0	0	0	0	0	0	21	23	23	19	16	6	2	2	1	3	2	3	1	0	0	0	0	0	0	9
PFPF15	4	1	0	10	13	9	9	3	4	8	11	14	11	5	2	1	2	8	6	3	3	2	3	2	3	0	0
PFPF16	4	2	0	8	8	7	5	1	1	3	3	5	3	3	2	0	2	9	10	6	3	1	2	2	2	0	5
PFPF17	4	3	0	0	1	1	0	0	2	3	0	2	1	0	1	0	5	17	18	10	3	0	0	0	1	1	2
PFPF18	6	5	0	0	0	0	0	0	0	3	3	1	1	1	1	3	7	13	9	6	2	0	0	0	0	0	0
PFPF19	4	1	0	0	0	0	0	0	0	0	0	0	0	1	0	0	0	2	1	1	0	2	1	1	1	0	0
PFPF20	2	1	0	0	0	0	0	0	0	0	0	0	0	1	1	0	0	0	2	3	0	1	1	1	1	0	0
PFPF21	2	0	1	0	0	0	0	0	0	0	0	0	2	5	3	2	2	0	0	0	1	0	0	0	0	0	0
PFPF22	0	0	0	0	0	0	0	0	0	0	1	2	4	5	3	3	3	0	0	0	0	1	0	0	0	0	0
PFPF23	0	1	2	2	0	0	0	0	0	0	0	0	1	0	0	1	2	1	1	0	0	0	0	0	0	0	0
PFPF24	1	1	2	2	0	0	0	0	0	0	0	0	1	0	0	0	0	0	0	0	0	0	0	0	0	0	0

Table A15 Overview about the number of common peaks of fractions of the PYE (#10) and PFP column (#15).

Fractions	PYEF4	PYEF5	PYEF6	PYEF7	PYEF8	PYEF9	PYEF10	PYEF11	PYEF12	PYEF13	PYEF14	PYEF15	PYEF16	PYEF17	PYEF18	PYEF19	PYEF20	PYEF21	PYEF22	PYEF23	PYEF24	PYEF25	PYEF26	PYEF27	PYEF28	PYEF29	PYEF30	PYEF31	PYEF32	PYEF33	PYEF34	PYEF35
PFPF2	233	99	58	66	36	36	26	23	32	30	7	10	9	7	4	3	3	2	3	0	1	5	9	7	1	0	0	1	3	1	5	5
PFPF3	107	42	22	30	35	23	33	16	29	25	7	9	10	13	7	9	0	3	8	5	1	2	6	5	0	1	3	2	1	2	1	0
PFPF4	35	37	22	36	17	13	16	35	38	35	13	12	13	10	1	10	6	7	4	2	1	3	2	4	6	4	6	5	0	0	0	1
PFPF5	14	9	19	27	23	19	22	22	35	32	26	26	21	12	3	10	4	3	1	2	5	4	2	5	3	1	2	2	0	0	0	0
PFPF6	15	20	14	20	13	15	17	14	17	24	18	19	21	18	36	16	5	5	2	2	2	4	1	1	2	1	2	2	3	6	4	2
PFPF7	5	19	35	36	14	10	5	8	9	32	25	43	35	26	17	13	6	4	4	4	8	7	7	3	1	2	2	2	3	12	2	8
PFPF8	4	5	9	10	8	5	7	8	25	31	20	45	27	21	13	12	13	6	2	3	5	6	5	7	1	2	1	0	1	0	0	7
PFPF9	8	3	2	9	11	5	10	9	17	22	21	32	38	31	18	33	16	16	8	6	1	2	3	5	5	0	0	0	0	0	0	3
PFPF10	2	0	0	3	2	2	9	3	14	20	16	49	54	33	16	21	10	10	9	5	2	3	1	3	3	1	1	0	1	0	1	2
PFPF11	1	1	0	1	0	0	2	4	11	8	2	17	21	11	4	7	2	7	9	15	13	4	0	4	1	2	4	5	4	3	1	2
PFPF12	1	1	0	1	0	0	0	5	5	2	1	10	14	9	6	9	8	6	8	13	4	4	1	3	0	1	3	3	1	1	2	0
PFPF13	1	0	0	1	1	2	6	5	3	1	1	3	3	5	6	7	2	1	0	5	6	28	40	13	6	5	0	0	1	2	1	0
PFPF14	0	0	0	0	4	4	4	0	0	4	6	5	5	5	2	7	4	1	4	11	2	11	16	15	14	16	28	3	0	0	0	0
PFPF15	0	1	0	3	6	3	1	2	3	3	3	6	11	10	4	3	2	1	4	13	9	13	8	13	13	12	7	0	0	12	5	0
PFPF16	0	1	0	1	1	4	6	3	3	4	2	2	2	2	2	2	1	1	4	6	7	9	4	5	10	10	17	11	5	7	4	0
PFPF17	0	1	0	0	0	2	3	2	1	3	2	1	1	2	1	3	2	5	14	15	10	11	3	3	2	5	3	6	8	6	0	0
PFPF18	0	0	0	1	0	1	2	2	1	1	0	4	5	7	2	0	0	2	9	10	7	10	4	4	2	2	0	0	2	6	10	1
PFPF19	0	0	0	0	0	0	0	0	0	0	0	4	5	6	1	0	0	0	0	0	2	0	1	1	5	3	3	2	1	1	6	4
PFPF20	0	0	0	0	0	0	0	0	1	0	0	1	1	1	1	0	0	0	1	1	0	0	1	2	4	4	5	1	1	0	1	0
PFPF21	0	0	0	0	0	0	0	0	0	0	0	0	3	0	0	0	0	0	0	0	0	1	1	1	1	1	1	0	0	0	5	5
PFPF22	0	0	0	0	0	0	0	0	0	0	0	0	0	0	0	0	0	0	0	0	0	1	1	0	0	1	1	0	0	1	7	5
PFPF23	0	1	0	0	0	0	1	0	1	0	0	1	2	3	10	12	9	2	4	5	7	8	6	1	2	1	2	1	2	1	2	0
PFPF24	0	1	0	0	1	0	0	0	0	0	0	0	1	0	0	0	0	0	0	0	0	0	1	2	2	2	1	0	0	1	2	1

Table A16 Percentage of bins that are containing at least one peak in the corresponding column pair plot.

Column pair	Percentage of bins that are containing at least one peak
C18 (#2) vs. PFP (15)	49%
C18 (#2) vs. PYE (#10)	77%
C18 (#2) vs. NH2 (#9)	85%
NH2 (#9) vs. PFP (15)	73%
NH2 (#9) vs. PYE (#10)	86%
PYE (#10) vs. PFP (15)	88%

References

1. US-EPA (2012): Estimation Programs Interface Suite™ for Microsoft® Windows, v. 4.11 edn. United States Environmental Protection Agency, Washington, DC, USA.
2. Doupe A, Landis S, Patterson P (1985) Environmental influences in the development of neural crest derivatives: glucocorticoids, growth factors, and chromaffin cell plasticity. The Journal of Neuroscience 5 (8):2119-2142
3. Wilson VS, Lambright C, Ostby J, Gray LE (2002) In Vitro and in Vivo Effects of 17β-Trenbolone: A Feedlot Effluent Contaminant. Toxicol Sci 70 (2):202-211. doi: https://10.1093/toxsci/70.2.202
4. Streck G (2009) Chemical and biological analysis of estrogenic, progestagenic and androgenic steroids in the environment. TrAC, Trends Anal Chem 28 (6):635-652. doi:https://doi.org/10.1016/j.trac.2009.03.006
5. Thomas KV, Hurst MR, Matthiessen P, McHugh M, Smith A, Waldock MJ (2002) An assessment of in vitro androgenic activity and the identification of environmental androgens in United Kingdom estuaries. Environ Toxicol Chem 21:1456-1461
6. Sohoni P, Sumpter JP (1998) Several environmental oestrogens are also anti-androgens. J Endocrinol 158 (3):327-339
7. Alvarez-Muñoz D, Indiveri P, Rostkowski P, Horwood J, Greer E, Minier C, Pope N, Langston WJ, Hill EM (2015) Widespread contamination of coastal sediments in the Transmanche Channel with anti-androgenic compounds. Marine Pollution Bulletin 95 (2):590-597. doi:https://doi.org/10.1016/j.marpolbul.2014.11.014
8. Rice SL, Hale RC (2009) Parameters for Ultra-Performance Liquid Chromatographic/Tandem Mass Spectrometric Analysis of Selected Androgens versus Estrogens in Aqueous Matrices. Anal Chem 81 (16):6716-6724. https://doi:10.1021/ac900134m
9. Schindler AE, Campagnoli C, Druckmann R, Huber J, Pasqualini JR, Schweppe KW, Thijssen JHH Classification and pharmacology of progestins. Maturitas 46:7-16. https://doi:10.1016/j.maturitas.2003.09.014
10. Fang H, Tong WD, Branham WS, Moland CL, Dial SL, Hong HX, Xie Q, Perkins R, Owens W, Sheehan DM (2003) Study of 202 natural, synthetic, and environmental chemicals for binding to the androgen receptor. Chem Res Toxicol 16 (10):1338-1358
11. Rostkowski P, Horwood J, Shears JA, Lange A, Oladapo FO, Besselink HT, Tyler CR, Hill EM (2011) Bioassay-Directed Identification of Novel Antiandrogenic Compounds in Bile of Fish Exposed to Wastewater Effluents. Environ Sci Technol 45 (24):10660-10667. doi:10.1021/es202966c
12. Grignard E, Lapenna S, Bremer S (2012) Weak estrogenic transcriptional activities of Bisphenol A and Bisphenol S. Toxicology in Vitro 26 (5):727-731. doi:https://doi.org/10.1016/j.tiv.2012.03.013
13. Gunde Egeskov Jensen NGN, Karin Dreisig, Anne Marie Vinggaard and Jay Russel Niemelä (2012) QSAR Model for Androgen Receptor Antagonism - Data from CHO Cell Reporter Gene Assays. Journal of Steroids & Hormonal Science
14. Araki N, Ohno K, Nakai M, Takeyoshi M, Iida M (2005) Screening for androgen receptor activities in 253 industrial chemicals by in vitro reporter gene assays using AR-EcoScreenTM cells. Toxicology in Vitro 19 (6):831-842. doi:https://doi.org/10.1016/j.tiv.2005.04.009

15. Kojima H, Katsura E, Takeuchi S, Niiyama K, Kobayashi K (2004) Screening for estrogen and androgen receptor activities in 200 pesticides by in vitro reporter gene assays using Chinese hamster ovary cells. Environ Health Perspect 112 (5):524-531
16. Weiss JM, Hamers T, Thomas KV, van der Linden SC, Leonards P, Lamoree M (2009) Masking effect of anti-androgens on androgenic activity in European river sediment unveiled by effect-directed analysis. Anal Bioanal Chem 394:1385-1397
17. Urbatzka R, van Cauwenberge A, Maggioni S, Viganò L, Mandich A, Benfenati E, Lutz I, Kloas W (2007) Androgenic and antiandrogenic activities in water and sediment samples from the river Lambro, Italy, detected by yeast androgen screen and chemical analyses. Chemosphere 67 (6):1080-1087. doi:https://doi.org/10.1016/j.chemosphere.2006.11.041
18. Pluskal T, Castillo S, Villar-Briones A, Oresic M (2010) MZmine 2: Modular framework for processing, visualizing, and analyzing mass spectrometry-based molecular profile data. Bmc Bioinformatics 11 (1):1-11. doi:Artn 395
Doi 10.1186/1471-2105-11-395

Appendix B

Supplementary information for chapter 3

A1 Materials and Methods

Table B1 List of solvents and reagents with a purity of at least 97% used in this study.

Reagent / solvent	Supplier
4-Methyl-7-diethylaminocoumarin	Sigma-Aldrich
4-Methyl-7-ethylaminocoumarin	TCI
4-Methyl-7-aminocoumarin	Sigma-Aldrich
Ciclopiroxolamine	Glentham Life Science
Flutamide	Sigma-Aldrich
17α-methyltestosterone	Sigma-Aldrich
Verapamil-d6 hydrochloride	Campro Scentific
Atrazine-$^{13}C_3$	Sigma-Aldrich
Bezafibrate-d4	Campro Scentific
Deuterium oxide (99.9 atom % D)	Sigma-Aldrich
Methan-d1-ol (99.8 atom % D)	Sigma-Aldrich
Ammonium acetate	Sigma-Aldrich
Ammonium bicarbonate	Sigma-Aldrich
Isopropanol	Sigma-Aldrich
Acetone, HPLC grade (Chromasolv)	Sigma-Aldrich
Ammonium hydroxide solution in water ≥ 25%	Sigma-Aldrich
Ethyl acetate, LC-MS grade (Chromasolv)	Sigma-Aldrich
Dimethylsulfoxid	Sigma-Aldrich
Methanol, gradient grade (LiChrosolv)	Merck
Methanol, LC-MS grade (Chromasolv)	Sigma-Aldrich
Water, LC-MS grade (Chromasolv)	Sigma-Aldrich
Formic acid, LC-MS grade	Sigma-Aldrich

B1.1 Extraction and Fractionation procedure

In total, 5 L of water were filtered through a glass fiber filter (GF/F, Whatman) and extracted using a cartridge containing the non-polar sorbents Chromabond HR-X (MN) in the upper and a mixture of Isolute ENV+ (Biotage), a weak anion exchanger (Chromabond HR-XAW, MN), and a weak cation exchanger (Chromabond HR-XCW, MN) in the lower layer. The layers were separated by a PP frit. The sample was eluted with methanol/ethyl acetate (50:50; v:v) containing 2 vol.-% of aqueous ammonium solution (25%) and methanol/ethyl acetate (50:50; v:v) containing 1.7 vol.-% of formic acid.

350 mL water equivalent were fractionated on a octadecyl-, pentafluorophenyl-, aminopropyl and pyrenyl ethyl-modified silica using optimized water/methanol gradients containing 0.1% of formic acid.

Table B2 Used gradients for fractionation on different columns.

Stationary Phase	Flow rate in mL/min	% Eluent B in Eluent A			
		0 min	1 min	31 min	41 min
Nucleodur C18 Gravity	2.8	50	50	95	95
Hypersil Gold PFP	2.8	60	60	95	95
Unison NH2	2.8	5	5	95	95
Cosmosil PYE	0.8	60	60	95	95

Table B3 Overview of fractions derived by fractionation on four orthogonal columns in parallel.

	Retention time window of fractions [min]			
Fraction name	**Nucleodur C18 Gravity**	**Hypersil Gold PFP**	**Unison NH2**	**Cosmosil PYE**
F1	1-10	3-10	1-3	2-3
F2	10-14	10-12	3-4	3-6
F3	14-15	12-13	4-5	6-9
F4	15-16	13-14	5-6	9-12
F5	16-17	14-15	6-7	12-13
F6	17-18	15-16	7-8	13-14
F7	18-19	16-17	8-9	14-15
F8	19-20	17-18	9-10	15-16
F9	20-21	18-19	10-11	16-17
F10	21-22	19-20	11-12	17-18
F11	22-23	20-21	12-13	18-19
F12	23-24	21-22	13-14	19-20
F13	24-25	22-23	14-15	20-21
F14	25-26	23-24	15-16	21-22
F15	26-27	24-25	16-17	22-23
F16	27-28	25-26	17-18	23-24
F17	28-29	26-27	18-19	24-25
F18	29-30	27-28	19-20	25-26
F19	30-31	28-29	20-21	26-27
F20	31-32	29-30	21-22	27-28
F21	32-33	30-31	22-23	28-29
F22	33-34	31-32	23-24	29-30
F23	34-40	32-40	24-25	30-31
F24	40-49	40-50	25-26	31-32
F25			26-27	32-33
F26			27-28	33-34
F27			28-29	34-35
F28			29-30	35-36
F29			30-35	36-37
F30			35-40	37-38
F31			40-46	38-39
F32				39-40
F33				40-42
F34				42-44
F35				44-46

All fractions were diluted in order to reach a maximal content of 10 vol.-% of methanol, frozen at -80°C, freeze dried and redissolved in 0.35 mL methanol (i.e., REF 1000). A blank sample for each column was prepared by the same fractionation and solvent exchange procedure but without sample injection.

B1.2 Gradient elution program for LC-HRMS

Table B4 Gradient elution program used for the chromatographic separation prior to mass spectrometric detection with (a) LTQ Orbitrap XL and (b) Q-Exactive Plus.

Time	0.1% FA in H_20	0.1% FA in MeOH	Isopropanol/Aceton 50/50 (v/v)	Flow rate
(a) Kinetex C18, 100 x 3 mm, 2.6 µm particle size, Phenomenex				
0.0 min	90%	10%	0%	0.20 mL/min
1.0 min	90%	10%	0%	0.20 mL/min
21.0 min	5%	95%	0%	0.20 mL/min
36.0 min	5%	95%	0%	0.20 mL/min
37.0 min	90%	10%	0%	0.20 mL/min
52.0 min	90%	10%	0%	0.20 mL/min
(b) Kinetex 2.6 µm EVO C18, 50 x 2.1 mm, Phenomenex				
0.0 min	95%	5%	0%	0.30 mL/min
1.0 min	95%	5%	0%	0.30 mL/min
13.0 min	0%	100%	0%	0.30 mL/min
24.0 min	0%	100%	0%	0.30 mL/min
24.1 min	5%	10%	85%	0.35 mL/min
26.2 min	5%	10%	85%	0.35 mL/min
26.3 min	95%	5%	0%	0.35 mL/min
32.0 min	95%	5%	0%	0.30 mL/min

A1.3 Structure elucidation of the antiandrogenic compounds

Settings of MZmine

The Thermo raw files of the active LC fractions were converted to mzML format by ProteoWizard [1] and non-target peaks were identified by MZmine 2.17 [2].

For mass detection the noise cutoff within individual scans was set to 200. Chromatograms were built using a minimum time span of 0.15 min, a minimum height of 10000 a.u. and a m/z tolerance of 0.001 m/z. Smoothing of chromatograms by the smoothing function was done with a filter width of 7. For deconvolution by local minimum search applied settings were: chromatographic threshold 89%, search minimum in RT range 0.3 min, minimum relative height 5%, minimum absolute height 10 000 a.u., min ratio of peak top/edge 1.5 and

peak duration range 0.2 to 10 min. The peak lists of all active fractions and the method blanks were aligned using joint alignment at a m/z tolerance of 0.001 m/z and a RT range of 0.5 min. The aligned peak list was exported to Microsoft Excel. It includes the retention time, accurate mass, height and area of the non-target peaks.

Non-target peaks with a sample-to-blank intensity ratio <10, an area-to-height ratio >100 (i.e., those not resembling Lorentzian peak shapes stemming from background noise, see [3]) and an intensity $<10^4$ were subtracted from the peak list using RStudio Version 0.98.501.

Hydrogen-Deuterium Exchange (HDX). Hydrogen-deuterium exchange (HDX) LC-HRMS was used for a further discrimination of candidate structures by the determination of the number of exchangeable hydrogen atoms of the candidate peak. To this end deuterated and non-deuterated water and methanol was used as the LC mobile phase [4-6]. All candidates with a structure in disagreement with the observed numbers of exchanged hydrogen atoms were removed from the candidate list.

Eluent A was deuterium oxide (99.9 atom % D, Sigma-Aldrich) with 0.1% formic acid and eluent B methan-d1-ol (99.8 atom % D, Sigma-Aldrich). The HDX full scan spectra were analyzed manually using the Xcalibur QualBrowser by the evaluation of the mass difference, corresponding to the number of exchanged hydrogen atoms of non-targets obtained by the use of deuterated and non-deuterated mobile phase. The number of heteroatom-attached hydrogens was calculated by the substructure search function of JChem for Excel (version 16.1.4, Chemaxon) [7].

pH-Dependent LC Retention. The LC retention times of the candidate peaks at pH 2.6, 6.4 and 10.0 were compared to obtain information on the presence of ionizable functional groups. pH-dependent charge of ionizable compounds results in LC retention time shifts allowing for the exclusion of candidate peaks with pK_a values that are not compatible with the change in retention [8]. The acidic and basic pK_a values of candidate compounds were calculated using JChem for Excel (version 16.1.4, Chemaxon) [7].

Aliquots of the of the active fraction collected via the fractionation using the C18 phase were separated with a Kinetex EVO C18 column (50 x 2.1 mm, particle size 2.6 µm) using the same elution program and eluents as shown in Table S5b for pH 2.6. For pH 6.4 eluents were water and MeOH with 2.5 mM ammonium acetate (pH was adjusted using ammonia solution in

water or MeOH), and for pH 10 H2O and MeOH with 2.5 mM ammonium bicarbonate (pH adjusted with ammonia solution). The column was rinsed with isopropanol:acetone 50:50 for 2 minutes and re-equilibrated to the initial conditions for 6 minutes for all pH conditions. Full scan chromatograms were received using ESI positive mode at the Q-Exactive instrument with a nominal resolving power of 140,000 (at m/z 200) in the mass range of 100-700 m/z.

B2 Results

B2.1 Biotests I

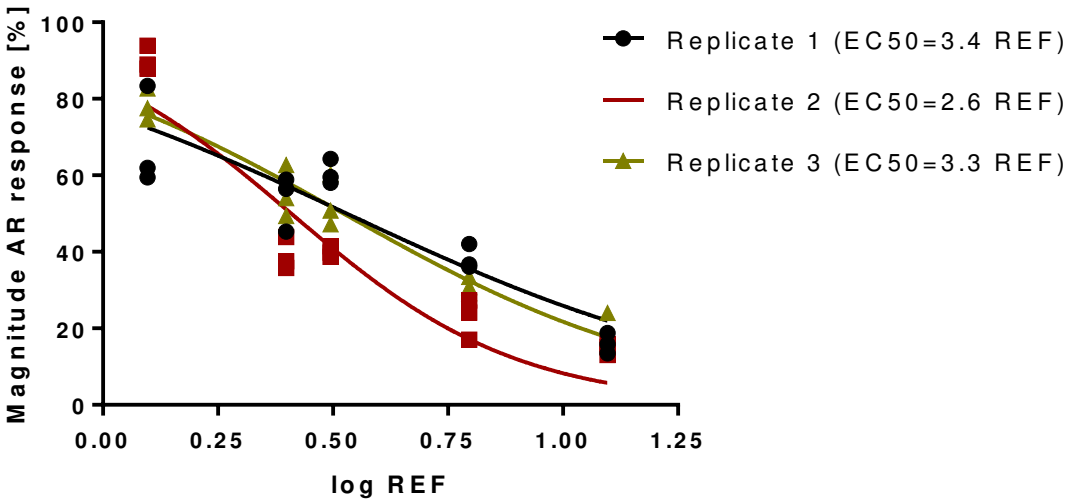

Figure B1 Magnitude of AR response versus the REF of the water extract in the antiAR-CALUX assay. Average EC50-value of the triplicate is 3.059 with a 95% confidence interval of 2.51 to 3.706.

B2.2 Chemical Analysis

Table B5 Overview of 36 androgenic endocrine disrupting compounds. Analytes were separated on a Kinetex C18 and a Nucleodur C18 silica phase.

Compound	CAS	logKow (EpiSuite)	Biological activity	Retention Time [min] on Nucleodur C18 Gravity	Retention Time [min] on Kinetex EVO C18
Steroids					
Dexamethasone	50-02-2	1.72	Antiandrogenic	20.57	10.59
17β-Trenbolone	10161-33-8	2.65	Androgenic	22.29	10.87
Norethindrone	68-22-4	2.99	Androgen receptor affinity	23.74	11.28
Androsterone	53-41-8	3.07	Androgenic	30.70	13.58
Epi-Androsterone	481-29-8	3.07	Androgenic	28.26	12.18
Dihydrotestosterone	521-18-6	3.07	Androgenic	28.98	12.65
Testosterone	58-22-0	3.27	Androgenic	25.64	11.54
Levonorgestrel	797-63-7	3.48	Androgen receptor affinity	26.62	11.88
Medroxyprogesterone	520-85-4	3.5	Androgen receptor affinity	28.60	12.26
Isopimaric Acid	5835-26-7	6.45	Antiandrogenic	41.23	14.95
Abietic Acid	514-10-3	6.46	Antiandrogenic	41.23	14.95
Progesterone	57-83-0	3.67	Antiandrogenic	30.25	12.01
Hydrocortisone	50-23-7	1.62	Androgen receptor affinity	17.94	9.95
Phenols					
Bisphenol S	80-09-1	1.65	Androgen receptor affinity	9.29	7.59
Isoeugenol	97-54-1	2.65	Androgen receptor affinity	21.39	10.11
2-Naphthol	135-19-3	2.69	Antiandrogenic	19.26	9.51
2,2´-Dihydroxybiphenyl	1806-29-7	2.8	Antiandrogenic	19.05	9.38
Genistein	446-72-0	2.84	Androgen receptor affinity	17.88	9.97
Propylparaben	94-13-3	2.98	Androgen receptor affinity	20.75	10.22
3-Hydroxybiphenyl	580-51-8	3.28	Androgen receptor affinity	23.69	10.54
Benzophenone-3	131-57-7	3.52	Antiandrogenic	29.46	12.08

1-Hydroxypyrene	5315-79-7	4.45	Antiandrogenic	31.32	12.34
Zearalenone	17924-92-4	3.58	Antiandrogenic	26.26	11.71
Others					
Procymidone	32809-16-8	2.59	Antiandrogenic	27.47	11.70
N-Benzylphthalimide	2142-01-0	3.22	Androgen receptor affinity	25.66	11.37
Carbaryl	63-25-2	2.35	Androgen receptor affinity	17.13	9.48
Propanil	709-98-8	2.88	Antiandrogenic	24.95	10.91
Tris (1-chloro-2-propoyl) phosphate	13674-84-5	2.89	Antiandrogenic	24.55	11.51
Linuron	330-55-2	2.91	Antiandrogenic	24.30	10.95
Metolachlor	51218-45-2	3.24	Androgen receptor affinity	27.95	12.01
Flutamide	13311-84-7	3.51	Antiandrogenic	24.99	11.35
Flavone	525-82-6	3.51	Androgen receptor affinity	26.26	11.54
Methylparathion	298-00-0	2.75	Antiandrogenic	23.94	11.08
Fenthion	55-38-9	4.08	Antiandrogenic	30.15	11.32
Triphenylphosphat	115-86-6	4.7	Androgen receptor affinity	29.75	12.85
Benzylbutylphthalate	85-68-7	4.84	Antiandrogenic	32.47	13.28

B2.3 Suspect screening for known Antiandrogens

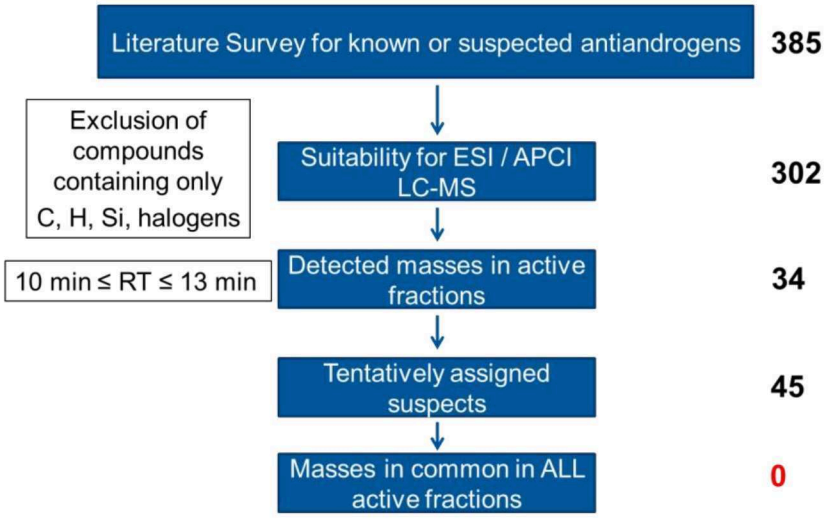

Figure B2 Applied workflow for suspect screening.

B2.4 Non-target analysis and confirmation of identity

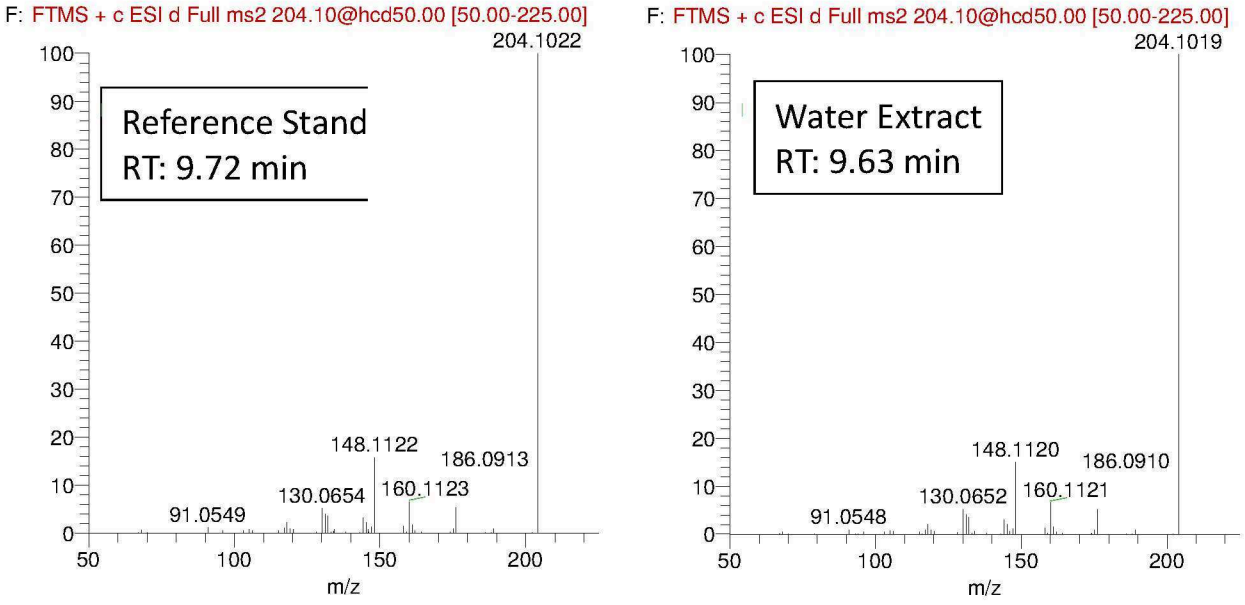

Figure B3 Fragment ion spectra (HCD 50) of the peak #4 with with m/z 204.1014 at RT 9.63 min from the water extract (REF 76) and of 4-methyl-7-ethylaminocoumarin. The mass spectrum is available in MassBank (https://massbank.eu/MassBank) with accession UA006501 (splash10-0iz0000000-ce6eebb08ff797995ed6).

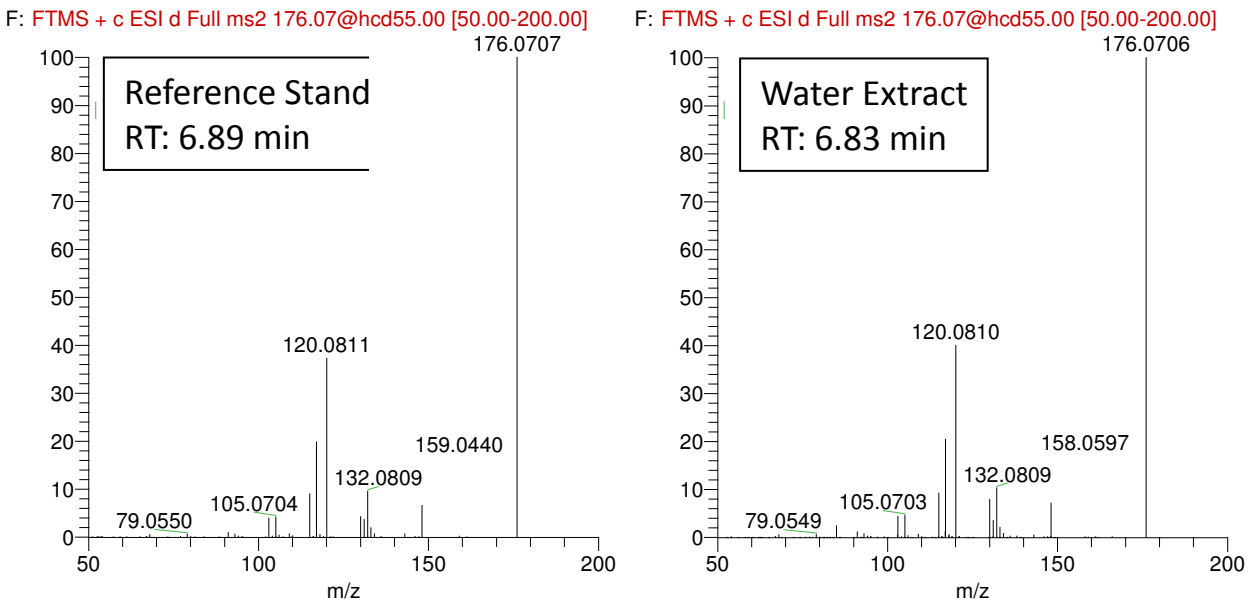

Figure B4 Fragment ion spectra (HCD 55) of the peak #5 with m/z 176.0706 at RT 6.83 min from the water extract (REF 76) and of 7-Amino-4-methylcoumarin. The mass spectrum is available in MassBank (https://massbank.eu/MassBank) with accession UA006601 (splash10-0z00000000-5680bff27334a4128e4c).

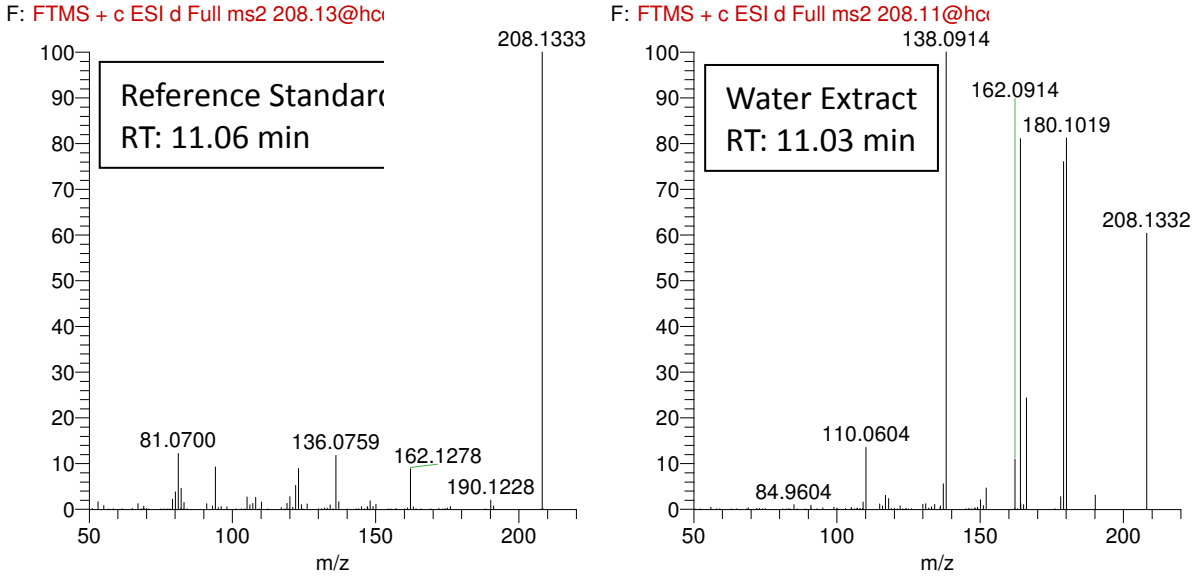

Figure B5 Fragment ion spectra (HCD50) of peak #3 with with m/z 208.1328 at RT 11.03 min from the water extract (REF 76) and of Ciclopirox.

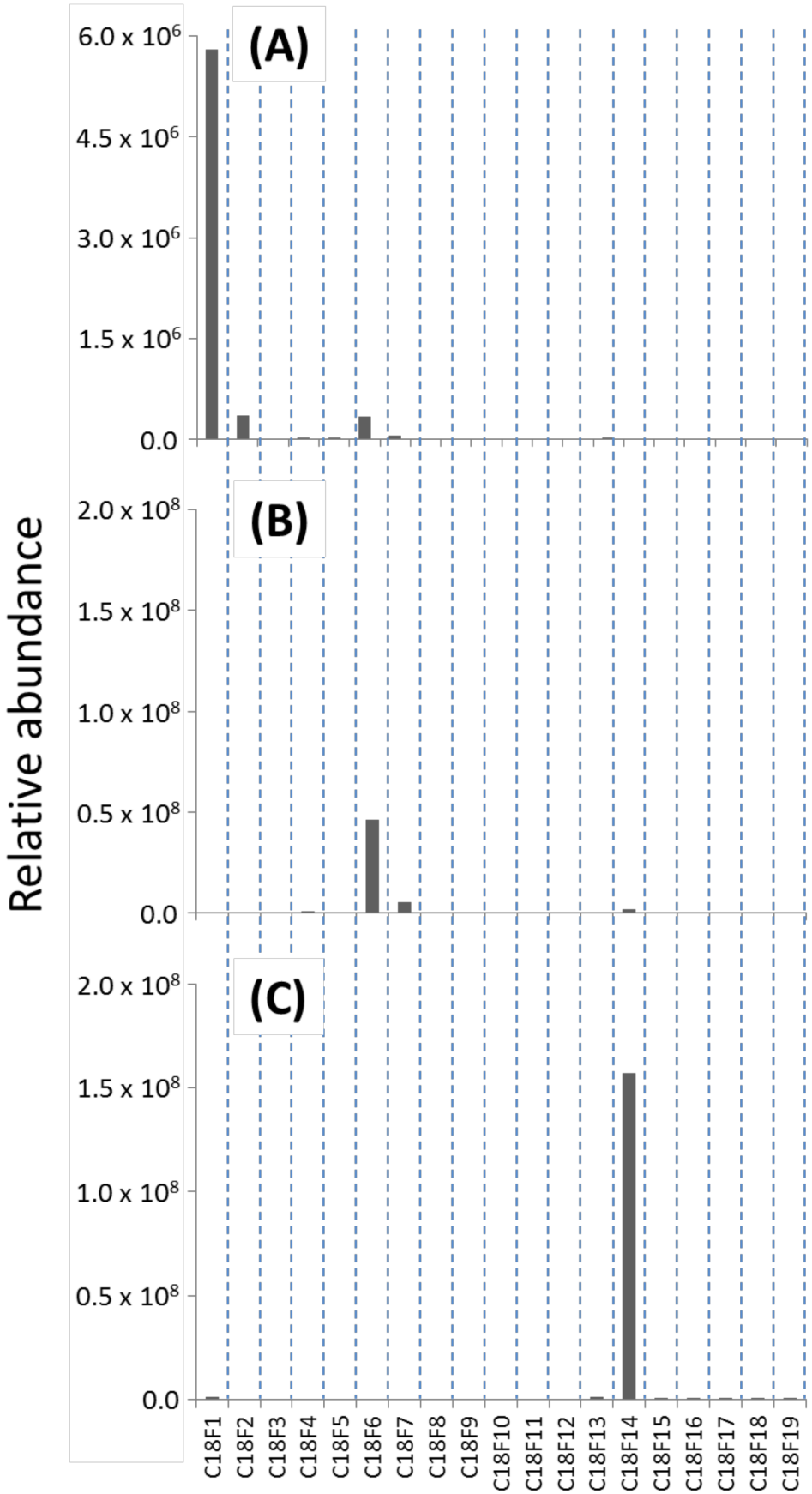

Figure B6 Peak heights of (a) C47T2, (b) C47T1 and (c) C47 within the fractions of the octadecyl silica phase.

B2.5 Biotests II

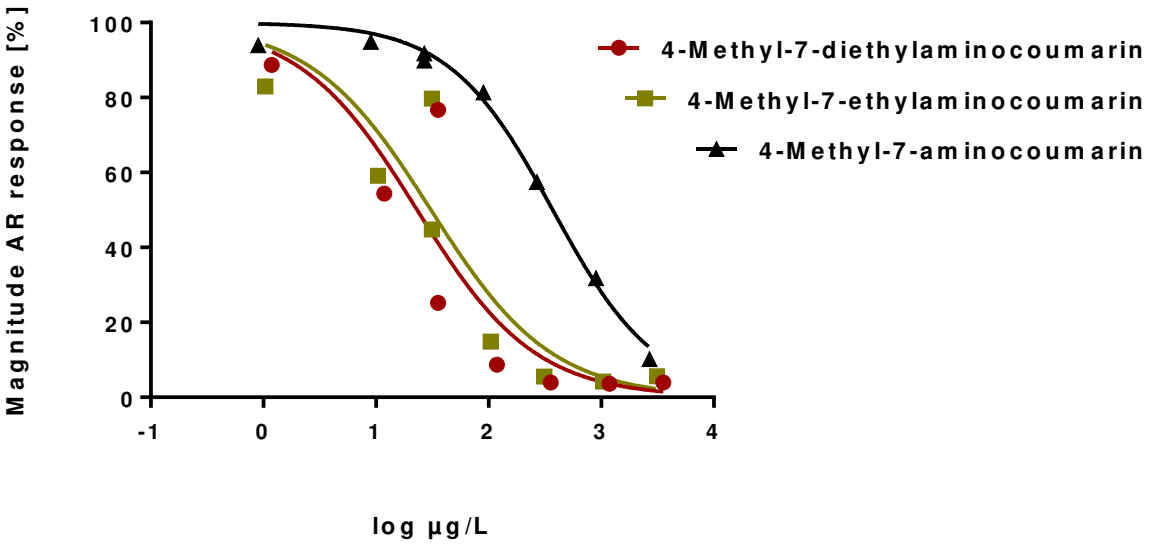

Figure B7 Magnitudes of AR response versus concentrations of 4-Methyl-7-diethylaminocoumarin (EC50=23 µg/L), 4-Methyl-7-ethylaminocoumarin (EC50=32 µg/L) and 4-Methyl-7-aminocoumarin (EC50=371 µg/L) in the antagonistic AR-CALUX assay.

Table B6 Overview of in the anti-AR-CALUX assay observed EC50-values of the water extract (three replicates), of the identified compounds and the EC50-values of the simultaneously measured flutamide standards. The concentrations of the identified compounds in the water extract (REF=1) and the resulting FEqs are also displayed.

		DHT EC_{50}	DHT EC_{50} (Flutamide)	resulting $Feq_{bio/chem}$
Water Extract	Replicate 1	3.4 REF	194.7 µg/L	57.5 µgFEq/L
	Replicate 2	2.6 REF	135.0 µg/L	52.6 µgFEq/L
	Replicate 3	3.3 REF	87.8 µg/L	26.3 µgFEq/L
	average			45.5 (±13.7 SD) µgFEq/L
Identified compounds	C47 (13.7 µg/L)	23.2 µg/L	120.9 µg/L	71.4 µgFEq/L
	C47T1 (3.9 µg/L)	30.8 µg/L	114.1 µg/L	14.5 µgFEq/L
	C47T2 (1.1 µg/L)	371.1 µg/L	64.2 µg/L	0.2 µgFEq/L

B2.6 Rapid Estrogen ACtivity Test *In Vivo* (REACTIV) assay

In order to detect any potential estrogen axis activity of C47, C47T1 and C47T2, day post hatch zero medaka fry harboring the chgh-gfp transgene (REACTIV assay) were exposed to the three coumarins for 24 h as described in Spirhanzlova et al. [9]. The following changes were made to the previously published protocol. Eight medaka fry rather than twenty used per exposure group in a single well of a six-well plate. A Leica MZ10F fluorescent (Leica Microsystems) fitted with a TXD 14C camera (Baumer), ET-GFP long-pass filters (excitation 480/40, emission 510LP, Leica) and a 200 W Lumen fluorescence source (Prior Scientific) was used to capture a color image of the liver of each fry.

Two independent replicate experiments were carried out. The two replicate experiments gave similar results, therefore data from all groups were normalized to the mean of the ethinylestradiol (EE2) 488 ng/L group and pooled.No pro-estrogenic effect was observed for the two transformation products (Figure S 10). However, a slight pro-estrogenic effect was detected for C47 itself.

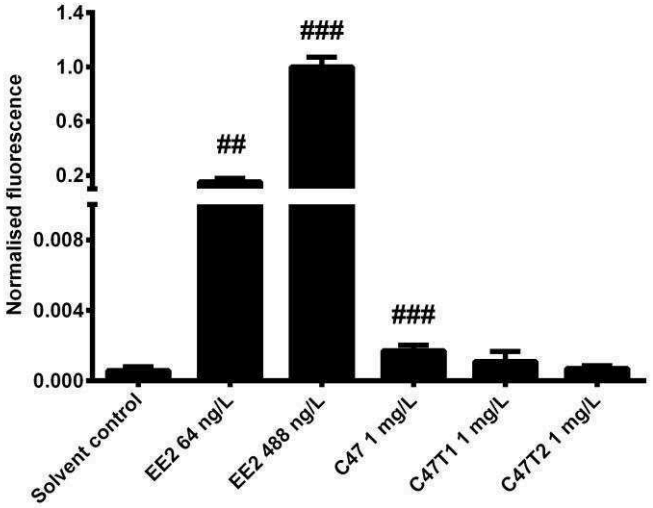

Figure B8 Quantification of estrogen axis activity of C47 and its transformation products *in vivo* using the chgh-gfp transgenic medaka fry (REACTIV assay). The compounds were tested at 1 mg/L. C47, but not its transformation products shows weak estrogenic activity. Note that the y-axis is cut to highlight the slight increase in estrogenic activity induced by C47. The reference synthetic estrogen ethinylestradiol (EE2) was tested in parallel for comparison. Statistical significance is shown compared to the solvent control group, indicated by: ## (P < 0.01) and ### (P < 0.001).

Table B7 In the literature reported compounds with antiandrogenic activity.

#	Compound	CAS	logKow	Smiles	References
1	5α-Androstane-3,11,17-trione	1482-70-8	1.21	[C@@H]13[C@@]4([C@@H](CC[C@H]1[C@H]2[C@](C(=O)CC2)(C)CC3=O)CC(=O)CC4)C	[10]
2	Hydrocortisone	50-23-7	1.62	[C@H]34[C@H]2[C@@H]([C@@]1(C(=CC(=O)CC1)CC2)C)[C@@H](O)C[C@@]3([C@](C(CO)=O)(O)CC4)C	[10]
3	4‘-Chloroacetoacetanilide	101-92-8	1.65	C1=C(C=CC(=C1)NC(CC(C)=O)=O)Cl	[10]
4	Bispenol S	80-09-1	1.65	C2=C([S](C1=CC=C(O)C=C1)(=O)=O)C=CC(=C2)O	[10]
5	Dexamethasone	50-02-2	1.72	[C@H]34[C@H]2[C@@](F)([C@@]1(C(=CC(=O)C=C1)CC2)C)[C@@H](O)C[C@@]3([C@](O)([C@@H](C4)C)C(=O)CO)C	[10]
6	11-Ketotestosterone	564-35-2	1.92	O=C2C[C@]4([C@H]([C@@H]3CC\C1=C\C(=O)CC[C@]1(C)[C@@H]23)CC[C@@H]4O)C	[10]
7	Corticosterone	50-22-6	1.99	[C@@H]23[C@H]([C@H]1[C@]([C@@H](C(CO)=O)CC1)(C)C[C@@H]2O)CCC4=CC(=O)CC[C@]34C	[10]
8	3-Chlorophenol	108-43-0	2.16	C1=CC(=CC(=C1)Cl)O	[10]
9	4,4‘-Dihydoxybenzophenone	611-99-4	2.19	C2=C(C(C1=CC=C(O)C=C1)=O)C=CC(=C2)O	[10, 11]
10	Carbaryl	63-25-2	2.35	C1=CC=CC2=CC=CC(=C12)OC(NC)=O	[10]
11	Procymidone	32809-16-8	2.59	C3=C(N1C(C2(C(C1=O)(C)C2)C)=O)C=C(Cl)C=C3Cl	[10, 12, 13]
12	Isoeugenol	97-54-1	2.65	C1=C(C=CC(=C1OC)O)\C=C\C	[10]
13	Diethylphthalate	84-66-2	2.65	C1=C(C(=CC=C1)C(OCC)=O)C(OCC)=O	[10]
14	4-Hydroxybenzophenone	1137-42-4	2.67	C2=C(C(=O)C1=CC=CC=C1)C=CC(=C2)O	[10, 11]
15	2-Naphthol	135-19-3	2.69	OC1=CC2=CC=CC=C2C=C1	[14]
16	4-Chloro-2-methyl phenol	1570-64-5	2.7	C1=C(C(=CC(=C1)Cl)C)O	[10]
17	2-(4-OH-benzyl)isoindole-1,3-dione	24124-24-1	2.74	C1=CC=CC3=C1C(N(CC2=CC=C(O)C=C2)C3=O)=O	[10]
18	Methylparathion	298-00-0	2.75	C1=CC(=CC=C1O[P](OC)(OC)=S)[N+]([O-])=O	[10, 12]
19	4-Amino butylbenzoate	94-25-7	2.78	C1=C(C(OCCCC)=O)C=CC(=C1)N	[10]
20	2,2´-Dihydroxybiphenyl	1806-	2.8	OC1=CC=CC=C1C1=C(O)C=CC=C1	[14]

		29-7			
21	4‘-Hydroxyflavanone	6515-37-3	2.8	C1=CC(=CC=C1C3OC2=C(C=CC=C2)C(C3)=O)O	[10]
22	6-Hydroxyflavanone	4250-77-5	2.8	C1=CC(=CC3=C1OC(C2=CC=CC=C2)CC3=O)O	[10]
23	Estriol	50-27-1	2.81	[C@H]34[C@H]2[C@@H](C1=C(C=C(O)C=C1)CC2)CC[C@@]3([C@@H](O)[C@@H](C4)O)C	[10]
24	Genistein	446-72-0	2.84	C1=C(O)C=C(C2=C1OC=C(C2=O)C3=CC=C(O)C=C3)O	[10]
25	Iprodione	36734-19-7	2.85	CC(C)NC(=O)N1CC(=O)N(C1=O)C1=CC(Cl)=CC(Cl)=C1	[15]
26	Spironolactone	52-01-7	2.88	O=C5O[C@@]4([C@@]3([C@H]([C@@H]2[C@H](SC(=O)C)C/C1=C/C(=O)CC[C@]1(C)[C@H]2CC3)CC4)C)CC5	[10, 11]
27	Propanil	709-98-8	2.88	C1=C(C=CC(=C1Cl)Cl)NC(CC)=O	[10, 12]
28	Tris (1-chloro-2-propoyl) phosphate	13674-84-5	2.89	CC(CCl)OP(=O)(OC(C)CCl)OC(C)CCl	[16]
29	Linuron	330-55-2	2.91	CON(C)C(=O)NC1=CC=C(Cl)C(Cl)=C1	[12, 15]
30	Vinclozoline metabolit M2	not available	2.95	CC(O)(C=C)C(=O)NC1=CC(Cl)=CC(Cl)=C1	[15]
31	2,4-dihydroxybenzophenone	131-56-6	2.96	C1=CC(=CC(=C1C(=O)C2=CC=CC=C2)O)O	[10, 11]
32	Propyl parabene	94-13-3	2.98	C1=C(C(OCCC)=O)C=CC(=C1)O	[10]
33	Norethindrone	68-22-4	2.99	O=C4\C=C3/[C@@H]([C@H]2CC[C@]1([C@@H](CC[C@]1(C#C)O)[C@@H]2CC3)C)CC4	[10]
34	Vinclozoline	50471-44-8	3.03	C1=C(C=C(C=C1Cl)Cl)N2C(C(OC2=O)(C=C)C)=O	[10, 12]
35	6-Hydroxyflavone	6665-83-4	3.03	C1=CC(=CC2=C1OC(=CC2=O)C3=CC=CC=C3)O	[10]
36	2-(4-nitro-benzyl)isoindole-1,3-dione	62133-07-7	3.03	C1=CC=CC3=C1C(N(CC2=CC=C([N+](=O)[O-])C=C2)C3=O)=O	[10]
37	Boldenone	46-48-0	3.05	C[C@]12CCC3C(CCC4=CC(=O)C=C[C@]34C)C1CC[C@@H]2O	[24]
38	5β-Dihydrotestosterone	571-22-2	3.07	O=C4C[C@H]3CC[C@@H]2[C@H](CC[C@]1(C)[C@@H](O)CC[C@H]12)[C@@]3(C)CC4	[10]
39	androsterone	53-41-8	3.07	[C@H]23[C@@H]([C@@]1([C@H](C[C@H](O)CC1)CC2)C)CC[C@]4([C@H]3CCC4=O)C	[10]
40	methyltrienolone	965-93-5	3.1	O=C4\C=C3/C(=C2/C=C\[C@]1([C@@H](CC[C@@]1(O)C)[C@@H]2CC3)C)CC4	[10]

41	benzophenone	119-61-9	3.15	C1=CC=CC=C1C(C2=CC=CC=C2)=O	[10]
42	4‘-hydroxychalcone	2657-25-2	3.18	C1=CC(=CC=C1C(\C=C\C2=CC=CC=C2)=O)O	[10]
43	4-hydroxychalcone	20426-12-4	3.18	c1ccc(cc1)C(=O)/C=C\c2ccc(cc2)O	[10]
44	2-benzyl-isoindole-1,3-dione	2142-01-0	3.22	C1=CC=CC3=C1C(N(CC2=CC=CC=C2)C3=O)=O	[10]
45	metolachlor	51218-45-2	3.24	C1=CC=C(C(=C1CC)N(C(COC)C)C(CCl)=O)C	[10]
46	Chloroxylenol	88-04-0	3.25	CC1=CC(O)=CC(C)=C1Cl	[14]
47	2,4,5-T	93-76-5	3.26	C1=C(Cl)C(=CC(=C1OCC(O)=O)Cl)Cl	[10]
48	Epitestosterone	481-30-1	3.27	CC12CCC3C(CCC4=CC(=O)CCC34C)C1CC[C@H]2O	[10]
49	flavanone	487-26-3	3.28	C1=CC=CC2=C1C(CC(O2)C3=CC=CC=C3)=O	[10]
50	4-hydroxybiphenyl	92-69-3	3.28	C2=C(C1=CC=CC=C1)C=CC(=C2)O	[10]
51	O,O-Dimethyl-O-4-nitro- m-tolylthiophosphat, Fenitrothion	122-14-5	3.3	COP(=S)(OC)OC1=CC=C(C(C)=C1)[N+]([O-])=O	[12, 15]
52	4-benzyloxylphenol	103-16-2	3.3	C2=C(OCC1=CC=CC=C1)C=CC(=C2)O	[10]
53	3-methylestriol	3434-79-5	3.37	[C@H]4([C@]3(C)[C@H]([C@@H]2CCC1=C(C=CC(=C1)OC)[C@H]2CC3)C[C@@H]4O)O	[10]
54	1-methoxy-4-[1-propenyl]benzene	4180-23-8	3.39	C1=CC(=CC=C1\C=C\C)OC	[10]
55	4-tert-butylphenol	98-54-4	3.42	C1=C(C(C)(C)C)C=CC(=C1)O	[10]
56	4-hydroxy-estradiol	5976-61-4	3.46	Oc1ccc2c(c1O)CC[C@@H]3[C@@H]2CC[C@@]4([C@@H](O)CC[C@@H]34)C	[10]
57	2-OH-estradiol	362-05-0	3.46	[C@]24([C@H]([C@@H]1CCC3=C([C@H]1CC2)C=C(C(=C3)O)O)CC[C@@H]4O)C	[10]
58	2-sec-butylphenol	89-72-5	3.46	C1=CC=CC(=C1C(CC)C)O	[10]
59	4-sec-butylphenol	99-71-8	3.46	C1=C(C=CC(=C1)O)C(CC)C	[10]
60	Norgestrel	797-63-7	3.48	[H][C@@]12CC[C@@](O)(C#C)[C@@]1(CC)CC[C@]1([H])[C@@]3([H])CCC(=O)C=C3CC[C@@]21[H]	[10]

61	fenpicionil	74738-17-3	3.48	C2=C(C1=C(C(=CC=C1)Cl)Cl)C(=C[NH]2)C#N	[10]
62	Medroxyprogesterone	520-85-4	3.5	O=C4\C=C2/[C@]([C@H]1CC[C@@]3([C@@](O)(C(=O)C)CC[C@H]3[C@@H]1C[C@@H]2C)C)(C)CC4	[10]
63	endosulfan	115-29-7	3.5	O=[S]2OCC1C3(Cl)C(Cl)(Cl)C(Cl)(C1CO2)C(=C3Cl)Cl	[10]
64	Flutamide	13311-84-7	3.51	CC(C)C(=O)NC1=CC(=C(C=C1)[N+]([O-])=O)C(F)(F)F	[11]
65	Norethynodrel	68-23-5	3.51	[H][C@@]12CC[C@@](O)(C#C)[C@@]1(C)CC[C@]1([H])C3=C(CC[C@@]21[H])CC(=O)CC3	[10]
66	Flavone	525-82-6	3.51	C1=CC=CC2=C1C(C=C(O2)C3=CC=CC=C3)=O	[10]
67	Vinclozoline metabolit M1	119209-27-7	3.52	CC(OC(=O)NC1=CC(Cl)=CC(Cl)=C1)(C=C)C(O)=O	[11, 15]
68	Oxybenzone	131-57-7	3.52	COC1=CC=C(C(=O)C2=CC=CC=C2)C(O)=C1	[11, 14, 17]
69	4,4‘-Dihydroxystilbene	659-22-3	3.56	C2=C(\C=C\C1=CC=C(O)C=C1)C=CC(=C2)O	[10]
70	Bisphenol A	80-05-7	3.64	CC(C)(C1=CC=C(O)C=C1)C1=CC=C(O)C=C1	[11]
71	4’Propoxy-2-methylpropiophenon	64436-60-8	3.65	CCCOC1=CC=C(C=C1)C(=O)C(C)C	[16]
72	Chalcone	94-41-7	3.66	O=C(\C=C\C1=CC=CC=C1)C1=CC=CC=C1	[10]
73	Progesterone	57-83-0	3.67	[H][C@@]12CC[C@H](C(C)=O)[C@@]1(C)CC[C@@]1([H])[C@@]2([H])CCC2=CC(=O)CC[C@]12C	[10, 11]
74	Equol	531-95-3	3.67	[C@H]1(CC2=C(OC1)C=C(C=C2)O)C3=CC=C(C=C3)O	[10]
75	Mibolerone	3704-09-4	3.69	O=C4\C=C3/[C@@H]([C@H]2CC[C@]1([C@@H](CC[C@@]1(O)C)[C@@H]2[C@H](C)C3)C)CC4	[10]
76	Ketoconazole	65277-42-1	3.7	[H][C@]1(COC2=CC=C(C=C2)N2CCN(CC2)C(C)=O)CO[C@H](O1)[C@H](N1C=CN=C1)C1=CC=C(Cl)C=C1Cl	[15]
77	Ethylparathion	56-38-2	3.73	C1=C(O[P](=S)(OCC)OCC)C=CC(=C1)[N+]([O-])=O	[10, 12]
78	Dihydroxymethoxychlor olefin	14868-03-2	3.75	C2=C(C(C1=CC=C(O)C=C1)=C(Cl)Cl)C=CC(=C2)O	[10]
79	16β-OH-16α-Me-3-Me-estradiol	5108-94-1	3.83	[C@]34([C@H]([C@H]2[C@@H](C1=C(C=C(OC)C=C1)CC2)CC3)C[C@]([C@@H]4O)(C)O)C	[10]
80	4-Androstenediol	1156-92-9	3.9	C[C@]12CCC3C(CCC4=C[C@@H](O)CC[C@]34C)C1CC[C@@H]2O	[10]

81	Androstenediol	521-17-5	3.9	O[C@@H]4C/C3=C/C[C@@H]1[C@H](CC[C@@]2([C@@H](O)CC[C@@H]12)C)[C@@]3(C)CC4	[10]
82	4-tert-Pentylphenol	80-46-6	3.91	C1=C(C(CC)(C)C)C=CC(=C1)O	[10]
83	17α-Estradiol	57-91-0	3.94	[C@@H]12CCC4=C([C@H]1CC[C@@]3([C@@H](CC[C@@H]23)O)C)C=CC(=C4)O	[10]
84	Estradiol (E2)	50-28-2	3.94	[C@H]34[C@H]2[C@@H](C1=C(C=C(O)C=C1)CC2)CC[C@@]3([C@@H](O)CC4)C	[10, 11]
85	Stanozolol	10418-03-8	3.96	[H][C@@]12CC[C@](C)(O)[C@@]1(C)CC[C@@]1([H])[C@@]2([H])CC[C@@]2([H])CC3=NNC=C3C[C@]12[H]	[18]
86	Androstanediol	571-20-0	3.98	[H][C@@]12CC[C@H](O)[C@@]1(C)CC[C@@]1([H])[C@@]2([H])CC[C@@]2([H])C[C@@H](O)CC[C@]12C	[10]
87	3α-Androstanediol	1852-53-5	3.98	O[C@@H]4CC[C@]3([C@@H](CC[C@H]2[C@@H]1CC[C@H](O)[C@@]1(C)CC[C@@H]23)C4)C	[10]
88	N-[4-Phenylamino)phenyl]-benzamide	Not available	4	O=C(NC1=CC=C(NC2=CC=CC=C2)C=C1)C1=CC=CC=C1	[16]
89	trans-4-Hydroxystilbene	3839-46-1	4.04	C1=CC(=CC=C1\C=C\C2=CC=CC=C2)O	[10]
90	Fenthion	55-38-9	4.08	COP(=S)(OC)OC1=CC=C(SC)C(C)=C1	[12, 15]
91	6α-Me-17α-OH-Progesterone acetate	71-58-9	4.09	C[C@H]1C[C@@H]2[C@H](CC[C@]3([C@H]2CC[C@@]3(C(=O)C)OC(=O)C)C)[C@@]4(C1=CC(=O)CC4)C	[10]
92	beta-Zearalenol	71030-11-0	4.09	[C@H]2(OC(=O)C1=C(C=C(O)C=C1O)\C=C\CCC[C@H](O)CCC2)C	[10]
93	Ethynylestradiol	57-63-6	4.12	[C@H]12[C@@]([C@@](C#C)(O)CC1)(CC[C@H]3[C@H]2CCC4=C3C=CC(=C4)O)C	[10, 11]
94	p-Cumyl phenol	599-64-4	4.12	C2=C(C(C1=CC=CC=C1)(C)C)C=CC(=C2)O	[10]
95	Prochloraz	67747-09-5	4.13	CCCN(CCOC1=C(Cl)C=C(Cl)C=C1Cl)C(=O)N1C=CN=C1	[12, 13, 15]
96	Bisphenol B	77-40-7	4.13	C2=C(C(C1=CC=C(O)C=C1)(CC)C)C=CC(=C2)O	[10]
97	Cyproterone acetate	427-51-0	4.18	[H][C@@]12CC[C@](OC(C)=O)(C(C)=O)[C@@]1(C)CC[C@@]1([H])C2C=C(Cl)C2=CC(=O)[C@@H]3C[C@@H]3[C@]12C	[11, 15]
98	Chlorophene	120-32-1	4.18	OC1=CC=C(Cl)C=C1CC1=CC=CC=C1	[14]
99	Diisobutyl adipate	141-04-8	4.19	C(OC(=O)CCCCC(=O)OCC(C)C)C(C)C	[10]
100	Promegestone	34184-77-5	4.2	CCC(=O)[C@@]1(C)CC[C@H]2[C@@H]3CCC4=CC(=O)CCC4=C3CC[C@]12C	[10]
101	3,4-diphenyltetrahydrofuran	93433-	4.21	c1ccc(cc1)C2COCC2c3ccccc3	[10]

		53-5			
102	Lindane (γ-HCH)	58-89-9	4.26	C1(Cl)C(Cl)C(Cl)C(Cl)C(Cl)C1Cl	[10]
103	Monohydroxymethoxychlor olefin	75938-34-0	4.31	C2=C(C(C1=CC=C(O)C=C1)=C(Cl)Cl)C=CC(=C2)OC	[10]
104	Dibutyl adipate	105-99-7	4.33	C(C)CCOC(CCCCC(OCCCC)=O)=O	[10]
105	Dichlorophene	1322-43-6	4.34	OC1=CC=C(Cl)C=C1CC1=C(O)C=CC(Cl)=C1	[14]
106	Phenanthrene	85-01-8	4.35	C1=CC2=C(C=C1)C1=CC=CC=C1C=C2	[16]
107	1-Hydroxypyrene	5315-79-7	4.45	OC1=C2C=CC3=C4C(C=CC(C=C1)=C24)=CC=C3	[11, 14]
108	di-i-Butyl phthalate (DIBP)	84-69-5	4.46	C1=CC=CC(=C1C(OCC(C)C)=O)C(OCC(C)C)=O	[10, 11]
109	4-Heptyloxyphenol	13037-86-0	4.54	C1=CC(=CC=C1OCCCCCCC)O	[10]
110	HPTE	2971-36-0	4.55	C2=C(C(C1=CC=C(O)C=C1)C(Cl)(Cl)Cl)C=CC(=C2)O	[10, 11]
111	Dibutylphthalate	84-74-2	4.61	C1=C(C(=CC=C1)C(OCCCC)=O)C(OCCCC)=O	[10, 13]
112	3,3‘-Dihydroxyhexestrol	79199-51-2	4.64	C1=C(O)C(=CC=C1C(C(C2=CC(=C(C=C2)O)O)CC)CC)O	[10]
113	Nordihydroguaiaretic acid	500-38-9	4.64	[C@H]([C@H](CC1=CC(=C(O)C=C1)O)C)(CC2=CC(=C(O)C=C2)O)C	[10]
114	Triclosane	3380-34-5	4.66	OC1=CC(Cl)=CC=C1OC1=CC=C(Cl)C=C1Cl	[11, 14]
115	Dimethylstilbestrol	552-80-7	4.66	C2=C(C(=C(C1=CC=C(O)C=C1)\C)/C)C=CC(=C2)O	[10]
116	Triphenylphosphate	115-86-6	4.7	c1ccc(cc1)OP(=O)(Oc2ccccc2)Oc3ccccc3	[10]
117	7-Oxobenz[de]anthracene	82-05-3	4.73	O=C1C2=C(C=CC=C2)C2=CC=CC3=CC=CC1=C23	[19]
118	2,3,4,5,6-Pentachlorophenol, Pentachlorophenol	87-86-5	4.74	OC1=C(Cl)C(Cl)=C(Cl)C(Cl)=C1Cl	[15]
119	Testosterone propionate	57-85-2	4.77	[H][C@@]12CC[C@H](OC(=O)CC)[C@@]1(C)CC[C@@]1([H])[C@@]2([H])CCC2=CC(=O)CC[C@]12C	[10]
120	Triphenylsilanol	791-31-1	4.79	c1ccc(cc1)[Si](c2ccccc2)(c3ccccc3)O	[10]
121	Benzylbutylphthalate	85-68-7	4.84	CCCCOC(=O)C1=CC=CC=C1C(=O)OCC1=CC=CC=C1	[10, 20]

122	Igepal CO-210	not available	4.84	CCCCCCCCCOC1=CC=C(OCCOCCO)C=C1	[10]
123	Zearalanone	5975-78-0	4.86	[C@H]2(OC(=O)C1=C(C=C(O)C=C1O)CCCCCC(=O)CCC2)C	[10]
124	p,p‘-Methoxychlor olefin	2132-70-9	4.87	C1=CC(=CC=C1C(C2=CC=C(OC)C=C2)=C(Cl)Cl)OC	[10, 12]
125	4-Methyl-phenanthrene	832-64-4	4.89	CC1=C2C(C=CC3=CC=CC=C23)=CC=C1	[16]
126	4-heptyloxybenzoic acid	15872-42-1	4.9	C1=CC(=CC=C1OCCCCCCC)C(O)=O	[10]
127	Kepone	143-50-0	4.91	O=C4C1(Cl)C2(Cl)C5(Cl)C3(Cl)C(Cl)(C1(Cl)C2(Cl)C3(Cl)Cl)C45Cl	[10]
128	Fluoranthene	206-44-0	4.93	C1=CC=C2C(=C1)C1=CC=CC3=C1C2=CC=C3	[11, 16, 21]
129	Pyrene	129-00-0	5	C1=CC2=CC=C3C=CC=C4C=CC(=C1)C2=C34	[11, 16, 21]
130	2,4‘-Dichlorobiphenyl	34883-43-7	5.05	C1=CC(=CC=C1C2=CC=CC=C2Cl)Cl	[10, 11]
131	5α-Androstan-17β-ol	1225-43-0	5.12	[H][C@@]12CC[C@H](O)[C@@]1(C)CC[C@@]1([H])[C@@]2([H])CC[C@@]2([H])CCCC[C@]12C	[10]
132	5α-Androstan-3β-ol	1224-92-6	5.12	O[C@@H]3C[C@@H]2CC[C@H]1[C@H]4[C@@](CC[C@@H]1[C@@]2(C)CC3)(C)CCC4	[10]
133	4-tert-Octylphenol	140-66-9	5.28	CC(C)(C)CC(C)(C)C1=CC=C(O)C=C1	[11, 15]
134	β-Zearalanol	42422-68-4	5.37	[C@H]2(OC(C1=C(C=C(O)C=C1O)CCCCC[C@H](O)CCC2)=O)C	[10]
135	3,3‘,5,5‘-Tetrachloro-4,4‘-biphenyldiol	13049-13-3	5.37	C2=C(C1=CC(=C(C(=C1)Cl)O)Cl)C=C(C(=C2Cl)O)Cl	[10]
136	Dieldrin	60-57-1	5.45	ClC5(Cl)[C@]3(Cl)C(\Cl)=C(\Cl)[C@@]5(Cl)[C@H]4[C@H]1C[C@H]([C@@H]2O[C@H]12)[C@@H]34	[2, 5]
137	17-Deoxyestradiol	53-63-4	5.48	[C@@H]23[C@H]([C@H]1[C@](CCC1)(C)CC2)CCC4=C3C=CC(=C4)O	[10]
138	Triphenylethylene	58-72-0	5.49	c1ccc(cc1)C=C(c2ccccc2)c3ccccc3	[10]
139	4-n-Octylphenol	1806-26-4	5.5	C1=C(C=CC(=C1)CCCCCCCC)O	[10]
140	Benz[a]anthracene	56-55-3	5.52	C1=CC=C2C=C3C(C=CC4=CC=CC=C34)=CC2=C1	[11, 16, 21]

141	o-Terphenyl	84-15-1	5.52	C1=CC=C(C=C1)C1=CC=CC=C1C1=CC=CC=C1	[16]
142	p-Terphenyl	92-94-4	5.52	C1=CC=C(C=C1)C1=CC=C(C=C1)C1=CC=CC=C1	[16]
143	p,p′-Methoxychlor	72-43-5	5.67	C1=CC(=CC=C1C(C2=CC=C(OC)C=C2)C(Cl)(Cl)Cl)OC	[10, 11]
144	1,3-bis(1,1-Dimethylethyl)-benzene	1014-60-4	5.81	CC(C)(C)C1=CC(=CC=C1)C(C)(C)C	[16]
145	Hydroxytamoxifen	68047-06-3	5.82	CC\C(=C(/C1=CC=C(O)C=C1)C1=CC=C(OCCN(C)C)C=C1)C1=CC=CC=C1	[20]
146	2,3,4,5-Tetrachloro-4′-biphenylol	67651-34-7	5.85	C1=C(Cl)C(=C(C(=C1C2=CC=C(C=C2)O)Cl)Cl)Cl	[10]
147	Heptachlor	76-44-8	5.86	C2(Cl)C1C3(Cl)C(Cl)(Cl)C(Cl)(C1C=C2)C(=C3Cl)Cl	[10]
148	p,p´-Dichlordiphenyldichlorethan	72-54-8	5.87	ClC(Cl)C(C1=CC=C(Cl)C=C1)C1=CC=C(Cl)C=C1	[11, 15]
149	o,p´-Dichlordiphenyldichlorethan	53-19-0	5.87	C2=C(C(C1=CC=C(Cl)C=C1)C(Cl)Cl)C(=CC=C2)Cl	[10]
150	9,10-Di(chloromethyl)anthracene	10387-13-0	5.95	ClCC1=C2C=CC=CC2=C(CCl)C2=C1C=CC=C2	[14]
151	Nonylphenol	25154-52-3	5.99	CCCCCCCCCC1=CC=C(O)C=C1	[15]
152	p,p´-Dichlordiphenyldichlorethen,	72-55-9	6	ClC(Cl)=C(C1=CC=C(Cl)C=C1)C1=CC=C(Cl)C=C1	[12, 13, 20]
153	1,4-Dibenzylbenzene	793-23-7	6.04	C(C1=CC=CC=C1)C1=CC=C(CC2=CC=CC=C2)C=C1	[16]
154	Hexestrol monomethyl ether	13026-26-1	6.16	C2=C(C(C(C1=CC=C(C=C1)O)CC)CC)C=CC(=C2)OC	[10]
155	Galaxolide	1222-05-5	6.26	CC1C(C)(C)C2=C(C=C3C(C)COCC3=C2)C1(C)C	[19]
156	Chlordane	57-74-9	6.26	C3C1C(C2(C(=C(C1(C2(Cl)Cl)Cl)Cl)Cl)Cl)C(Cl)C3Cl	[10]
157	Tamoxifen	10540-29-1	6.3	C1=CC(=CC=C1\C(=C(C2=CC=CC=C2)\CC)C3=CC=CC=C3)OCCN(C)C	[10]
158	Traseolide	68140-48-7	6.31	O=C(c1cc2c(cc1C)C(C(C2C(C)C)C)(C)C)C	[19]
159	2,2′,4,4′-tetrachlorobiphenyl	2437-79-8	6.34	C1=CC(=CC(=C1C2=C(C=C(Cl)C=C2)Cl)Cl)Cl	[10]
160	Tonalide	1506-02-1	6.35	O=C(c1c(cc2c(c1)C(CC(C)C2(C)C)(C)C)C)C	[19]
161	Primaric acid	127-27-	6.45	[H][C@]12CC[C@@](C)(C=C)C=C1CCC1[C@@](C)(CCC[C@]21C)C(O)=O	[14]

		5			
162	Isopimaric acid	5835-26-7	6.45	[H][C@]12CC[C@@](C)(CC1=CC[C@@]1([H])[C@@](C)(CCC[C@]21C)C(O)=O)C=C	[14]
163	Abietic acid	514-10-3	6.46	[H][C@]12CCC(=CC1=CC[C@@]1([H])[C@@](C)(CCC[C@]21C)C(O)=O)C(C)C	[14]
164	5α-Androstan	438-22-2	6.65	[C@H]23[C@@H]([C@@]1([C@H](CCCC1)CC2)C)CC[C@]4([C@H]3CCC4)C	[10]
165	Clomiphene	911-45-5	6.74	C3=C(\C(C1=CC=CC=C1)=C(\C2=CC=CC=C2)Cl)C=CC(=C3)OCCN(CC)CC	[10]
166	Aldrin	309-00-2	6.75	ClC34C1C(C2C=CC1C2)C(C3(Cl)Cl)(Cl)C(=C4Cl)Cl	[10]
167	p,p´-Dichlordiphenyltrichlorethan	50-29-3	6.79	ClC1=CC=C(C=C1)C(C1=CC=C(Cl)C=C1)C(Cl)(Cl)Cl	[12, 20]
168	o,p'-Dichlordiphenyltrichlorethan	789-02-6	6.79	C1=CC=CC(=C1C(C(Cl)(Cl)Cl)C2=CC=C(Cl)C=C2)Cl	[10, 12]
169	Mirex	2385-85-5	7.01	ClC53C1(Cl)C4(Cl)C2(Cl)C1(Cl)C(Cl)(Cl)C5(Cl)C2(Cl)C3(Cl)C4(Cl)Cl	[15]
170	Nafoxidine	1845-11-0	7.2	C1=CC(=CC3=C1C(=C(C2=CC=CC=C2)CC3)C5=CC=C(OCCN4CCCC4)C=C5)OC	[10]
171	1,3-Diphenyltetramethyldisiloxane	56-33-7	7.2	C[Si](C)(c1ccccc1)O[Si](C)(C)c2ccccc2	[10]
172	4-Dodecylphenol	104-43-8	7.46	C1=C(CCCCCCCCCCCC)C=CC(=C1)O	[10]
173	4-(3,5-Diphenylcyclohexyl)phenol	33330-65-3	7.6	C1=CC(=CC=C1C3CC(C2=CC=CC=C2)CC(C3)C4=CC=CC=C4)O	[10]
174	p-Dicyclohexylbenzene	1087-02-1	7.63	C1CCC(CC1)C1=CC=C(C=C1)C1CCCCC1	[16]
175	6-Phenyldodecane	2719-62-2	7.87	CCCCCCC(CCCCC)C1=CC=CC=C1	[16]
176	bis(n-Octyl)phthalate	117-84-0	8.54	C1=CC=CC(=C1C(OCCCCCCCC)=O)C(OCCCCCCCC)=O	[10]
177	Diisononylphthalate	28553-12-0	9.37	C1=CC=CC(=C1C(OCCCCCCC(C)C)=O)C(OCCCCCCC(C)C)=O	[10]
178	Tris(2-ethylhexy)phosphate	78-42-2	9.49	O=P(OCC(CC)CCCC)(OCC(CCCC)CC)OCC(CC)CCCC	[19]
179	Chlorobenzilate	510-15-6	3.99	Clc1ccc(cc1)C(O)(c2ccc(Cl)cc2)C(=O)OCC	[12]
180	Heptachlor epoxide	1024-	4.56	C12C(C(C3C1O3)Cl)C4(C(=C(C2(C4(Cl)Cl)Cl)Cl)Cl)Cl	[12]

		57-3			
181	Dicofol	115-32-2	5.81	C1=CC(=CC=C1C(C2=CC=C(C=C2)Cl)(C(Cl)(Cl)Cl)O)Cl	[12]
182	trans-Chlordane	5566-34-7	6.26	C1C2C(C(C1Cl)Cl)C3(C(=C(C2(C3(Cl)Cl)Cl)Cl)Cl)Cl	[12]
183	cis-Chlordane	5103-71-9	6.26	C1[C@H]2[C@@H]([C@H]([C@H]1Cl)Cl)[C@@]3(C(=C([C@]2(C3(Cl)Cl)Cl)Cl)Cl)Cl	[12]
184	alpha-Endosulfan	959-98-8	3.59	C1[C@@H]2[C@H](CO[S+](O1)[O-])[C@@]3(C(=C([C@]2(C3(Cl)Cl)Cl)Cl)Cl)Cl	[12]
185	Chlornitrofen	1836-77-7	4.96	C1=CC(=CC=C1[N+](=O)[O-])OC2=C(C=C(C=C2Cl)Cl)Cl	[12]
186	Chlomethoxyfen	32861-85-1	4.4	COC1=C(C=CC(=C1)OC2=C(C=C(C=C2)Cl)Cl)[N+](=O)[O-]	[12]
187	Nitrofen	1836-75-5	4.32	C1=CC(=CC=C1[N+](=O)[O-])OC2=C(C=C(C=C2)Cl)Cl	[12]
188	CNP-amino	73166-60-6	4.23	C1=CC(=CC=C1N)OC2=C(C=C(C=C2Cl)Cl)Cl	[12]
189	Oxyfluorfen	42874-03-3	5.21	CCOC1=C(C=CC(=C1)OC2=C(C=C(C=C2)C(F)(F)F)Cl)[N+](=O)[O-]	[12]
190	Bifenox	42576-02-3	4.15	COC(=O)C1=C(C=CC(=C1)OC2=C(C=C(C=C2)Cl)Cl)[N+](=O)[O-]	[12]
191	Acifluorfen-methyl	50594-67-7	4.47	COC(=O)C1=C(C=CC(=C1)OC2=C(C=C(C=C2)C(F)(F)F)Cl)[N+](=O)[O-]	[12]
192	Anilofos	64249-01-0	3.89	CC(C)N(C1=CC=C(C=C1)Cl)C(=O)CSP(=S)(OC)OC	[12]
193	EPN	2104-64-5	4.47	CCOP(=S)(C1=CC=CC=C1)OC2=CC=C(C=C2)[N+](=O)[O-]	[12]
194	Prothiofos	34643-46-4	6.34	CCCSP(=S)(OCC)Oc1ccc(cc1Cl)Cl	[12]
195	Tolclofos-methyl	57018-04-9	4.77	Cc1cc(c(c(c1)Cl)OP(=S)(OC)OC)Cl	[12]
196	Piperophos	24151-93-7	4.23	CCCOP(=S)(OCCC)SCC(=O)N1CCCCC1C	[12]
197	Ethion	563-12-2	5	CCOP(=S)(OCC)SCSP(=S)(OCC)OCC	[12]
198	Butamifos	36335-	4.52	CCC(C)NP(=S)(OCC)Oc1cc(ccc1[N+](=O)[O-])C	[12]

		67-8			
199	Phosalone	2310-17-0	4.29	CCOP(=S)(OCC)SCn1c2ccc(cc2oc1=O)Cl	[12]
200	Dichlofenthion	97-17-6	5.2	CCOP(=S)(OCC)Oc1ccc(cc1Cl)Cl	[12]
201	Cyanophos	2636-26-2	2.76	COP(=S)(OC)Oc1ccc(cc1)C#N	[12]
202	Bromophos-ethyl	4824-78-6	6.09	CCOP(=S)(OCC)Oc1cc(c(cc1Cl)Br)Cl	[12]
203	Quinalphos	13593-03-8	3.04	CCOP(=S)(OCC)Oc1cnc2ccccc2n1	[12]
204	Isofenphos	103982-06-5	4.4	CCOP(=S)(NC(C)C)OC1=CC=CC=C1C(=O)OC(C)C	[12]
205	Flucythrinate	70124-77-5	6.56	CC(C)C(c1ccc(cc1)OC(F)F)C(=O)OC(C#N)c2cccc(c2)Oc3ccccc3	[12]
206	Fenvalerate	51630-58-1	6.76	CC(C)C(c1ccc(cc1)Cl)C(=O)OC(C#N)c2cccc(c2)Oc3ccccc3	[12]
207	Cyfluthrin	68359-37-5	5.74	CC1([C@H]([C@H]1C(=O)O[C@@H](C#N)c2ccc(c(c2)Oc3ccccc3)F)C=C(Cl)Cl)C	[12]
208	Etofenprox	80844-07-1	7.47	CCOc1ccc(cc1)C(C)(C)COCc2cccc(c2)Oc3ccccc3	[12]
209	Methiocarb	2032-65-7	3.33	Cc1cc(cc(c1SC)C)O/C(=N/C)/O	[12, 22]
210	Thiobencarb	28249-77-6	3.9	CCN(CC)C(=O)SCc1ccc(cc1)Cl	[12]
211	Thenylchlor	125034-10-8	4.21	Cc1cccc(c1N(Cc2c(ccs2)OC)C(=O)CCl)C	[12]
212	Mefenacet	73250-68-7	2.8	CN(c1ccccc1)C(=O)COc2nc3ccccc3s2	[12]
213	Alachlor	15972-60-8	3.37	CCc1cccc(c1N(COC)C(=O)CCl)CC	[12]
214	Pencycuron	66063-05-6	5.51	c1ccc(cc1)NC(=O)N(Cc2ccc(cc2)Cl)C3CCCC3	[12]
215	Diuron	330-54-1	1.19	CN(C)/C(=N\c1ccc(c(c1)Cl)Cl)/O	[12]
216	Bromopropylate	18181-80-1	4.9	CC(C)OC(=O)C(c1ccc(cc1)Br)(c2ccc(cc2)Br)O	[12]

217	Pendimethalin	40487-42-1	4.82	CCC(CC)Nc1c(cc(c(c1[N+](=O)[O-])C)C)[N+](=O)[O-]	[12]
218	Bitertanol	55179-31-2	4.07	CC(C)(C)C(C(n1cncn1)Oc2ccc(cc2)c3ccccc3)O	[12]
219	Triflumizole	99387-89-0	1.5	CCCOC/C(=N\c1ccc(cc1C(F)(F)F)Cl)/n2ccnc2	[12]
220	Imazalil	35554-44-0	4.1	C=CCOC(Cn1ccnc1)c2ccc(cc2Cl)Cl	[12]
221	2-Phenylphenol	90-43-7	3.28	c1ccc(cc1)c2ccccc2O	[12]
222	Pyrazoxyfen	71561-11-0	4.97	Cc1c(c(n(n1)C)OCC(=O)c2ccccc2)C(=O)c3ccc(cc3Cl)Cl	[12]
223	Propiconazole	60207-90-1	4.13	CCCC1COC(O1)(Cn2cncn2)c3ccc(cc3Cl)Cl	[12]
224	Fenarimol	162707-16-6	3.62	c1ccc(c(c1)C(c2ccc(cc2)Cl)(c3cncnc3)O)Cl	[12]
225	Ethoxyquin	91-53-2	3.87	CCOc1ccc2c(c1)C(=CC(N2)(C)C)C	[12]
226	3,3´-Dichlorobenzidine	91-94-1	3.21	c1cc(c(cc1c2ccc(c(c2)Cl)N)Cl)N	[11, 17]
227	4,4´-[1-[4-[1-(4-Hydroxyphenyl)-1-methylethyl]phenyl]ethylidene]bis[phenol]	110726-28-8	6.99	CC(C)(c1ccc(cc1)C(C)(c2ccc(cc2)O)c3ccc(cc3)O)c4ccc(cc4)O	[11, 17]
228	2,4,6-Trichlorophenylhydrazine	5329-12-4	2.73	c1c(cc(c(c1Cl)NN)Cl)Cl	[11, 17]
229	4-(Phenylpropyl)pyridine	2057-49-0	4.04	c1ccc(cc1)CCCc2ccncc2	[12]
230	4-Diethylaminobenzaldehyde	120-21-8	2.87	CCN(CC)c1ccc(cc1)C=O	[12]
231	4-Methoxy-2-methyldiphenylamine	41317-15-1	3.92	Cc1cc(ccc1Nc2ccccc2)OC	[11, 17]
232	2,4-Diphenyl-4-methylpentene-1	6362-80-7	6.51	CC(C)(CC(=C)c1ccccc1)c2ccccc2	[17]
233	2,2-Bis(4-cyanophenyl)propane	1156-51-0	1.83	CC(C)(c1ccc(cc1)OC#N)c2ccc(cc2)OC#N	[11, 17]
234	Benzo[b]fluorene	243-17-4	5.19	c1ccc2cc-3c(cc2c1)Cc4c3cccc4	[21]
235	Chrysene	218-01-9	5.52	c1ccc2c(c1)ccc3c2ccc4c3cccc4	[11, 21]

236	Benzo[k]fluoranthene	207-08-9	6.11	c1ccc2cc-3c(cc2c1)-c4cccc5c4c3ccc5	[11, 21]
237	Indeno[1,2,3-cd]pyrene	193-39-5	6.7	c1ccc-2c(c1)-c3ccc4ccc5cccc6c5c4c3c2c6	[21]
238	Benzo[ghi]perylene	191-24-2	6.7	c1cc2ccc3ccc4ccc5cccc6c5c4c3c2c6c1	[21]
239	Epoxiconazole	106325-08-0	3.47	c1ccc(c(c1)[C@@H]2[C@@](O2)(Cn3cncn3)c4ccc(cc4)F)Cl	[13]
240	DEHP	117-81-7	8.39	CCCCC(CC)COC(=O)c1ccccc1C(=O)OCC(CC)CCCC	[13]
241	Paracetamol	103-90-2	8.76	C/C(=N\c1ccc(cc1)O)/O	[13]
242	finasteride	98319-26-7	6.77	C[C@]12CC[C@H]3[C@H]([C@@H]1CC[C@@H]2/C(=N/C(C)(C)C)/O)CC[C@@H]4[C@@]3(C=CC(=N4)O)C	[23]
243	Deltamethrin	52918-63-5	6.18	CC1([C@H]([C@H]1C(=O)O[C@H](C#N)c2cccc(c2)Oc3ccccc3)C=C(Br)Br)C	[22]
244	Simazine	122-34-9	2.4	CC/N=c\1/[nH]/c(=N\CC)/nc([nH]1)Cl	[22]
245	Tribenuron-methyl	101200-48-0	2.55	Cc1nc(nc(n1)OC)N(C)C(=O)NS(=O)(=O)c2ccccc2C(=O)OC	[22]
246	Dilazep	35898-87-4	3.09	C(OCCCN1CCCN(CC1)CCCOC(C1=CC(OC)=C(C(OC)=C1)OC)=O)(C1=CC(OC)=C(C(OC)=C1)OC)=O	[11]
247	3,3'-Dimethoxy-4,4'-biphenyldiamin	119-90-4	2.08	C1(C2=CC(OC)=C(C=C2)N)=CC(OC)=C(C=C1)N	[11]
248	2-Dibutylaminoethanol	102-81-8	2.01	C(N(CCO)CCCC)CCC	[11]
249	N,N-Diethylcyclohexanamine	91-65-6	3.29	C1(CCCCC1)N(CC)CC	[11]
250	Busulfan	55-98-1	-0.68	C(OS(C)(=O)=O)CCCOS(C)(=O)=O	[11]
251	2,3-Dihydro-1,4-benzodioxin-2-ylmethanol	3663-82-9	1	C12=C(OC(CO2)CO)C=CC=C1	[11]
252	Biphenylamine	90-41-5	2.84	C1(C2=C(C=CC=C2)N)=CC=CC=C1	[11]
253	2-Anthracenamine	613-13-8	3.43	C12=CC3=C(C=CC(N)=C3)C=C1C=CC=C2	[11]
254	2,4-Dimethoxy-1-nitrobenzene	4920-84-7	1.97	C1(N(=O)=O)=C(C=C(C=C1)OC)OC	[11]

255	Aminopyrene	1606-67-3	4.02	C12=C3C4=C(C=CC3=CC=C2)C=CC(N)=C4C=C1	[11]
256	4-Benzylpyridine	2116-65-6	3.06	C1(CC2=CC=NC=C2)=CC=CC=C1	[11]
257	Betapar	1247-42-3	2.01	C(CO)(C1(C2(C(CC1C)C1C(C(C2)=O)C2(C(CC1)=CC(C=C2)=O)C)C)O)=O	[11]
258	Dimethoxymethyl-benzene	1125-88-8	1.44	C1(C(OC)OC)=CC=CC=C1	[11]
259	2-Hydroxyflutamide	52806-53-8	2.8	C(C1=C(C=CC(NC(C(O)(C)C)=O)=C1)N(=O)=O)(F)(F)F	[11]
260	21-O-Acetyl-corticosterone	1173-26-8	1.74	C12=CC(CCC1(C)C1C(CC2)C2C(CC1O)(C(CC2)C(COC(C)=O)=O)C)=O	[11]
261	Acetylnaphthalene	941-98-0	2.85	C(C1=C2C(C=CC=C2)=CC=C1)(C)=O	[11]
262	4-Methylthiophenol	106-45-6	3.23	C1(S)=CC=C(C=C1)C	[11]
263	Thenylchlor	96491-05-3	4.21	Cc1cccc(c1N(Cc2c(ccs2)OC)C(=O)CCl)C	[11]
264	Bicalutamide	90357-06-5	2.3	C(C1=C(C=CC(NC(C(CS(C2=CC=C(C=C2)F)(=O)=O)(O)C)=O)=C1)C#N)(F)(F)F	[11]
265	p-Chlorocresol	59-50-7	2.7	C1(Cl)=C(C=C(C=C1)O)C	[11]
266	Nilutamide	63612-50-0	1.31	CC1(C(=O)N(C(=O)N1)c2ccc(c(c2)C(F)(F)F)[N+](=O)[O-])C	[11]
267	(2,4-Dimethoxyphenyl)(4-hydroxyphenyl)methanone	20-30-3	2.83	C1(C(C2=C(C=C(C=C2)OC)OC)=O)=CC=C(C=C1)O	[11]
268	4-(2,4,6-Trichlorophenoxy)aniline	26306-61-6	4.23	C1(Cl)=C(C(Cl)=CC(Cl)=C1)OC1=CC=C(C=C1)N	[11]
269	2,3',4,4'-Tetrahydroxybenzophenone	61445-50-9	2	C1(C(C2=C(C=C(C=C2)O)O)=O)=CC(O)=C(C=C1)O	[11]
270	2,3,4,4'-Tetrahydroxybenzophenone	311127-54-5	2.42	C1(C(C2=C(C(O)=C(C=C2)O)O)=O)=CC=C(C=C1)O	[11]
271	TBHQ	1948-33-0	2.94	C(C1=C(C=CC(O)=C1)O)(C)(C)C	[11]
272	N-(3,5-Dichlorophenyl)-2-hydroxy-2-methyl-3-butenamide	83792-61-4	2.95	C(NC1=CC(Cl)=CC(Cl)=C1)(C(C=C)(O)C)=O	[11]
273	2,5-Biphenyldiol	1079-	2.8	C1(C2=C(C=CC(O)=C2)O)=CC=CC=C1	[11]

		21-6			
274	17,20-Dihydroxypregn-4-en-3-one	1662-06-2	2.66	C12=CC(CCC1(C)C1C(CC2)C2C(CC1)(C(CC2)(C(O)C)O)C)=O	[11]
275	Mifepristone	84371-65-3	5.39	CC#C[C@@]1(CC[C@@H]2[C@@]1(C[C@@H](C3=C4CCC(=O)C=C4CC[C@@H]23)c5ccc(cc5)N(C)C)C)O	[11]
276	3-Methyl-1-hexene	3404-61-3	3.37	C(C(CCC)C)=C	[11]
277	3-Hydroxybenzophenone	13020-57-0	2.67	C1(C(C2=CC(O)=CC=C2)=O)=CC=CC=C1	[11]
278	2-(4-Fluorophenyl)propene	350-40-3	3.64	C(C1=CC=C(C=C1)F)(C)=C	[11]
279	(2,4-Dihydroxyphenyl)(4-hydroxyphenyl)methanone	1470-79-7	2.48	C1(C(C2=C(C=C(C=C2)O)O)=O)=CC=C(C=C1)O	[11]
280	2,3,4-Trihydroxybenzophenone	1143-72-2	2.91	C1(C(C2=C(C(O)=C(C=C2)O)O)=O)=CC=CC=C1	[11]
281	Tebuconazole	107534-96-3	3.89	C(C(CN1C=NC=N1)(CCC1=CC=C(C=C1)Cl)O)(C)(C)C	[11]
282	Diallyl phthalate	131-17-9	3.36	C(OCC=C)(C1=C(C=CC=C1)C(OCC=C)=O)=O	[11]
283	4,4'-Methandiyldibenzolol	620-92-8	3.06	C1(O)=CC=C(C=C1)CC1=CC=C(C=C1)O	[11]
284	Bis(2,4-dihydroxyphenyl)methanone	131-55-5	2.78	C1(C(C2=C(C=C(C=C2)O)O)=O)=C(C=C(C=C1)O)O	[11]
285	3,4-Bis(3-hydroxybenzyl)dihydro-2(3H)-furanone	76543-15-2	2.73	C1(C(C(CO1)CC1=CC(O)=CC=C1)CC1=CC(O)=CC=C1)=O	[11]
286	Mevastatin	73573-88-3	4.18	C12=CCCC(OC(C(CC)C)=O)C1C(C(C=C2)C)CCC1CC(CC(O1)=O)O	[11]
287	O-Demethylangolensin	21255-69-6	3.14	C(C(C1=CC=C(C=C1)O)C)(C1=C(C=C(C=C1)O)O)=O	[11]
288	Nookatone	4674-50-4	4.46	C12=CC(CC(C)C1(CC(CC2)C(C)=C)C)=O	[11]
289	4-p-Chlorobenzoylphenol	20-30-4	3.31	C1(C(C2=CC=C(C=C2)O)=O)=CC=C(C=C1)Cl	[11]
290	2-Fluorobiphenyl	321-60-8	3.96	C1(C2=C(C=CC=C2)F)=CC=CC=C1	[11]
291	o-Benzoylphenol	117-99-7	3.44	C1(C(C2=C(C=CC=C2)O)=O)=CC=CC=C1	[11]

292	2,3,5,6-Tetrachloro-1,4-benzenediol	87-87-6	3.61	C1(Cl)=C(C(O)=C(C(Cl)=C1O)Cl)Cl	[11]
293	1,1'-[Methylenebis(4,1-phenyleneoxy)]bis(3-chloro-2-propanol)	20-30-5	3.98	C1(OCC(CCl)O)=CC=C(C=C1)CC1=CC=C(C=C1)OCC(CCl)O	[11]
294	Pryfon	25311-71-1	4.4	C(OC(C)C)(C1=C(C=CC=C1)OP(OCC)(NC(C)C)=S)=O	[11]
295	Acetylpyrene	3264-21-9	4.61	C(C1=C2C3=C(C=C1)C=CC1=C3C(C=C2)=CC=C1)(C)=O	[11]
296	Fenarimol	60168-88-9	3.62	C1(C(C2=CC=C(C=C2)Cl)(C2=C(C=CC=C2)Cl)O)=CN=CN=C1	[11]
297	Lovastatin	75330-75-5	4.6	C12=CC(C)CC(OC(C(CC)C)=O)C1C(C(C=C2)C)CCC1CC(CC(O1)=O)O	[11]
298	Anthracene	120-12-7	4.35	C12=CC3=C(C=CC=C3)C=C1C=CC=C2	[11]
299	Dioxybenzone	131-53-3	3.82	C1(C(C2=C(C=C(C=C2)OC)O)=O)=C(C=CC=C1)O	[11]
300	2,6-Di-tert-butyl-4-hydroxymethylphenol	88-26-6	3.56	C(C1=C(C(C(C)(C)C)=CC(CO)=C1)O)(C)(C)C	[11]
301	Phenanthrindene	203-64-5	4.6	C12=C3C4=C(C=CC=C4C2)C=CC3=CC=C1	[11]
302	Hexylresorcinol	136-77-6	4.04	C1(CCCCCC)=C(C=C(C=C1)O)O	[11]
303	2,2'-Dihydroxy benzophenone	835-11-0	3.74	C1(C(C2=C(C=CC=C2)O)=O)=C(C=CC=C1)O	[11]
304	Benalaxyl-M	98243-83-5	3.69	C1(C)=C(C(C)=CC=C1)N(C(C(OC)=O)C)C(CC1=CC=CC=C1)=O	[11]
305	Amiodarone	1951-25-3	8.81	C1(C(C2=C(CCCC)OC3=C2C=CC=C3)=O)=CC(I)=C(C(I)=C1)OCCN(CC)CC	[11]
306	1-Nitropyrene	5522-43-0	4.75	C12=C3C4=C(C=CC3=CC=C2)C=CC(N(=O)=O)=C4C=C1	[11]
307	Pcb 1	2051-60-7	4.4	C1(C2=C(C=CC=C2)Cl)=CC=CC=C1	[11]
308	(2-Hydroxy-3-methylphenyl)(phenyl)methanone	4072-08-6	3.99	C1(C(C2=C(C(C)=CC=C2)O)=O)=CC=CC=C1	[11]
309	Zearalenone	17924-92-4	3.58	C1(C2=C(C=C(C=C2O)O)C=CCCCC(CCCC(O1)C)=O)=O	[11]
310	2-Benzoyl-4-chlorophenol	85-19-8	4.09	C1(C(C2=C(C=CC(Cl)=C2)O)=O)=CC=CC=C1	[11]

311	1,1'-[2,2-Propanediylbis(4,1-phenyleneoxy)]bis(3-chloro-2-propanol)	4809-35-2	4.57	C1(C(C2=CC=C(C=C2)OCC(CCl)O)(C)C)=CC=C(C=C1)OCC(CCl)O	[11]
312	Simvastatin	79902-63-9	5.19	C(OC1C2C(C=CC(C2CCC2CC(CC(O2)=O)O)C)=CC(C1)C)(C(CC)(C)C)=O	[11]
313	9-Methylanthracene	779-02-2	4.89	C12=CC3=C(C=CC=C3)C(C)=C1C=CC=C2	[11]
314	3,5-Dichloro-4-biphenylol	1137-59-3	4.57	C1(C2=CC(Cl)=C(C(Cl)=C2)O)=CC=CC=C1	[11]
315	4,4'-Dichlorobenzilic acid isopropyl ester	5836-10-2	4.41	C(OC(C)C)(C(C1=CC=C(C=C1)Cl)(C1=CC=C(C=C1)Cl)O)=O	[11]
316	2,4-Di-t-butylphenol	96-76-4	5.33	C(C1=C(C=CC(C)(C)C)C=C1)O)(C)(C)C	[11]
317	3,3'-PCB	2050-67-1	5.05	C1(C2=CC(Cl)=CC=C2)=CC(Cl)=CC=C1	[11]
318	2,2'-Dichlorobiphenyl	13029-08-8	5.05	C1(C2=C(C=CC=C2)Cl)=C(C=CC=C1)Cl	[11]
319	PCB 5	16605-91-7	5.05	C1(C2=C(C(Cl)=CC=C2)Cl)=CC=CC=C1	[11]
320	2,6-PCB	33146-45-1	5.05	C1(C2=C(C=CC=C2Cl)Cl)=CC=CC=C1	[11]
321	3,5-Dichlorobiphenyl	34883-41-5	5.05	C1(C2=CC(Cl)=CC(Cl)=C2)=CC=CC=C1	[11]
322	9,10-Dimethylanthracene	781-43-1	5.44	C1(C)=C2C(C=CC=C2)=C(C2=C1C=CC=C2)C	[11]
323	Homosalate	118-56-9	6.16	C(OC1CC(CC(C1)C)(C)C)(C1=C(C=CC=C1)O)=O	[11]
324	9,10-DICHLOROANTHRACENE	605-48-1	5.63	C1(Cl)=C2C(C=CC=C2)=C(C2=C1C=CC=C2)Cl	[11]
325	Benzocaine	50-32-8	6.11	C12=C3C4=C(C=CC3=CC=C2)C=C2C(C=CC=C2)=C4C=C1	[11]
326	Benz[j]fluoranthene	205-82-3	6.11	C12=CC=C3C4=CC=CC5=C4C(C3=C1C=CC=C2)=CC=C5	[11]
327	Agricide	8001-35-2	6.79	C1(C2(C(C(C1)C(C2Cl)Cl)(CCl)C(Cl)Cl)Cl)CCl)(Cl)Cl	[11]
328	2,4,4'-Trichlorobiphenyl	7012-37-5	5.69	C1(C2=C(C=C(C=C2)Cl)Cl)=CC=C(C=C1)Cl	[11]
329	2,4,6-Trichlorobiphenyl	35693-92-6	5.69	C1(C2=C(C=C(C=C2Cl)Cl)Cl)=CC=CC=C1	[11]

330	2,3',5'-PCB	37680-68-5	5.69	C1(C2=C(C=CC=C2)Cl)=CC(Cl)=CC(Cl)=C1	[11]
331	2,2',6-PCB	38444-73-4	5.69	C1(C2=C(C=CC=C2Cl)Cl)=C(C=CC=C1)Cl	[11]
332	2,3,4'-PCB	38444-85-8	5.69	C1(C2=C(C(Cl)=CC=C2)Cl)=CC=C(C=C1)Cl	[11]
333	3,4',5-PCB	38444-88-1	5.69	C1(C2=CC(Cl)=CC(Cl)=C2)=CC=C(C=C1)Cl	[11]
334	2,3,6-PCB	55702-45-9	5.69	C1(C2=C(C(Cl)=CC=C2Cl)Cl)=CC=CC=C1	[11]
335	3-Bromo-4-(2,4-dibromophenoxy)phenol	20-21-7	5.4	C1(OC2=C(C=C(C=C2)Br)Br)=C(C=C(C=C1)O)Br	[11]
336	Dipentyl phthalate	131-18-0	5.59	C(OCCCCC)(C1=C(C=CC=C1)C(OCCCCC)=O)=O	[11]
337	Dicyclohexyl phthalate	84-61-7	6.2	C(OC1CCCCC1)(C1=C(C=CC=C1)C(OC1CCCCC1)=O)=O	[11]
338	2,4-Dibromo-1-(2-bromo-4-methoxyphenoxy)benzene	20-21-8	5.96	C1(OC2=C(C=C(C=C2)Br)Br)=C(C=C(C=C1)OC)Br	[11]
339	1,1'-(Chlorophenylmethylene)bis(4-methoxybenzene)	40615-36-9	5.74	C1(C(C2=CC=C(C=C2)OC)(C2=CC=C(C=C2)OC)Cl)=CC=CC=C1	[11]
340	Retene	483-65-8	6.35	C1(C)=CC=CC2=C3C(C=C(C=C3)C(C)C)=CC=C12	[11]
341	2,4-Dibromo-1-(4-bromophenoxy)benzene	41318-75-6	5.88	C1(OC2=CC=C(C=C2)Br)=C(C=C(C=C1)Br)Br	[11]
342	Tribromodiphenyl ether	49690-94-0	5.88	C1(Br)=C(C=C(C=C1)OC1=C(C=CC=C1)Br)Br	[11]
343	DMBA	57-97-6	6.62	C12=CC=C3C(C)=C4C(C=CC=C4)=C(C3=C1C=CC=C2)C	[11]
344	Triphenylchloromethane	76-83-5	5.58	C1(C(C2=CC=CC=C2)(C2=CC=CC=C2)Cl)=CC=CC=C1	[11]
345	2,3',4,4'-PCB	32598-10-0	6.34	C1(C2=C(C=C(C=C2)Cl)Cl)=CC(Cl)=C(C=C1)Cl	[11]
346	2,4,4',6-PCB	32598-12-2	6.34	C1(C2=C(C=C(C=C2Cl)Cl)Cl)=CC=C(C=C1)Cl	[11]
347	2,4,4',5-PCB	32690-93-0	6.34	C1(C2=C(C=C(C(Cl)=C2)Cl)Cl)=CC=C(C=C1)Cl	[11]
348	2,3,5,6-PCB	33284-54-7	6.34	C1(C2=C(C(Cl)=CC(Cl)=C2Cl)Cl)=CC=CC=C1	[11]
349	2,2',4,5'-PCB	41464-	6.34	C1(C2=C(C=C(C=C2)Cl)Cl)=C(C=CC(Cl)=C1)Cl	[11]

		40-8			
350	2,2',3,6'-PCB	41464-47-5	6.34	C1(C2=C(C(Cl)=CC=C2)Cl)=C(C=CC=C1Cl)Cl	[11]
351	2,3,4',6-PCB	52663-58-8	6.34	C1(C2=C(C(Cl)=CC=C2Cl)Cl)=CC=C(C=C1)Cl	[11]
352	γ-linolenicacid	506-26-3	7.3	C(CCCCC=CCC=CCC=CCCCCC)(O)=O	[11]
353	1-Chloro-2-[2,2-dichloro-1-(4-chlorophenyl)vinyl]benzene	3424-82-6	6	C1(C(C2=C(C=CC=C2)Cl)=C(Cl)Cl)=CC=C(C=C1)Cl	[11]
354	Pentachlorodibenzofuran	57117-31-4	6.94	C12=C(C=C(C(Cl)=C2)Cl)OC2=C1C=C(C(Cl)=C2Cl)Cl	[11]
355	2,3-Dibromo-4-(2,4-dibromophenoxy)phenol	602326-22-7	6.29	C1(O)=C(C(Br)=C(C=C1)OC1=C(C=C(C=C1)Br)Br)Br	[11]
356	2,5-Dibromo-4-(2,4-dibromophenoxy)phenol	602326-23-8	6.29	C1(Br)=C(C=C(C(OC2=C(C=C(C=C2)Br)Br)=C1)Br)O	[11]
357	1,4-Dibromo-2-(2,4-dibromophenoxy)-5-methoxybenzene	602326-26-1	6.29	C1(Br)=C(C=C(C(OC2=C(C=C(C=C2)Br)Br)=C1)Br)OC	[11]
358	2,3-Dibromo-1-(2,4-dibromophenoxy)-4-methoxybenzene	602326-25-0	6.29	C1(OC)=C(C(Br)=C(C=C1)OC1=C(C=C(C=C1)Br)Br)Br	[11]
359	Dihexyl phthalate	84-75-3	6.57	C(OCCCCCC)(C1=C(C=CC=C1)C(OCCCCCC)=O)=O	[11]
360	Tris(4-chlorophenyl)methanol	3010-80-8	6.31	C1(C(C2=CC=C(C=C2)Cl)(C2=CC=C(C=C2)Cl)O)=CC=C(C=C1)Cl	[11]
361	Tetrabromodiphenyl ether	40088-47-9	6.77	C1(Br)=C(C(Br)=C(C=C1)OC1=CC(Br)=CC=C1)Br	[11]
362	bis(2,4-dibromophenyl) ether	5436-43-1	6.77	C1(OC2=C(C=C(C=C2)Br)Br)=C(C=C(C=C1)Br)Br	[11]
363	1,2,3,6,7,8-Hexachlorooxanthrene	57653-85-7	8.21	C1(Cl)=C(C(Cl)=C2C(OC3=C(C(Cl)=C(C=C3O2)Cl)Cl)=C1)Cl	[11]
364	2,2-Propanediyldi-4,1-phenylene bis(2-methylacrylate)	3253-39-2	5.6	C1(C(C2=CC=C(C=C2)OC(C(C)=C)=O)(C)C)=CC=C(C=C1)OC(C(C)=C)=O	[11]
365	2,3',4,4',5-PCB	31508-00-6	6.98	C1(C2=C(C=C(C(Cl)=C2)Cl)Cl)=CC(Cl)=C(C=C1)Cl	[11]
366	2,3,3',4,4'-Pentachlorobiphenyl	32598-14-4	6.98	C1(C2=C(C(Cl)=C(C=C2)Cl)Cl)=CC(Cl)=C(C=C1)Cl	[11]
367	PCB-126	57465-28-8	6.98	C1(C2=CC(Cl)=C(C(Cl)=C2)Cl)=CC(Cl)=C(C=C1)Cl	[11]

368	2,3,3',5,6-Pcb	74472-37-0	6.98	C1(C2=C(C(Cl)=CC(Cl)=C2Cl)Cl)=CC(Cl)=CC=C1	[11]
369	Docohexaenoic acid	6217-54-5	8.62	C(CCC=CCC=CCC=CCC=CCC=CCC=CCC)(O)=O	[11]
370	Bis(5-methylhexyl) phthalate	71888-89-6	7.41	CC(C)CCCCOC(=O)c1ccccc1C(=O)OCCCCC(C)C	[11]
371	2,3,6-Tribromo-4-(2,4-dibromophenoxy)phenol	20-22-3	7.18	C1(Br)=C(C(Br)=C(C(OC2=C(C=C(C=C2)Br)Br)=C1)Br)O	[11]
372	3,3',5,5'-Tetrabromobisphenol A	79-94-7	7.2	C1(C(C2=CC(Br)=C(C(Br)=C2)O)(C)C)=CC(Br)=C(C(Br)=C1)O	[11]
373	1,3,4-Tribromo-5-(2,4-dibromophenoxy)-2-methoxybenzene	20-22-4	7.74	C1(Br)=C(C(Br)=C(C(OC2=C(C=C(C=C2)Br)Br)=C1)Br)OC	[11]
374	2,2',3,4,4',5'-PCB	35065-28-2	7.62	C1(C2=C(C(Cl)=C(C=C2)Cl)Cl)=C(C=C(C(Cl)=C1)Cl)Cl	[11]
375	2,3,3',4,4',5-PCB	38380-08-4	7.62	C1(C2=C(C(Cl)=C(C(Cl)=C2)Cl)Cl)=CC(Cl)=C(C=C1)Cl	[11]
376	2,3',4,4',5,5'-PCB	52663-72-6	7.62	C1(C2=C(C=C(C(Cl)=C2)Cl)Cl)=CC(Cl)=C(C(Cl)=C1)Cl	[11]
377	2,3,3',4,4',5'-PCB	69782-90-7	7.62	C1(C2=C(C(Cl)=C(C=C2)Cl)Cl)=CC(Cl)=C(C(Cl)=C1)Cl	[11]
378	2,2’,4,4’,5-Pentabromodiphenyl ether	60348-60-9	7.66	C1(Br)=C(C=C(C(OC2=C(C=C(C=C2)Br)Br)=C1)Br)Br	[11]
379	1,2,3-Tribromo-4-(2,4-dibromophenoxy)benzene	182346-21-0	7.66	C1(Br)=C(C(Br)=C(C=C1)OC1=C(C=C(C=C1)Br)Br)Br	[11]
380	1,3,5-Tribromo-2-(2,4-dibromophenoxy)benzene	189084-64-8	7.66	C1(Br)=C(C(Br)=CC(Br)=C1)OC1=C(C=C(C=C1)Br)Br	[11]
381	p-Cresol, 2,2'-methylenebis[6-tert-butyl-	119-47-1	7.97	C(C1=C(C(CC2=C(C(C(C)(C)C)=CC(C)=C2)O)=CC(C)=C1)O)(C)(C)C	[11]
382	2,2',3,3',5,5',6,6'-PCB	2136-99-4	8.91	C1(C2=C(C(Cl)=CC(Cl)=C2Cl)Cl)=C(C(Cl)=CC(Cl)=C1Cl)Cl	[11]
383	2,2'-Methylenebis(6-tert-butyl-4-ethylphenol)	88-24-4	8.95	C(C1=C(C(CC2=C(C(C(C)(C)C)=CC(CC)=C2)O)=CC(CC)=C1)O)(C)(C)C	[11]
384	m-Cresol, 4,4'-butylidenebis[6-tert-butyl-	85-60-9	9.09	C(C1=C(C=C(C(C(CCC)C2=C(C=C(C(C(C)(C)C)=C2)O)C)=C1)C)O)(C)(C)C	[11]
385	1,2,3,4,5-Pentabromo-6-(2,4-dibromophenoxy)benzene	189084-67-1	9.44	C1(Br)=C(C(Br)=C(C(Br)=C1OC1=C(C=C(C=C1)Br)Br)Br)Br	[11]

References

1. Chambers, M.C., et al., *A cross-platform toolkit for mass spectrometry and proteomics.* Nat Biotech, 2012. **30**(10): p. 918-920.
2. Pluskal, T., et al., *MZmine 2: Modular framework for processing, visualizing, and analyzing mass spectrometry-based molecular profile data.* Bmc Bioinformatics, 2010. **11**.
3. Hug, C., et al., *Identification of novel micropollutants in wastewater by a combination of suspect and nontarget screening.* Environmental Pollution, 2014. **184**(0): p. 25-32.
4. Prakash, C., C.L. Shaffer, and A. Nedderman, *Analytical strategies for identifying drug metabolites.* Mass Spectrometry Reviews, 2007. **26**(3): p. 340-369.
5. Pfeifer, T., J. Tuerk, and R. Fuchs, *Structural Characterization of Sulfadiazine Metabolites Using H/D Exchange Combined with Various MS/MS Experiments.* Journal of the American Society for Mass Spectrometry, 2005. **16**(10): p. 1687-1694.
6. Liu, D.Q., et al., *On-line H/D exchange LC–MS strategy for structural elucidation of pharmaceutical impurities.* Journal of Pharmaceutical and Biomedical Analysis, 2007. **44**(2): p. 320-329.
7. *ChemAxon JChem for Excel 15.7.2700.2799. http://www.chemaxon.com.*
8. Muz, M., et al., *Mutagenicity in Surface Waters Synergistic Effects of Carboline Alkaloids and Aromatic Amines.* Environmental Science & Technology, 2017.
9. Spirhanzlova, P., et al., *Oestrogen reporter transgenic medaka for non-invasive evaluation of aromatase activity.* Comparative Biochemistry and Physiology Part C: Toxicology & Pharmacology, 2016. **179**(Supplement C): p. 64-71.
10. Fang, H., et al., *Study of 202 natural, synthetic, and environmental chemicals for binding to the androgen receptor*. Chemical Research in Toxicology, 2003. 16(10): p. 1338-1358.
11. Jensen GE, Nikolov NG, Dreisig K, Vinggaard AM, Niemelä JR (2012) QSAR Model for Androgen Receptor Antagonism - Data from CHO Cell Reporter Gene Assays. J Steroids Horm Sci S2:006. doi: 10.4172/2157-7536.S2-006
12. Kojima, H., et al., *Screening for estrogen and androgen receptor activities in 200 pesticides by in vitro reporter gene assays using Chinese hamster ovary cells*. Environmental Health Perspectives, 2004. 112(5): p. 524-531.
13. Mandrup, K.R., et al., *Mixtures of environmentally relevant endocrine disrupting chemicals affect mammary gland development in female and male rats*. Reproductive Toxicology, 2015. 54(Supplement C): p. 47-57.
14. Rostkowski, P., et al., *Bioassay-Directed Identification of Novel Antiandrogenic Compounds in Bile of Fish Exposed to Wastewater Effluents*. Environmental Science & Technology, 2011. 45(24): p. 10660-10667.
15. Urbatzka, R., et al., *Androgenic and antiandrogenic activities in water and sediment samples from the river Lambro, Italy, detected by yeast androgen screen and chemical analyses*. Chemosphere, 2007. 67(6): p. 1080-1087.
16. Weiss, J.M., et al., Masking effect of anti-*androgens on androgenic activity in European river sediment unveiled by effect-directed analysis*. Analytical and Bioanalytical Chemistry, 2009. 394: p. 1385-1397.

17. Araki, N., et al., *Screening for androgen receptor activities in 253 industrial chemicals by in vitro reporter gene assays using AR-EcoScreenTM cells*. Toxicology in Vitro, 2005. 19(6): p. 831-842.
18. Chang, H., et al., *Occurrence of androgens and progestogens in wastewater treatment plants and receiving river waters: Comparison to estrogens*. Water Research, 2011. 45(2): p. 732-740.
19. Weiss, J.M., et al., *Identification strategy for unknown pollutants using high-resolution mass spectrometry: Androgen-disrupting compounds identified through effect-directed analysis*. Analytical and Bioanalytical Chemistry, 2011. 400(9): p. 3141-3149.
20. Sohoni, P. and J.P. Sumpter, Several environmental oestrogens are also anti-*androgens*. Journal of Endocrinology, 1998. 158(3): p. 327-339.
21. Alvarez-Muñoz, D., et al., *Widespread contamination of coastal sediments in the Transmanche Channel with anti-androgenic compounds*. Marine Pollution Bulletin, 2015. 95(2): p. 590-597.
22. Birkhøj, M., et al., *The combined antiandrogenic effects of five commonly used pesticides*. Toxicology and Applied Pharmacology, 2004. 201(1): p. 10-20.
23. Christiansen, S., et al., *Synergistic Disruption of External Male Sex Organ Development by a Mixture of Four Antiandrogens*. Environmental Health Perspectives, 2009. 117(12): p. 1839-1846.
24. Thomas, K.V., et al., *An assessment of in vitro androgenic activity and the identification of environmental androgens in United Kingdom estuaries*. Environmental Toxicology and Chemistry, 2002. 21: p. 1456-1461.

Appendix C

Supplementary information for chapter 4

C1 Material and Methods

C1.1 Study Area

Table C1 Overview of sampling site number and corresponding site name with geographical coordinates.

Sampling site number	Sampling site name	Latitude	Longitude
3	Wernigerode	51°49'04.3''N	10°43'43.9''E
5	Braunes Wasser (Tributary)	51°49'10.9"N	10°44'29.9"E
8	Zillierbach (Tributary)	51°50'01.0"N	10°46'48.0"E
9	Upstream rainwater drainage	51°50'49.7''N	10°47'29.6''E
11	Upstream Barrenbach	51°51'48.1''N	10°49'52.8''E
12	Barrenbach (Tributary)	51°51'52.0"N	10°49'54.3"E
13	Upstream Silstedter Bach	51°51'53.4''N	10°50'46.2''E
14	Silstedter Bach (Tributary)	51°51'47.6"N	10°50'44.7"E
15	Upstream WWTP Silstedt	51°51'54.1"N	10°51'31.0"E
17	Downstream WWTP Silstedt	51°51'59.3"N	10°52'47.0"E
18	Upstream Derenburg	51°52'00.4''N	10°54'25.0''E
19	Rothe (Tributary)	51°52'08.8"N	10°54'28.9"E
20	Hellbach/Mühlenbach (Tributary)	51°52'32.1''N	10°54'43.1''E
21	Downstream Derenburg	51°52'37.5''N	10°54'46.7"E
22	Pegel Mahndorf	51°53'06.2''N	10°57'47.2''E
23	Ströbecker Fließ (Tributary)	51°53'32.3"N	10°58'36.5"E
24	Downstream Ströbecker Fließ	51°53'34.9''N	10°59'56.0''E
25	Upstream Halberstadt	51°53'48.2''N	11°01'11.3''E
26	Halberstadt upstream rainwater drainage	51°54'11.6''N	11°03'28.2''E
29	WWTP Halberstadt (Tributary)	51°54'16.8''N	11°03'47.1''E
31	Downstream WWTP Halberstadt	51°54'25.8"N	11°04'12.6"E
34	Upstream Asse	51°55'21.9''N	11°06'25.8''E
35	Asse (Tributary)	51°55'27.4"N	11°06'16.6"E
36	Upstream Weir Gross Quenstedt	51°55'24.3"N	11°06'36.3"E
38	Nienhagen	51°56'29.7"N	11°09'31.1"E
39	Ditch Nienhagen (Tributary)	51°56'57.3''N	11°10'08.0''E
40	Upstream Salzgraben	51°57'01.6''N	11°10'33.4''E
41	Salzgraben (Tributary)	51°57'01.4"N	11°10'38.7"E
42	Mouth	51°57'47.8"N	11°10'57.7"E

C1.2 Chemical analysis using LC-HRMS/MS

Table C2 Gradient program for LC-HRMS screening method.

Time [min]	0.1% formic acid in H_2O [%]	0.1% formic acid in methanol [%]	Isopropanol/Acetone 50/50 (v/v) [%]	Flow rate [mL/min]
0.0	95	5	0	0.30
1.0	95	5	0	0.30
13.0	0	100	0	0.30
24.0	0	100	0	0.30
24.1	5	10	85	0.35
26.2	5	10	85	0.35
26.3	95	5	0	0.35
31.9	95	5	0	0.35
32.0	95	5	0	0.30

Table C3 MDL of the coumarin derivatives in the retrospective analysis.

	Water (direct injection) in ng/L	Water (extracted by LVSPE) in ng/L	Sediment in ng/g TOC	*Gammarus pulex* in ng/g wet weight
C47	2.7	0.4	5.0	0.2
C47T1	3.9	1.2	8.0	0.3
C47T2	6.2	0.9	7.8	0.3

C1.3 Analytical method for sediment sorption experiment

For LC, an Agilent 1260 system was used. Compounds were separated by gradient elution on a C18 column (Kinetex C18, 50x 3 mm, 2.6 µm particle size, with pre-column 5x 3 mm and in-line filter) using 0.1% formic acid (eluent A) and methanol containing 0.1% of formic acid (eluent B) at a flow rate of 400 µL min^{-1} and a column temperature of 40°C. The gradient program started at 5% of B, held for 1 minute, increasing linearly in 5.2 minutes to 95% of B, held for 5.2 minutes, followed by re-equilibration.

For ionisation, a Turbo V ESI source operated in positive ion mode was used. The QTrap 6500 MS was operated in multiple reaction monitoring mode using the following settings:

Compound	Retention time [min]	Q1 mass	Q3 mass	DP [V]	CE [V]	CXP [V]
7-Amino-4-methylcoumarin	6.1	176.1	120.0	101	31	8
		176.1	103.0	101	37	12
7-Ethylamino-4-methylcoumarin	7.2	204.1	148.1	131	31	8
		204.1	130.1	131	37	10
7-Diethylamino-4-methylcoumarin	7.9	232.1	188.0	151	39	16
		232.1	132.0	151	53	6

C2 Results and Discussion

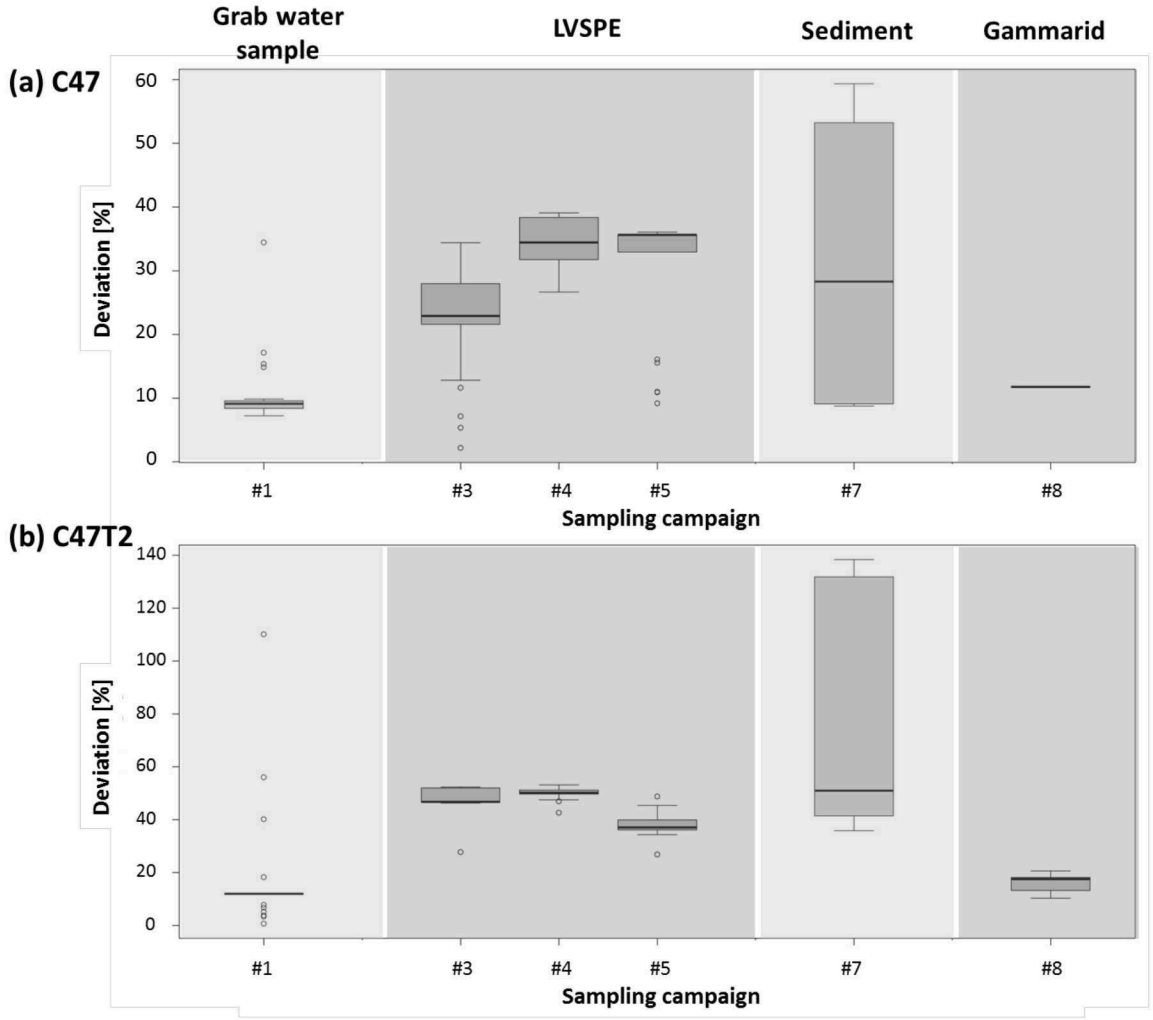

Figure C1 Deviation [%] of the simultaneous and retrospective quantification of (a) C47 and (b)C47T2 in grab water, LVSPE, sediment and gammarid samples.

Table C4 Variability [%] of the coumarin derivatives in the retrospective analysis.

	Water (non-concentrated)	Water (extracted by LVSPE)	Sediment / *Gammarus pulex*
C47	10.0	12.8	22.8
C47T1	11.9	10.5	20.5
C47T2	21.3	8.2	12.1
average	14.4	10.5	18.4

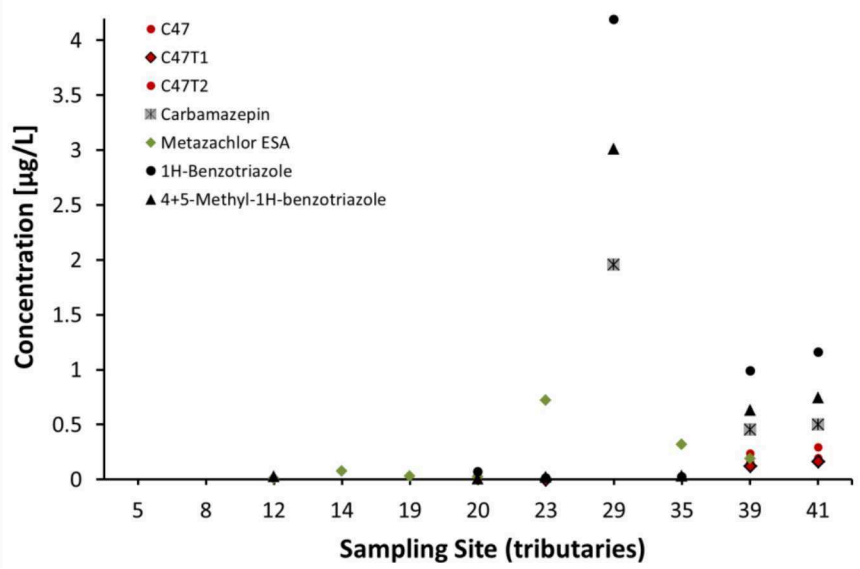

Figure C2 Concentration profiles of C47, C47T1, C47T2, the persistent wastewater tracers carbamazepine, 4+5-Methylbenzotriazole and Benzotriazole, as well as the groundwater marker Metazachlor ESA at tributaries of the Holtemme on 06 Oct 2015.

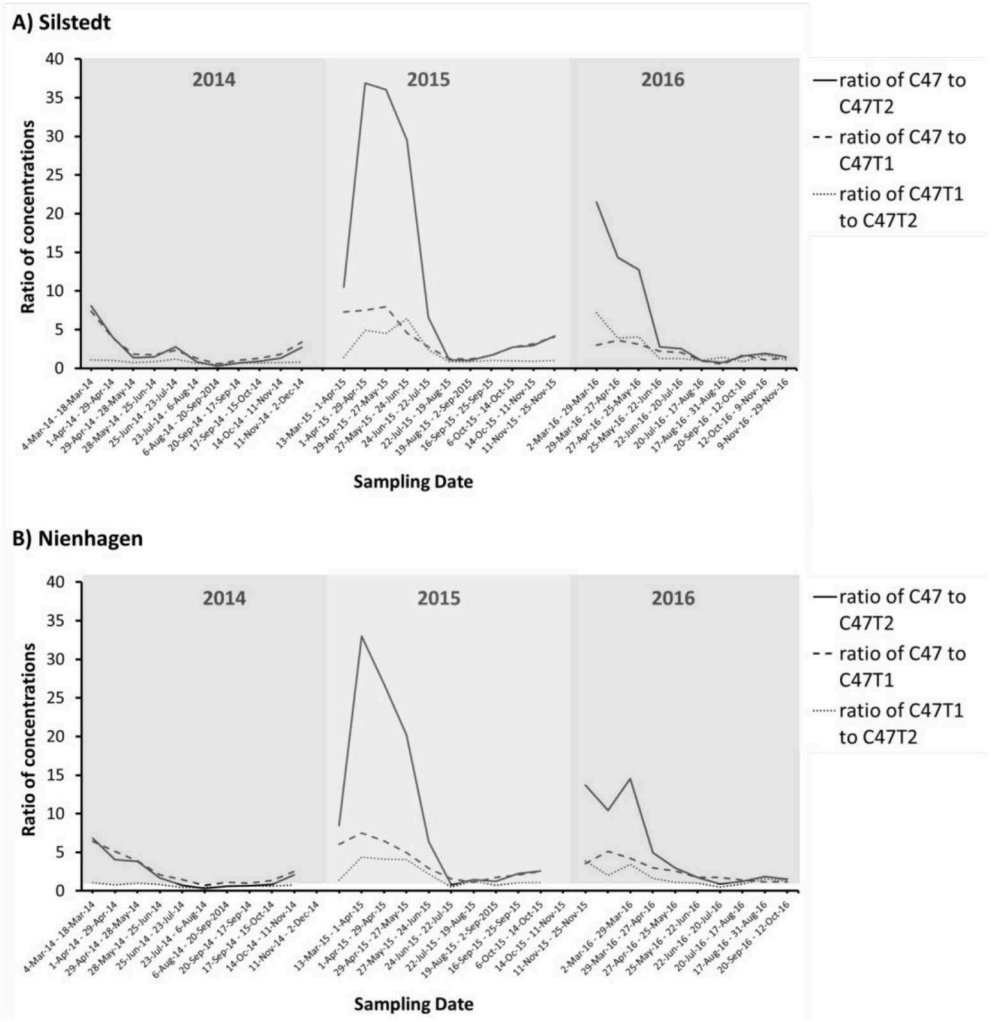

Figure C3 Ratios of concentrations in 28 days composite LVSPE samples of C47, C47T1 and C47T2 collected at Silstedt (17) and Nienhagen (38) between 2014 and 2016.

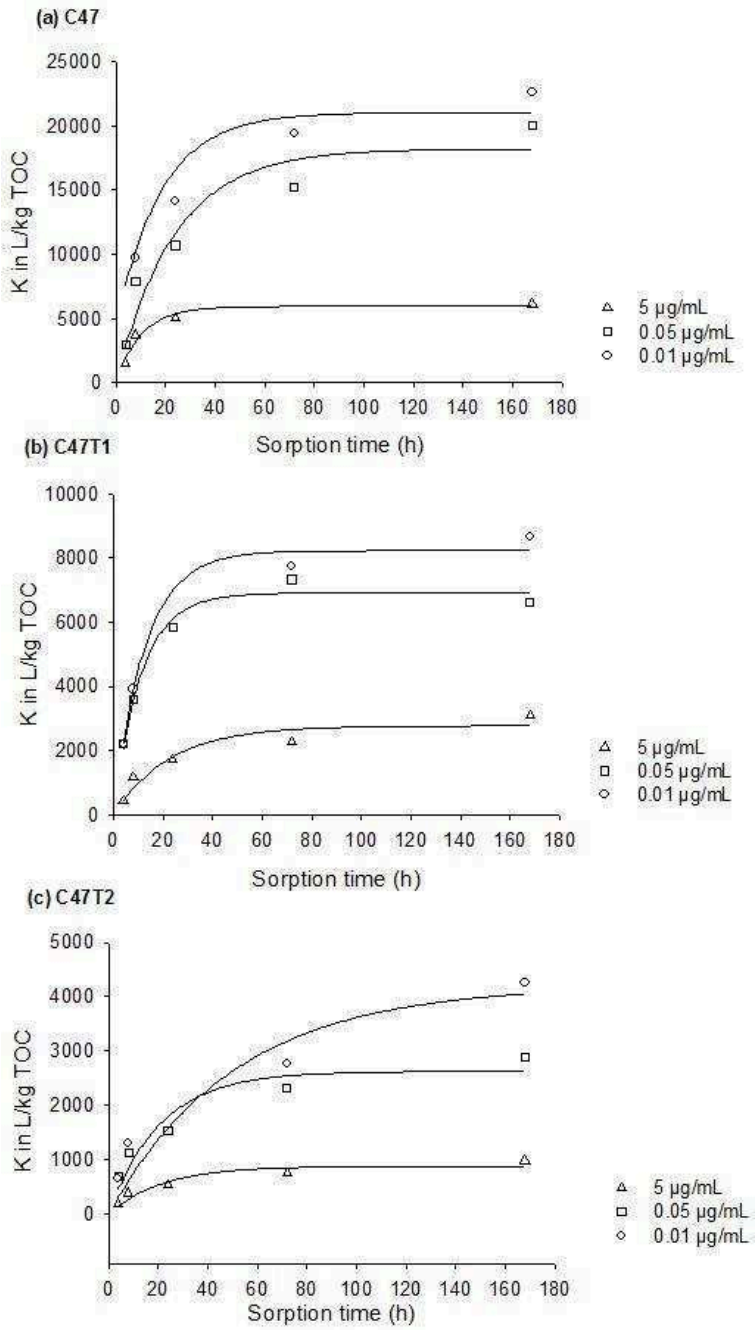

Figure C4 Sediment-water partitioning constant K of (a) C47, (b) C47T1 and (c) C47T2 as a function of sorption time to sediment at initial aqueous concentrations of 0.01, 0.05 and 5 µg/mL.

Table C5 Overview of predicted partitioning coefficients $K_{OC,\ pred.}$ and the for initial water concentrations of 5, 0.05 and 0.01 µg/mL experimentally derived, concentration dependent partitioning coefficients $K_{OC,\ exp.}$ of C47, C47T1 and C47T2. Prediction was carried out in EPI Suite v4.11 (US EPA, 2012).

Compound	Initial water concentration of partitioning batch experiment (µg/mL)	$K_{OC,\ pred.}$ (L/kg TOC)	$K_{OC,\ exp.}$ (L/kg TOC)
C47	5	376	5944
C47	0.05	376	18205
C47	0.01	376	21030
C47T1	5	105	2768
C47T1	0.05	105	6909
C47T1	0.01	105	8224
C47T2	5	29	888
C47T2	0.05	29	2629
C47T2	0.01	29	4204

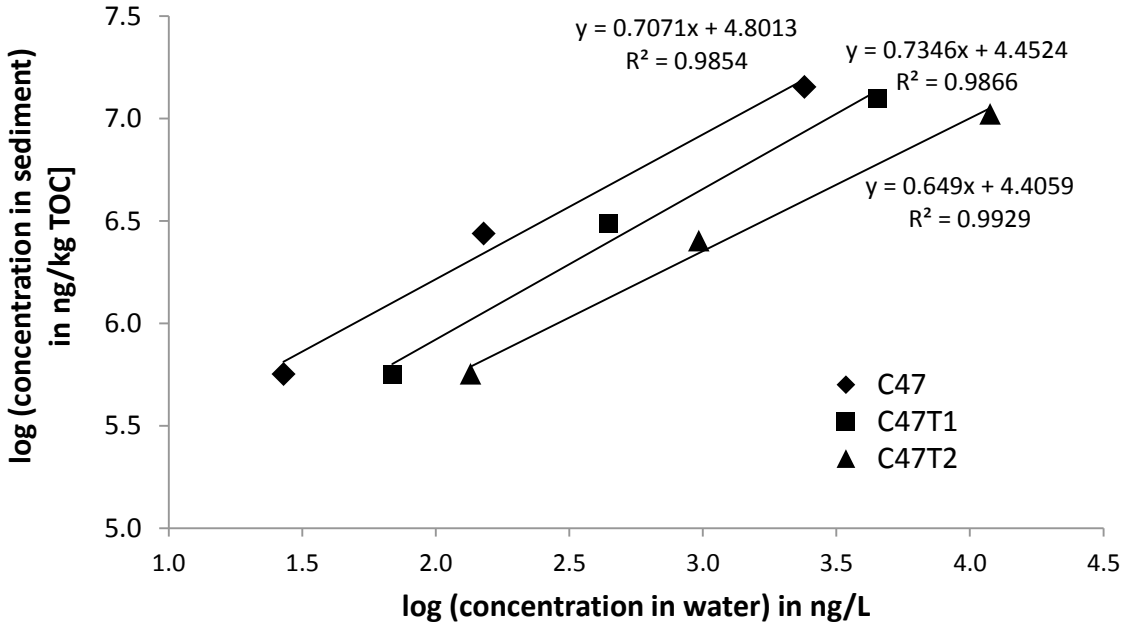

Figure C5 Isotherm of the sorption of C47, C47T1 and C47T2 to sediment in equilibrium of partitioning. Equations of the linearized Freundlich isotherms and the corresponding coefficients of determination (R^2) are displayed.

Table C6 Overview about measured concentrations of C47, C47T1 and C47T2 at three sampling sites in sediment (c_s) and water ($c_{fd,W}$). Displayed are also accordingly to the Freundlich Isotherm calculated freely dissolved sediment concentration $c_{fd,\,S}$ exp. and the freely dissolved sediment concentration $c_{fd,\,S}$ pred. based on predicted K_{OC} values. Prediction was carried out in EPI Suite v4.11 (US EPA, 2012). Predicted and experimental ratios of freely dissolved concentrations and the corresponding partitioning constants are also shown.

Site	Compound	c_s (µg/kg TOC)	$c_{fd,\,W}$ (ng/L)	$c_{fd,\,S}$ pred. (µg/L)	$c_{fd,\,S}$ exp. (ng/L)	log K_{OC} pred.	log K_{OC} exp.	Sediment - water ratio: $c_{fd,\,S}$ pred. / $c_{fd,W}$ pred.	Sediment - water ratio: $c_{fd,\,S}$ exp. / $c_{fd,W}$ exp.
Silstedt (17)	C47	8	2897	0	0	2.6	5.2	0.06	0.00002
Quenstadt (36)	C47	9042	945	376	1115	2.6	3.9	398	1.2
Nienhagen (38)	C47	8040	945	313	945	2.6	4.0	332	1.0
Silstedt (17)	C47T1	10	1238	1	0	2.0	4.6	1	0.0002
Quenstadt (36)	C47T1	2765	293	411	511	2.0	3.8	1403	1.7
Nienhagen (38)	C47T1	3177	293	443	617	2.0	3.7	1510	2.1
Silstedt (17)	C47T2	188	202	50	22	1.5	3.9	246	0.1
Quenstadt (36)	C47T2	1044	90	555	305	1.5	3.6	6143	3.4
Nienhagen (38)	C47T2	2355	90	1174	1070	1.5	3.4	12988	11.8

Acknowledgements

I am really grateful to PD Dr. Werner Brack who gave me the chance to conduct my PhD work in his working group. I do not take it for granted that your door was always open when I needed an opinion or advice. My special thanks goes to my second supervisor Dr. Martin Krauss, who always were available to support me with its immense knowledge, patience and indispensable experience. Also I would like to thank Prof. Dr. Henner Hollert for accepting me as a PhD student, for the very fruitful and pleasant collaboration concerning the biotests and for evaluating this dissertation.

This PhD work was mainly financed by the SOLUTIONS project under the grant agreement 603437 and partially financed by the TOX-BOX project (grant agreement no. 02WRS1282C; http://www.bmbf.riskwa.de) and also by the EDA EMERGE ITN project within the EU Seventh Framework Program (FP7-PEOPLE-2011-ITN) under the grant agreement number 290100.

I want to thank all members of the working group of effect-directed analysis. First thanks to Margit Petre and Marion Heinrich for the help in the lab. Without them, I would probably still be searching for chemicals or other equipment. Many thanks to Erik Müller for the invaluable help in using the software R. Thanks to Dr. Arnold Bahlmann for his help in the beginning of my PhD time. Thanks to Jörg Ahlheim, Dr. David López Herráez, Liza-Marie Beckers, Denise Kurth, Robert Bloch, Meng Hu and Arslan Hashmi for being my companions on this journey. Thanks to Dr. Tobias Schulze for his help concerning the fractionation apparatus. Thanks to Aleksandra Piotrowska for conducting the partitioning experiments.

Besides I want to thank my colleagues from RWTH Aachen: Thanks to Dr. Carolina di Paolo for always being available to discuss the biotest results. I am also thankful about the very nice collaboration with Kristina Kirchner regarding the anti-AR-CALUX assay, to Dr. Richard Ottermanns for his explanations of statistics to a non-statistican, as well as to Dr. Thomas-Benjamin Seiler, Monika Lam, Jochen Kuckelkorn and Simone Hotz for the support with the bioassays.

Many thanks to Dr. Andrew Tindall from WatchFrog who significantly contributed to the EDA study with its in vivo test system and who was very helpful in revising the manuscript.

I am very thankful that I met people from all over the world that are not just colleagues but became important to me as friends: Melis M., Riccardo M., Pedro I. and Harry B. Thinking back I always will be very thankful about the support of Angelika. H.
At the end, I would like to give my gratitude to my family. This work would not have been done without your support.

Curriculum Vitae

Name: Matthias Muschket

Address: Braustraße 23, 04107 Leipzig, Germany

Email: matthias.muschket@ufz.de

Date of Birth: 04.07.1982

Place of Birth: Bad Salzungen

Research Experience

09/2017 – 07/2018

Helmholtz Centre for Environmental Research, Department of Analytical Chemistry, Leipzig, Germany

Research fellow

Object of research: Analytics of transformation products of polyfluorinated precursors in soil and plants

03/2013 – 10/2017

Helmholtz Centre for Environmental Research, Department of Effect-Directed Analysis, Leipzig, Germany and RWTH Aachen University, Germany

PhD student, title of dissertation: „Effect-directed identification and fate analysis of potent antiandrogenic coumarin derivatives in a central European river“

11/2009 – 1/2010

Center for Biotechnology and Biomedicine, Research Group Bioanalytics, Leipzig, Germany

Research assistant

Focus: Peptide synthesis and their chromatographic purification

10/2006 – 02/2007

Center for Biotechnology and Biomedicine, Research Group Bioanalytics, Leipzig, Germany

Student assistant

Focus: Chemical analysis of peptides with MALDI-MS, synthesis of Amadori peptides

Education

11/2009

Graduated as a Diplom-Chemiker (equivalent to a Master of Science with thesis) at the Universität Leipzig

Publications

Muschket, M., et al., Identification of Unknown Antiandrogenic Compounds in Surface Waters by Effect-Directed Analysis (EDA) Using a Parallel Fractionation Approach. Environmental Science & Technology, 2018. 52(1): p. 288-297.

Di Paolo, C., [et al., including **Muschket, M.**], *Downscaling procedures reduce chemical use in androgen receptor reporter gene assay*. Science of The Total Environment, 2016. 571: p: 826-833.

Brack, W., [et al., including **Muschket, M.**], *Effect-directed analysis supporting monitoring of aquatic environments - An in-depth overview*. Science of The Total Environment, 2016. 544: p. 1073-1118.

Singer, D., [et al., including **Muschket, M.**], *Separation of Multiphosphorylated Peptide Isomers by Hydrophilic Interaction Chromatography on an Aminopropyl Phase*. Analytical Chemistry, 2010. 82(15): p. 6409-6414.

Oral Presentations

Muschket, M., Di Paolo, C., Tindall, A., Touak, G., Krauss, M., Kirchner, K., Hollert, H., Brack, W. (2017). A novel fractionation approach using four columns in parallel for effect-directed analysis of antiandrogenic compounds in a river water extract. Oral presentation in the Society of Environmental Toxicology and Chemistry (SETAC). Brussels, 7-11.5.2017

Muschket, M., Di Paolo, C., Krauss, M., Kirchner, K., Hollert, H., Brack, W. (2016). A novel fractionation approach using four columns in parallel for effect-directed analysis of antiandrogenic compounds in a river water extract. . Oral presentation in the Society of Environmental Toxicology and Chemistry (SETAC). Nantes, 22-26.5.2016

Muschket, M., Di Paolo, C., Krauss, M., Kirchner, K., Hollert, H., Brack, W. (2015). A novel fractionation approach using four columns in parallel for effect-directed analysis of antiandrogenic compounds in a river water extract. Oral presentation during the symposium of the NORMAN network. Rome, 2-4.12.2015

Poster Presentations

Muschket, M., Brack, W., Krauss, M. (2016). Orthogonal, Parallel Fractionation of Androgens and Antiandrogens by Liquid Chromatography. Poster presentation in the International Conference on Chemistry and the Environment (ICCE). Leipzig, 21-23.9.2016

Muschket, M., Brack, W., Krauss, M. (2015). A multidimensional fractionation approach for effect-directed analysis of antiandrogenic compounds in a river water extract. Poster presentation in the Society of Environmental Toxicology and Chemistry (SETAC). Barcelona, 3-7.5.2015